

VERIFICATION OF SOIL-STRUCTURE INTERACTION METHODS

C.A. Miller, C.J. Costantino, A.J. Philippacopoulos,
and M. Reich

Date Published — May 1985

DEPARTMENT OF NUCLEAR ENERGY, BROOKHAVEN NATIONAL LABORATORY
UPTON, NEW YORK 11973



Prepared for the U.S. Nuclear Regulatory Commission
Washington, D.C. 20555
Contract No. DE-AC02-76CH00016

VERIFICATION OF SOIL-STRUCTURE INTERACTION METHODS

**C.A. Miller, C.J. Costantino, A.J. Philippacopoulos,
and M. Reich**

**Manuscript Completed — February 1985
Date Published — May 1985**

**STRUCTURAL ANALYSIS DIVISION
DEPARTMENT OF NUCLEAR ENERGY
BROOKHAVEN NATIONAL LABORATORY
UPTON, NEW YORK 11973**

**Prepared for
OFFICE OF NUCLEAR REGULATORY RESEARCH
UNITED STATES NUCLEAR REGULATORY COMMISSION
WASHINGTON, D.C. 20555
CONTRACT NO. DE-AC02-76CH00016
FIN A-3242**

NOTICE

This report was prepared as an account of work sponsored by an agency of the United States Government. Neither the United States Government nor any agency thereof, or any of their employees, makes any warranty, expressed or implied, or assumes any legal liability or responsibility for any third party's use, or the results of such use, of any information, apparatus, product or process disclosed in this report, or represents that its use by such third party would not infringe privately owned rights.

The views expressed in this report are not necessarily those of the U.S. Nuclear Regulatory Commission.

Available from
Superintendent of Documents
U.S. Government Printing Office
P.O. Box 37082
Washington, DC 20013-7982
and
National Technical Information Service
Springfield, Virginia 22161

ABSTRACT

Soil-structure interaction (SSI) methods currently used by industry to evaluate the seismic response of nuclear power plant facilities are reviewed with the aim of evaluating those areas of uncertainty which still exist in the analytic approaches. The primary methodologies used by various agencies generally can be grouped into three areas, namely, lumped parameter methods, finite element methods of combined soil/structure systems, and substructuring methods of analysis. Each of these are discussed in the report.

In general, it was found that lumped parameter approaches yield reasonable results provided that the site is relatively uniform and the seismic inputs are low enough such that nonlinear effects are unimportant. The finite element results are reasonable provided that extreme care is taken in determining mesh geometry, boundary conditions, 3D effects, etc. Similar conclusions can be applied to the substructuring approaches.

EXECUTIVE SUMMARY

Soil-structure interaction (SSI) methods currently used by industry to evaluate the seismic response of nuclear power plant facilities are reviewed in this report with the aim of evaluating those areas of uncertainty which still exist in the various analytic approaches used to evaluate structural response. The primary methodologies can be conveniently grouped into three analytic approaches, namely, lumped parameter methods, finite element methods of combined soil/structure systems and substructuring method of analyses. This latter approach has not been specifically evaluated herein since many of its characteristics are similar to those of the finite element methods. Differences can only be expected to occur from specific computer code implementations.

The lumped parameter approach makes use of a detailed model of the structure coupled to the free-field soil or rock by means of springs and dashpots, whose function is to represent the interaction process. Typically, a seismic disturbance, defined as if the structural facility were not present, is input to the spring/damper SSI models. The fundamental assumption of this approach is that the motion of the structure, moving in response to the input seismic disturbance, does not influence the incoming free-field motion. It is typically argued that the structural motion may in fact modify the very near field motion, but will not seriously change the far field motion at some distance from the structure. This area, however, is clearly an area of uncertainty which must be considered.

Solutions to the interaction equations of motion are carried out in either the time or frequency domain, which depending on the analysis method used, leads to two further areas of concern, namely, (a) the use of modal damping, and (b) the frequency dependence of the interaction parameters. Typically SSI damping is relatively high while structural damping is low which can lead to errors in the computation if undamped modal equations of motion are used, as is often the case. In addition, when the solution is carried out in the time domain, the frequency dependence of the interaction parameters,

particularly the damping parameters, can also lead to errors in the computation. Other uncertainties (i.e., affect of noncircular foundation shape, foundation flexibility, depth of burial, unhomogeneity of free-field, etc.) were also considered in the study. The results indicate that the lumped parameter approach yields reasonable simulation provided that the site is uniform and the seismic input levels low enough so as to make nonlinear effects unimportant.

The finite element model is typically based in the use of a single model to represent both the free-field and the structure. Due to the size limitations of the computer hardware and software, these models are usually taken as two-dimensional slices through the facility and the free-field, leading to an area of major uncertainty. The free-field mesh is typically bounded by three artificially placed boundaries to limit the mesh size, leading to the second area of concern, associated with the imposed boundary conditions. In addition, the seismic disturbance is input at the bottom boundary, leading to the requirement for ascertaining seismic motions at depth near the specified surface criteria motion (convolution problem). Coupled with these problems is the requirement associated with mesh size used in the typical computation to ensure that the frequency transmission capability of the mesh is adequate for the computation.

The concept of the finite element method clearly has the potential for creating a better model of the SSI problem than does the lumped parameter method. Comparisons with measured data from uniform site indicates that results from the computation are adequate, provided that care is taken in specifying mesh characteristics, transmitting boundaries, etc.

ACKNOWLEDGEMENTS

The authors wish to express their appreciation to Mr. Herman Graves of the Structural Engineering Research Branch of the NRC for his support and encouragement in the conduct of this study. In addition, we would also like to thank Dr. J. Costello for the Structural Engineering Branch of the NRC for his valuable comments and criticisms.

Special thanks are also due to Dr. H. Tanaka of Tokyo Electric Power for providing measured data from the Fukushima Nuclear Power Plant, and to Dr. Neil Higgins of Applied Research Associates for providing inputs from the SIMQUAKE experiments. The cooperation of the Electric Power Research Institute in making available the data utilized by Dr. Higgins is also greatly appreciated.

Finally, we wish to acknowledge the efforts of Ms. Joan Murray and Ms. Liz Gilbert for compiling and typing the manuscript.

TABLE OF CONTENTS

	Page
ABSTRACT	iii
EXECUTIVE SUMMARY	iv
ACKNOWLEDGEMENTS	vi
1.0 INTRODUCTION	1
2.0 UNCERTAINTIES IN SOIL/STRUCTURE INTERACTION METHODS	3
2.1 Lumped Parameter Models	3
2.1.1 General Description	3
2.1.2 Interaction Parameters	5
2.1.2.1 Base Interaction	5
2.1.2.2 Sidewall Interaction	7
2.1.3 Uncertainties in Lumped Parameter Method	8
2.2 Finite Element Method	9
2.2.1 General Description	9
2.2.2 Free Field Model	11
2.2.3 Input Motion	12
2.2.4 Soil/Structure Interface	12
2.2.5 Uncertainties	13
2.3 Substructuring Method	14
2.3.1 General Description	14
2.3.2 Uncertainties	15

TABLE OF CONTENTS (Cont'd)

	Page
3.0 EXPERIMENTAL DATA RELATING TO SOIL/STRUCTURE INTERACTION	15
3.1 Summary of Literature Review	15
3.1.1 Rating System	15
3.1.2 Available Data	17
3.1.2.1 Actual Earthquake Data	17
3.1.2.2 Earthquake Simulation With Explosives	18
3.1.2.3 Department of Defense Field Tests	19
3.1.2.4 Laboratory Scale Tests	21
3.2 Data Selected For Use	21
4.0 COMPARISONS OF EXPERIMENTAL DATA WITH CALCULATED RESULTS	22
4.1 Lumped Parameter SSI Model	22
4.2 Finite Element SSI Models	24
REFERENCES	26
APPENDIX A Correlation of Fukushima Data with Lumped Parameter Codes	A-1
APPENDIX B Correlation of SIMQUAKE II Data With Lumped Parameter Codes	B-1
APPENDIX C Correlation of Fukushima Data With Finite Element Codes	C-1

1.0 INTRODUCTION

This report describes work performed at Brookhaven National Laboratory (BNL) on the program "Benchmarking of Structural Analysis Problems". The work reported here is concerned with the task "Verification of Soil/Structure Interaction (SSI) Methods". The overall objective of the "Verification of Soil/Structure Interaction (SSI) Methods" task is to utilize existing experimental data to quantify and hopefully to reduce the uncertainties which exist in the various techniques used to treat SSI.

The SSI methods currently used by the industry to evaluate the seismic response of nuclear power plant facilities are first reviewed so that the major uncertainties of each method may be identified. Many state of the art reports on SSI (e.g., Ref. 1) exist and it is not the intent of this report to duplicate such work. Rather the report will present each of the methods only insofar as is required to develop the uncertainties which exist. The following comments are given to clarify the type of uncertainties which are to be included in the study:

1. The various SSI methods are often identified with one or more computer codes. The intent of this program is to focus on the methodology and not the computer codes. Methodologies will be verified during the course of the study; computer codes will not be validated.
2. The report focuses on those uncertainties which are centered around the SSI process. There are other uncertainties which exist (e.g., specification of the free field motion, numerical methods used to implement the various methods). To the extent that it is possible to uncouple this type of uncertainty from those associated with the interaction processs they are not included within the scope of this study.
3. The review of SSI methods centers on the normal engineering application of the method. In many instances better use of the method could be made than is standard practice. Economics and/or time constraints often result in a less sophisticated application than is possible. The intent

of this study is to develop data which may be used to assess the level of sophistication that may be advisable in performing a SSI analysis for a given site.

There are three primary methods currently being used to solve SSI problems: lumped parameter models; finite element models of the free field and structure; and substructuring methods. Each of these are discussed in the following sections of the report resulting in a list of uncertainties associated with each of the methods.

Applied Research Associates (ARA) on subcontract to BNL performed a comprehensive literature review (Ref. 2) in which the available experimental data describing the SSI process is discussed. This review was conducted in parallel with the task defining the SSI uncertainties so that the effort could be directed to those sources of experimental data which are most applicable. The data sources considered included: seismic measurements on actual structures; high explosive simulation loading on full scale or model structures; Department of Defense (DOD) experiments conducted in support of weapon system development; and laboratory simulations. Each data source was evaluated in terms of its applicability to the uncertainties of interest. This work is summarized in Section 3.0.

The comparisons between the experimental data and analytical predictions are discussed in Section 4.0. Complete details of the comparisons are contained in the appendices to the report with the results summarized in Section 4.0. Two data sources are considered: data from the Fukushima Nuclear Power Plant taken during a 7.4 M earthquake; and data from the SIMQUAKE II experiment. The Fukushima data is compared with predictions made with the lumped parameter and the finite element methods. The SIMQUAKE II data is compared with predictions made with the lumped parameter method.

During the course of the program the CLASSI Code (Ref. 3) was made available to BNL. This computer code is a substructuring code where the coupling between the structure and free field is through impedance functions. These functions are based on analytic solutions to the half-space steady state vibration problem. This code was made operational and tested on the BNL computer. The results of this work will be reported separately.

Conclusions drawn from the study are discussed in Section 4.0. This section of the report also contains a discussion of those areas which require further work.

2.0 UNCERTAINTIES IN SOIL/STRUCTURE INTERACTION METHODS

Three methods of performing SSI analyses are currently used to evaluate the seismic response of nuclear power plant facilities. The lumped parameter method is most popular because of its simplicity. The relatively low cost of obtaining solutions with this method allows for the variation of model parameters. The finite element method is more elegant than the lumped parameter method and can give good results if it is carefully applied. Solutions obtained using the finite element method are costly, however. The substructuring method is relatively new and found more in research studies than in actual practice.

Each of these methods are discussed with the objective of identifying the major uncertainties which exist for each. No attempt is made to completely describe the methods and all of the appropriate literature. Such discussions are available in the literature (Ref. 1).

2.1 Lumped Parameter Models

2.1.1 General Description

The lumped parameter method is based upon a finite element model of the structure coupled to the free field with springs and dashpots intended to represent the interaction process. A free field disturbance is input to the spring/damper model of the SSI. A very fundamental assumption of this method is that motion of the structure does not effect the free field motion (i.e., the effect of scattering of the incident wave by the rigid foundation is neglected). The free field pulse is used in the analysis with no possibility considered of the pulse being modified as a result of the structural motion. It is argued that the structural motion may influence the very near field motion but will not seriously alter the free field motion at reasonable distances from the structure. The structural motion is more sensitive to the

motion of the large mass of soil surrounding the structure than it is to local perturbations to this motion which may occur in the immediate vicinity of the structure. This clearly is an area of uncertainty which must be considered.

The heart of this method lies in the selection of the spring damper interaction parameters. This is discussed in the following section. Solutions to the resulting equations of motion are carried out in either the time or frequency domain. The choice is largely a matter of computational convenience. The method of computation does have an effect on the interaction model in two respects. One is associated with the use of composite damping in modal analysis methods and the other with the frequency dependence of the interaction parameters.

SSI damping is relatively high (up to 50% of critical) and structural damping is low (2-10% of critical). One method of solution proceeds by calculating the fixed base modes of the structure with the SSI springs and dampers acting in series with the structural finite elements. When the modal equations of motion are integrated in the time domain, one is faced with the dilemma of selecting a single value of modal damping to represent the high interaction damping and the low structural damping. A composite damping (Ref. 4) is often used to calculate an "average" damping. This has been shown (Ref. 5 and 6) to lead to unconservative results, however. The difficulty can be avoided if the solution is carried out in the frequency domain, or if the interaction forces are treated as modal loads applied to a free-free model of the structure. While this is a major uncertainty in seismic response calculations, it does not result from a lack of knowledge of the interaction process. As such, it is not treated as an uncertainty for this program.

The frequency dependence of the interaction parameters (as discussed in the next section) places a second restriction on the computational method. When the solution is carried out in the time domain, it is not possible to consider the frequency dependence of the parameters. Average values representative of frequency ranges of interest are used. Of course solutions carried out in the frequency domain could consider the frequency dependent

parameters. Since most lumped parameter solutions are carried out in the time domain, the replacement of frequency dependent interaction parameters with average values is treated as an uncertainty.

2.1.2 Interaction Parameters

The values used for the interaction parameters (springs and dampers) are based on analytic, steady state solutions to the problem of a rigid foundation vibrating on an elastic half space. Two contributions have been considered, namely the forces acting on the base of the structure and the interaction forces acting on the sidewalls of the structure. Each of these is considered.

2.1.2.1 Base Interaction

Bycroft (Ref. 7) developed one of the earlier solutions for a rigid circular foundation vibrating on the surface of a homogeneous elastic half space. Solutions were found for vertical translation, horizontal translation, rocking about a horizontal axis and torsional motion about a vertical axis. These solutions are in the form of integrals of special functions but numerical results are available for several cases of interest. The resulting displacement and stress components of the solution may then be combined to obtain equivalent springs and dampers. These springs and dampers are found to be functions of the frequency of excitation.

Many studies have been conducted to refine and extend the original results of Bycroft with Luco, et al. (Ref. 8) probably providing the most complete presentation. The set of curves given in Figs. 1 through 3 showing the frequency dependent springs and dampers are taken from Ref. 8. The interaction coefficients used in most of the lumped parameter codes are taken as frequency independent and are given as

$$K_H = \frac{28.8 G R (1-u)}{(7-8 u)}$$

$$C_H = \frac{18.24 \rho_c R^2 (1-u)}{(7-8 u)}$$

$$K_V = \frac{4GR}{(1-u)}$$

$$C_V = \frac{3.4 R^2 \rho_c}{(1-u)}$$

$$K_T = \frac{2.13 G R^3}{(1-u)}$$

$$C_T = \frac{0.4 \rho_c R^2}{(1-u)}$$

$$\text{where } \rho_c = \sqrt{\gamma G}$$

- K = spring constant
- C = damper constant
- H, T, V = horizontal, rocking, vertical
- G = shear modulus of soil
- u = Poisson's ratio of soil.
- R = Radius of foundation
- γ = mass density of soil

It may be seen that these "average" spring coefficients correspond to the zero frequency values from Fig. 1 while the dampers correspond to a non-dimensional frequency in the range of 1 to 2. The form of the equations giving the interaction parameters and the extent to which they are sensitive to the frequency of the disturbance are important uncertainties.

There are three areas where additional information is needed. These are: foundation properties, half space non-homogenities and half space nonlinearities. Each of these are discussed.

All of the available solutions are for a rigid circular foundation resting on the surface of an elastic half space. Many actual foundations, however, have noncircular shapes. Whitman (Ref. 9) has developed approximate methods for extending the circular solutions to include rectangular foundations. The extent to which these approximations represent experimental data and the interaction parameters for other shaped foundations is an uncertainty.

A recent paper (Ref. 10) by Luco examines the effect of foundation flexibility on the interaction parameters. Significant changes in the parameters are found for realistic values of the foundation's flexibility. This should be considered.

Some analytic solutions are available (Ref. 11) for a layered half space. Very few numerical evaluations for these solutions are available. The effect of layering on the interaction parameters must be considered as an uncertainty.

The presence of the water table near to the foundation has been shown (Ref. 12) to greatly influence the values of the interaction parameters. This factor is usually not considered in performing a lumped parameter interaction analysis and must be treated as an uncertainty.

All of the available solutions are for a linearly elastic half space. Nonlinearities of two types may be important. First, the stresses across the soil/structure interface may tend to tensile values in which case the two would separate. This uplift problem is nonlinear and should be considered. Second, the soil properties themselves are nonlinear, being heavily dependent on strain level. This nonlinearity is usually treated with an iterative linear process. Further justification of this process is required.

2.1.2.2 Sidewall Interaction

There are two approaches currently used to represent the effects of sidewall interaction. The first (Ref. 13) is based on a horizontal plane stress slice taken in the free field with a circular hole representing the sidewall of the building. The sidewall is assumed to be rigid and analytic solutions are developed for the steady state vibration of this system. Displacement and stress solutions to the problem may then be combined to generate equivalent springs and dampers to represent the sidewall interaction. These parameters are again found to be functions of the input frequency. All of the uncertainties listed above for the base interaction parameters apply here as well. The foundation flexibility limitation is now more serious because this solution requires the foundation to be rigid along

the length of the wall. In addition is an uncertainty associated with the appropriateness of the plane stress solution.

The second (Ref. 14) method uses springs and dampers to couple the sidewall to the adjacent soil. The values of the parameters have been developed from empirical methods. While the form of the equations used to represent these parameters is qualitatively plausible, the values used have been developed from small scale experiments for foundation geometries which are more like missile silos than nuclear power plant structures. The accuracy of these parameters needs to be validated with experimental data that is representative of nuclear power plant geometries and for seismic disturbances.

The method of constructing nuclear power plants will almost always have a backfill material near the sidewall which has quite different properties than the free field. The existing solutions for sidewall interaction parameters do not take this into account.

2.1.3 Uncertainties in Lumped Parameter Method

Based on the above discussion the following uncertainties will be considered during this program (As stated in the Introduction, the inclusion of an uncertainty does not imply that nothing is known on the topic nor tht it is not properly considered in current engineering practic. Items are included as uncertainties which are not an as firm a base as other aspects of the method.):

1. The scattering effect of structural motion on the free field disturbance is not considered in the lumped parameter modeling methodology. The important issue to resolve is not whether the very near motion is effected but whether the use of an unmodified far field motion results in an adequate solution for the structural response.
2. The frequency dependence of the base interaction parameters is usually not considered. It is important to determine whether a single value gives reasonable results for disturbances which contain the frequency content of a typical earthquake.

3. The effect of noncircular foundation shapes on the base interaction parameters should be considered. While methods currently exist to extend the circular base solutions to other shapes, there is a requirement to validate these methods.
4. The influence of foundation flexibility on the base interaction parameters is not known. It is generally felt that NPP foundations are rigid, but there is little quantitative data generally available to substantiate this result.
5. Half space non-homogeneties such as layering and the presence of a water table may effect the values used for base interaction parameters. Criteria are needed to quantify where these non-homogeneties should be included in the analysis.
6. Potential non-linearities such as debonding at the soil/structure interface and soil material properties have not been adequately considered to date.
7. The general form of the interaction parameters used to represent sidewall interaction must be validated. The uncertainties represented in Items 2 through 6 above apply as well to sidewall interaction as they do to base interaction.
8. The effect of backfill material around the sidewall may influence the the interaction process. This should be considered in more detail and is an uncertainty.

2.2 Finite Element Method

2.2.1 General Description

The finite element method is based on the use of a single model to represent both the free field and the structure. Because of the size limitations of current computer hardware and software, these models are usually taken as two-dimensional slices through the facility and the free field. This approximation is one of the major uncertainties in the method.

The free field model is bounded by the surface and three artificial boundaries. The bottom boundary is taken to be horizontal and placed at a depth corresponding to some bedrock interface. If there is not a distinct bedrock interface within a reasonable depth, this boundary is established at a depth where there is a marked increase in the media shear wave velocity or at a depth that is sufficiently far from the facility so as to not overly effect the facility motion. Two vertical boundaries are established at some distance from the facility. These boundaries are located based on two conflicting requirements. First, they should be sufficiently far from the facility so that reflections from these artificial boundaries will not have a significant influence on the response of the structure. This distance is controlled by the boundary conditions assumed in the computation. Second, they must be close enough so that the number of elements required to model the free field is within the capability of the computer system.

The structure itself is modeled with finite elements. The structural model is often transformed to modal equations prior to carrying out the solution. This option is for numerical convenience and has no bearing on the interaction problem. The interface between the structure and the free field is usually modeled so that there is displacement and pressure continuity across the interface. This, of course, is the heart of the interaction problem and does represent a major source of uncertainty in the method except for the potential liftoff problem.

The free field motion is input as a horizontal disturbance at the bottom boundary. Since the seismic disturbance is most often specified at a location at or near the surface, some form of deconvolution is required to determine a consistent bedrock motion.

The concept of the finite element method clearly has the potential of creating a better model for soil/structure interaction than does the lumped parameter method. If a three-dimensional model of unlimited size could be used it would undoubtedly give better results than the lumped parameter model. Computer limitations, however, place severe restrictions on the size of the problem that is possible to solve. It is important, therefore, that uncertainties in this method be identified in terms of model sizes that are possible to use.

2.2.2 Free Field Model

The model used to represent the free field is greatly restricted by the size limitations of the computer and software being used to solve the problem. The first compromise that is used is to reduce the problem from three to two dimensions. A plane stress or strain model is taken through the facility and free field. The facility is limited in extent in this direction while the free field is not. A somewhat arbitrary decision must be made then for the relative amount of soil and structure mass to include in the model. Artificial viscosity can be added (Ref. 15) to the two-dimensional model to approximate the energy that would be radiated into the third dimension. This is clearly a major uncertainty of the method.

The element size used to construct the free field model is an important factor influencing the accuracy of the solution. Quadrilateral elements are usually used. If these elements have aspect ratios greater than two or three one would expect large errors to occur. The size of the elements also determines the frequency content that can be transmitted through the element. An estimate of the required element size to transmit a given frequency is (Ref. 16):

$$a = c/4f$$

where, a = maximum element size

c = dilatational wave speed

f = maximum frequency of interest

The element acts as a filter to eliminate frequencies higher than those which can be passed.

The element size is therefore determined by the required frequency content of the solution. The permissible degrees of freedom are limited by the computer hardware and software (and perhaps the cost of obtaining a solution). Any limitation of degrees of freedom, of course, restricts the number of elements which may be used. Since the element size is restricted and the number of elements used is limited, the geometric size of the free field model is limited. This limitation is often severe. The user must therefore place the "bedrock" and two vertical boundaries so that these geometric limitations are satisfied.

When bedrock is not located near to the surface, an artificial boundary is established to reduce the degrees of freedom required in the model. Ideally the vertical boundaries would be placed sufficiently far from the facility so that reflections from the boundary would not reach the facility in times of interest to the problem. This is not possible because of the degree of freedom limitations in the problem. Quiet boundaries are (Ref. 17) used to reduce the reflections at the vertical boundaries. A quiet boundary should absorb all of the energy reaching the boundary and reflect none. There are no quiet boundaries which satisfy this requirement completely.

The finite element models are based on elastic constitutive models of the free field material. Consideration should be given to nonlinear aspects of soil behavior since both the shear modulus and material damping of soil is strongly strain dependent. The free field is often a two phase material (soil and water). The influence of the water table on the propagation of seismic disturbances through the media must be considered.

2.2.3 Input Motion

A seismic disturbance is usually specified in the form of a response spectra at or near the surface. Wave forms are fit to the criteria spectra and then used for analysis. Input to the finite element model is usually specified at the bottom bedrock interface. This motion is generated by deconvoluting the horizontal criteria motion from the surface to bedrock. Steady state vertically propagating shear waves are the basis for this deconvolution.

Serious questions naturally arise when the bedrock boundary is not horizontal. Any input along such a boundary would contain strong coupling between the vertical and horizontal motions.

2.2.4 Soil/Structure Interface

The standard finite element solution assumes displacement and pressure continuity across the soil/structure interface. This is equivalent to the assumption that points on the structure's foundation are welded to adjacent

points in the free field. In many respects this may not be a good representation of the actual boundary conditions. The surfaces will separate whenever tensile stresses tend to occur. The surfaces will slip relative to each other whenever the shear stress at the interface exceeds some value that would be limited by the friction between the soil and structure or the shear strength of the soil. The latter phenomena will be significant when the structure exhibits rocking motion relative to the free field. As the structure rocks, the soil applies a restraining moment due to vertical shear forces which develop along the sidewalls of the structure. The magnitude of this restraining moment would be limited whenever the soil would slip along the sidewall of the structure.

A crack model has been proposed (Ref. 15) which accounts for many of these conditions. All of these effects are nonlinear so that the inclusion of any of the more involved interface conditions require a nonlinear finite element code.

2.2.5 Uncertainties

Based on the above discussion the following uncertainties are identified for the finite element method:

1. All of the finite element solutions employ two dimensional models. The extent to which this can represent the actual three dimensional conditions must be considered. The use of damping boundary conditions and the relative mass of the structure and soil are particular items to be investigated.
2. Errors which result because of mesh size limitations are inherently a part of the problem when finite element methods are used. In particular it is important to establish the element size and form of the boundary conditions to be applied along the vertical boundaries (i.e., quiet boundaries).

3. The potential impact of nonlinear soil properties should be considered. In particular the strain and strain rate dependency of the shear modulus and material damping is important. Another potentially important characteristic of soil behavior is the two-phase aspect of the material behavior when the water table is close to the facility.
4. The input is specified at the bedrock. Errors which occur because of the deconvolution process using shear beam models should be considered. In addition there are many difficulties which arise when the orientation of bedrock is not horizontal.
5. The interface between the soil and structure contains many nonlinearities which are not considered in the standard welded boundary conditions assumed in a linear finite element computer code. In particular the possibility of separation and slipping along the interface should be considered.

2.3 Substructuring Method

2.3.1 General Description

The substructuring method consists in the combination of three solutions. First, a solution to the free field problem is found. This is treated as a plane strain problem with the seismic disturbance applied at a horizontal boundary representing bedrock. Second, solutions are found for unit impulses applied to the free field at the interface surface between the structure and the free field. Asymmetric models of the free field adequately represents this problem. Third, solutions are found for unit impulses applied to the structural model at the interface locations. Many unit impulse solutions must be obtained with the location of the point of application of the impulse varied. Finally the three solutions may be combined by insisting on compatibility of forces and displacements across the soil/structure interface. This is a rather new method and has not been widely used in practice.

2.3.2 Uncertainties

This method is very much like the finite element method. It has the advantage of being able to treat the three dimensional aspects of the problem because it takes advantage of the usual circular symmetry of the soil/structure interface. It has a disadvantage in that it relies totally on superposition so that there are no possibilities of incorporating nonlinear effects into the solution.

The uncertainties are therefore the same as listed in Section 2.2.5 except that the first may be eliminated. If items 3 and 4 of Section 2.2.5 should be important then this method has no possibility for refinement while the finite element method could be adopted to include nonlinear effects.

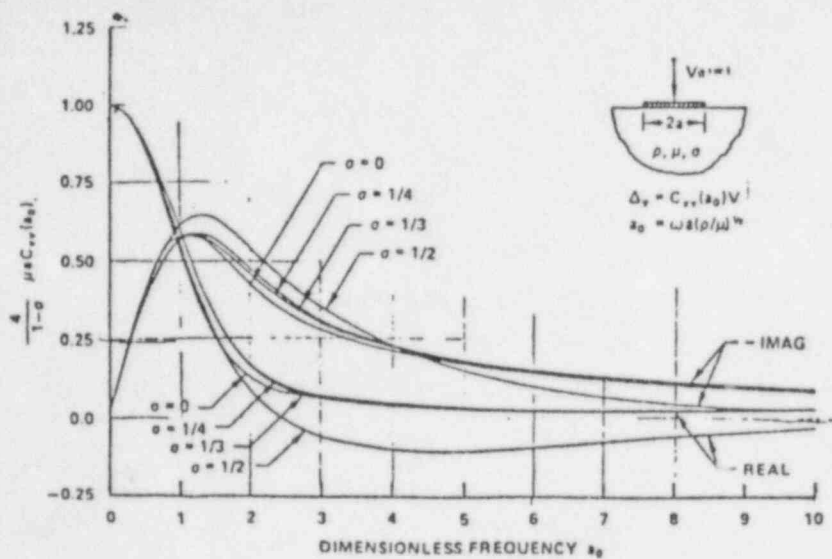
3.0 EXPERIMENTAL DATA RELATING TO SOIL/STRUCTURE INTERACTION

The primary objective of the work reported here is to compare solutions generated with the various soil/structure interaction methods with applicable experimental data. Applied Research Associates, on subcontract to BNL, performed a comprehensive literature review (Ref. 2). The results of that literature review are summarized in this section of the report. The final selection of data used for the study is then discussed.

3.1 Summary of Literature Review

3.1.1 Rating System

The ideal data source for the study would be measurements of the response of an actual nuclear power plant to a seismic disturbance. Data is only useful, however, if there are a sufficient number of measurements taken in both the structure and the free field. The site geological characteristics must also be of the type where SSI effects would be expected to be significant. Unfortunately there are no ideal data sources so that less than ideal sources must be considered. Most of the data taken during actual earthquakes is limited in that there are few if any free field measurements taken to compare with the in-structure measurements. A rating system is established to assess the adequacy of the "less than ideal" data sources.



LEGEND:

μ = Shear Modulus

σ = Poisson's Ratio

$$\alpha_0 = \omega a \sqrt{\frac{\rho}{\mu}}$$

ρ = Soil Mass Density

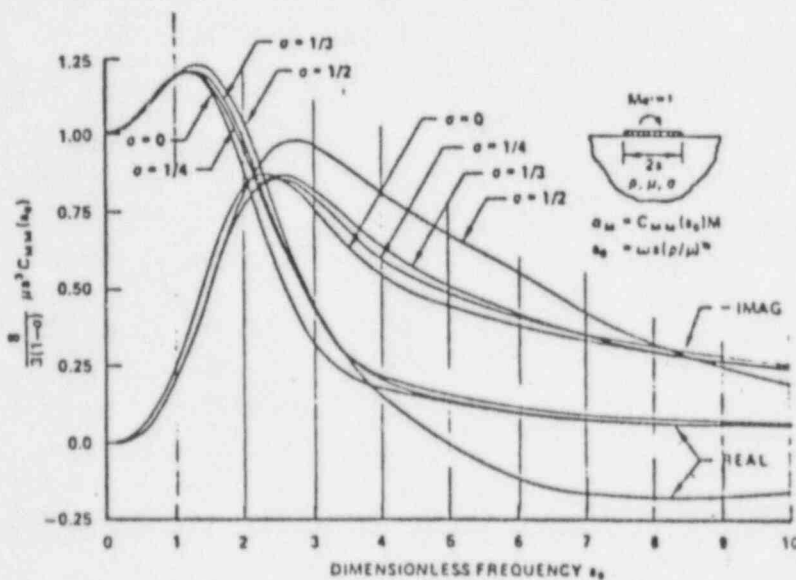


Fig. 2. Rocking Interaction Parameters

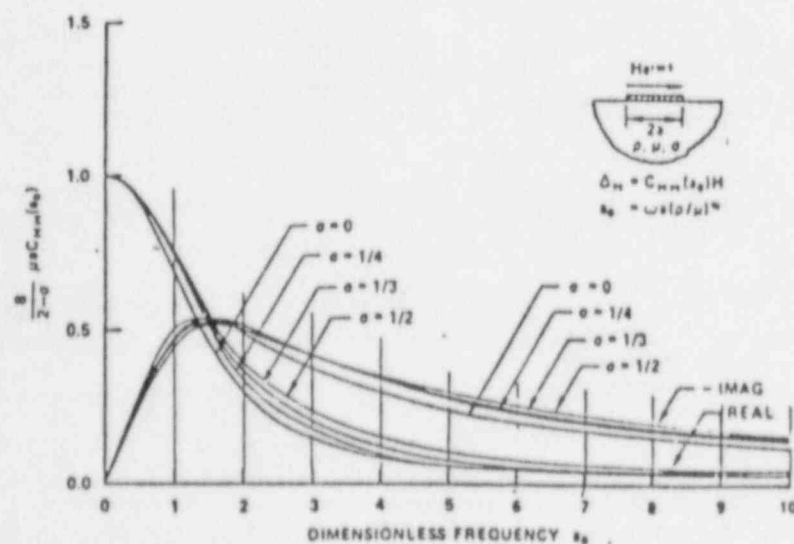


Fig. 3. Horizontal Interaction Parameters

The primary items on the rating system are the geometry of the structures and the characteristics of the input disturbance. The structural parameters of interest are the mass distribution of the structure relative to the foundation; the shape of the foundation; and the structural frequencies of vibration. The peak acceleration; duration of the pulse; and pulse frequency content are the input waveform characteristics of particular interest.

The secondary items of the rating system deal with characteristics of the soil/structure interface. Interface behavior includes mechanisms of stress transfer; bonding-debonding characteristics; and relative slip. The extent to which nonlinear properties of the soil influenced the measurements is also included.

Each potential data source considered during the review is evaluated by comparing the data source to an actual nuclear power plant with respect to the above parameters. A rating system (0-10) is used to indicate the degree of relevancy.

3.1.2 Available Data

Four general types of data are considered: actual earthquake data; earthquake simulation with explosives; Department of Defense field tests; and Laboratory scale tests. Each of these are discussed.

3.1.2.1 Actual Earthquake Data

Two data sources have been considered in detail, Fukushima and Humboldt Bay. A review of other data sources have indicated a lack of sufficient data to be of interest to this study.

The Fukushima Nuclear Power Plant is located on the eastern coast of Japan. It is a BWR type 460 MWe plant. The reactor containment structure is instrumented with four accelerometers mounted at different levels in the facility. There are four free field accelerometers. These gages are placed

at various elevations below the foundation ranging from the foundation level to about 36 meters below the foundation. The plant was subjected to a 7.4 magnitude earthquake on June 12, 1978. Records from all eight accelerometers were obtained from Dr. Hiroshi Tanaka of Tokyo Electric Power Company Inc. His cooperation is gratefully acknowledged. This is an excellent data source in that the plant structure is typical of most nuclear facilities. There is rather complete instrumentation in both the structure and the free field for a large magnitude earthquake.

The Humboldt Bay Power Plant is located in Eureka, California. The plant is unusual in that the reactor is located in a structure which is embedded in soil for about 70% of its height. One accelerometer is located in the Reactor Caisson, one in the Refueling Building, and one in a storage building located about 100m south of the Refueling Building. The facility was subjected to a 5.5 magnitude earthquake on June 7, 1975. This data source could be useful because of the extreme embedment of the Reactor Caisson which would be useful in evaluating sidewall interaction effects. There is not sufficient instrumentation in the free field or in any one structure however for this to be a good source for verification of SSI methods.

3.1.2.2 Earthquake Simulation With Explosives

The SIMQUAKE and HDR explosive simulations were considered in detail. References to other explosive tests are given in Ref. 2.

The SIMQUAKE tests were designed to simulate the effects of earthquake-like ground motion on generic nuclear power plant models using arrays of high explosive (DIHEST). The first experiment in the series was called Mini-SIM-QUAKE and evaluated the use of a time-sequenced double explosive array for producing ground motions with an acceptable duration. The second experiment was scheduled to be larger but the second explosive array failed to fire. SIMQUAKE II was then conducted and both arrays fired successfully. Six model containment structures were located in the experiment with scale factors ranging from 1/24 to 1/8. Extensive instrumentation was located in both the free field and in the test structures. This data is useful because of the completeness of the instrumentation. Unfortunately, liftoff effects occurred for all of the test structures so that the interaction effects may not be directly applicable to real nuclear power plant structures.

The HDR is a decommissioned 100 megawatt superheated steam reactor in the Federal Republic of Germany. Four types of experiments were performed to evaluate the dynamic response of the HDR containment structure: vibrational excitation with mechanical shakers; impulsive containment excitation with solid propellant rocket to simulate impact; snapback testing of components; and blast testing with small buried point charges. The last test is of interest to SSI studies. The resultant input is of rather lower amplitude however.

3.1.2.3 Department of Defense Field Tests

The Department of Defense has conducted extensive field testing in support of the development of the ground facilities for missile weapon systems. In general their interest has been in loadings acting on the structures arising from an attack with nuclear weapons. Both air blast pressures and ground shock act on the structures with the levels of loadings significantly higher than those which could occur during an earthquake. It is to be expected therefore that the structural shapes and load characteristics will differ from those applicable to the seismic response of nuclear power plants. Nonetheless the data is worth considering because of its extent and the extensive instrumentation used for all of the tests. Eight particular test series are briefly described more complete details are given in Ref. 2.

GOLIATH and HERCULES

Dynamic load tests were conducted on circular composite slabs similar to those used for missile launch facility closures. The slabs were subjected to overpressure loading (up to several thousand psi) and were founded on a rock. It would be expected that the rock/structure interaction effects would not be significant.

HANDEC

HANDEC was a series of two tests run by the Air Force which subjected surface-flush vertical silo-type structures to simulated nuclear loads. Both airblast-induced and direct-induced ground shocks were produced using the HEST and DIHEST techniques. HEST produced a vertically propagating wave while DIHEST produced a horizontally propagating wave. These data may be useful for investigating sidewall interaction effects but the load environments are substantially different from those encountered in a seismic environment.

ESSEX

Essex was a program designed to study the effects resulting from the detonation of low yield nuclear devices by modeling such detonations with HE sources. Surface and buried structures of the box and arch types were used during the program. The duration of the applied ground motion was probably too short for this data to be of direct applicability to the seismic problem.

DNA SBS

Seven HEST tests on shallow buried reinforced concrete boxes were conducted. The loading was generated in the Waterways Experiment Station Blast Load Simulator and as such resulted in vertically propagating P waves. The waves had large peak values and rather short durations. Considerable attention was given during these tests in establishing the effect of "arching" of the soil around the buried structure. This may be of interest in developing a better understanding of the behavior of the soil/structure interface as interaction occurs.

HAVE HOST

Horizontal and vertical cylindrical buried structures were subjected to both air blast and ground shock loadings. The loadings were of large amplitude and short duration.

DSOT AND VHS

Buried horizontal cylindrical structures were subjected to airblast induced ground shock loadings. The geometry of the structure, backfill, loading and material properties of the structure were varied during the test series. This offers a rather wide variation of parameters.

KACHINA

Buried arch and box type structures were subjected air blast loadings using HEST technique. Interface pressure measurements were made giving data directly applicable to the SSI problem. However the loading primarily consisted of vertical propagating P waves driving the structures deeper into the soil. This is quite different than seismic loading on structures.

3.1.2.4 Laboratory Scale Tests

Laboratory tests have been conducted with the objective of defining the conditions which exist at the soil/structure interface. None of these are directly useful in providing data that may be used to qualify SSI methods. They do however shed some light on characteristics that should be included in the SSI model if it is to represent the phenomena. A complete listing of the pertinent literature is given in Ref. 2.

3.2 Data Selected For Use

The Fukushima and SIMQUAKE data were selected for detailed study during this program. The Fukushima data was selected because it represents data collected from an operating nuclear power plant during a rather large magnitude earthquake. There is also enough data collection stations in both the structure and the free field so that meaningful comparisons with analysis results are possible. A complete description of this data is given in Appendix A. As mentioned above the data was obtained in digitized form from Dr. Tanaka of Tokyo Electric Power Company.

The SIMQUAKE data is selected because of the extensive set of instrumentation which was used. The experiment was also designed to simulate the SSI problem associated with the seismic response of nuclear power plants. A complete description of this data is given in Appendix B. The data was obtained in digitized form from Applied Research Associates.

4.0 COMPARISONS OF EXPERIMENTAL DATA WITH CALCULATED RESULTS

Comparisons of data from the Fukushima and SIMQUAKE data sources with predictions made using the various SSI methods are discussed in this section of the report. The Appendices to the report contain a detailed description of the work performed for each of the comparisons. The objective here is to briefly describe what was done and to relate the conclusions drawn during the study to the uncertainties for each of the methods which were developed and described in Section 2. The uncertainties which have not been resolved then form the basis for recommending additional work to be performed.

4.1 Lumped Parameter SSI Model

The lumped parameter SSI method is used to make predictions for both the Fukushima data and SIMQUAKE data. The comparisons with the Fukushima data is discussed in Appendix A while the comparisons with the SIMQUAKE data are contained in Appendix B. The specific conclusions drawn from each of these studies are presented in the last section of each of the Appendices. In general the comparisons with the Fukushima data are quite good while the comparisons with the SIMQUAKE data are poor.

The Fukushima comparisons indicate that the lumped parameter method can be expected to give reasonable results when the site is rather uniform. It should be noted that sidewall interaction effects were relatively small for the Fukushima facility so that no comment is possible regarding the reasonableness of the lumped parameter methodology for treating sidewall

interaction. Both the soil properties and soil/structure interface conditions are linear. The good correlation of the Fukushima data with lumped parameter methods should not therefore be extrapolated to problems which contain significant nonlinear components.

The poor correlation of the lumped parameter predictions with the measured SIMQUAKE data is attributed to the nonlinear interface conditions which existed for the experiment. The ground motion input during the SIMQUAKE experiment was sufficiently high to cause liftoff. This nonlinear effect was found to cause serious discrepancies between the measured and computed rocking and vertical structural motion components. It had little effect on the translational motion of the structure as evidenced by the good correlation of the measured and computed horizontal motion. Errors in both frequency content and motion amplitude were observed. An attempt was made to modify the interaction parameters to account for the effect to liftoff. This was found not to be possible so that it was concluded that the linear lumped parameter method should not be used where significant liftoff has occurred.

Each of the uncertainties identified in Section 2.1.3 are now discussed:

1. Scattering effects from the structure to the free field are found not to be significant. Of course this conclusion may not extend to the case where interest is in predicting the response of a light structure located close to a massive structure.
2. The constant interaction parameters are found to give good results for the case where the site is relatively uniform and significant nonlinear effects are not present. There is some indication that a frequency dependent interaction damper may give better results than the frequency independent damper. This could be resolved if data were available for different earthquakes (with different frequency contents) acting on the same facility.
3. The Fukushima foundation is square and the application of the generally accepted methods for converting the circular foundation solutions to a rectangular foundation were used and found to give acceptable results.

4. The foundations of both Fukushima RCB and SIMQUAKE structures were rigid so that foundation flexibility effects could not be investigated. This uncertainty could be investigated by using some of the DOD data (e.g., DNA SBS, HAVE HOST, and DSOT and VHS... see Section 3.1.2.3).
5. Soil properties for both data sources were fairly homogeneous. It is recommended that nonhomogenities due to both layering and water table effects be investigated. This could be done by conducting numerical experiments using computer codes that treat both nonhomogenities and which have to some extent been validated during this study.
6. Liftoff has been shown to be a very significant effect and one which cannot be treated with the standard lumped parameter methodology. It is recommended that this be considered further to define the earthquake magnitudes for which such effects are important.
7. Sidewall interaction effects were not significant for either data source. It is recommended that the Humboldt Bay data be used to study sidewall interaction effects.
8. Backfill effects were not important for either of the data sources used on this study.

4.2 Finite Element SSI Models

The finite element SSI method is used to make predictions for the Fukushima data. The comparisons of these predictions with the measured data is discussed in Appendix C. Specific conclusions based on these comparisons are given in the last section of the Appendix.

The comparisons of the computed and the measured floor response data indicate a fair correlation with the possibility of obtaining good results with the finite element method provided that care is taken in developing the mesh characteristics used to model the soil. The frequency transmission capability of the mesh between the input source motion and the structure is found to be particularly important. A fine mesh located around the structure

and made coarser as one moves away from the structure is found to be an unacceptable strategy to reduce the problem size. Frequency transmission characteristics of all elements in the mesh must be larger than frequencies of interest in the final solution. Quiet vertical boundaries are found to be adequate. Once again these conclusions are limited to uniform homogeneous sites such as exist at Fukushima.

Each of the uncertainties identified in Section 2.2.5 are discussed:

1. The two dimensional slice taken through the Fukushima site was found to give reasonable results. Damping boundary elements were used to account for the energy transmitted out from the slice. These dampers did not significantly effect the results.
2. The computed responses are significantly effected by the mesh size. Much better results are found for meshes that can transmit 17 or 35 cps than for meshes that can transmit only 9 cps. The transmitting boundary appears to give good results so that the vertical boundaries can be placed rather close to the facility.
3. Nonlinear soil characteristics were not important at the Fukushima site and were therefore not considered.
4. A rather extensive deconvolution study was conducted using the four Fukushima free field measurements. This is reported in Appendix A as it was required for the lumped parameter studies. It generally showed that the deconvolution process works well with the possible exception that a better soil damping model is required.
5. Shear separation of the sidewall interface was considered in this study and found to have little effect on the results.

REFERENCES

1. J.J. Johnson, "Soil Structure Interaction: The Status of Current Analysis Methods and Research", NUREG/CR-1780, January 1981.
2. W.C. Dass, C.J. Higgins, "Benchmarking of Structural Engineering Computer Codes: Soil-Structure Interaction Data Sources Bibliography", Applied Research Associates, June 1983.
3. J.J. Johnson, et al., "Seismic Safety Margins Research Program Phase I Final Report", NUREG/CR-2015, June 1982.
4. J.M. Roesset, R.W. Whitman, R. Dobry, "Modal Analysis of Structures with Foundation Interaction," Journal of the Structural Division, ASCE, March 1973.
5. D.A. Gasparini, A.D. Choudry, L.W. Curvy, "Damping for Frames with Constrained Viscoelastic Layers", Journal of Structural Division, ASCE, January 1980.
6. C.A. Miller, C.J. Costantino, A.J. Philippacopoulos, "High Soil/Structure Interaction Combined with Low Structural Damping", Proceedings, 7th SMIRT Conference, August 1983.
7. G.N. Bycroft, "Forced Vibrations of a Rigid Circular Plate on a Semi-Infinite Elastic Space and on an Elastic Structure", Philo. Trans., Royal Society of London, January 1956.
8. J.E. Luco, R.A. Westmann, "Dynamic Response of Circular Footings", Journal of Engineering Mech., ASCE, October 1971.

REFERENCES (Cont'd)

9. R.V. Whitman, "Soil-Structure Interaction Seismic Design for Nuclear Power Plant", MIT Press 1970.
10. J.J. Johnson, et al., "SSI Sensitivity Studies and Model Improvement for the USNRC Seismic Safety Margins Research Program", NUREG/CR-4018, November 1984.
11. J.E. Luco, "Impedance Functions for a Rigid Foundation on a Layered Medium", Nuclear Engineering and Design, Vol. 31.
12. R. Lung, "Dynamic Response of Combined Soil/Water Systems", Thesis submitted to CCNY, June 1976.
13. Y.O. Beredugo, M. Doval, "Coupled Horizontal and Rocking Vibration of Embedded Footings", Canadian Geotechnical Journal, 1972.
14. C.J. Costantino, E. Vey, "Response of Buried Cylinders Encased in Foam", Journal of Soil Mechanics, ASCE, September 1969.
15. Lysmer, et al., "FLUSH - A Computer Program for Approximate 3-D Analysis of Soil-Structure Interaction Problems", Report EERC 75-30, Univ. of California, 1975.
16. C.J. Costantino, C.A. Miller and L.A. Lufrano, "Mesh Size Criteria for Soil Amplification Studies", Proceedings, SMIRT 3 Conference, September 1975.
17. G. Wass, "Linear Two Dimensional Analysis of Soil Dynamic Problem in Semi-Infinite Layered Media", Thesis to Univ. of California, 1972.

Correlation of Fukushima Data with Lumped
Parameter Codes

Appendix A

CORRELATION OF FUKUSHIMA DATA WITH LUMPED PARAMETER CODES

1.0 INTRODUCTION

This Appendix describes the work performed on one of the tasks of the "Soil/Structure Interaction Verification" program. The objective of this program is to correlate the results of the standard SSI methods of analysis with measured SSI data. The methods of analysis considered on the program are: the lumped parameter SSI model, the finite element model, and the substructuring method. Potential data sources for making the correlations include: measurements taken at the Fukushima Nuclear Power Plant, the SIMQUAKE experiment performed to model the seismic response of nuclear power plant containment structures, and Department of Defense experiments performed to validate the response of missile launch facilities to nuclear weapon induced ground shock. This Appendix contains comparisons between the Fukushima measured data and predictions made using the lumped parameter methodology.

The Fukushima Nuclear Power Plant, located in Japan, was subjected to a large (magnitude 7.4) earthquake on June 12, 1978. Measurements were obtained from four accelerometers located in the free field and four accelerometers mounted on the structure. The objective of this study is to compare predictions made with the lumped parameter method of performing SSI calculations to actual measurements made on the Fukushima plant. Hopefully, these comparisons will lead to quantification of the magnitude of the uncertainties which exist in the lumped parameter method, and perhaps a resolution of some of the uncertainties.

The lumped parameter method is based upon a finite element model of the structure coupled to the free field with springs and dampers intended to represent the interaction process. The free field motion is input to the base of the spring/damper interaction model. There are two major areas of uncertainty which arise in the use of the lumped parameter method to solve soil/structure interaction problems. The first is concerned with the numerical values to be assigned to the springs and dampers used to couple the

structure to the soil. Spring-damper models are used to represent the interaction process between the soil and the base of the structure and between the soil and the sidewalls of the structure (if it is embedded in the soil). The second area of uncertainty is concerned with the scattering of the free field seismic motion to be used as input to the model by the structure. The lumped parameter method neglects any such scattering from the structure to the free field and uses as input the free field motion which would be expected at the site if the structure were not there. Each of these areas is considered.

Application of the lumped parameter method to real problems often requires the calculation of a consistent set of free field time histories. For example, if the free field criteria motion is given at the surface, a calculation must be made to determine the free field motion at the elevation of the structure's foundation. This is done based upon a model which assumes that the free field disturbance originates in the bedrock and propagates as vertically traveling shear waves up to the surface of the site. Convolution methods are used to make the calculations with the soil modeled as a linear elastic material having hysteretic damping. An iterative solution is often used with the soil properties determined based on an average soil strain.

Two computer codes are used to perform these studies. SIM Code (Ref. 1) is used to perform the lumped parameter SSI calculations, and SLAVE Code (Ref. 2) is used to calculate free field motion at any location in the site given a measured motion at one location and the soil properties. It should be emphasized, however, that these codes are typical of those used by the industry. It should be expected that conclusions drawn from this study are applicable to any lumped parameter code.

The Fukushima plant and actual measurements taken are described in Section 2.0. The free field computations performed with SLAVE Code are discussed in Section 3.0 with Section 4.0 containing a description of the SIM Code results. The conclusions of the study are given in Section 5.0

2.0 DESCRIPTION OF FUKUSHIMA DATA

This section of the report contains a description of the Fukushima Nuclear Power Plant and the measurements taken during the Miyagiken-Oki earthquake. The Fukushima nuclear power plant is first described. The June 12, 1978 earthquake is then discussed including a description of the accelerograms collected during the earthquake. Prior studies performed using this data are also discussed.

2.1 Fukushima Power Plant

The Fukushima Power Plant contains two BWR reactors each having a generating capacity of 460 MWe. The station is located on the coastline in northern Honshu about 100 km south of Sendai, Japan. The plant was completed in 1970 and began commercial operation in 1971.

The reactor building is founded on mudstone and is embedded in the soil about 14 meters as shown in Fig. A.1. The reactor building is located adjacent to the turbine and rad-waste buildings but is structurally isolated from them. The soil properties (Ref. 3) indicate shear wave velocities varying from 180 mps at the surface to 530 mps at depths greater than 10 meters below the surface. The reported soil damping ratio is 10%. A detailed discussion of soil property data is contained in Section 3.0. While mudstone is a rock material, it is referred to as soil in this report because it has a shear wave velocity close to a stiff sand.

The reactor building is about 40 meters square in plan and has an overall height of about 59 meters. The structure is reinforced concrete up to the level of the operating floor, and steel frame from the operating floor to the roof. The operating floor is 43 meters above the base of the foundation slab. The foundation slab has a thickness of about 2.8 meters with much thicker sections around the reactor cavity. The plan dimensions of the building are reduced to 30 meters by 40 meters at elevations more than 30 meters above the foundation level. The total weight of the structure and equipment is about 67,000 tons. A more complete description of this structure is given in Section 4.2 when the lumped parameter structural model is described.

2.2 Measured Seismic Data

The Miyagiken-Oki earthquake occurred on June 12, 1978. No damage was reported at the plant. There was considerable structural damage reported around Sendai which was close to the epicenter of the earthquake. The earthquake had a magnitude of 7.4 as measured on the Richter scale.

The plant had eight moving coil type accelerometers, four located in the soil and four in the structure. Data from these gages was obtained on a magnetic tape from Dr. Hiroshi Tanaka of the Nuclear Power Research and Development Institute of Japan. The four located on the structure are shown in Fig. A.1. Four located in the free field as shown in Fig. A.3. Three of the free field instruments were under the centerline of the reactor building: directly under the basemat (Elev. -4 M); Elev. -14 M; and Elev. -40 M. The fourth measurement was taken at the level of the foundation but 55 meters east of the centerline of the reactor building. All measurements were made for the north-south component of motion (parallel to the long axis of the turbine building). A complete discussion of the free field measurements is given in Section 3.0. The time histories for the four free field measurements are shown of Figs. A.4 through A.7. Response spectra (2% damping) for these measured responses are shown on Figs. A.8 through A.11. A comparison of the -14 M and -40 M spectra show the motions to be quite similar for frequencies above 5 cps. The -14 M spectra has a significant peak at 2.6 cps which is not evident in the spectra for the motion at the deeper depth. The spectra for the motion at the basemat level shows that the 2.6 cps response has been amplified (0.63 G's at the basemat and 0.44 G's at a depth of 33 feet). Note that the 2.6 cps spectral peak for the measurement taken to the side of the structure is 0.40 G's. This increase of the 2.6 cps spectral peak in the vicinity of the structure is probably caused by the soil/structure interaction frequencies as discussed below. The spectral peaks at frequencies above 5 cps are damped out in the surface spectra (0.37 G's at 5 cps for the 33 feet deep measurement and 0.24 G's for the same frequency at the surface). The surface measurement taken to the side of the structure has a spectral peak of 0.27 G's at 5 cps.

The four measurements made in the structure are taken at: the basemat (Elev. -1.2 M); Elev. 25.9 M; at the operating floor (Elev. 38.9 M); and at the top of the structure (Elev. 54.9 M). Spectra (2%) for these measured accelerograms are shown on Fig. A.2. The first three are in the concrete portion of the structure while the third is at the top of the steel structure. The peak measured accelerations (ZPA) are: 0.08 G's, 0.14 G's, 0.20 G's, and 0.60 G's respectively from the bottom measurement to the top. The free field ZPA at the foundation level is about 0.09 G's. These data indicate that there is significant rocking interaction since the peaks increase from 0.09 G's at the foundation to 0.60 G's at the roof. The free field spectra directly under the basemat is very close to the basemat spectra indicating that the soil in the immediate vicinity of the structure moves with the structure. The structural spectra have significant peaks at 2.6 cps, 3.5 cps, 4.8 cps, and 11 cps. Spectral values at these peaks are given on Table 2.1.

Table 2.1
Peak Measured Spectral Accelerations (G's)

Frequency (cps)	Free Field Locations		Structural Locations	
	To Side	Under Basemat	Basemat	Operating Floor
2.0	0.18	0.40	0.40	0.60
2.6	0.40	0.60	0.72	1.30
3.5	0.33	0.36	0.40	1.70
4.8	0.26	0.24	0.26	0.40
11.0	0.22	0.22	0.22	0.25
ZPA	0.07	0.08	0.09	0.20

A comparison of the basemat peaks with the free field peaks demonstrate that the basemat has the same motion as the free field near to the structure. These peaks are amplified relative to the free field to the side of the structure for frequencies below 3.5 cps with essentially no amplification above this frequency. In Section 4.2 the coupled interaction frequencies are shown to be 3.6 cps and 11.0 cps. For a system having these frequencies one

would expect amplifications of spectral peaks for frequencies below 3.6 cps with little amplification of the peaks at the higher frequencies. This would indicate that the interaction springs, upon which the interaction frequencies are based, are consistent with the measured data. The higher amplification of the operating floor peaks indicate that rocking motion of the structure is significant. Note that there is a much higher amplification of the 3.5 cps peak. This is one of the interaction frequencies and it is more associated with rocking of the plant than with translational motion.

2.3 Prior Studies of Fukushima Data

Tanaka and Nakahara (Ref. 3) have performed an analysis of the Fukushima data. Their model consisted of lumped mass cantilever models for the structure and the soil. The structure was modeled with two beams; one represented the inner walls and one the outer walls. The soil was modeled with five shear beams representing the distant soil, intermediate soil, near soil, adjacent soil, and soil under the structure. Soil masses were lumped at nodes in the shear beam with springs used between nodes to represent the soil stiffnesses. The nodes of the soil columns were tied together with springs. The embedded nodes on the structure were tied to the adjacent soil column nodes to model the horizontal interaction forces. Rocking springs and dampers were used to tie the foundation to the Elev. -40 M depth level. The soil columns extended down to Elev. -40 M.

The first five modes of the combined soil/structure system were found to have frequencies of: 2.5 cps; 3.1 cps; 3.9 cps; 4.8 cps; and 5.5 cps. The first, third, and fifth modes were found to have the largest participation factors. The mode shapes show that the first mode involved shear deformations of the free field and rocking motion of the structure. The third and fifth mode involved cantilever deformations of the steel portion of the structure.

The measured motion at Elev. -40 M was then input to the base of the soil. Response spectra were generated for the motion at points in the structure where the measured responses were taken. The calculated response

spectra were compared to the measured spectra. The computed spectra generally agree with the measured spectra. There is some disagreement above 4 cps with the disagreement becoming more pronounced for higher frequencies and for higher locations in the structure.

Muto and Omatsuzawa (Ref. 4) performed a study of the response of this plant to an earthquake which occurred on May 26, 1970. This earthquake was of much smaller magnitude. The basemat free field ZPA was 0.01 G's. A lumped parameter model of the structure was tied to the free field with interaction springs and dampers. Data is not available describing these parameters. The first five modes of the combined structure/interaction element system was found to have frequencies of: 4 cps; 5.5 cps; 11.2 cps; 13.0 cps; and 19.6 cps. The measured acceleration at the basemat was used as input. Comparisons were made between spectra for the measured and calculated responses. Good agreement was noted. Once again the agreement was better at the lower frequencies and the lower locations in the structure. The spectra of the input motion indicated that the primary frequency content of the input was about 10 cps.

3.0 FREE FIELD STUDIES

This section of the report presents the results of convolution analyses performed with SLAVE Code, the purpose of which is to develop free field time histories to be used as input to the structural analysis phase of the study (with SIM Code). As is described in the following section, the input required to SIM Code is the motion time history (accelerogram) which would have developed at the elevation of the structural foundation, assuming that the reactor structure were not present. This (fictitious) computed accelerogram is therefore only controlled by the constitutive properties of the soil/rock of the foundation as well as the known parameters of the accelerogram measured at some deeper depth in the foundation. In this section, only horizontal motion studies are considered.

The analysis performed in SLAVE Code is the exact deconvolution analysis for a horizontal accelerogram input to a horizontally bedded soil/rock system at a given elevation. The output of the calculation is the corresponding horizontal accelerogram developed at any other desired elevation, assuming that the motions developed in the rock free field is caused by vertically propagating shear waves. In the deconvolution analysis, the soil/rock overburden is represented as a vertical column (linear shear beam) to which the specified criteria motion is input. For this study, the criteria input motion is the known Fukushima horizontal accelerogram measured at elevation -40 meters. The output in each case is the calculated accelerograms at elevations -14 and -4 meters, at which elevations recorded spectra are available. The -4 meter elevation corresponds to the elevation of the foundation of the reactor building. The accelerogram computed at this elevation is then used as input to SIM Code, from which structural responses are calculated.

3.1 SLAVE Code Analysis

In SLAVE Code, Fourier transform methods of analysis are used. A linear spring-dashpot representation for the material constitutive law is assumed, wherein the spring coefficient represents the stiffness of the soil/rock, and the damping coefficient represents any nonlinear dissipation which would occur in the material during cyclic loadings.

SLAVE Code can be used in one of two ways. Firstly, the stiffness and damping data of all the soil/rock layers can be input and the desired responses generated. Alternatively, if laboratory data for the material is available as a function of peak shear strain (from say, resonant column testing), SLAVE Code can be run in an iterative manner so as to generate the proper stiffness/damping parameters for a particular problem. After each cycle, the peak shear strain in each soil layer is computed that will be developed by the input accelerogram. The first approach is used in this study, since no strain variation data is available for the rock at the site.

If the criteria motion input to SLAVE Code is an acceleration pulse, the first step in the analysis is to decompose the time history into its Fourier component, as

$$\ddot{y}_n(t) = \sum_{n=1}^N C_n \sin \omega_n(t+t_n) \quad (3.1)$$

where C_n is the magnitude of the mode components of the pulse and t_n is the modal phase time. The modal circular frequency is given by

$$\omega_n = 2\pi n/T \quad (3.2)$$

where T is the total duration of the specified pulse. In SLAVE Code, the maximum frequency content of the pulse is determined such that at least 8 time points of the pulse can be utilized in any one cycle at the highest frequency. Therefore

$$\omega_N = 2\pi/(8\Delta t) \quad (3.3)$$

where Δt is the specified time increment of the criteria pulse and ω_N is the

highest circular frequency considered. Higher frequencies than those specified by equation 3.3 will lead to significant errors in the computation. The maximum number of mode components used in the deconvolution analysis is then given by

$$N = T/(8\Delta t) \quad (3.4)$$

Thus, if an input accelerogram has a 20 second duration with a 10 millisecond time increment (as is typically the case), the number of modes used in the analysis would be restricted to 250, with frequencies varying from 0.05 cps to 12.5 cps, in increment of 0.05 cps. Computations at higher frequencies would be in serious error.

The soil system is considered to be a vertical soil column composed of an arbitrary number of uniform damped/elastic soil layers. Each soil layer is assumed to behave in a linear fashion, with all actual nonlinearities "lumped" into an equivalent damping term. For each layer, the shear stress-shear strain relation is written as

$$\tau = G\gamma + n\dot{\gamma} \quad (3.5)$$

where τ is the shear stress, γ the shear strain, $\dot{\gamma}$ the corresponding shear strain rate, G the shear modulus, and n the viscosity coefficient. Each layer is assumed to possess constant properties G , n , and ρ , where ρ is the mass density of the material. Substituting the constitutive law of equation 3.5 into the shear wave equation leads to a second order linear differential equation at each modal frequency for each soil layer. Satisfying the interface conditions between each layer and the ground surface leads to the development of a linear set of algebraic equations which can be easily solved; that is, given the modal input at one location, the corresponding modal output at any other location in the soil/rock column can be determined. Combining the results at each frequency leads to a time history (accelerogram) at any output station in the column.

As mentioned above in equation 3.5, each soil material in the column is modeled as a linear material with both shear stiffness and damping properties specified. This linear relation has been found adequate for typical seismic problems, provided that the damping parameter is interpreted as representing the nonlinear hysteretic behavior of the soil under cyclic loadings, as found from resonant column testing for example. The energy lost per cycle of loading due to nonlinear soil behavior is measured by the hysteretic damping ratio, D , which has been found experimentally to be essentially independent of frequency. If the measured energy loss per cycle is equated to the corresponding loss due to the viscous term in equation 3.5, the hysteretic damping ratio is found to be related to the viscosity coefficient by

$$D = \eta \omega / 2G \quad (3.6)$$

where D is the hysteretic damping ratio, and ω is the circular frequency.

3.2 Site Description

A general description of the site is presented in Ref. 3, and is shown in Fig. A.3. The entire soil overburden was initially removed from the site at the time of the site preparation, leaving the current elevation of the ground surface at 10 meters above sea level. The reactor building is thus founded in a mudstone rock to a depth of 14 meters, the average properties of which are specified as follows:

Shear Wave Speed:	530 mps
Compressive Wave Speed:	1700-1740 mps
Shear Modulus:	8590 ksf
Poisson's Ratio:	0.42
Unit Weight:	106 pcf

No specific information is presented in Ref. 3 concerning the tests that were performed to obtain this data, nor the variation of these properties with depth. Below the mudstone, at a depth of 160 meters is a sandstone basement

rock. The only specific information available for this material is the compressional wave speed listed in Fig. A.3.

A series of free field accelerometers were located at the site, four of which are shown in Fig. A.3. These were used to measure the horizontal motions developed during the 1978 earthquake. The digitized records are used in this study and compared with the analytical computations performed with SLAVE Code. The measured time histories from these four gages are shown in Figs. A.4 through A.7. As may be noted from these records, the period of primary energy input is the first 30 seconds of the pulse, followed by a quiescent period of 30 seconds. The corresponding response spectra for these records are shown in Figs. A.8 through A.11. In each case, the criteria spectrum obtained from Reg. Guide 1.60 is also shown for comparison purposes. The criteria spectra are scaled to the peak measured accelerations (ZPA) from each gage. In each case, it may be noted that the criteria or "design" spectra exceed the measured data over a significant frequency range, except for specific frequencies. This exceedance is within the one sigma limit upon which the Reg. Guide criteria is based so that the exceedance may not be significant. The following analysis shows that these frequencies are associated with the soil column.

It may be shown that the frequencies associated with a vertically propagating shear wave in a material having a shear velocity of V_s and a length L is,

$$f_n = V_s (2n-1)/(4L) \quad (3.7)$$

where n is the wave number. Therefore the first 4 shear column frequencies are: 0.8 cps; 2.4 cps; 3.9 cps; and 5.5 cps. These correspond to the frequencies at which the measured spectra exceed the Reg. Guide spectra. One may conclude that the Reg. Guide criteria should include amplifications at frequencies corresponding to the site frequencies.

A comparison of the measured spectra for three gages immediately below the RB is shown in Fig. A.12. As may be noted, the highest response was measured at the -4m gage immediately below the RB foundation slab. The peak spectral values occur at a frequency of 2.6 cps, and this peak is not in the

-40m record. A comparison of the two records measured at the -4m elevation, one at the side and one underneath the foundation slab, is presented in Fig. A.13. Again both these pulses have peak spectral values at 2.6 cps, although the spectra immediately below the foundation slab indicates higher response throughout the frequency range than the record to the side.

3.3 Analytic Comparisons

As mentioned in Section 3.1, SLAVE Code is used to generate a corresponding horizontal free field pulse, assuming that no structure existed at the site. This analysis further assumes that the horizontal motion that would have developed at the ground surface is derived primarily from vertically propagating shear waves. Theoretically, if the measured motion at -40m elevation were used as input to the soil column, the corresponding motion that would develop at -4m could be determined. The one remaining rock property that is required for this computation is the hysteretic damping ratio for which no firm data is available. A series of calculations were therefore performed varying the hysteretic rock damping from 2 percent to 20 percent. Pulses are generated at elevations -4 M, -14 M, and -25 M using the measured -40 M pulse at input. Spectra of these pulses are shown in Figs. A.14 through A.19 for soil damping ratios of 2%, 5%, 7%, 10%, 15%, and 20% respectively. The variation of spectra with depth can be seen in each of these figures. At low values of damping, two narrow banded column frequencies can be noted, one at 2.6 hz and one at about 7.8 hz. As rock damping is increased this higher frequency essentially disappears, being smeared over a wider frequency band. Note that the peak spectral acceleration at 2.6 cps for the -4 M spectra (Basemat location) decreases dramatically as the soil damping is increased. The peak is 2.8 G's for 2% soil damping, 1.0 G's for 10% soil damping, and 0.7 G's for 20% soil damping. It may also be observed that double peaks occur at 2.6 cps and 3.1 cps for low soil damping. After 7% soil damping these double peaks coalesce into a single peak at about 3.0 cps. Since these are the pulses to be used as input to the interaction model, it is clear that the actual soil damping is an important parameter.

A comparison between the computed and measured spectra at elevation -4m is shown in Figs. A.20 and A.21. Again, at the low damping values, the computed spectra are very much higher at the soil column frequencies than the measured spectra. The differences are not as great at the higher damping values. A similar comparison with the measured record at the side of the RB Figs. A.22 and A.23 leads to a similar conclusion, with however, not as good a correlation. For all of these comparisons it may be noted that the correlation between the spectra of the measured and calculated pulses is poor at the soil column frequency of 2.6 cps. This would indicate that the hysteretic soil damping model used in the analysis may not be adequate. There is apparently more energy being dissipated at this frequency than can be accounted for with the linear damping model.

4.0 LUMPED PARAMETER ANALYSIS OF FUKUSHIMA DATA

Lumped parameter models are most often used to perform seismic response calculations for nuclear power plant structures. These methods couple a structural model to the free field with springs and dampers used to represent the soil/structure interaction effects. The interaction forces are then proportional to the relative displacements and velocities between the structure and the free field. The free field motion is taken to be the motion which would occur in the free field if the structure were not there. This assumes that any modification of the input motion due to feedback from the structure to the free field is negligible. The validity of this assumption is one of the major uncertainties in the lumped parameter approach.

The other uncertainties in the method are centered around the values used for the spring/damper models of the interaction process. Two sets of springs/dampers are used. One represents interaction forces acting on the base of the structure and the second models the interaction forces which act on the side-wall of the structure if it is embedded in the soil. The equations used to calculate values for each of these models are based on analytic solutions for steady state vibrations of rigid foundations resting in an elastic homogeneous half space. The analytic solutions give equivalent springs and dampers which

depend on properties of the media, geometry of the foundation, and the frequency of vibration. An average frequency is assumed to obtain the frequency independent interaction parameters used in the lumped parameter method. The validity of this approach therefore depends on whether: frequency independent parameters are acceptable; the elastic homogeneous model of soil is acceptable; and nonlinear effects such as separation of soil and foundation occur.

The objective of this study is to analyze the Fukushima data using the lumped parameter method and to compare the measured data with the calculated data. The computer code (SIM) used to perform these analyses is discussed in Section 4.1. The model of the plant and interaction parameters is developed in Section 4.2, and the numerical results are given in Section 4.3. The free field inputs are developed in Section 3.0.

4.1 SIM Code

SIM Code (Ref. 1) is used to perform all of the lumped parameter calculations. This code has been extensively used to perform seismic response calculations for nuclear power plant structures. Earlier versions of the code (Ref. 5) were used to calculate the response of missile launch facilities to ground shock loading. Computations made with SIM Code will give the same results as similar calculations made with any of the other lumped parameter codes in routine use by the industry. Conclusions drawn from this study are therefore generic to the lumped parameter method and not specific to the SIM Code.

Two alternative methods of analysis are available in SIM Code. For the first, the structure is modeled with its free-free modes of vibration. The interaction forces are treated as forces acting on the free-free model of the structure. The modal equations of motion are numerically integrated with the interaction forces transformed to modal loads at each time step in the integration. This approach has an advantage in the treatment of damping effects. Structural damping is usually rather low (2-7%) while interaction damping is often high (on the order of 50%). With this approach the modal damping is

the structural damping with the interaction damping becoming part of the load applied to the free-free structure. The second method is based on the system modes of vibration of the structure which include the spring/damper models of the interaction process. The seismic disturbance is used as input to the model. One now must use some composite damping to represent an average modal damping which includes the effects of the low structural damping and the high interaction damping. For either method the modal equations are numerically integrated in the time domain using a fourth order Runge-Kutta scheme. After the solution is completed floor response spectra are generated at selected locations.

The structure is modeled with beams including both flexural and shear deformations. The geometry of the structure may be specified in three dimensions. The user has the option of allowing response in all three directions or restricting the response to one dimension. The structural modes of vibration are calculated using a power method and include rigid body modes for the free-free structural model discussed above. Three types of damping are permitted. The first is proportional damping where the damping matrix is made proportional to the stiffness and mass matrices so that the specified damping ratio (percent of critical damping) occurs for the first two modes. Damping ratios for the higher modes are then calculated, and are usually found to be close to the specified value. The second type of damping allows the user to specify the damping ratio for each mode. The third type is composite damping, wherein the user specifies the damping ratio for each element in the model. An average (composite) damping ratio for each mode is then determined based on the modal deformation of each element. The elements which have the largest deformation (expressed in terms of strain energy) have the most influence in setting the modal damping.

The interaction model is divided into two parts, one representing interaction effects at the base of the structure and the other representing sidewall effects. For each of these the user has the option of using a standard set of equations or independently setting the values. The standard equations are given in detail in the following section. Use of the standard equations requires the specification of soil parameters.

4.2 Fukushima Model

The lumped parameter model used to describe the Fukushima plant is described in this section. The models used for the structure and for the interaction parameters are presented. Solutions are obtained using both the free-free and fixed base approaches available in SIM Code. The differences in modeling for each are presented.

The reactor containment building is shown in Fig. A.24b. Since all of the measured data is in the North-South direction, the model of interest will be for structural displacements in this direction and for rotations about the East-West axis. A section through the center of the reactor building looking in the North direction is shown on Fig. A.24a. The model of the structure is shown on Fig. A.24b with node numbers as indicated and element numbers shown circled. Each node has two degrees of freedom, a displacement out of the page in the X direction (N-S motion) and a rotation about the Y axis (E-W axis). The same model is used for both the free-free and fixed base models. The base interaction forces are applied to node 1. The sidewall interaction forces are applied to nodes 1, 2 and 3 for the free-free model while equivalent sidewall forces are applied to node 1 for the fixed base model.

Each of the elements is modeled as a beam including both flexural and shear stiffnesses. The four vertical beams (A,B,C,D,E) represent the sections of the structure as shown on Fig. A.24a. The outer structure is represented with beams A, D and E. Beam B models the structure around the reactor while the reactor itself is modeled with Beam C. The portion of the structure below the operating floor is reinforced concrete and the beam cross section properties are calculated directly from the structural plans. The upper portion of the structure is a steel truss. Models of the steel truss structure are analyzed with the SAPV (Ref. 6) computer code. Unit loads acting in the X direction are placed on the truss and deformations determined. These data are then used to determine equivalent beam properties. The concrete has a Young's Modulus of 3300 ksi and Poisson's Ratio of 0.17. The steel has a Young's Modulus of 29,900 ksi and a Poisson's Ratio of 0.33. Steel member damping is taken to be 2% of critical and concrete member damping is 5% of critical.

Masses are lumped directly at the nodes. Structural weight is divided half to each of the member end nodes. The equipment weight acting on each floor is available, and is distributed equally to the nodes located on the floor. The total weight of the structure and equipment is 133,870 kips, about 10% of which is equipment. The center of gravity is located 64.5 feet above the base (one third of the height) and 1.7 feet to the west of the centerline of the reactor (1% of the basemat width).

The soil/structure interaction models are divided into two parts. One for interaction forces acting on the basemat and one for sidewall interaction. The basemat interaction model is identical for both the free-free and the fixed base models. The basemat interaction forces are applied to node 1. These forces (load in the X direction and moment about the Y axis) are calculated as the interaction spring times the relative displacement of node 1 and the input motion plus the interaction damper times the relative velocity of node 1 and the input disturbance. The model then requires four parameters; the horizontal spring and damper; and the moment spring and damper. The equations used to calculate these parameters are taken from Ref. 7 and are discussed in detail in the main body of the report. The soil properties used for these computations are:

Shear modulus = 8590 ksf = G

Poisson's ratio = 0.42 = μ

Unit weight = 0.106 k/cu.ft.

Resulting shear wave velocity = 1615 fps

The horizontal spring is calculated from,

$$K_H = 4(1 + \mu) B_x K_{1x} G \sqrt{cd}$$

$$K_H = 4(1 + 0.42) (0.9) (0.97) (8590) \sqrt{66.54 \times 66.54}$$

$$K_H = 2.834 \times 10^6 \text{ kips/ft}$$

The moment spring is given as,

$$K_{\theta} = 8G B_{\theta} K_{1\theta} cd^2/(1-\mu)$$

$$K_{\theta} = 8 (8590)(0.5)(0.86)(66.54)^3/(1-0.42)$$

$$K_{\theta} = 1.501 \times 10^{10} \text{ kip ft}$$

The percent of critical damping for horizontal damping is,

$$\beta_H = \frac{50 C_{1x} r_o^{1.5}}{V_s} \left[\frac{32(1-\mu)G}{(7-8\mu)K_{1x}M} \right]^{1/2}$$

$$\beta_H = \frac{50(0.58)(75.08)}{1615}^{1.5} \left[\frac{32(1-.42)8590}{(7-8 \times .42)(.97)(4157.4)} \right]^{1/2} = 38.5\%$$

The percent of critical damping for rocking motion is ,

$$\beta_{\theta} = \frac{50 C_{1\theta} r_o^{2.5}}{V_s} \left[\frac{8G}{3(1-\mu)K_{1\theta}I_{\theta}} \right]^{1/2} = 38.5\%$$

$$\beta_{\theta} = \frac{50(.12)(75.08)}{1615}^{2.5} \left[\frac{8(8590)}{3(1-.42)(.86)(2.794 \times 10^7)} \right]^{1/2} = 7.58\%$$

Different models are used for the sidewall interaction in the free-free and fixed base models. The fixed base sidewall interaction model is based on the work of Beredugo and Novak (Ref. 8). The effects of sidewall interaction are converted to equivalent springs and dampers acting on the base of the structure and are then simply additive to the base interaction parameters. Their solution is an analytic solution of the steady state vibration of a rigid circular cylindrical structure contained in an elastic strip of the same depth as the length of the cylinder. The basic result obtained is the force and moment acting on the cylinder for a given displacement and rotation. These data are then used in the reference to obtain equivalent springs and dampers.

The resulting horizontal spring is,

$$\bar{K}_H = G_S r_o \delta S_{u1}$$

$$\bar{K}_H = 8590 (75.08) \frac{45.9}{75.08} 4.1 = 1.613 \times 10^6 \text{ kips/ft}$$

The moment spring is,

$$\bar{K}_\theta = G_S r_o^3 \delta \left[(S_{\phi 1} + i S_{\phi 2}) + (S_{u1} + i S_{u2}) \left(\frac{8^2}{3} - \frac{\delta Z i}{r_o} + \frac{Z i^2}{r_o^2} \right) \right]$$

$$\bar{K}_\theta = 6.672 \times 10^9 \text{ kip ft}$$

Because of the translation of sidewall effects to the base of the structure there is a coupling term relating interaction moment to displacement. This is given as,

$$\bar{K}_{\theta H} = G_S r_o^2 \delta \left[(S_{u1} + i S_{u2}) \left(\frac{8}{2} - \frac{Z_o}{r_o} \right) \right]$$

$$\bar{K}_{\theta H} = 3.694 \times 10^7 \text{ kip}$$

Note that the sidewall springs are smaller than the base springs. The horizontal base spring is 1.76 times the sidewall spring while the base moment spring is 2.25 times the sidewall spring. The Fukushima data can therefore not be expected to shed much light on the validity of the sidewall interaction model.

The sidewall translational damper is given as,

$$\bar{C}_H = G_S r_o \delta S_{u2}$$

$$= 8590 (75.08) \left(\frac{45.9}{75.08} \right) 10.6 = 4.17 \times 10^6 \text{ kip sec/ft}$$

This is 129.2% of critical

The moment damper is,

$$\overline{C}_{\theta H} = 4.47 \times 10^8 \text{ kip ft sec}$$

This is 51.8% of critical

The coupling damper is,

$$\overline{C}_{\theta H} = 6.18 \times 10^6 \text{ kip sec}$$

The sidewall interaction model used for the free-free computations is based on the results in Ref. 5. The sidewall interaction forces are computed from interaction pressures acting normal to the wall with the pressures given as,

$$\sigma_n = k(\Delta w) + s(\Delta \dot{w})$$

These pressures are then integrated around the wall to find the interaction forces. The sidewall forces are applied to nodes 1, 2, and 3. If one converts these parameters to equivalent base springs, the horizontal spring is $4.55 \times E + 06$ kips per foot and the moment spring is $3.29 \times E + 09$ kip feet. The comparable Beredugo and Novak values are $1.61 \times E + 06$ kips per foot and $6.672 \times E + 09$ kip feet. These differences represent an uncertainty in the lumped parameter method. Since the sidewall interaction is not very significant for the Fukushima plant one cannot expect to resolve these differences with this data.

Vibration characteristics of the model described above are discussed before performing the data analyses. If the structure is taken to be rigid, the coupled frequencies associated with the interaction springs may be determined. The coupled frequencies are 3.6 cps and 10.5 cps. The first frequency is undoubtedly the major frequency shown on the spectra for the measured pulses as indicated in Section 2.2.

The first system twelve modes (including the interaction springs) of the structure are shown on Figs. A.25 through A.27. As may be seen the frequencies range from 2.5 cps to 20.0 cps. Actually 15 modes were included in the analysis with the fifteenth mode having a frequency of 22.9 cps. The first mode is identical to that found by Tanaka (Ref. 3). It should be noted that significant interaction effects occur (there are significant displacements of node 1) for modes 1, 4, 7, 10, and 11. This model requires that composite modal damping values be calculated. The damping ratios for the twelve modes are: 0.17, 0.06, 0.06, 0.37, 0.05, 0.04, 0.11, 0.06, 0.06, 0.05, 0.07, and 0.05. As may be seen the modes with the larger damping ratios are associated with deformations of the interaction springs.

The first mode of the free-free model of the structure has a frequency of 4.2 cps and the fifteenth mode has a frequency of 31.4 cps. Since only structural damping is included in the modal damping for this model, all damping ratios are in the range from 0.02 to 0.05.

4.3 Numerical Results

The major uncertainties in the "lumped parameter" SSI methodology lie in the selection of the interaction parameters and in the form of the seismic disturbance to be used as an input to the model. There are two basic types of wave forms that are used. The first are measured data in the vicinity of the basemat of the structure and the second are derived from a convolution analysis where the measured deep motion (at Elev.-40 M) is propagated up through the soil to the basemat location (as described in Section 3.0). There are two measured wave forms which are used; one is directly under the basemat while the second is about 55 M east of the reactor building centerline. The wave forms resulting from the convolution analysis depend on soil property data and in particular the soil damping. Since reliable data for soil damping is not available, solutions are found for soil damping values of 10%, 15%, and 20% of critical.

For each set of input wave forms the interaction parameters are varied to obtain a "best" fit of the data. Solutions are first found with the standard interaction parameters as described in Section 4.2. The parameters are then varied to make the calculated response spectra fit the spectra of the measured data. The results of these comparisons are then used to assess the adequacy of the standard interaction parameters. Spectral comparisons are made at four locations: basemat; half way between the basemat and operating floor; operating floor; and the roof.

4.3.1 Comparisons Using Measured Input

Seismic free field motions were measured directly under the centerline of the basemat and about 55 M to the east at the same elevation as the basemat. Response spectra generated from these measured motions are shown on Figs. A.8 and A.9. As may be seen the pulse from directly beneath the basemat has a much higher content at 2.6 cps.

The pulse measured to the side of the facility is used as input to both the free-free and fixed base models. For both problems the interaction parameters are varied to obtain a "best" fit of the spectra of the measured in-structure motion. The standard interaction springs are found to give the better results with 50% and 75% of the standard interaction dampers giving the best results for the fixed base and free-free models respectively. The spectral comparisons of the in-structure motions are shown on Figs. A.28 and A.29 for the free-free and fixed base models. The fits are reasonable with the free-free model giving slightly better results than the fixed base model. The use of this pulse as input best represents the intent of the lumped parameter method in that it is the free field pulse which would exist at the foundation level if the structure were not there. One may therefore conclude that the interaction springs are adequate but that the standard interaction dampers are perhaps a little too large. This could result from the neglect of the frequency dependence for the damping parameters. The analytic solutions upon which the interaction damping parameters are based indicate damping values which are frequency dependent. The dampers start at 0 for 0 frequency and increase in magnitude with frequency. Some "typical" frequency is selected to obtain the frequency independent values used in the lumped parameter calculations. If the Fukushima problem was sensitive to lower frequencies then the standard dampers would be too high.

The pulse directly under the basemat is used as input to the fixed base model. Once again the interaction parameters are varied to obtain a "best" fit. The resulting spectra comparisons are shown on Fig. A.30. The standard interaction parameters for both the springs and dampers are used for this model. The comparisons are better than those obtained using the pulse to the side of the building. These comparisons indicate that the standard interaction parameters work reasonably well when the input from directly beneath the structure is used as input.

Sensitivity of the results are tested by varying the interaction parameters for this case. The operating floor is selected for the purposes of comparison. As may be seen from Fig. A.30 spectral peaks occur at 2.0, 2.6, and 3.3 cps. Table 4.1 shows the variation of these peaks as the interaction dampers are varied.

Table 4.1

Effect of Interaction Damping on Spectral Peaks

Damping (% of Standard)		Peak Spectral Acceleration (G')		
Horizontal	Rocking	at 2.0 cps	at 2.6 cps	at 3.3 cps
Measured Data		0.65	1.35	1.95
40	40	1.39	3.82	0.93
60	60	1.28	2.95	0.79
100	100	1.11	2.05	0.69
100	40	1.25	2.70	0.76
100	60	1.20	2.43	0.73

Since the frequencies of the peaks in the calculated spectra occur at somewhat lower frequencies than for the measured spectra (2.6 cps versus 3.4 cps), the interaction springs are varied in an attempt to obtain a better fit of the data. The differences are more pronounced at the higher levels in the structure than near the basemat. The horizontal displacement spring is therefore not varied but the rocking spring is increased by 160%. The resulting spectra are shown on Fig. A.31. As may be seen this has very little effect.

4.3.2 Comparisons Using Convoluted Pulses

As discussed in Section 3.0 convolution methods are used to generate a pulse at the basemat location from the measured pulse at the 40 meter depth. Pulses are generated based on soil damping values of 10%, 15%, and 20% of critical. The generated pulses at the basemat are used as input to the SIM Code. The fixed base model is used for all cases.

The "best" fit in-structure spectra for the 10%, 15%, and 20% pulses are shown on Figs. A.32, A.33, and A.34 respectively. The theoretical interaction springs are used for the model upon which these spectra are based. The interaction dampers are however 200%, 150%, and 100% of the theoretical dampers. It should be noted that the most probable soil damping is about 10%. Therefore extra damping is required in either the soil or the interaction model to develop a good fit of the measured in-structure spectra.

A comparison of the measured and calculated spectra using the theoretical interaction parameters and the likely soil damping (10%) is shown on Fig. A.35. As may be seen the calculated values are rather conservative. This overestimate of the spectra is most likely due to the convolution process as discussed in Section 3.3. It appears that the simple hysteretic soil damping model used in the convolution analyses underestimates the soil damping effects at the resonant soil column frequencies. Some of this difference could be due to feedback effects from the RB and other nearby structures such as the turbine building. The comparisons made here support the conclusion that the standard base interaction parameters are correct but that the use of the convolution analyses may lead to rather conservative results.

5.0 CONCLUSIONS

A large earthquake occurred at the Fukushima nuclear power plant in 1978. Four accelerometers were located in the free field and four in the reactor containment building. These data are used to verify the lumped parameter method of performing soil/structure interaction analyses.

The free field data were first studied. Spectra generated from the measured data were compared with the shape of spectra as specified in Reg. Guide 1.60. The deepest measured pulse (Elev.-40 M) is then used to generate consistent pulses at the locations of the other measured free field pulses.

The measured pulses at the basemat location are then input to a lumped parameter model of the reactor containment building. Reasonable comparisons are found between the spectra from the calculated in-structure responses and the measured in-structure response spectra. The basemat location free field pulses convoluted from the -40 M measured pulse are then used as input. Much larger interaction damping values are required with these pulses to obtain good agreement between the spectra from the measured and calculated responses.

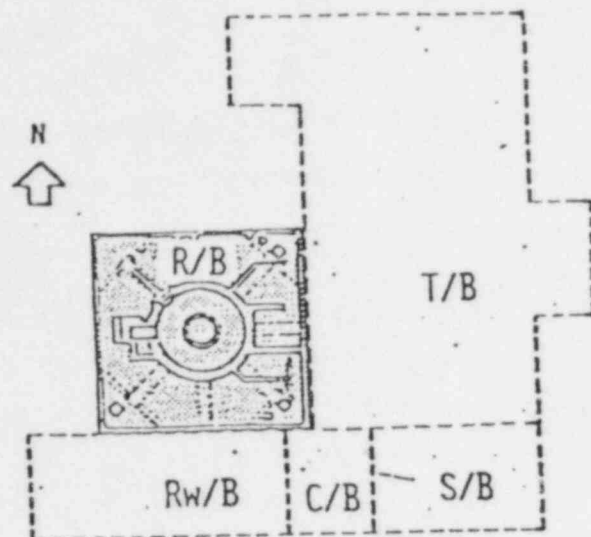
The following conclusions are drawn based on the results of these analyses:

1. Comparisons of the measured free field spectra with Reg. Guide 1.60 spectra (scaled to the measured ZPA) indicate that the Reg. Guide spectra envelop the measured spectra except at frequencies which correspond to the site soil column frequencies. For example, at 2.6 cps the Reg. Guide spectra at the -4 M elevation shows an acceleration of 0.4 G's while the measured acceleration is 0.6 G's. At -14 M elevation the difference is less (0.44 G's measured as compared to 0.39 G's criteria). The Reg. Guide criteria envelop one sigma of the measured data so that this exceedance may not be significant.

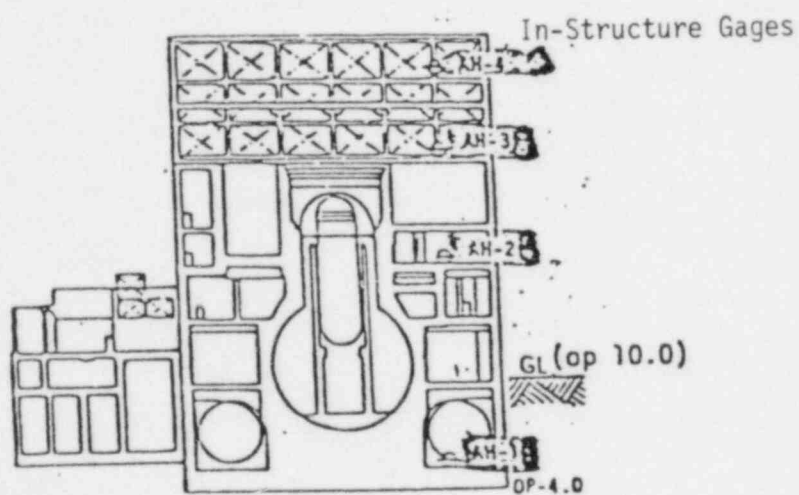
2. The concept of a vertically propagating shear wave, upon which the convolution methods are based, appears to be reasonable for sites such as Fukushima. Comparisons of spectra, for pulses generated from the -40 M elevation pulse, with measured pulses show good agreement in overall shape with some discrepancies in amplitude at soil column frequencies. The convoluted pulses result in larger amplitude spectral accelerations than the measured pulses. This would indicate that the hysteretic soil damping model used in the convolution analysis may not account for all of the damping which is present.
3. The general concepts of the lumped parameter soil/structure interaction method appear to adequately model the measured phenomena. The soil in the vicinity of the structure does move with the foundation of the structure. A comparison of the pulse at the -4 M elevation taken 55 M east of the structure to the basemat measured motion and the free field measured motion directly under the basemat supports this conclusion. A comparison of the amplifications which occur between these data also demonstrate that the basic concepts of the lumped parameter method are consistent with the data.
4. The standard methods of calculating the interaction springs and dampers give results which are compatible with the measured in-structure motions. The sidewall interaction parameters have a much smaller effect on the calculated results than do the base interaction parameters. These results therefore validate the base interaction parameters but not the sidewall parameters. The differences which are found between the measured and calculated spectra are attributable to the values of the interaction dampers. It may be that the use of frequency independent dampers should be re-evaluated. The theoretical solutions upon which the damper values are based indicate constantly increasing damping as the frequency of the response increases. If data from

another earthquake were available it could be used to further investigate this frequency dependence question. For example the lower magnitude earthquake reported in Ref. 4 had a higher frequency content than did the Miyagiken-Oki earthquake. If the interaction dampers were frequency dependent then one would expect the data from the lower magnitude earthquake to show larger damping effects.

5. Feedback effects from the reactor building do not appear to influence the free field or the building response calculations. It may be that the reactor building response would effect the response of the turbine building since the bearing pressure under the reactor building is larger than the bearing pressure under the turbine building. This question could be investigated if turbine building response data were available.

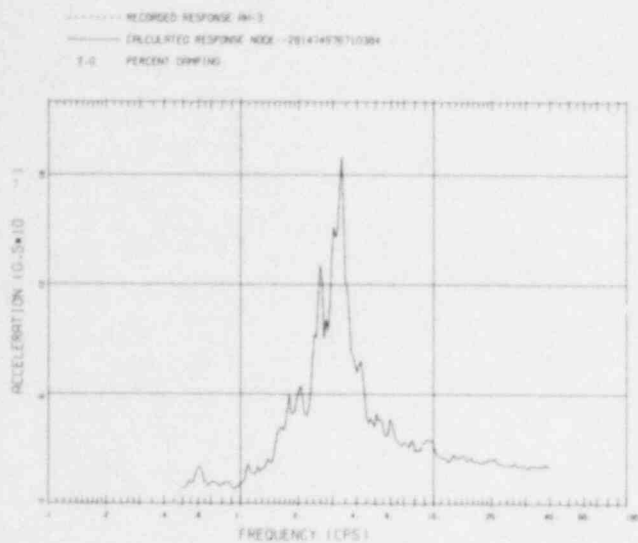


(a) BUILDING LAYOUT

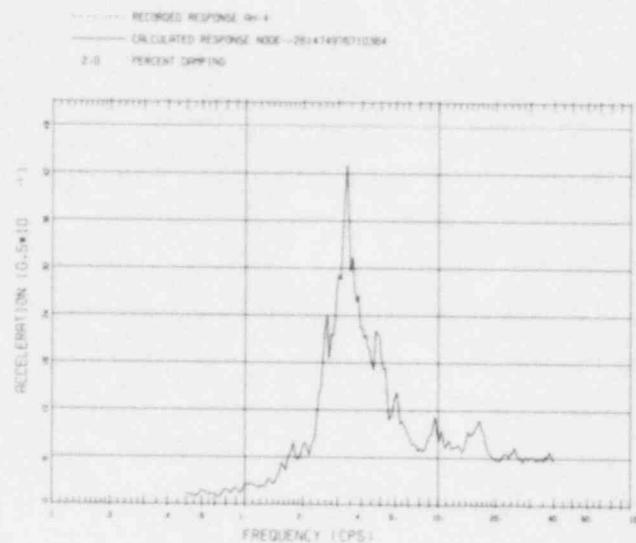


(b) N-S DIRECTION

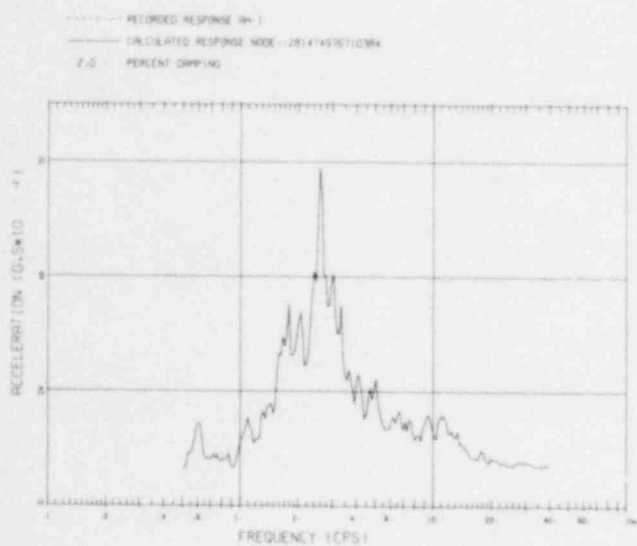
Fig. A.1 Fukushima Plant



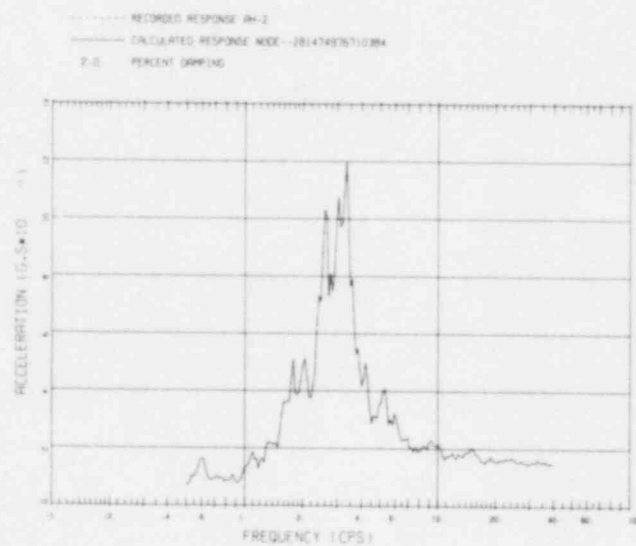
(c) Operating Floor



(d) Top of Structure



(a) Basemat



(b) Elev. 25.9 M

Fig. A.2 Spectra (2%) of Measured In-Structure Accelerograms

All Dimensions and
Elevations in Meters

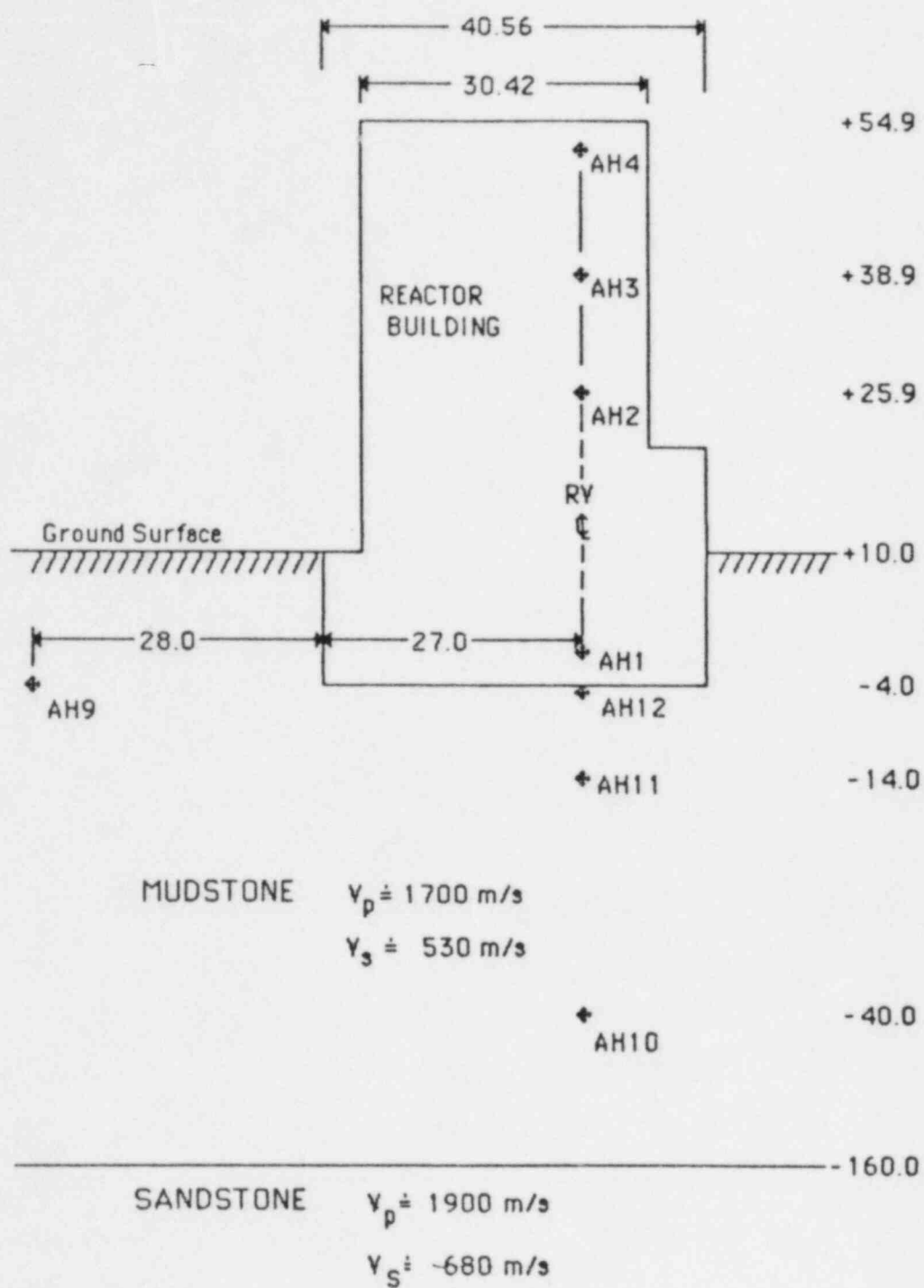


Fig. A.3 E-W Section of Reactor Building

Fig. A-4 -4M RECORDED SPECTRA UNDER REACTOR BUILDING

MEASURED FUKUSHIMA RECORD AT ELEV 1 (-4M), CL OF RB

NODE=1

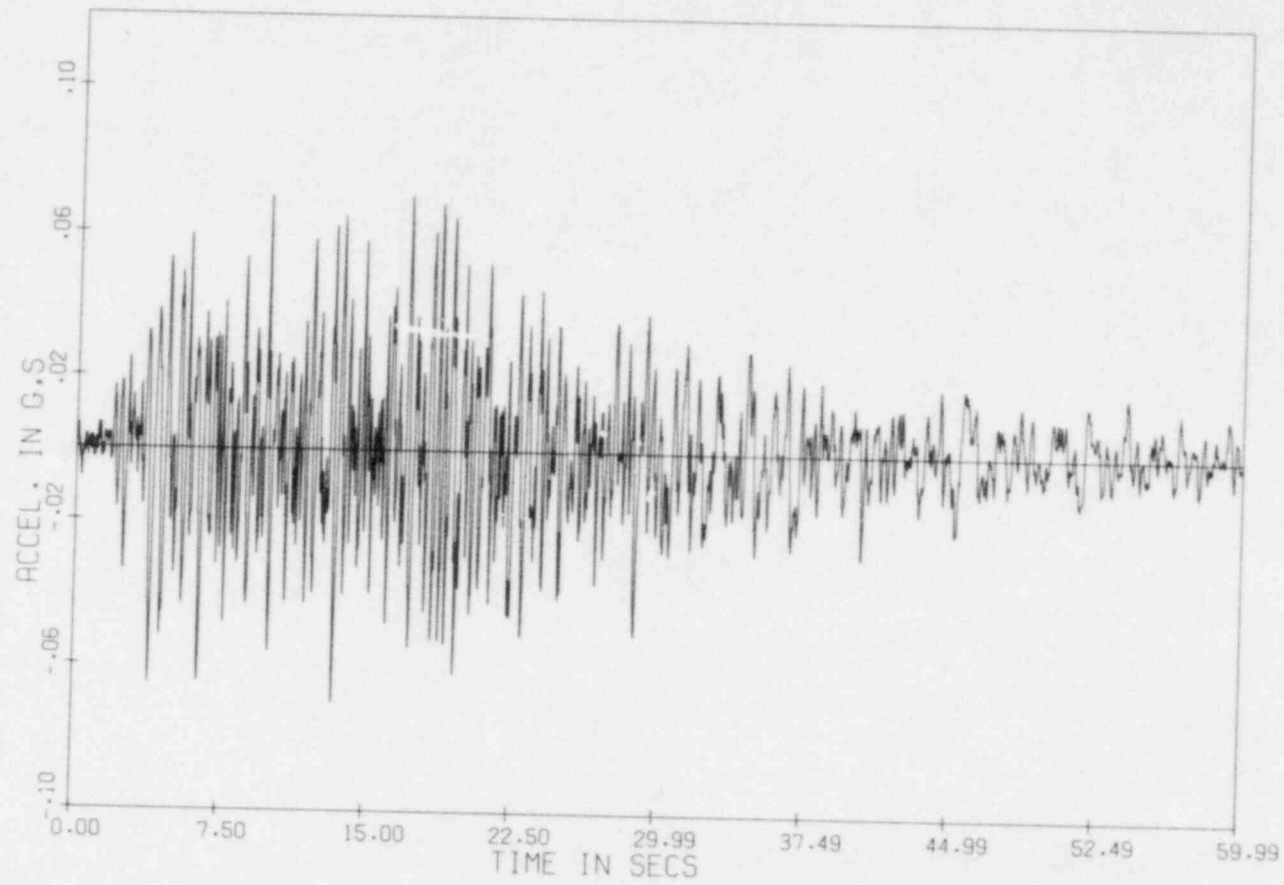


Fig. A.5 -4M RECORDED SPECTRA AT SIDE OF REACTOR BUILDING

MEASURED FUKUSHIMA RECORD AT ELEV 1 (-4M), SIDE OF RB

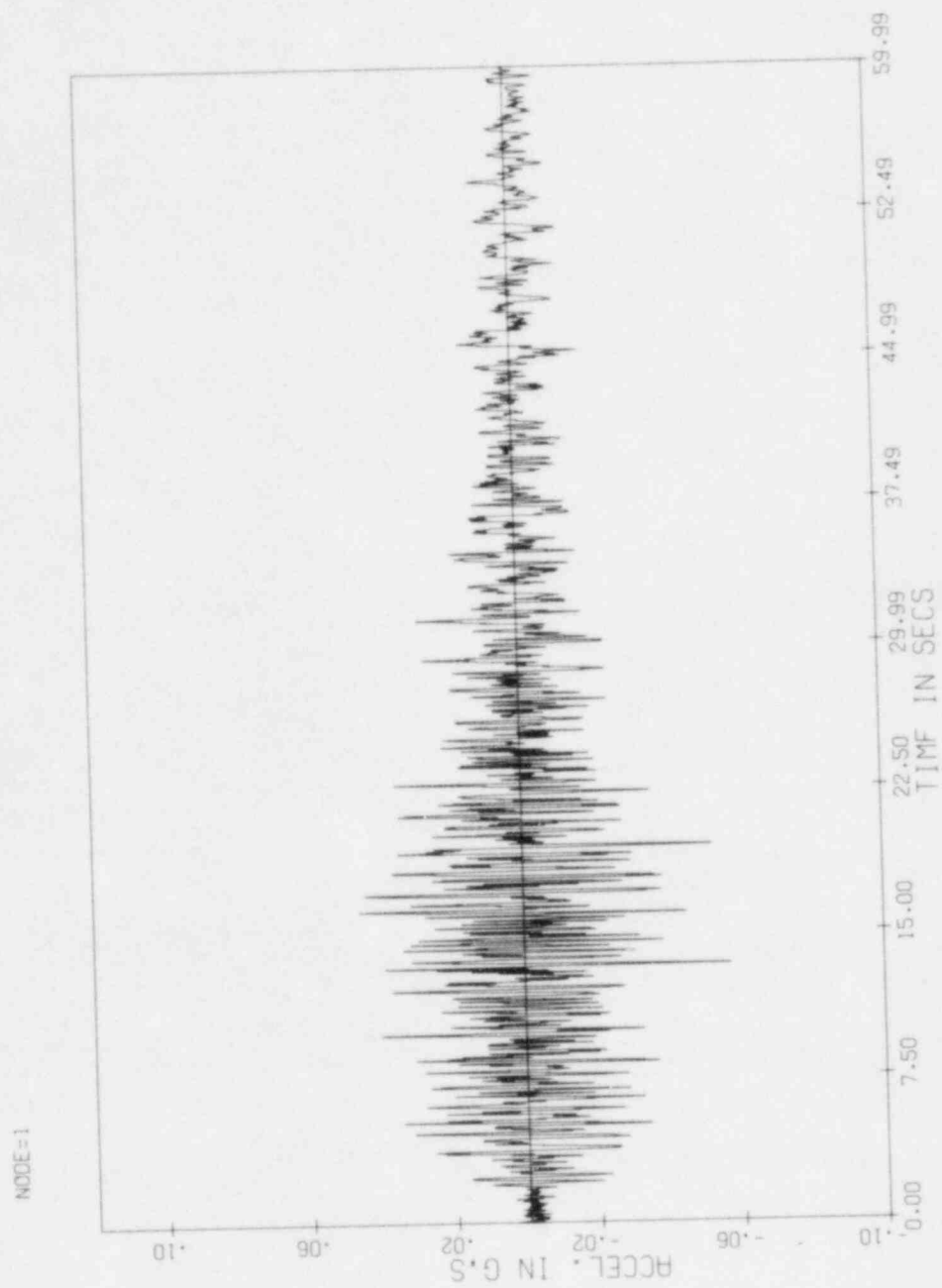


Fig. A.6 -14M RECORDED SPECTRA UNDER REACTOR BUILDING

MEASURED FUKUSHIMA RECORD AT ELEV 2 (-14M), CL OF RB

NODE=1

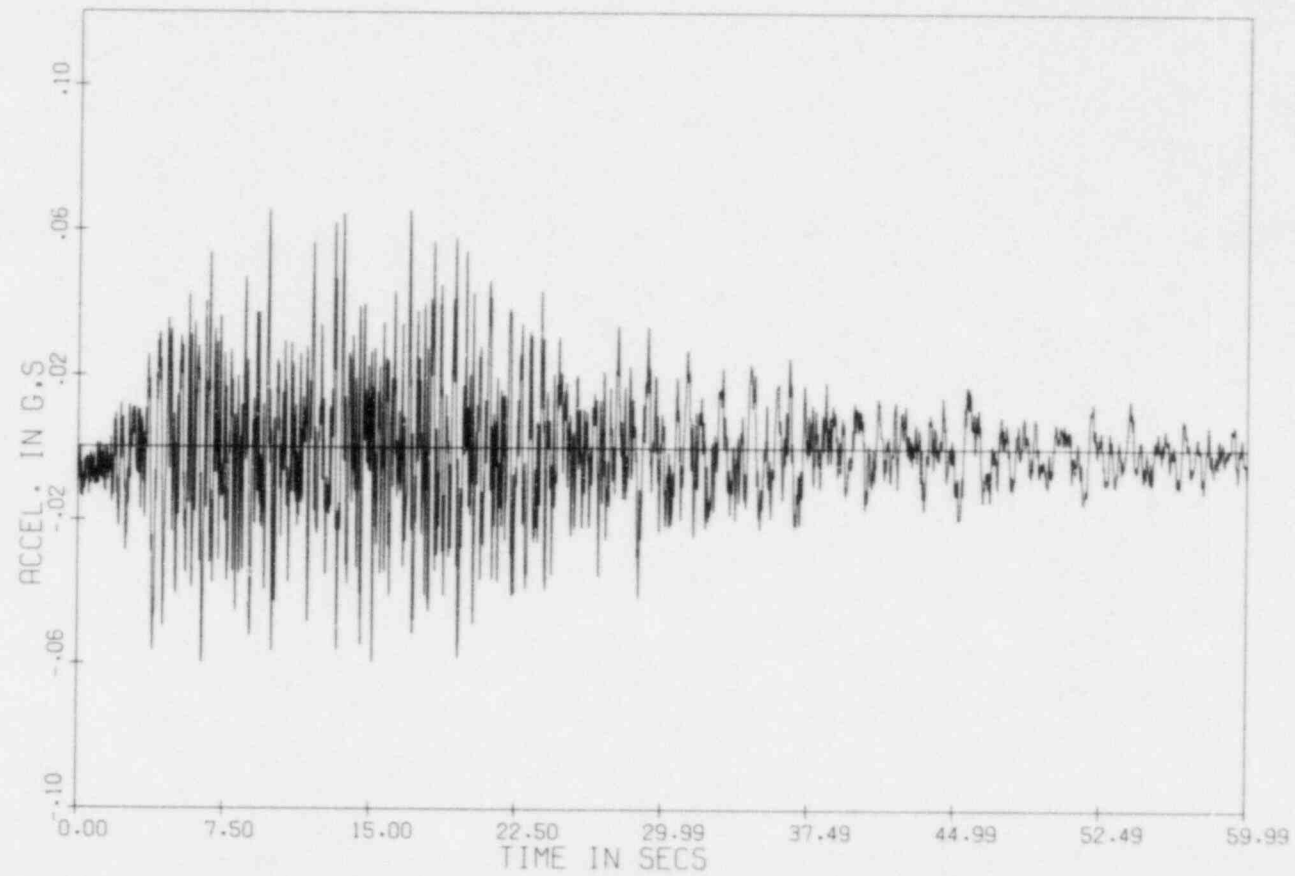


Fig. A.7 -40M RECORDED SPECTRA UNDER REACTOR BUILDING

NODE-1

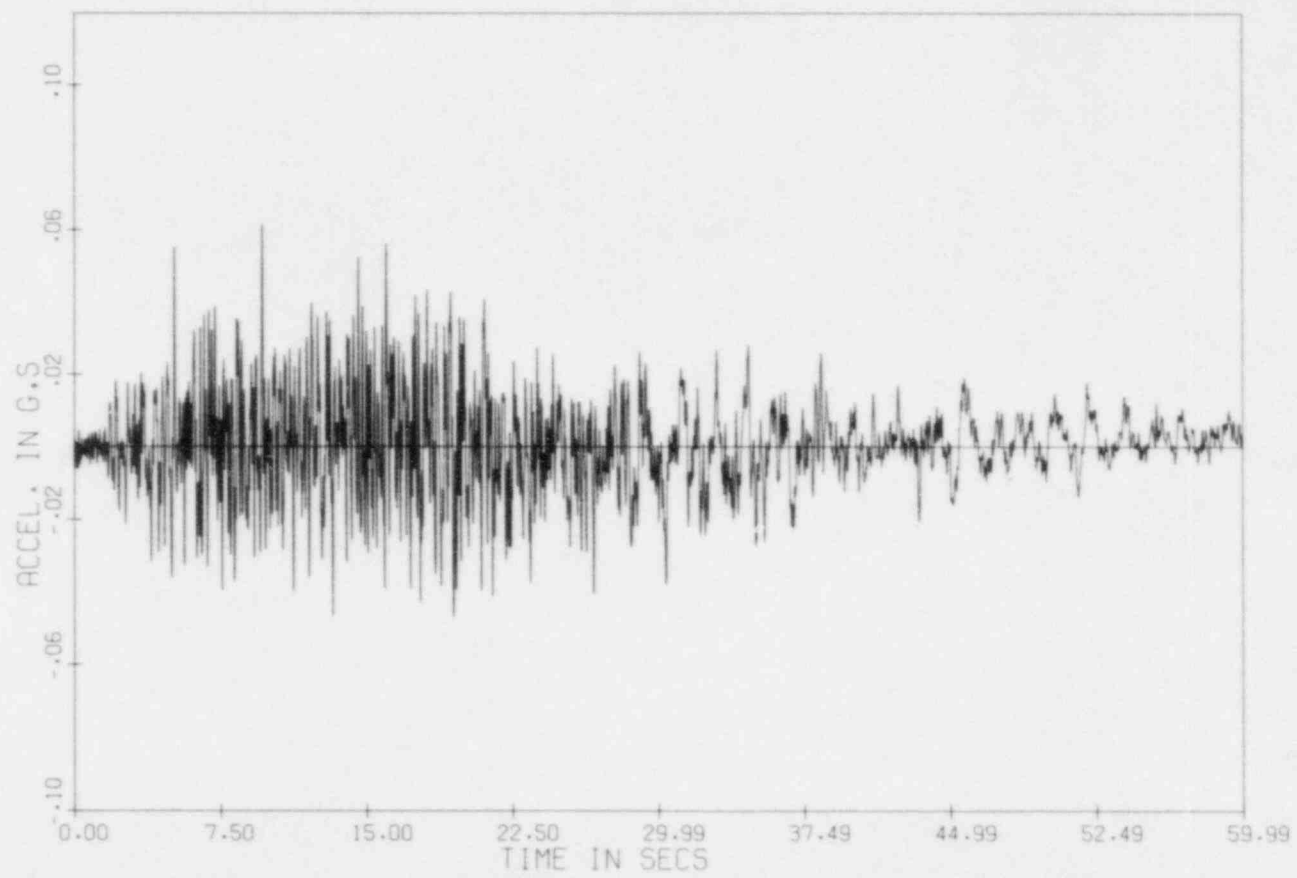


Fig. A.8 -4M RECORDED SPECTRA UNDER REACTOR BUILDING

2.0 PERCENT DAMPING

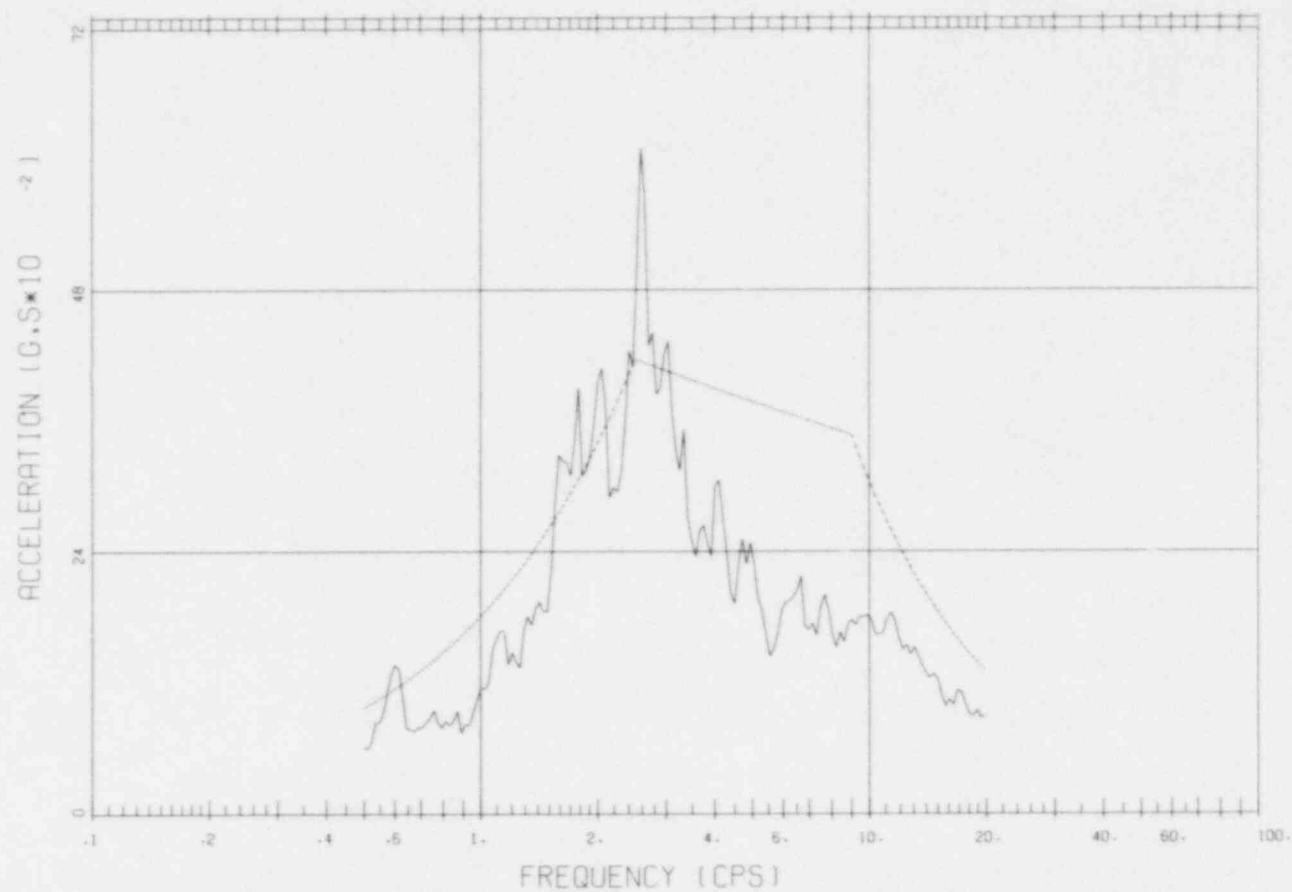


Fig. A.9 -4M RECORDED SPECTRA AT SIDE OF REACTOR BUILDING

2.0 PERCENT DAMPING

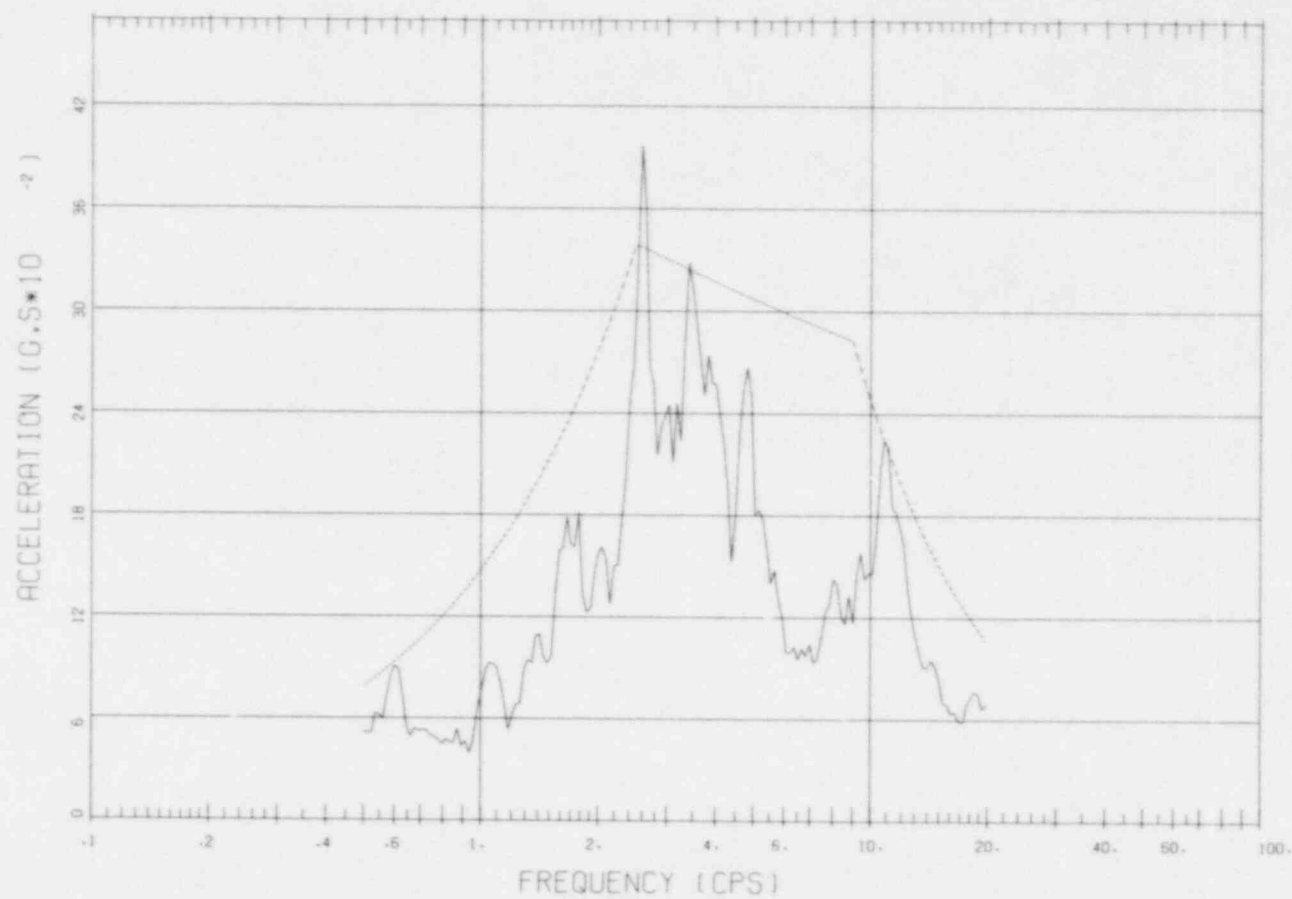


Fig. A.10 -14M RECORDED SPECTRA UNDER REACTOR BUILDING

2.0 PERCENT DAMPING

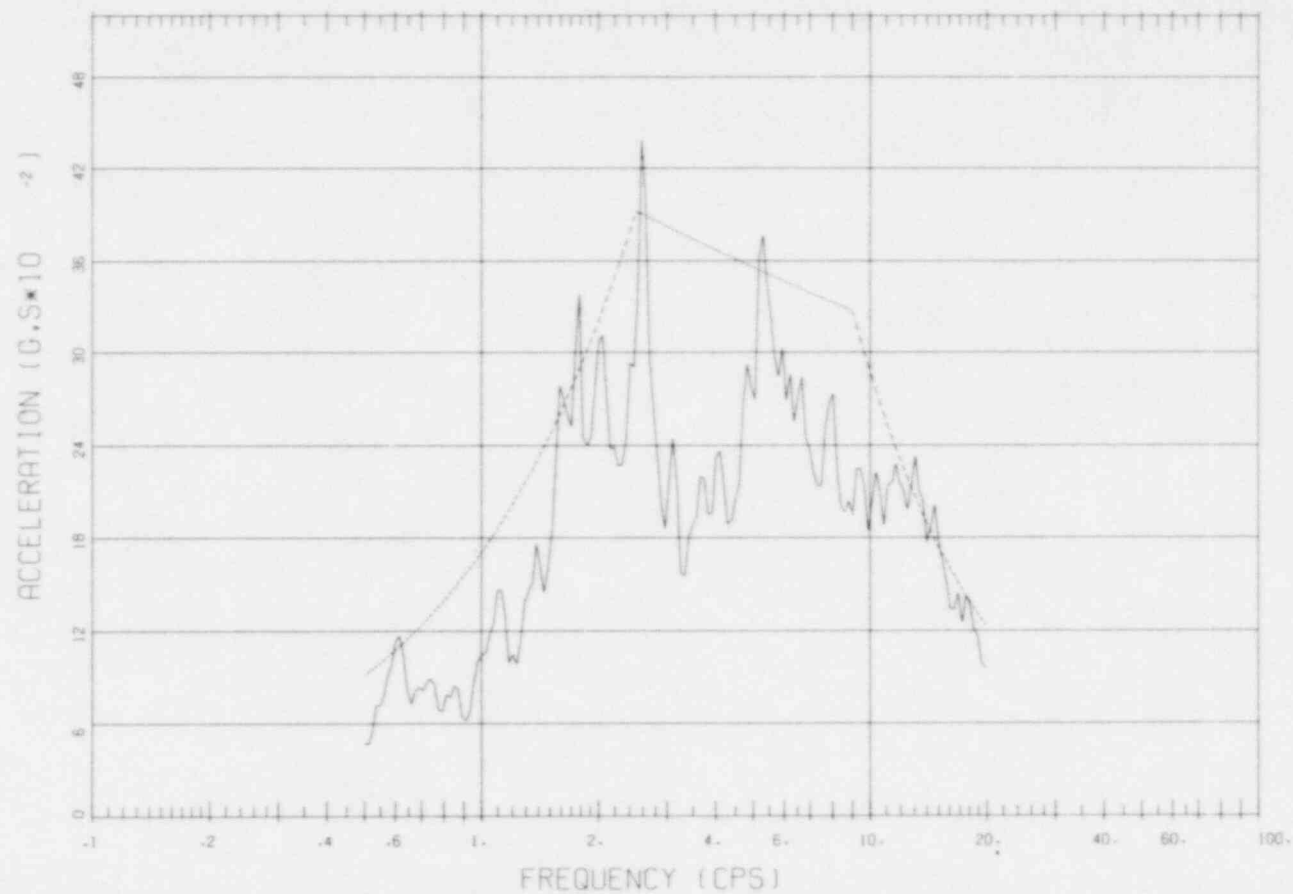


Fig. A.11 -40M RECORDED SPECTRA UNDER REACTOR BUILDING

2.0 PERCENT DAMPING

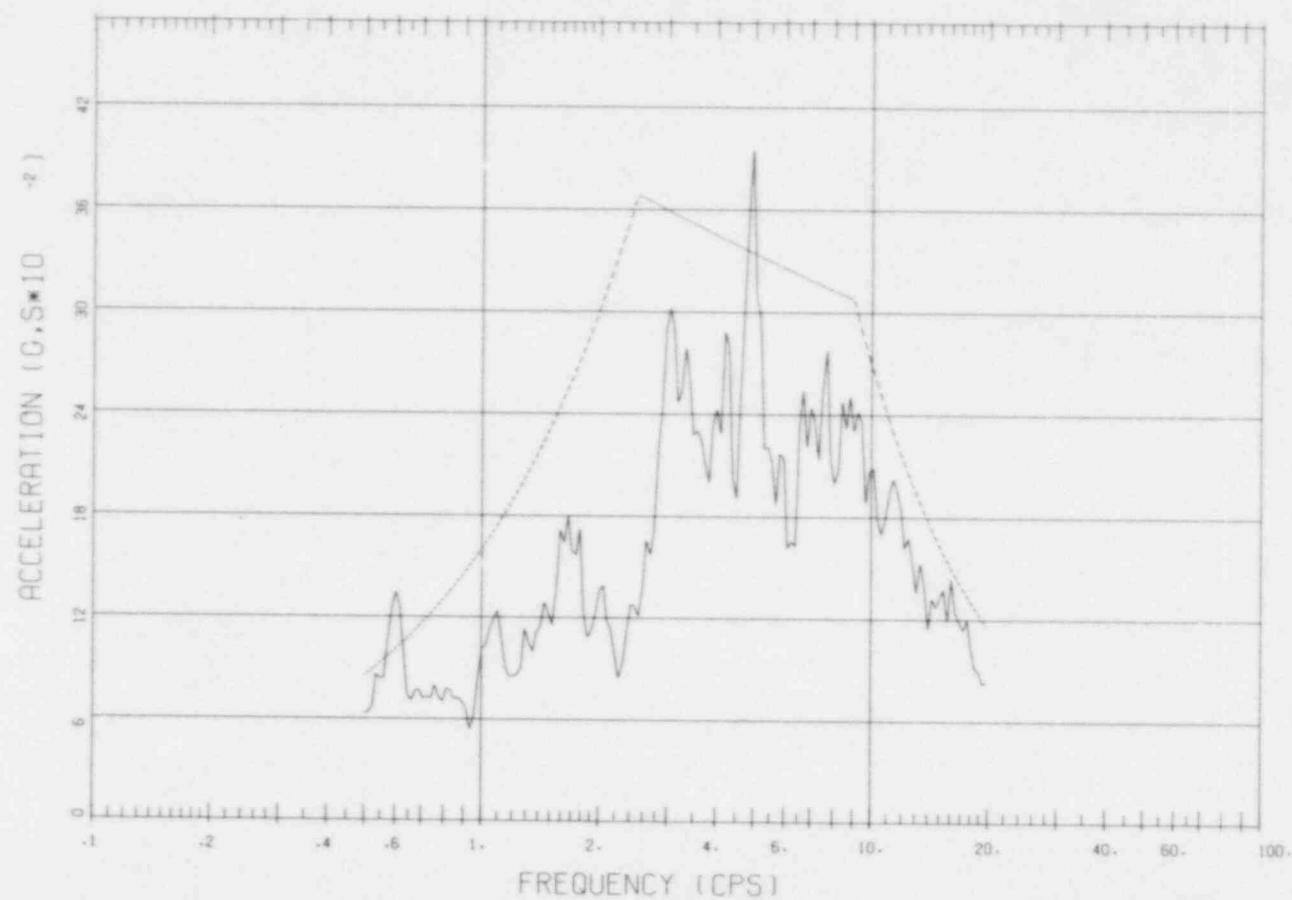


Fig. A.12 ACCELERATION SPECTRA FOR FUKUSHIMA PLANT, JUNE 1978
RECORDED SPECTRA UNDER REACTOR BUILDING

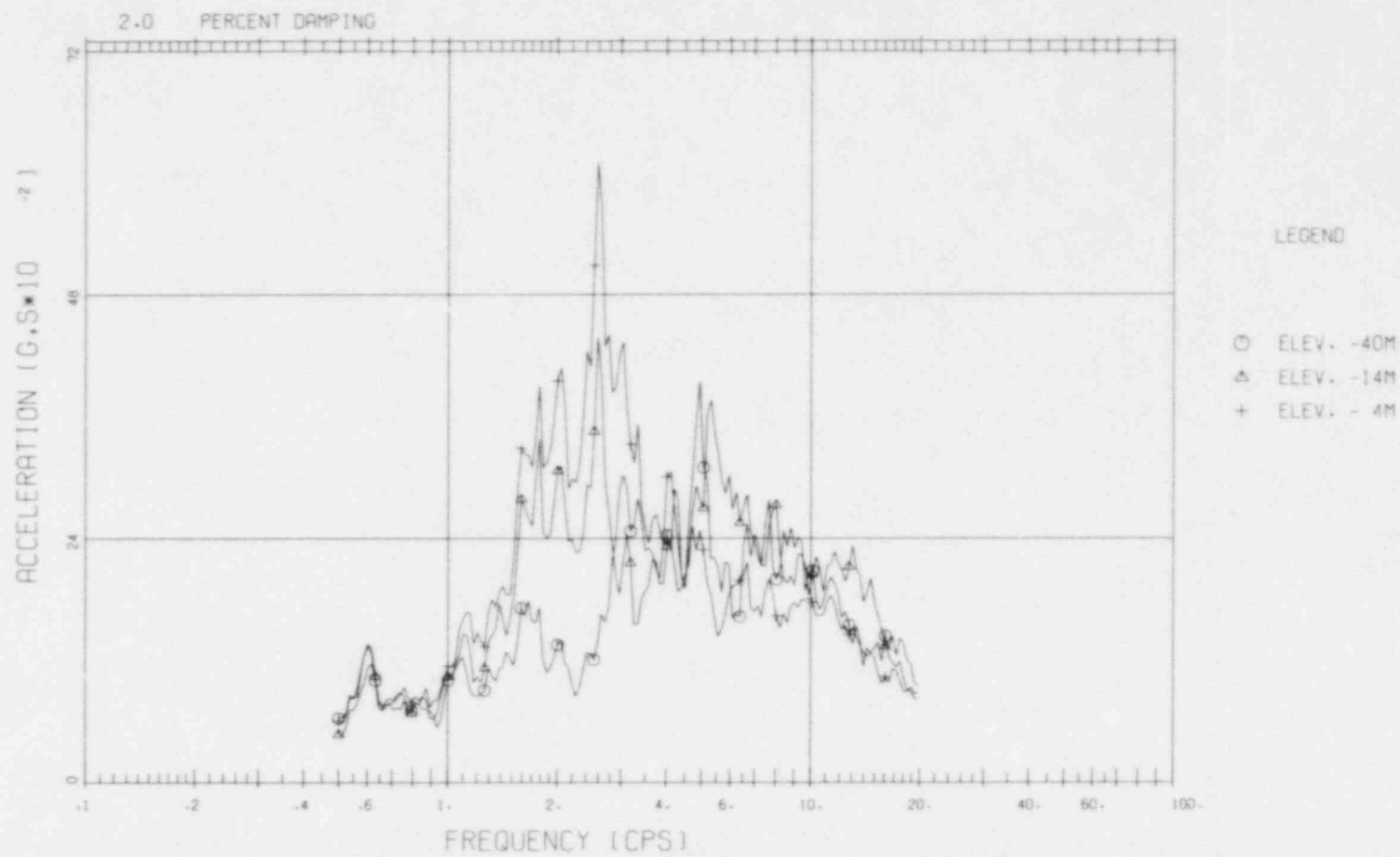


Fig. A.13 ACCELERATION SPECTRA FOR FUKUSHIMA PLANT, JUNE 1978
RECORDED SPECTRA AT ELEVATION -4 METERS

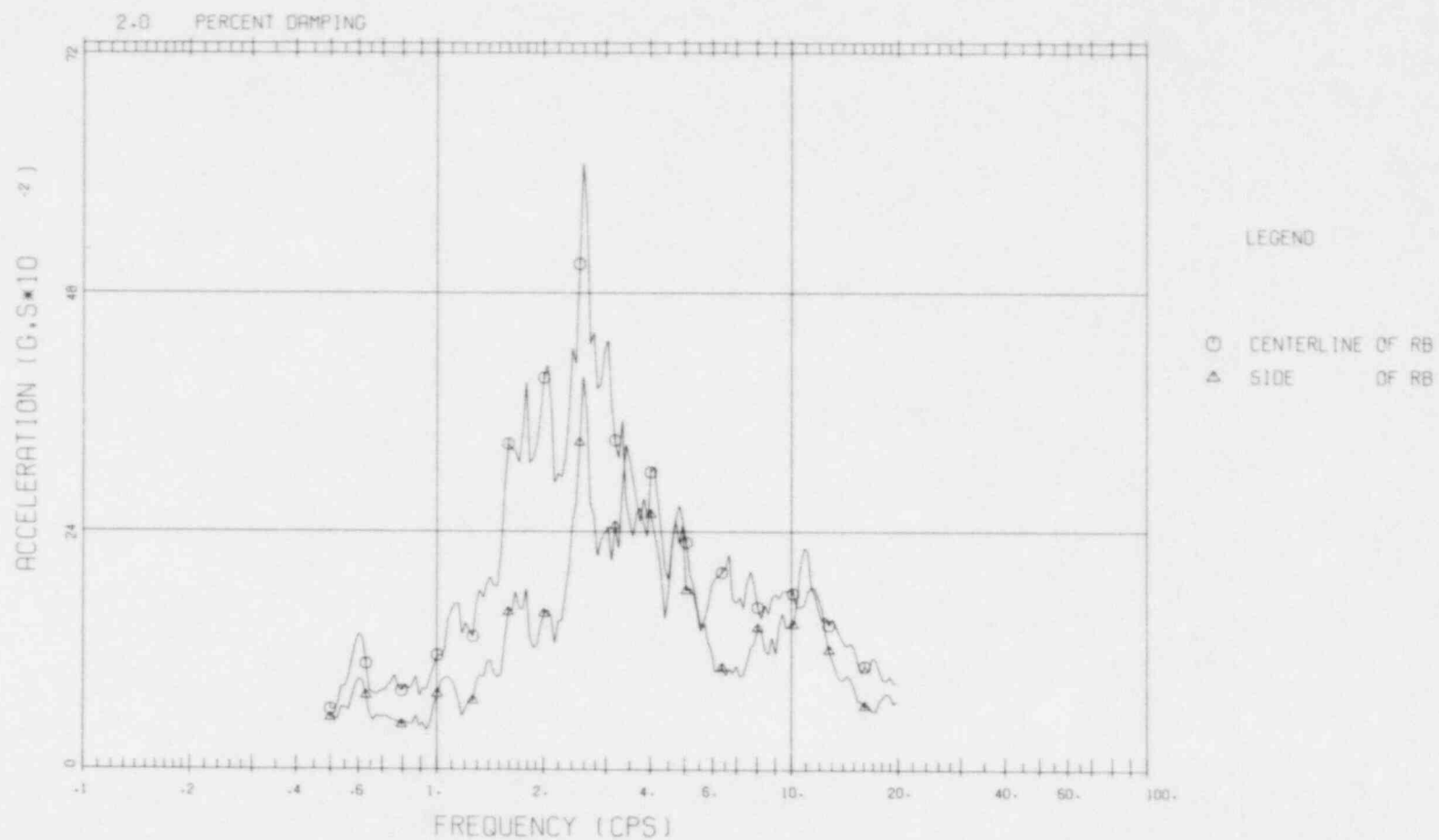


Fig. A.14 ACCELERATION SPECTRA FOR FUKUSHIMA PLANT, JUNE 1978
COMPUTED SPECTRA UNDER REACTOR BUILDING, 2 PCT ROCK DAMPING

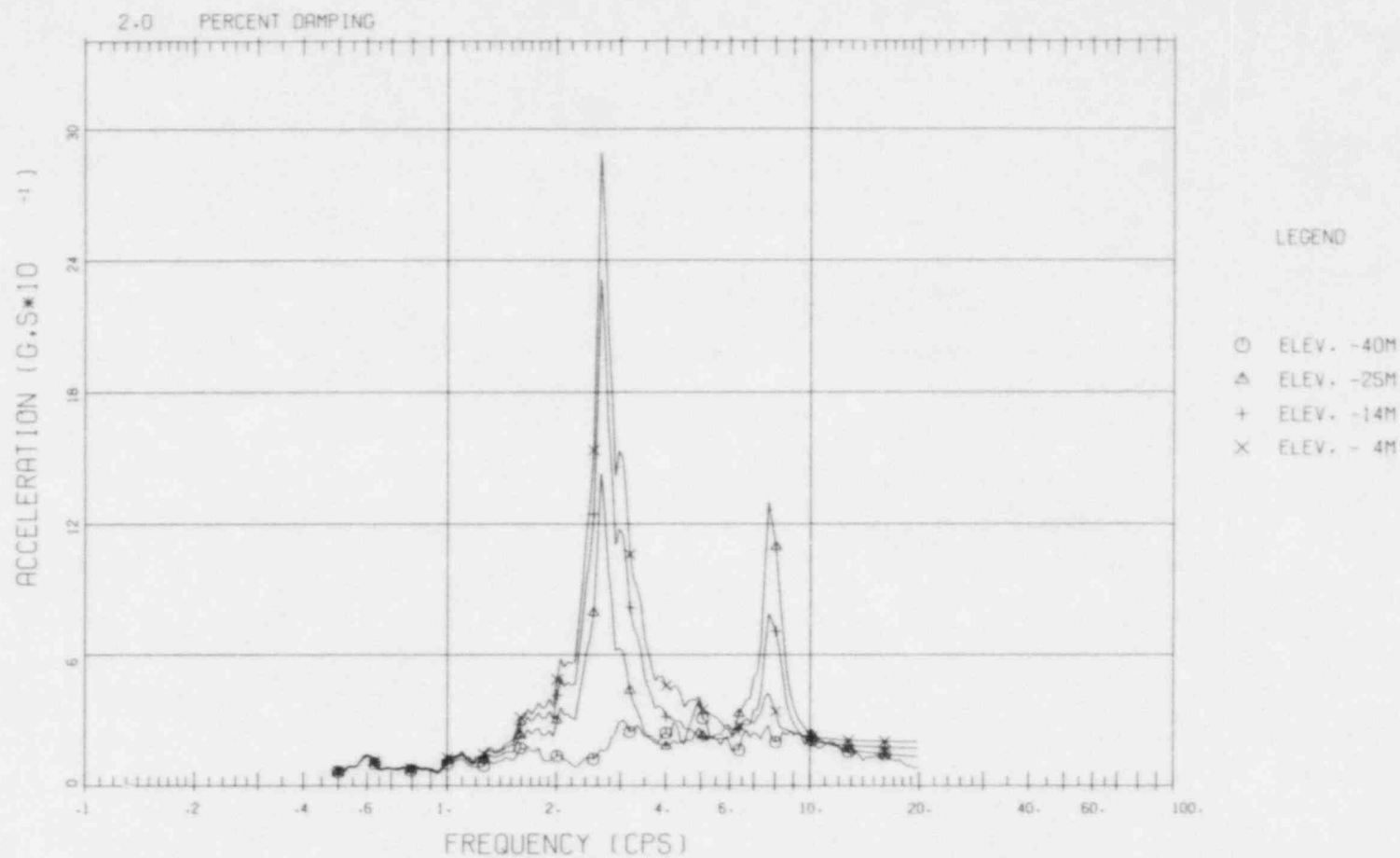


Fig. A.15 ACCELERATION SPECTRA FOR FUKUSHIMA PLANT, JUNE 1978
COMPUTED SPECTRA UNDER REACTOR BUILDING, 5 PCT ROCK DAMPING

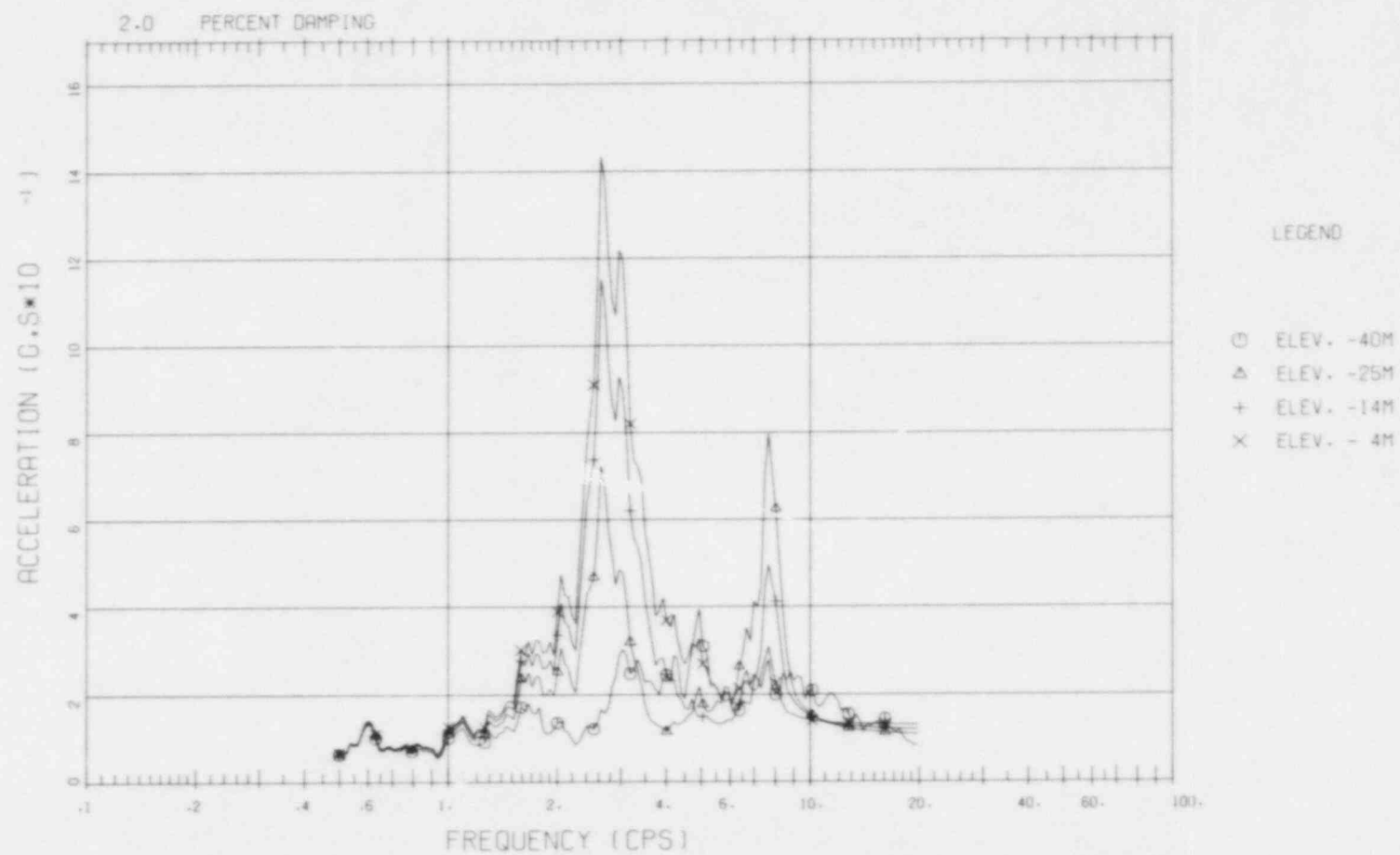


Fig. A.16 ACCELERATION SPECTRA FOR FUKUSHIMA PLANT, JUNE 1978
COMPUTED SPECTRA UNDER REACTOR BUILDING, 7 PCT ROCK DAMPING

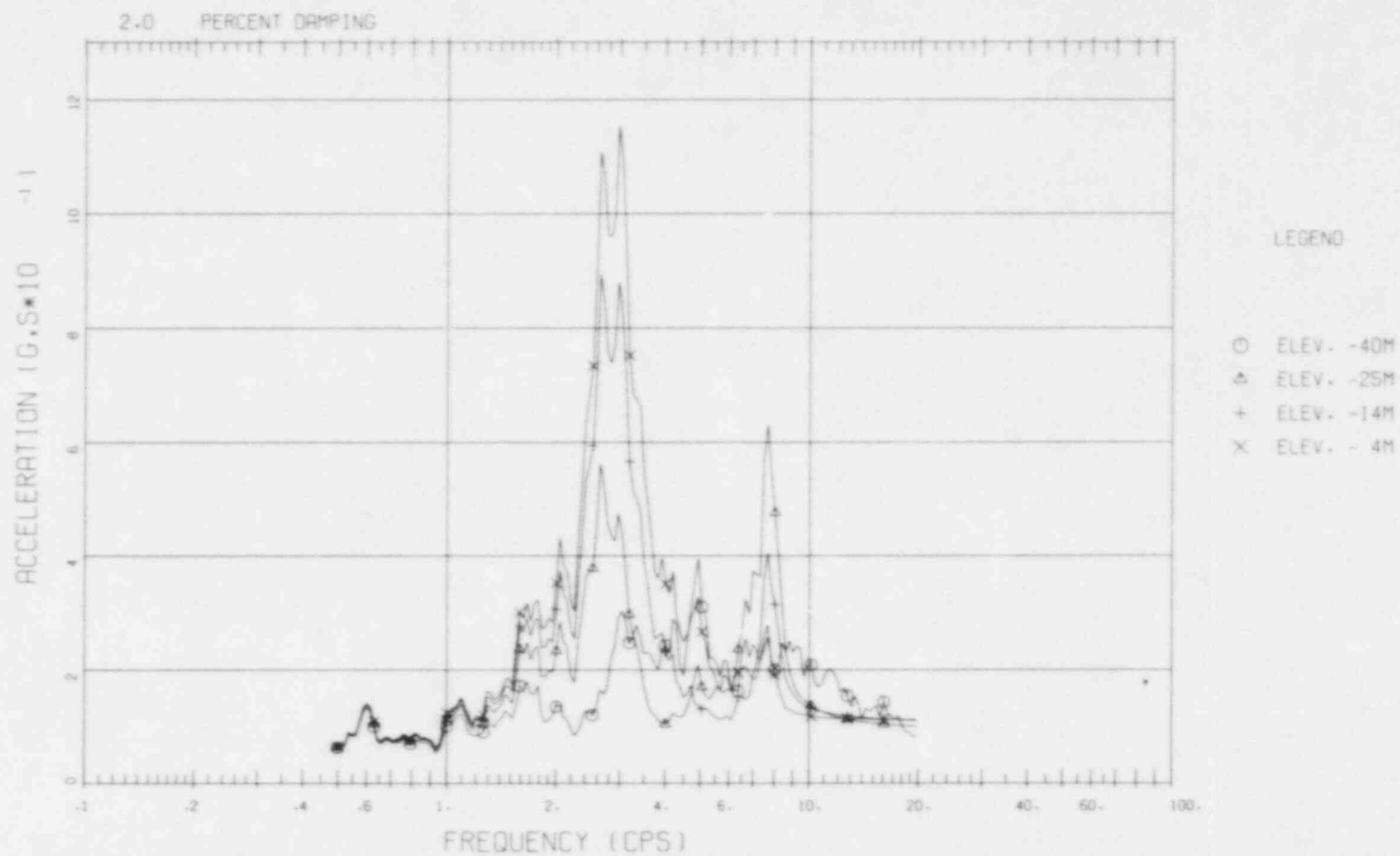


Fig. A.17 ACCELERATION SPECTRA FOR FUKUSHIMA PLANT, JUNE 1978
COMPUTED SPECTRA UNDER REACTOR BUILDING, 10 PCT ROCK DAMPING

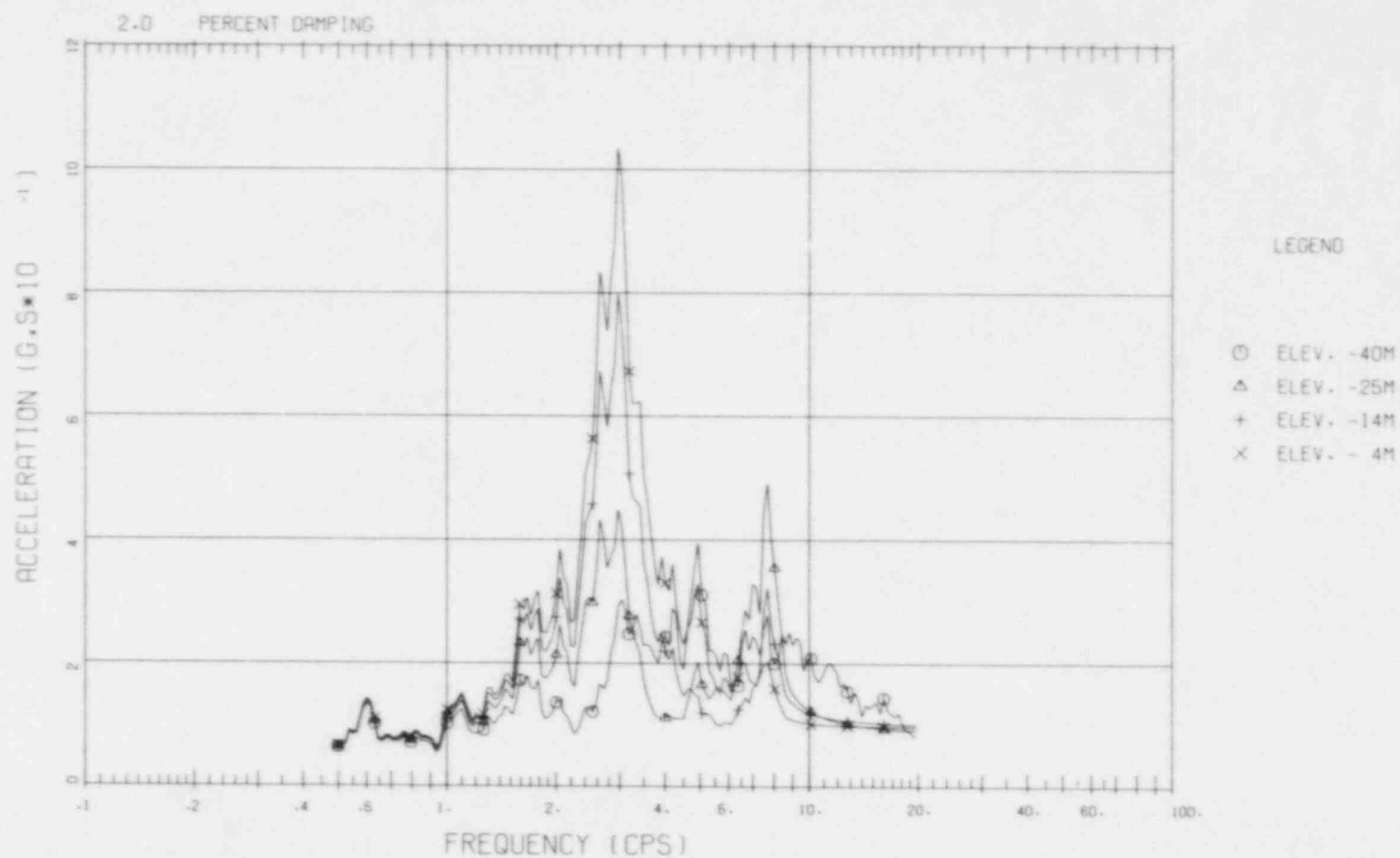


Fig. A.18 ACCELERATION SPECTRA FOR FUKUSHIMA PLANT, JUNE 1978
COMPUTED SPECTRA UNDER REACTOR BUILDING, 15 PCT ROCK DAMPING

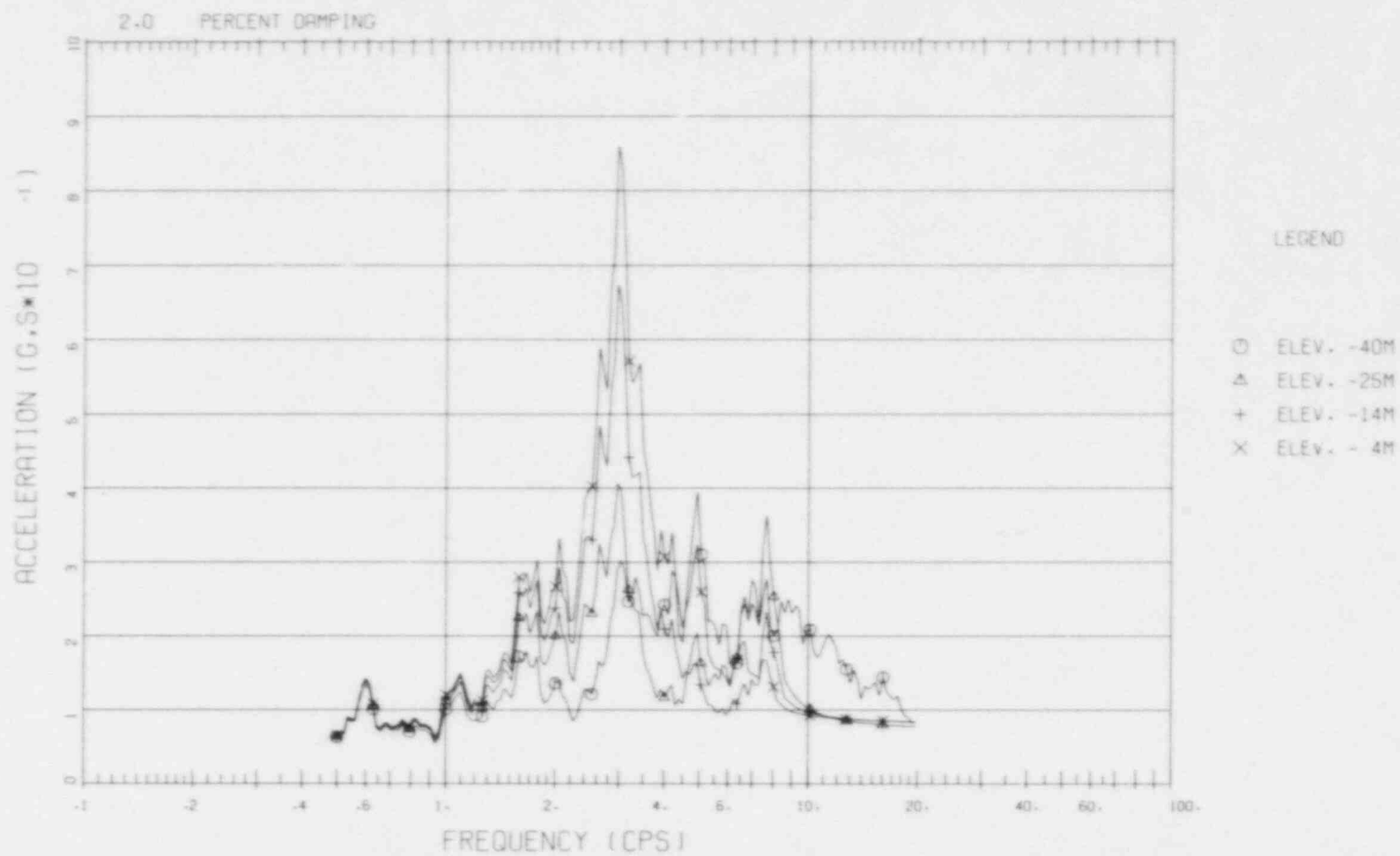


Fig. A.19 ACCELERATION SPECTRA FOR FUKUSHIMA PLANT, JUNE 1978
COMPUTED SPECTRA UNDER REACTOR BUILDING, 20 PCT ROCK DAMPING

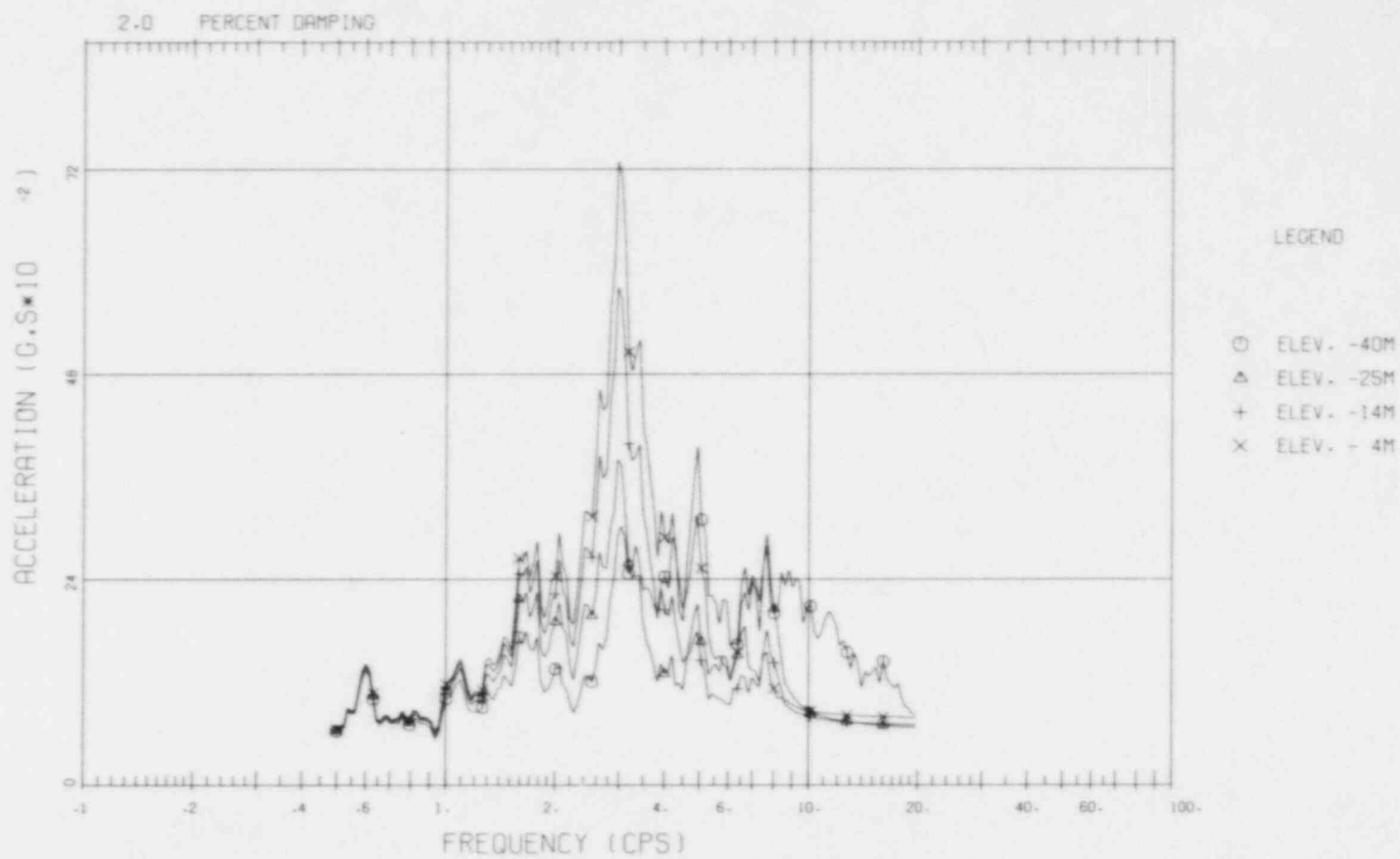


Fig. A.20 ACCELERATION SPECTRA FOR FUKUSHIMA PLANT, JUNE 1978
COMPUTED SPECTRA AT ELEV. -4M FOR VARYING ROCK DAMPING

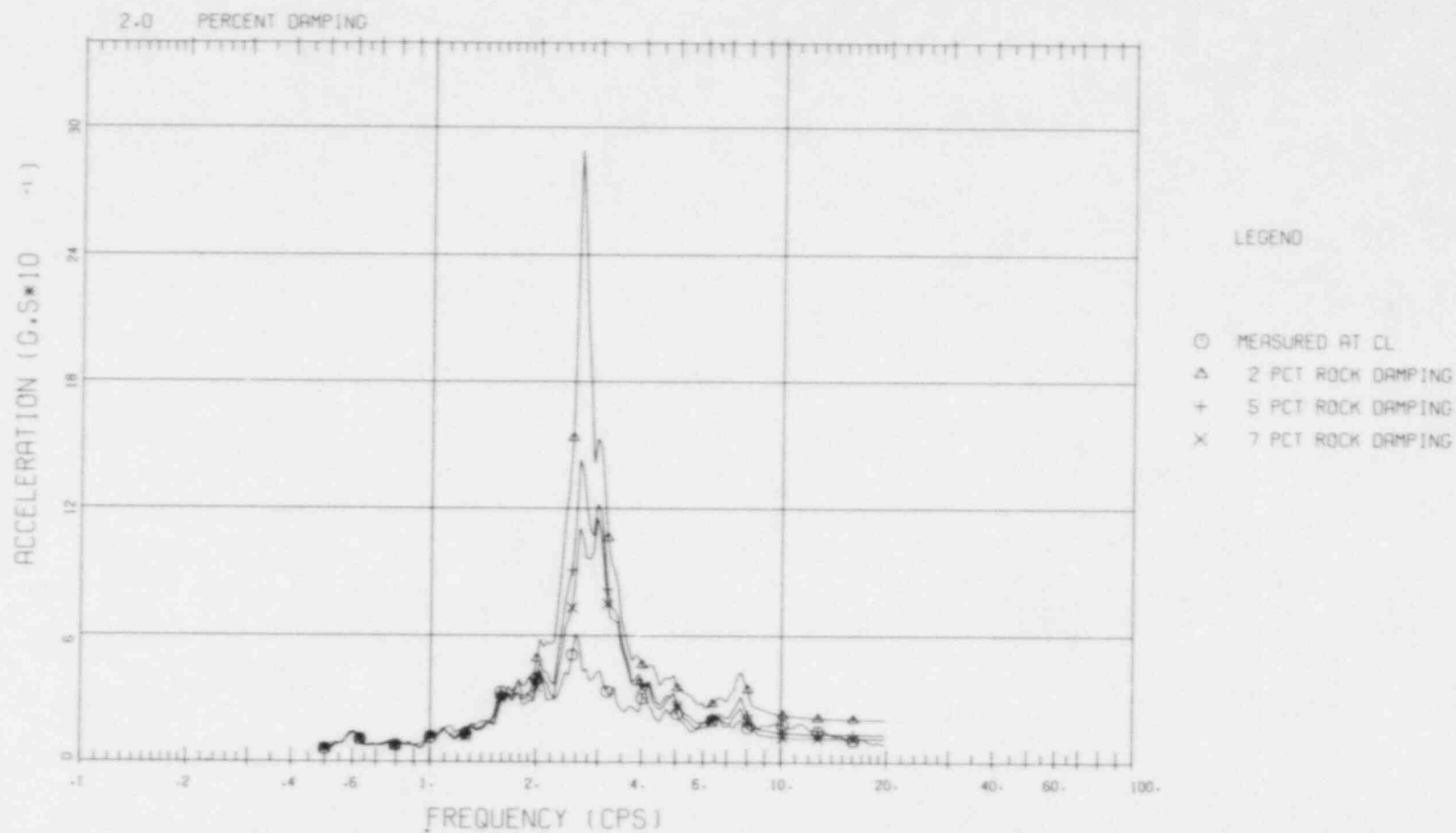


Fig. A.21 ACCELERATION SPECTRA FOR FUKUSHIMA PLANT, JUNE 1978
COMPUTED SPECTRA AT ELEV. -4M FOR VARYING ROCK DAMPING

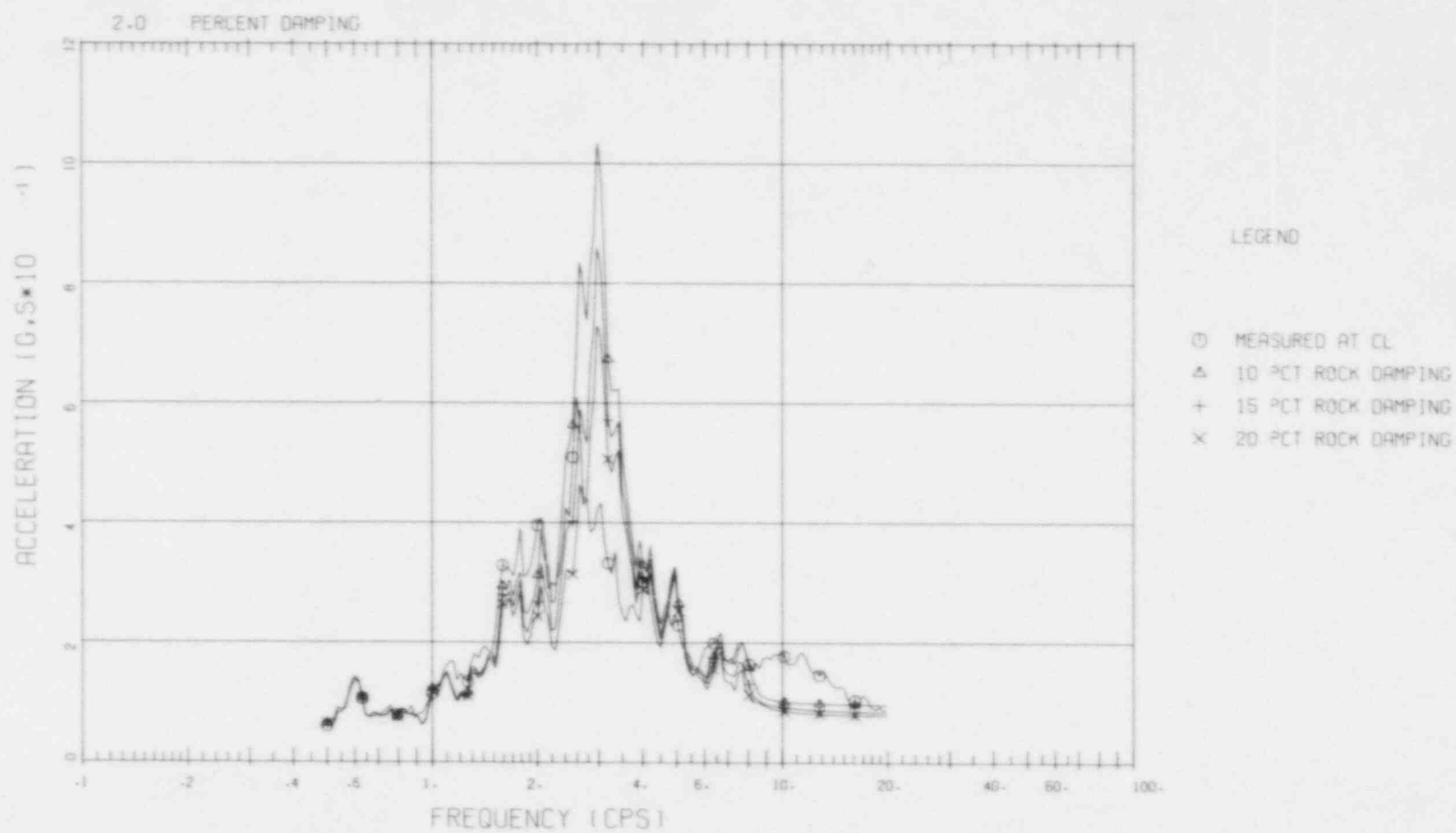


Fig. A.22 ACCELERATION SPECTRA FOR FUKUSHIMA PLANT, JUNE 1978
COMPUTED SPECTRA AT ELEV. -4M FOR VARYING ROCK DAMPING

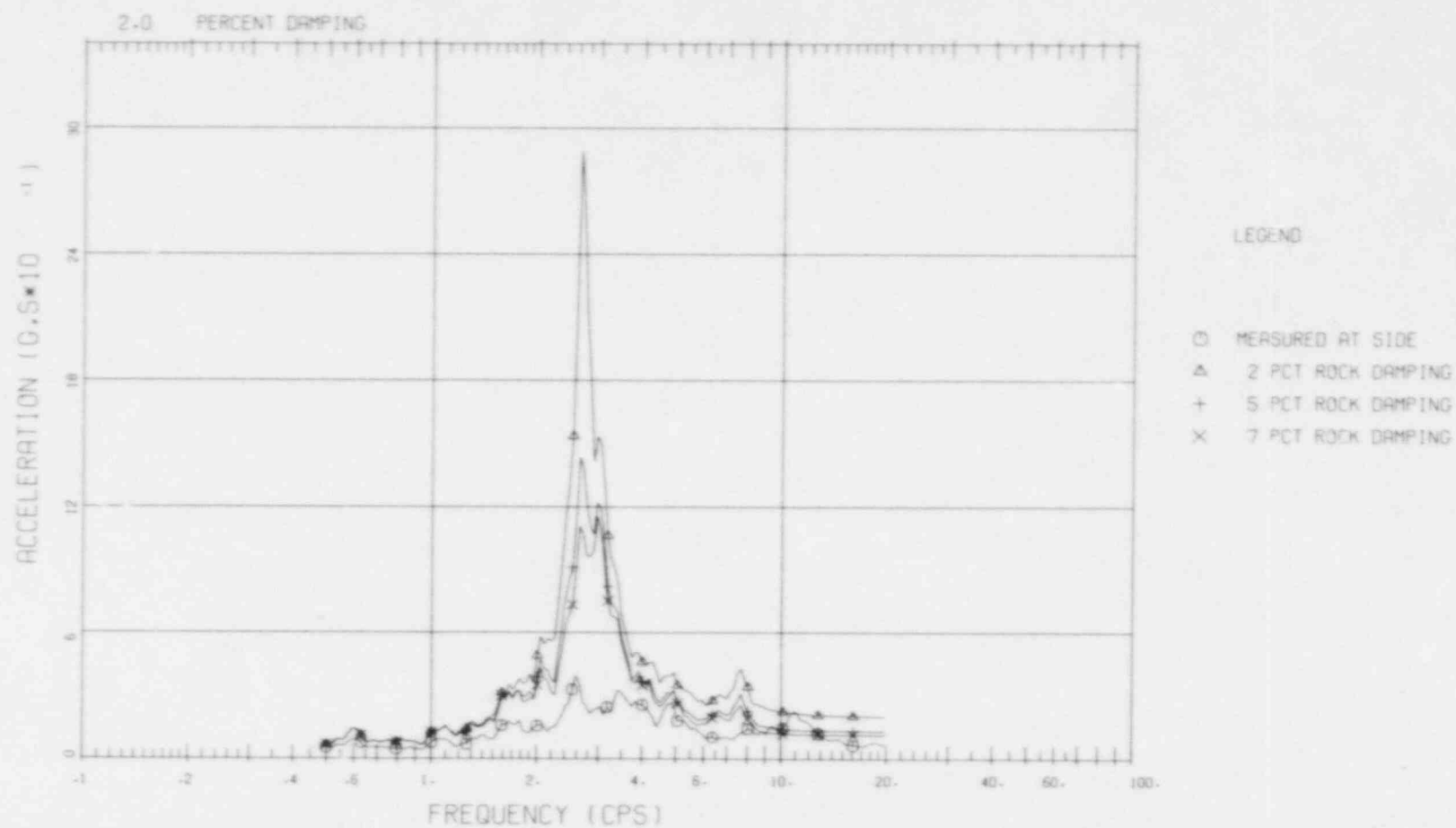
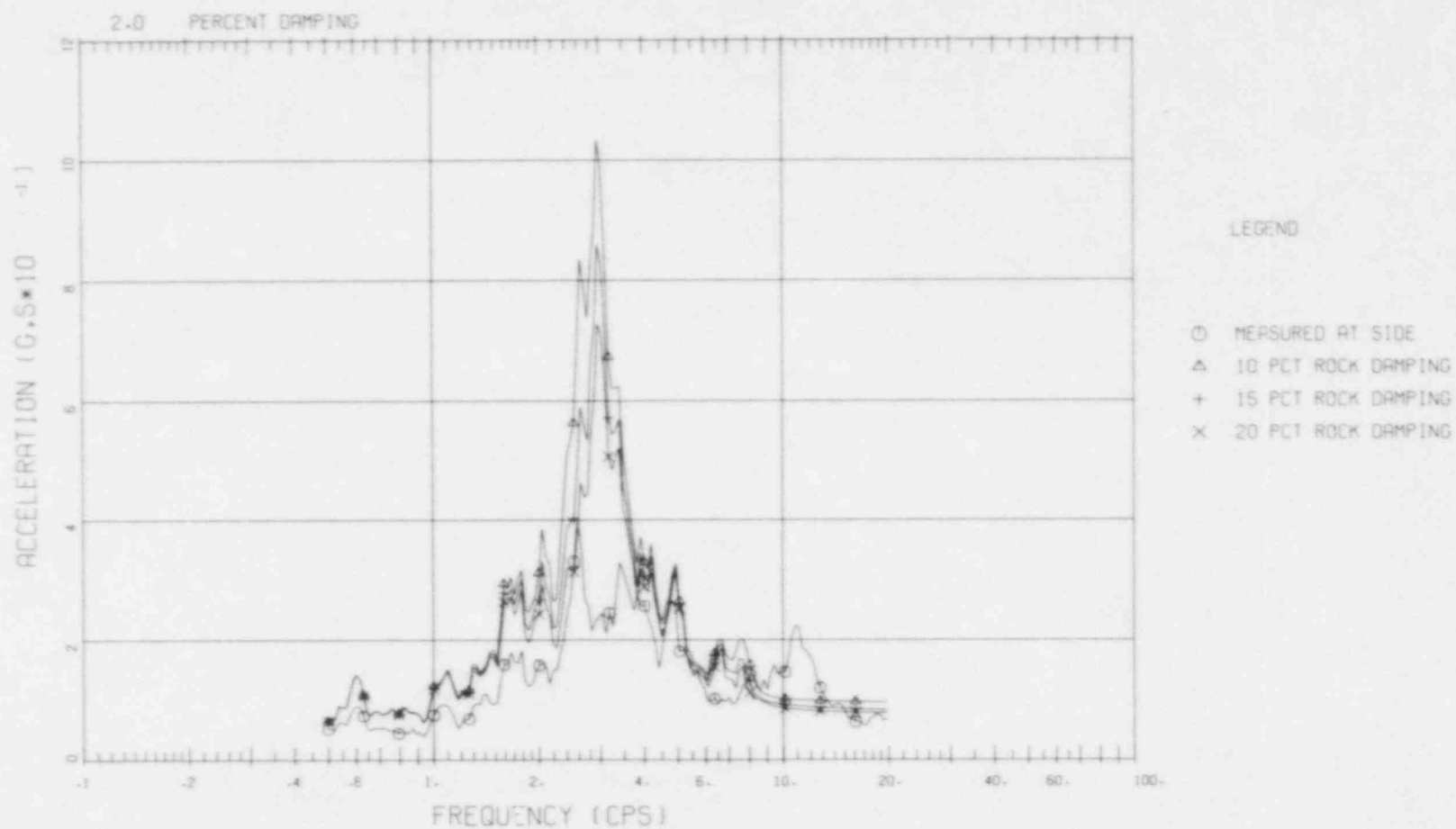
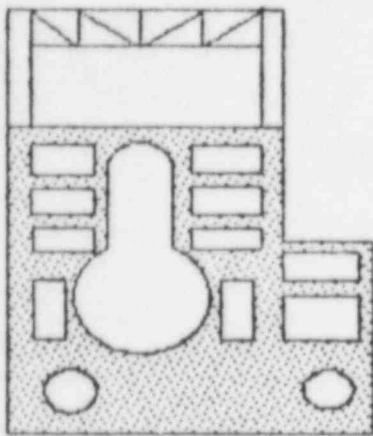
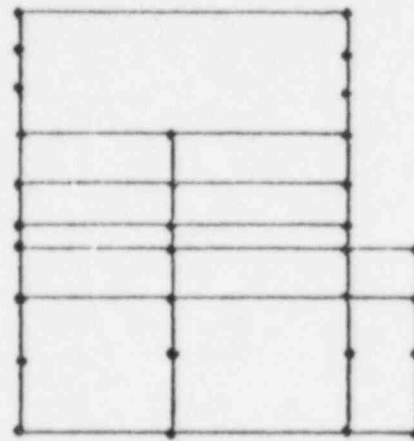


Fig. A.23 ACCELERATION SPECTRA FOR FUKUSHIMA PLANT, JUNE 1978
COMPUTED SPECTRA AT ELEV. -4M FOR VARYING ROCK DAMPING





(a) Building Cross Section



(b) Model

Fig. A.24 Reactor Containment Building Model

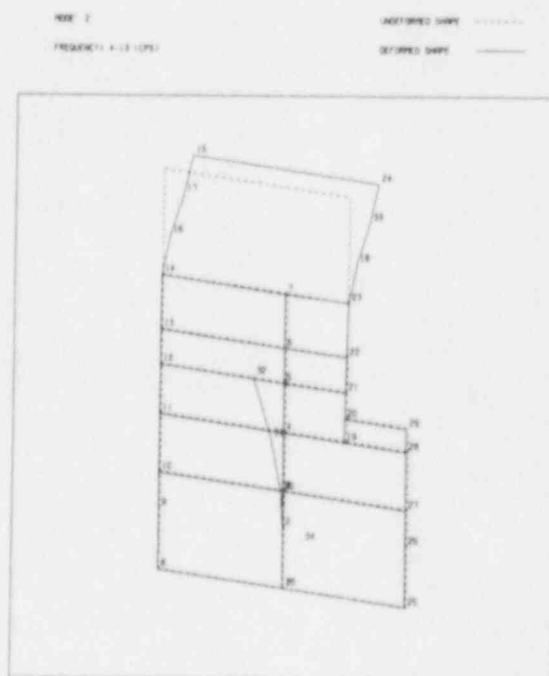
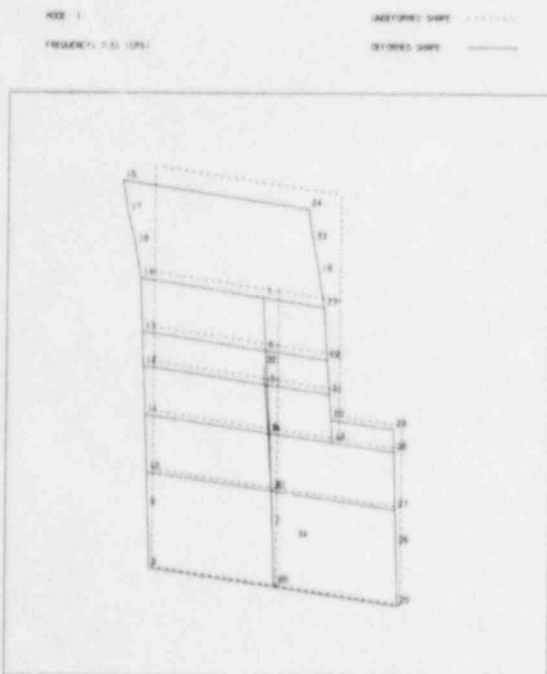
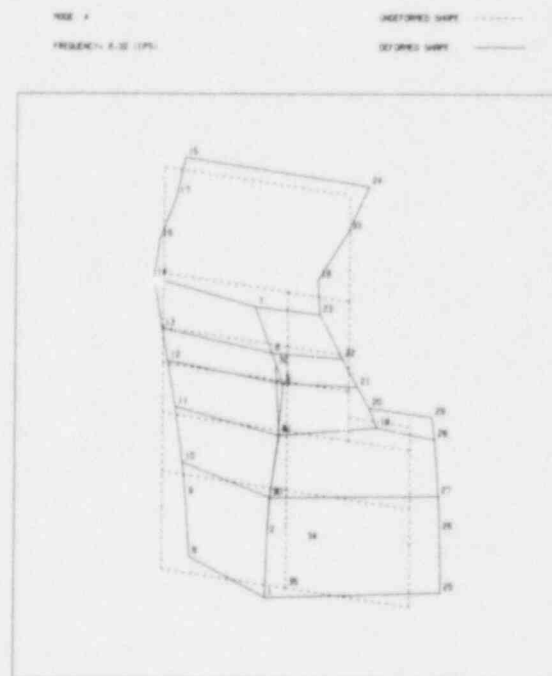
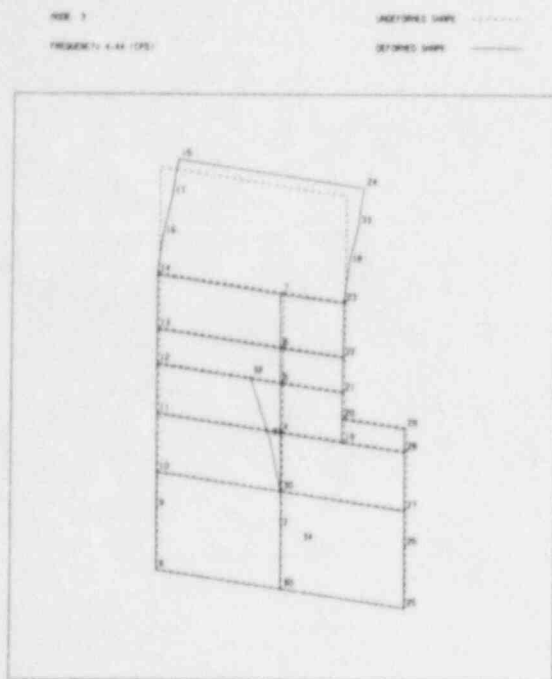


Fig. A.25 Fixed Base Mode Shapes 1-4

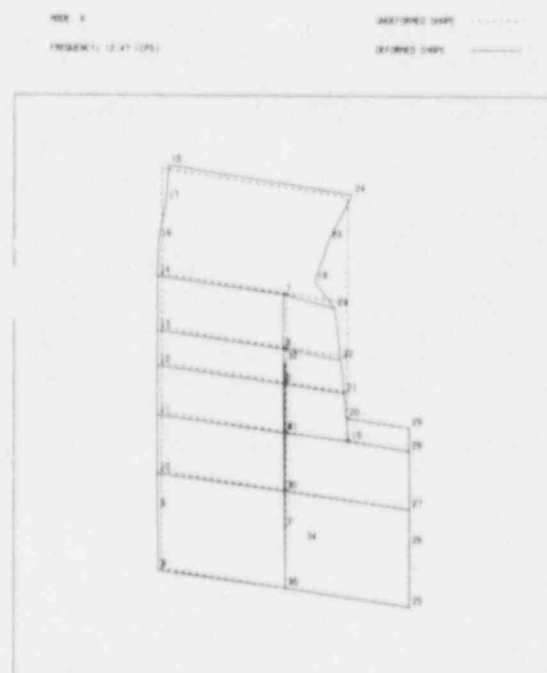
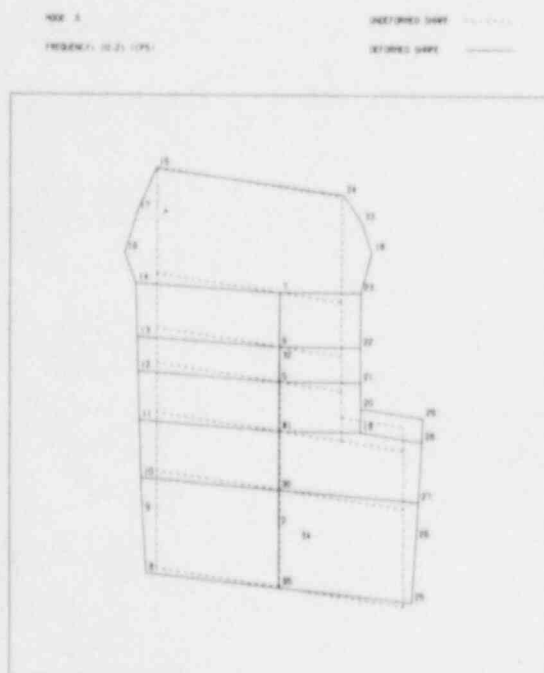
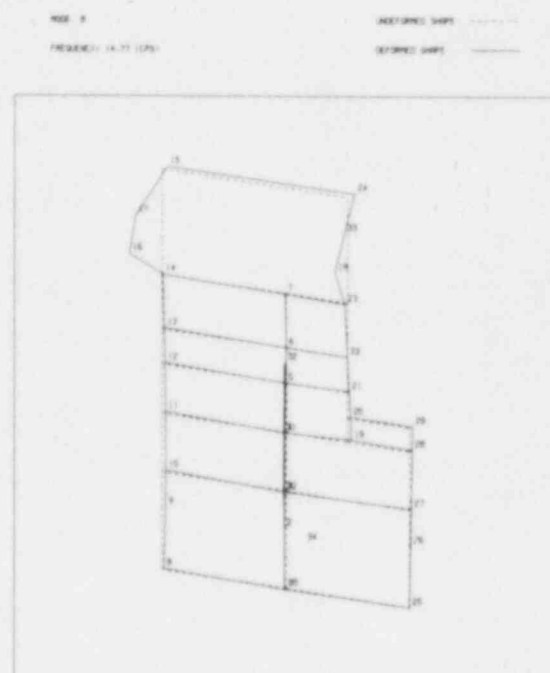
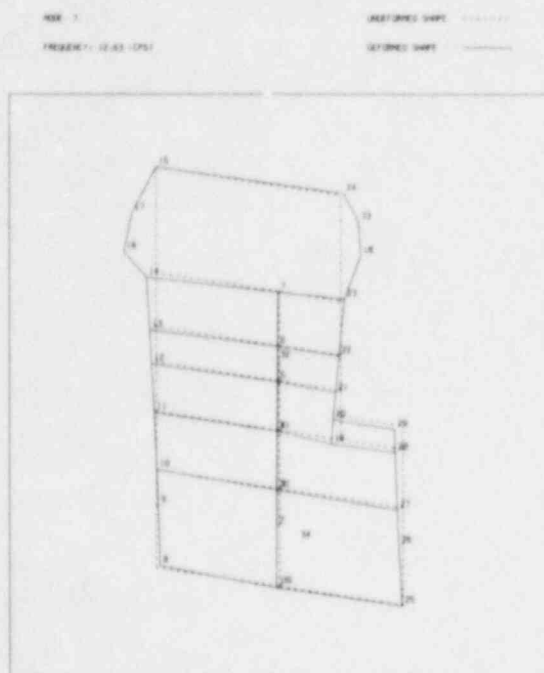


Fig. A.26 Fixed Base Mode Shapes 5-8

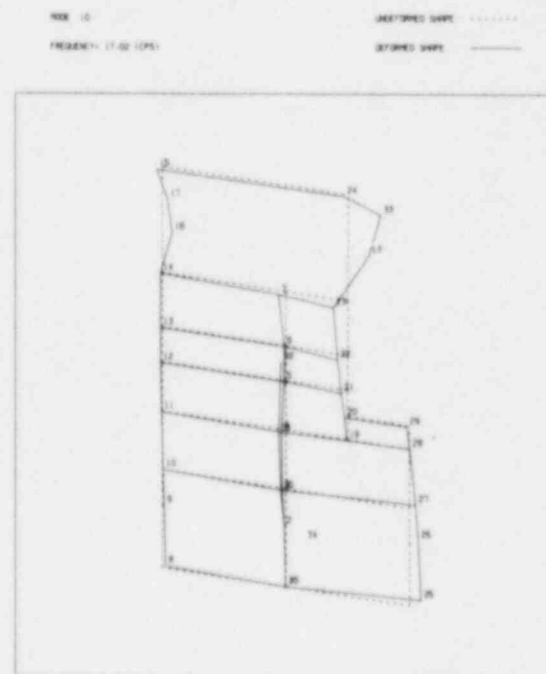
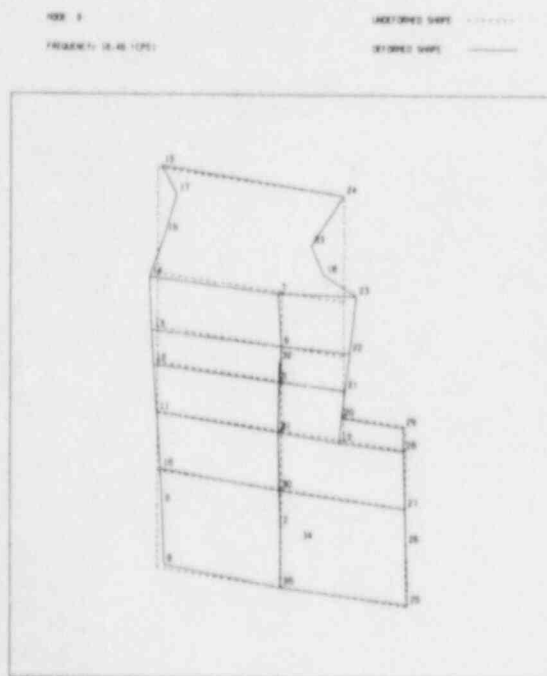
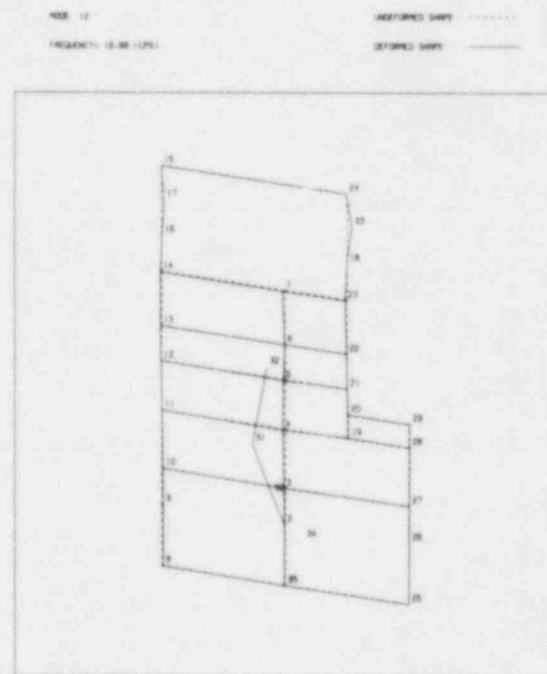
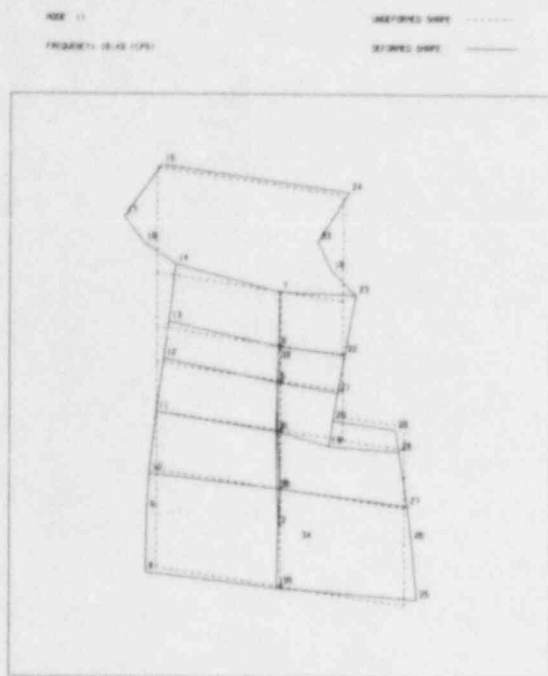
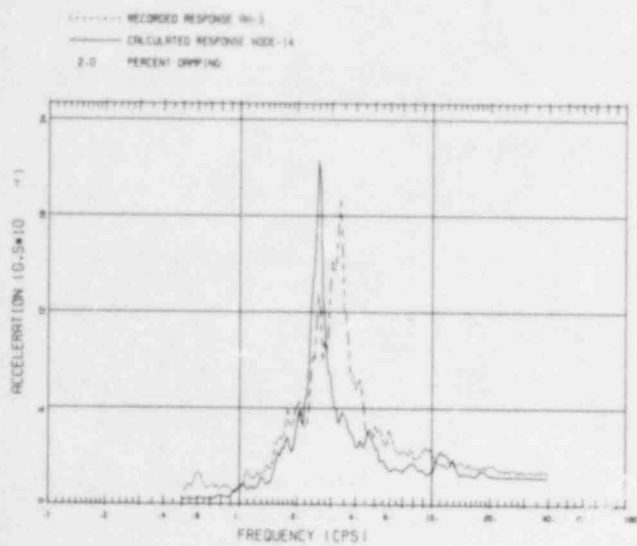
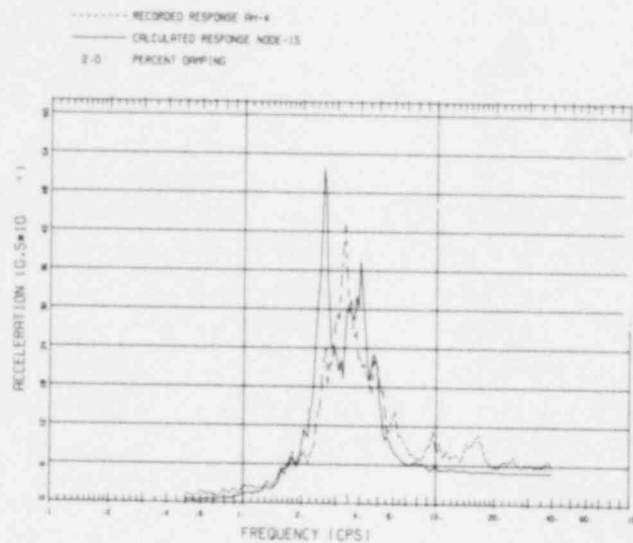


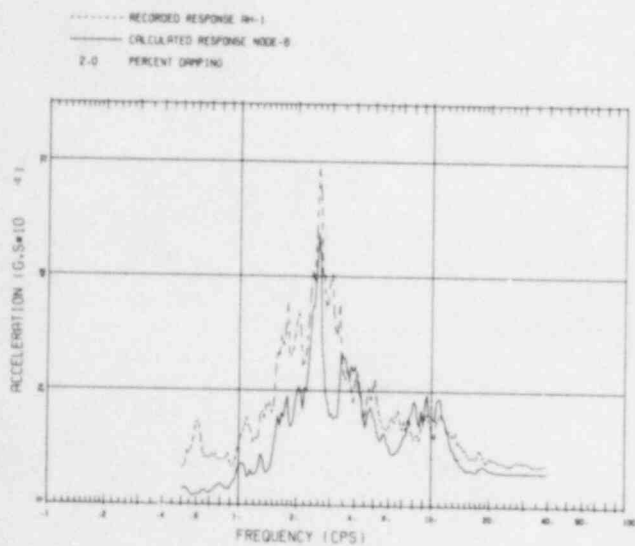
Fig. A.27 Fixed Base Mode Shapes 9-12



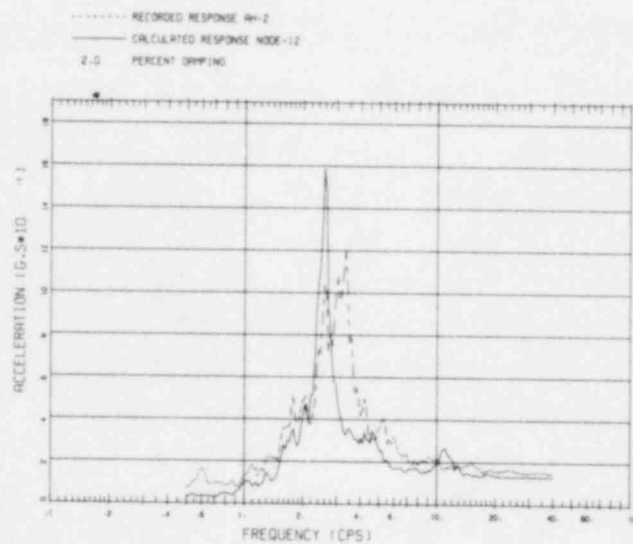
(c) Operating Floor



(d) Top of Structure

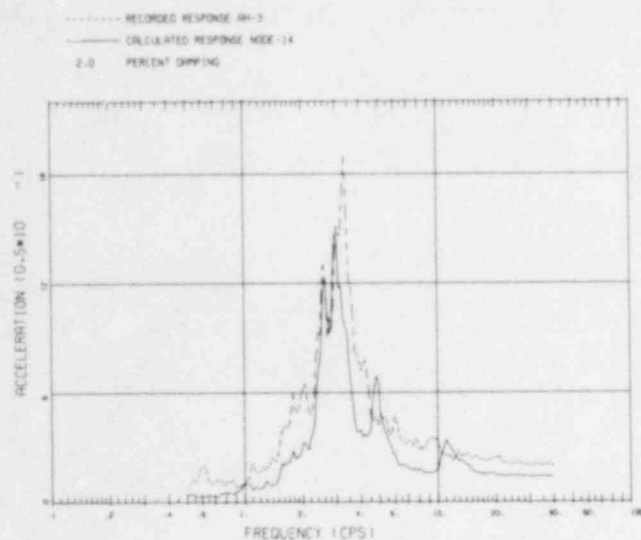


(a) Basemat

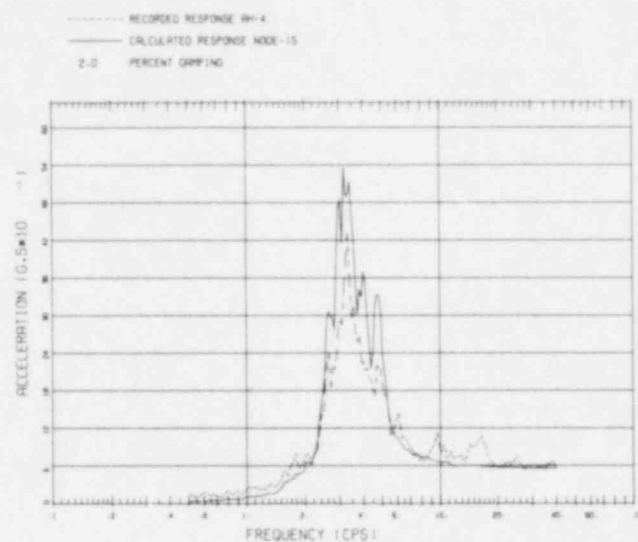


(b) Elev. 25.9 M

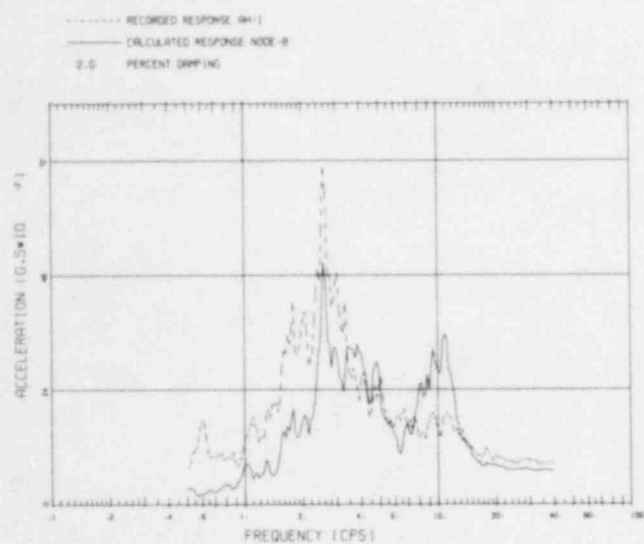
Fig. A.28 Comparison of Measured and Calculated Structural Spectra (Fixed Base Model; Measured Pulse to Side of RCB Input; Standard Interaction Springs; 50% of Standard Interaction Dampers)



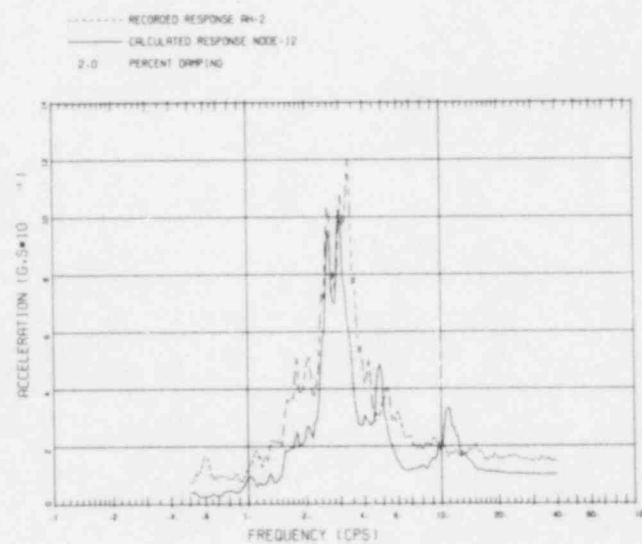
(c) Operating Floor



(d) Top of Structure

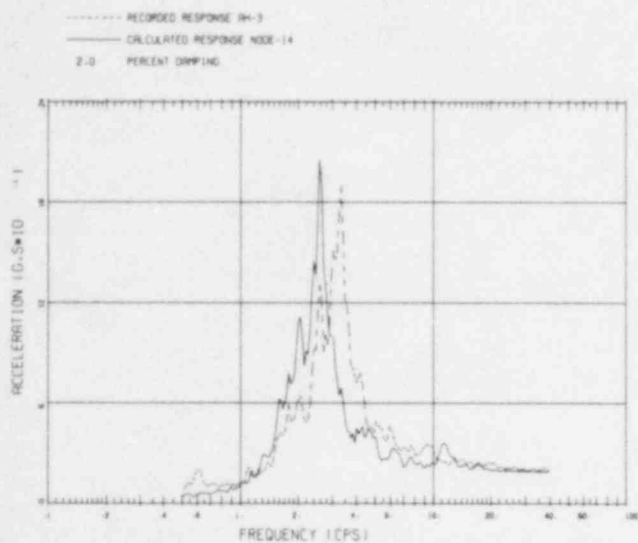


(a) Basemat

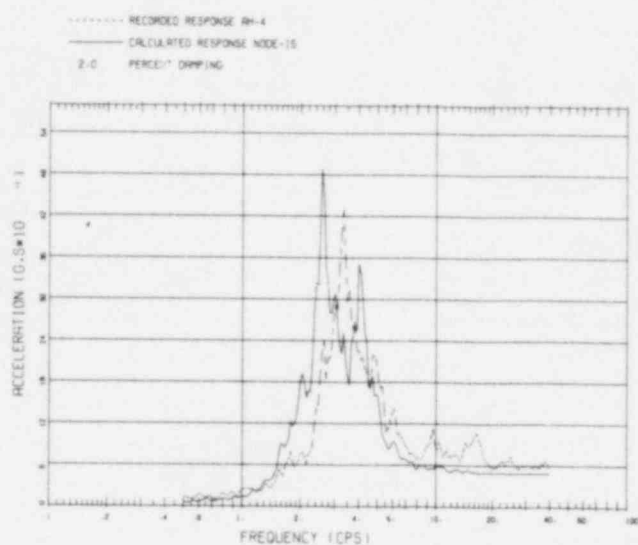


(b) Elev. 25.9 M

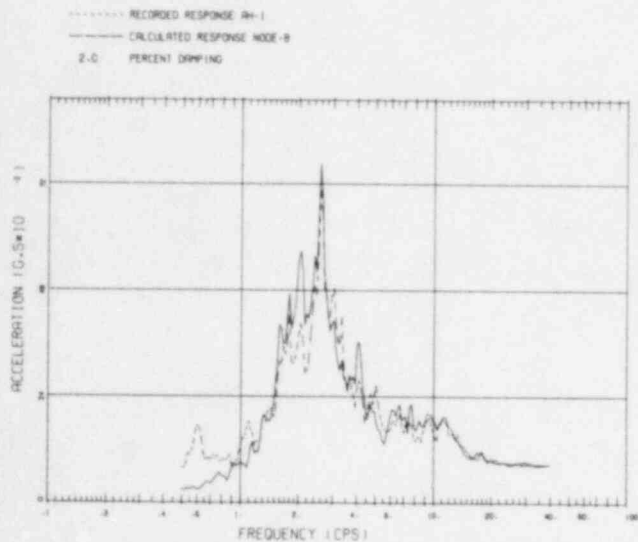
Fig. A.29 Comparison of Measured and Calculated Structural Spectra (Free-Free Model; Measured Pulse to Side of Structure Input; Standard Interaction Springs; 75% of Standard Interaction Dampers)



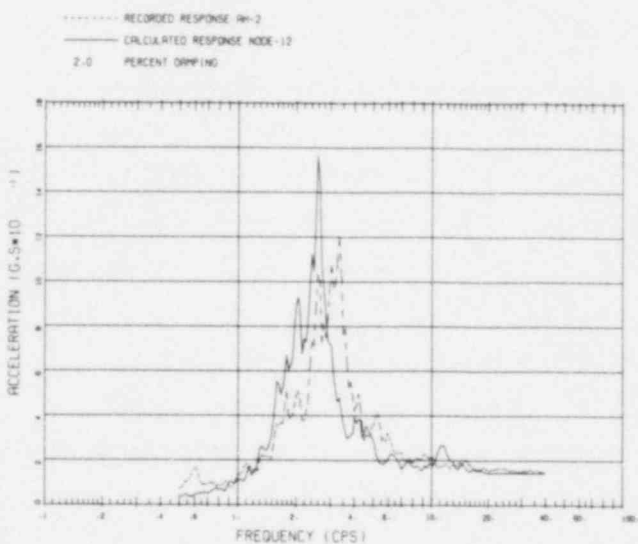
(c) Operating Floor



(d) Top of Structure

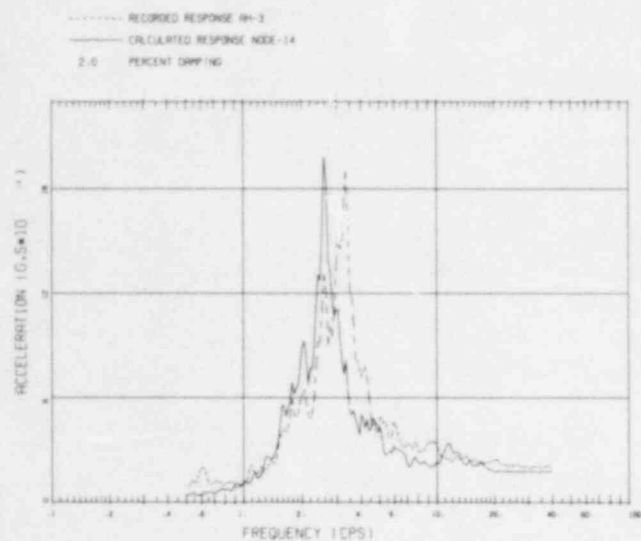


(a) Basemat

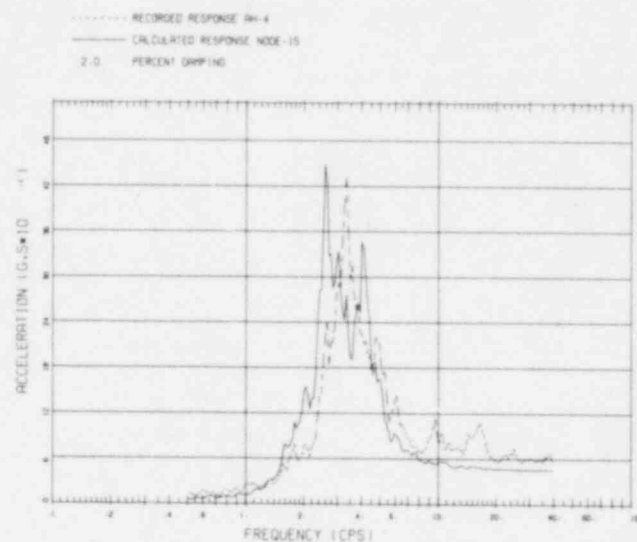


(b) Elev. 25.9 M

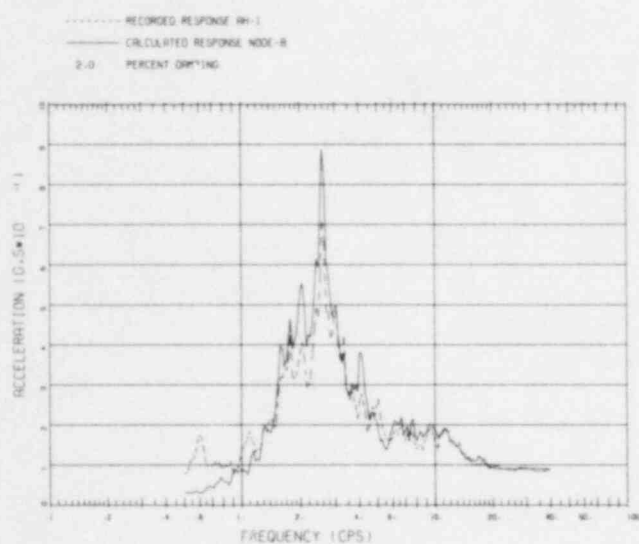
Fig. A.30 Comparison of Measured and Calculated Spectra for Fukushima Using Measured Input Motion and Standard Interaction Parameters



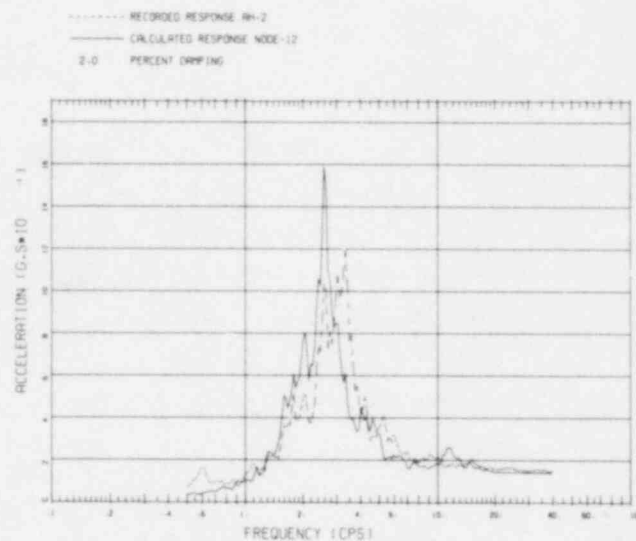
(c) Operating Floor



(d) Top of Structure

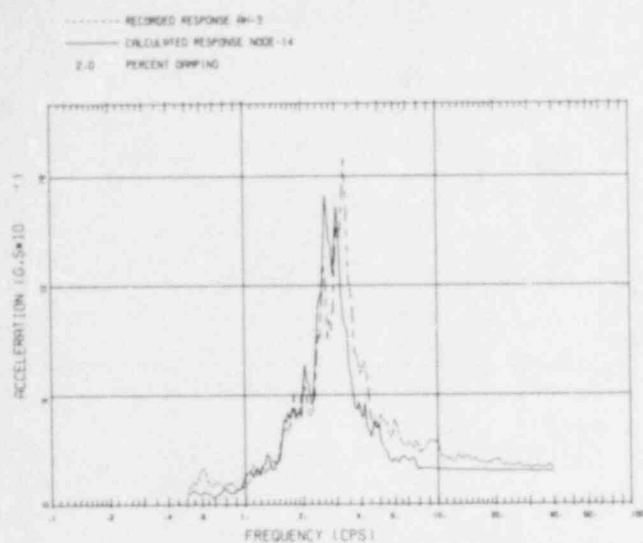


(a) Basemat

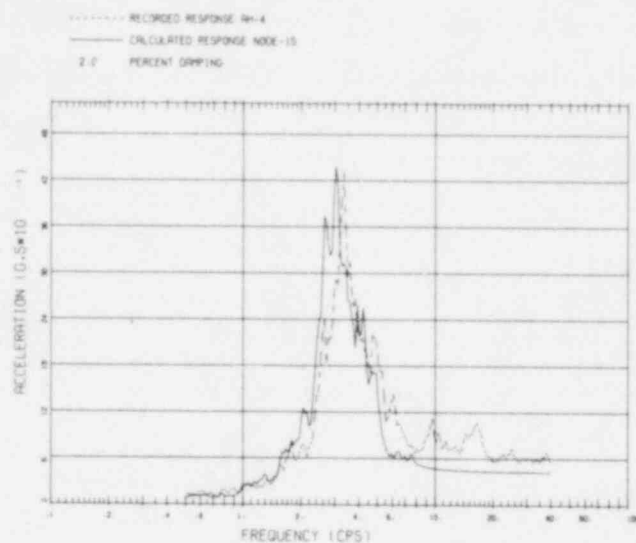


(b) Elev. 25.9 M

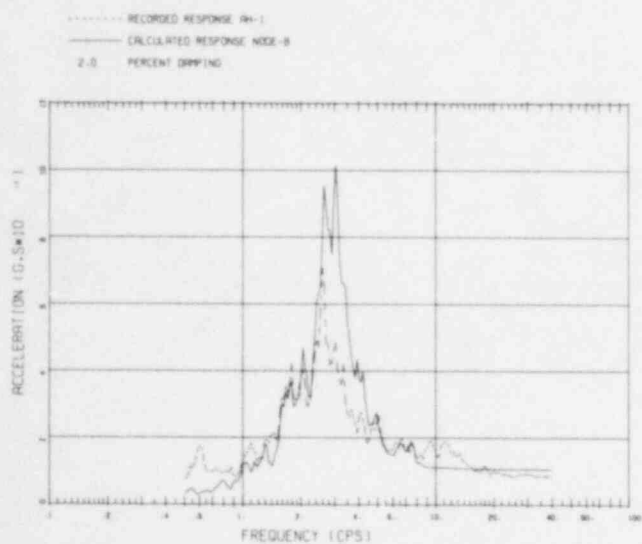
Fig. A.31 Comparison of Measured and Calculated Structural Spectra (Fixed Base Model; Measured Pulse Directly Under Basemat Input; Standard Interaction Parameters Except Moment Spring 160% of Standard)



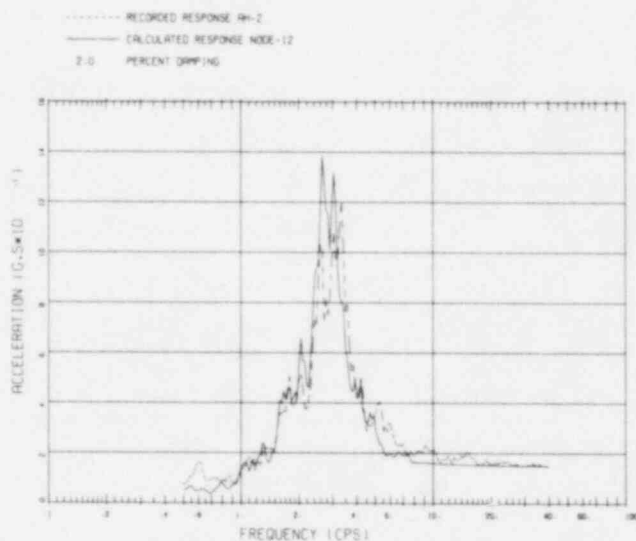
(c) Operating Floor



(d) Top of Structure

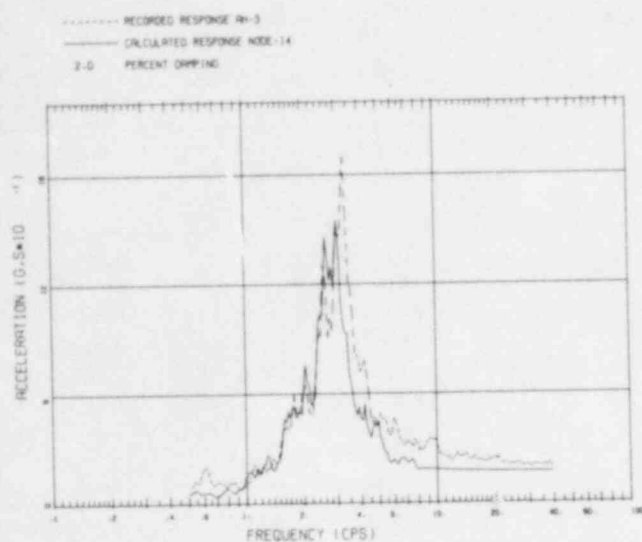


(a) Basemat

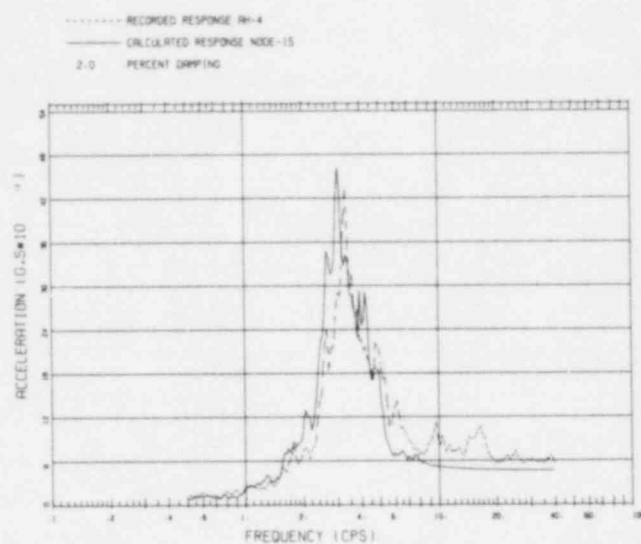


(b) Elev. 25.9 M

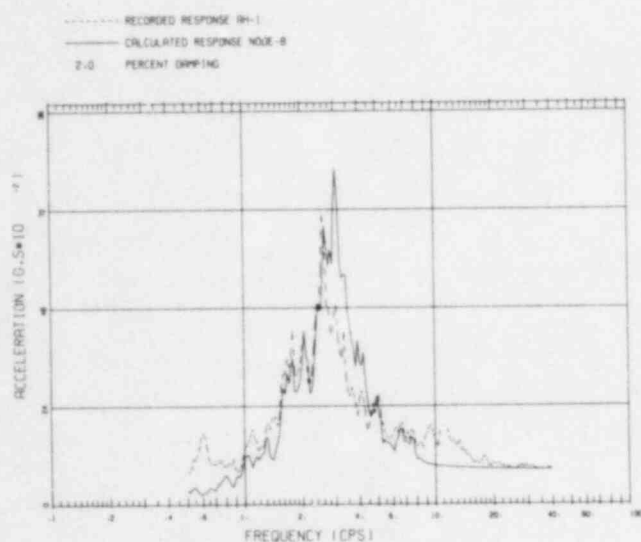
Fig. A.32 Comparison of Measured and Calculated Structural Spectra (Fixed Base Model; Calculated Pulse Using 10% Soil Damping Input; Standard Interaction Springs; 200% of Standard Interaction Dampers)



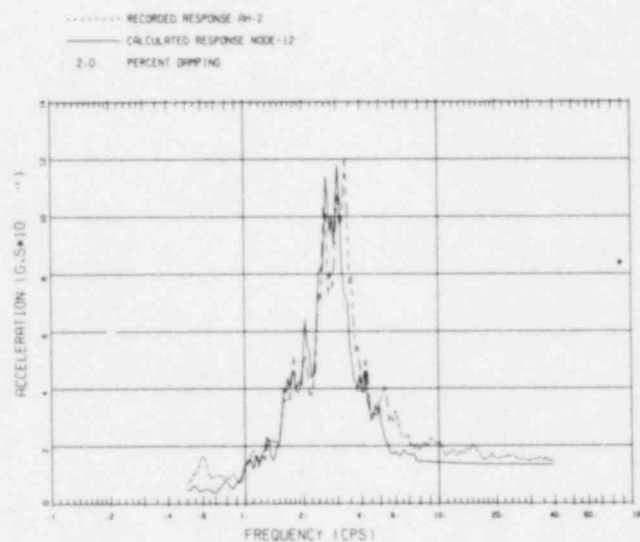
(c) Operating Floor



(d) Top of Structure

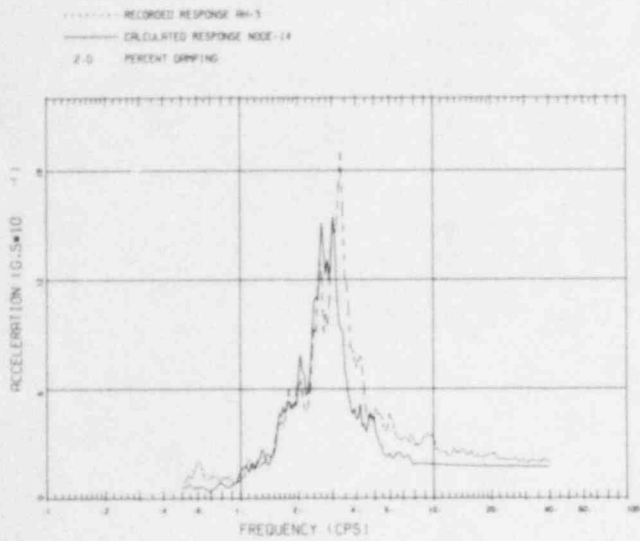


(a) Basemat

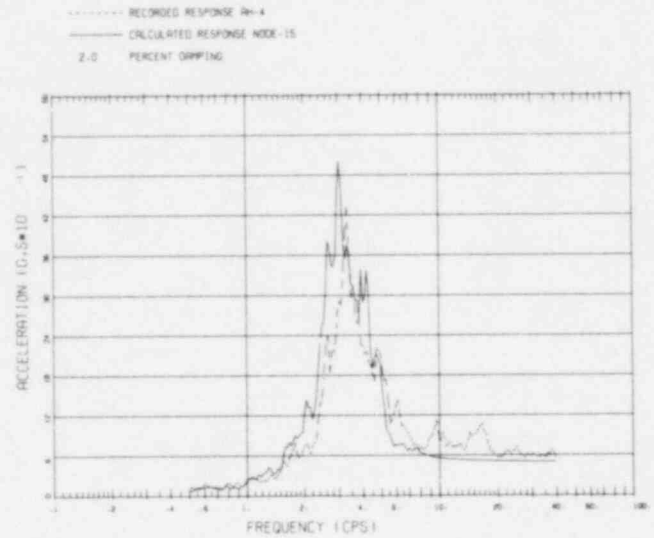


(b) Elev. 25.9 M

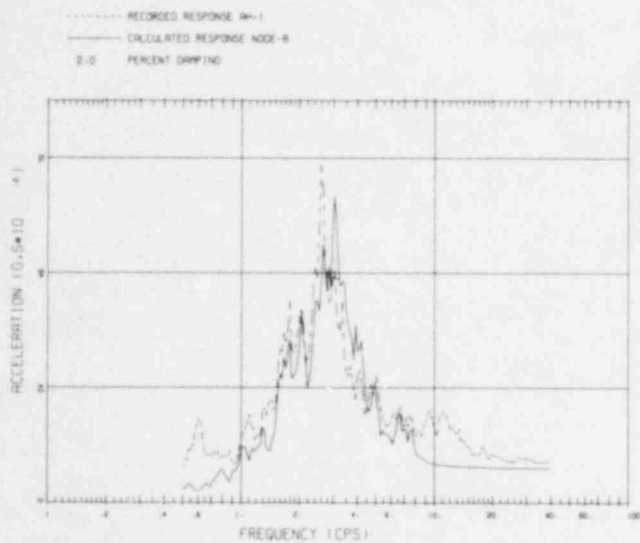
Fig. A.33 Comparison of Measured and Calculated Structural Spectra (Fixed Base Model; Calculated Pulse Using 15% Soil Damping Input; Standard Interaction Springs; 150% of Standard Interaction Dampers)



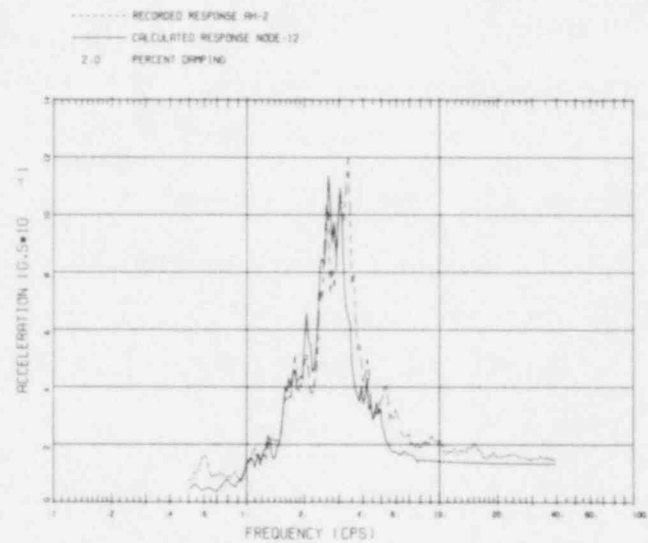
(c) Operating Floor



(d) Top of Structure

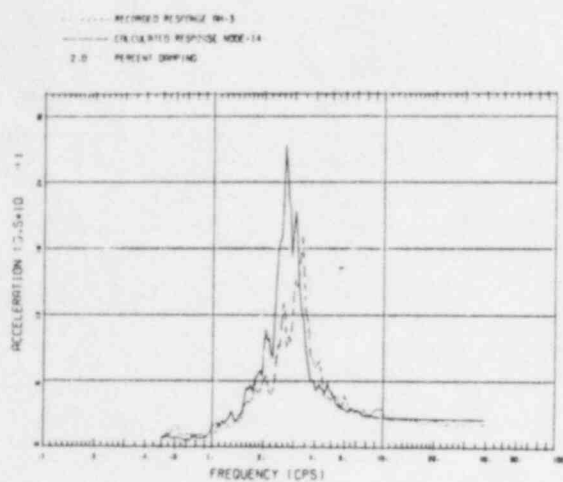


(a) Basemat

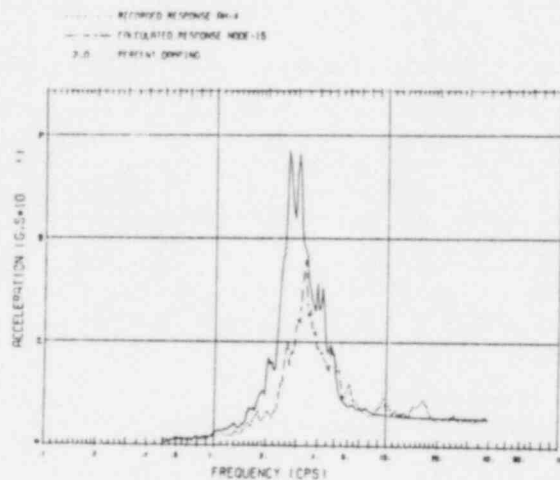


(b) Elev. 25.9 M

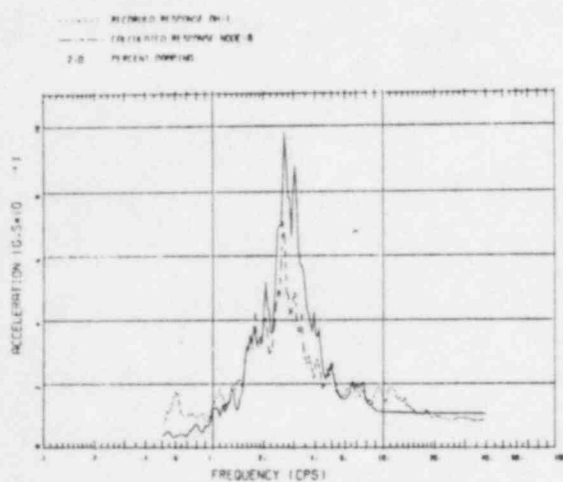
Fig. A.34 Comparison of Measured and Calculated Structural Spectra
(Fixed Base Model; Calculated Pulse Using 20% Soil Damping
Input; Standard Interaction Springs and Dampers)



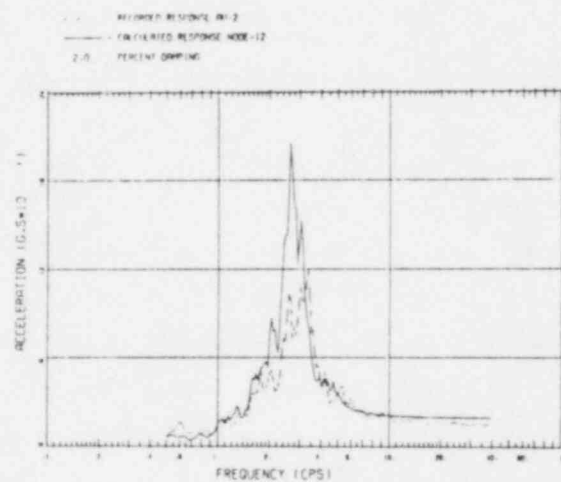
(c) Operating Floor



(d) Top of Structure



(a) Basemat



(b) Elev. 25.9 M

Fig. A.35 Comparison of Measured and Calculated Spectra (Fixed Base Model; Calculated Pulse Using 10% Soil Damping; Standard Interaction Springs and Dampers)

REFERENCES

1. C.A. Miller and C.J. Costantino, "Soil-Structure Interaction Methods-SIM Code", NUREG/CR-1717, Vol. III, Sept. 1979.
2. C.J. Costantino and C.A. Miller, "Soil-Structure Interaction Methods-SLAVE Code", NUREG/CR-1717, Vol. II, Sept. 1979.
3. H. Tanaka and M. Nakahara, "Investigation of Soil-Building Interaction Behavior of a BWR Plant During Miyagiken-Oki Earthquake of 1978".
4. K. Muto and K. Omatsuzawa, "The Earthquake Response Analysis for a BWR Nuclear Power Plant Using Recorded Data", First SMIRT, Sept. 1971.
5. C.J. Costantino and E. Vey, "Response of Buried Cylinders Encased in Foam", Journal of Soil Mechanics, ASCE, Sept. 1969.
6. R.J. Bathe, F.L. Wilson, and F.L. Peterson, "A Structural Analysis Program for Static and Dynamic Response of Linear Systems", Earthquake Engineering Research Center, University of California, June 1973.
7. R.V. Whitman, "Soil-Structure Interaction, Seismic Design for Nuclear Power Plants", MIT Press, 1970.
8. Y.O. Beredugo and M. Novak, "Coupled Horizontal and Rocking Vibration of Embedded Footings", Canadian Geotechnical Journal, 1972.

Correlation of SIMQUAKE II Data With
Lumped Parameter Codes
Appendix B

CORRELATION OF SIMQUAKE II DATA WITH LUMPED PARAMETER CODES

1.0 INTRODUCTION

This report describes the work performed on one of the tasks of the "Soil/Structure Interaction Verification" Program. The objective of this program is to correlate the results of the standard SSI methods of analysis with measured SSI data. The methods of analysis considered on the program are: the lumped parameter SSI model, the finite element model, and the substructuring method. Potential data sources for making the correlations include: measurements taken at the Fukushima Nuclear Power Plant, the SIMQUAKE experiment performed to model the seismic response of nuclear power plant containment structures, and the Department of Defense experiments performed to validate the response of missile launch facilities to nuclear weapon induced ground shock. This report contains comparisons between the SIMQUAKE II measured data and predictions made using the lumped parameter methodology.

The SIMQUAKE experiments were performed during the late 1970's at the University of New Mexico's McCormick Ranch test site south of Albuquerque, New Mexico. The objective of the test series was to simulate the effects of strong earthquake motions on nuclear power plant containment structures. High explosive charges were used to induce the ground motion. The containment structures were modeled with concrete cylinders founded on a circular foundation. The structures had scale factors ranging from 1/8 to 1/48. The total series consisted of three tests: Mini-SIMQUAKE, SIMQUAKE I, and SIMQUAKE II. This study uses the data from SIMQUAKE II since it most closely represents the earthquake motion levels of general interest. A complete description of the experiments is given in Refs. 1 and 2.

The lumped parameter method is based upon a finite element model of the structure coupled to the free field with springs and dampers intended to represent the interaction process. The free field motion is input to the base of the spring/damper interaction model. There are two major areas of

uncertainty which arise in the use of the lumped parameter method to solve soil/structure interaction problems. The first is concerned with the numerical values to be assigned to the springs and dampers used to couple the structure to the soil. Spring-damper models are used to represent the interaction process between the soil and the base of the structure and between the soil and the sidewalls of the structure (if it is embedded in the soil). The second area of uncertainty is concerned with the free field seismic motion to be used as input to the model. The lumped parameter method neglects any feedback from the structure to the free field and used as input the free field motions which would be expected at the site if the structure were not there. Each of these areas is considered.

The SIM Code (Ref. 3) is used to perform the lumped parameter SSI calculations. It should be emphasized, however, that this code is typical of those used by the industry. It should be expected that conclusions drawn from this study are applicable to any lumped parameter code.

The SIMQUAKE II experiment and actual measurements taken are described in Section 2.0. Section 3.0 contains a description of the SIM Code results. The conclusions of the study are given in Section 4.0.

2.0 DESCRIPTION OF SIMQUAKE II EXPERIMENT

This section of the report contains a description of the SIMQUAKE II experiment. Details of the experiment are given first. The measurements which were taken during the test are then described; some analyses of these data are made. Other studies which have been based on these data are then discussed.

2.1 SIMQUAKE II Experiment

The SIMQUAKE II experiment was conducted on June 2, 1977 at the University of New Mexico's McCormick Ranch test site south of Albuquerque, New Mexico. The test was conducted by the Civil Engineering Research Facility of the University for the Electric Power Research Institute. A summary report of the experiment is given in Ref. 1, while a more complete description is contained in the eight volume report of Ref. 4. The data used in this study is taken from Ref. 4 and a magnetic tape containing all of the recorded free field and in-structure measurements. This tape was obtained from EPRI through Applied Research Associates (Albuquerque, New Mexico).

Figures B.1 and B.2 show a plan and elevation taken through the test site. Specific details of the loading, structural models, instrumentation and soil properties are discussed in the following sections.

The loading was induced with two plane, high explosive arrays each covering a vertical plane about 200 feet wide and 75 feet deep. The top of the arrays were placed about 25 feet below the surface. The arrays were separated by 100 feet. The back array consisted of 12 explosive charges, each being 16 inches in diameter and 75 feet long. The front array contained 16 charges, each being 12 inches in diameter and 75 feet long. The back array was fired first and was followed 1.2 seconds later by the front array.

The test area containing the structural models were located about a line normal to the plane of the arrays and originating at the center of the

arrays. The closest structure was 200 feet from the front array while the furthest structure was located 250 feet from the front array. Six structures were placed in the test area. Structure S04 was isolated from its basemat and S03 was filled with water. Neither of these structures is considered in this study. A typical sketch of a test structure is shown on Fig. B.3. The structures consist of a concrete cylinder founded on a circular concrete slab. Steel plates are placed on the surface of the concrete to simulate the reinforcement. Structural frequencies of these structures are all over 40 cps. The structures are therefore considered to be rigid in all of these computations. Dimensions of the structure are shown on Table 2.1.

Table 2.1
Dimensions of Structural Models

Parameter*		S01	S02	S05	S06
Scale		1/8	1/12	1/24	1/12
Range	(feet)	200.	200.	225.	250.
D	(feet)	15.	10.	5.	10.
H	(feet)	22.50	15.30	7.50	15.30
B	(feet)	2.26	1.50	0.73	1.50
C	(feet)	1.51	1.00	0.50	1.50
Weight	(kips)	253.31	78.04	9.70	78.04
Embedment	(%)	25.00	25.00	25.00	25.00

* See Fig. B.3 for definition of parameters

The free field instrumentation was placed in eleven holes, labeled B01 through B11 on Figs. B.1 and B.2. The instrument number and type of measurement is noted on Fig. 2.2. The first letter designates the type of measurement (A = acceleration; V = velocity) while the second indicates the direction (H = horizontal; V = vertical; T = tangential). As may be seen there was extensive instrumentation placed in the test bed area at depths of 5 feet, 20 feet, 35 feet and 62.5 feet.

There were also extensive measurements taken on and in the immediate vicinity of each of the test structures. Horizontal accelerations were measured at the top and bottom of the structure. Vertical accelerations were measured at the upstream and downstream sides of the basemat. Rotational accelerations were measured at the middle of the basemat, and transverse accelerations were measured at the downstream side of the basemat. Interface pressure measurements were made along the side of the structure and on the bottom surface of the structure.

The top 26 feet of the soil at the test site consists of alternating layers of fine silts, clay and caliche. Dry cohesionless sand extends from this depth to an unknown depth. The ground water table is below 300 feet. Wave speed properties as determined from refraction surveys and uphole and crosshole measurements are given on Table 2.2.

Table 2.2
Seismic Properties of Test Site

Depth (feet)	P-Wave (ft/sec)	S-Wave (ft/sec)	Density (lb/cu. ft)
0- 6	1198	804	95
6-25	1952	951	113
25-90	2493	1099	120
90-	3199	unknown	unknown

2.2 SIMQUAKE II Free Field Measurements

The location of the free field, in-structure, and near structure measurements are discussed in the previous section. A complete listing of the data is contained in Ref. 4. The measured data in and near to the structures are

discussed in Section 3.0 where the comparisons are made between the measured and computed structural motions. Some of the free field measurements are discussed in this section for the purpose of defining the general level and characteristics of the free field motion.

Spectra (2% damping) of the measured free field pulses at a depth of 5 feet and ranges of 150 feet, 200 feet and 300 feet from the front array are shown on Figs. B.4 through B.6 respectively. A tabulation of the major peaks in the spectra are shown on Table 2.3.

Table 2.3
Free Field Spectral Peaks (G's) at Depth of Five Feet

Frequency (cps)	Range=150'	Range=200'	Range=300'
1.7	4.7	3.7	2.8
2.7	4.6	3.9	3.1
3.6	4.6	3.8	2.2
4.3	5.0	5.0	2.2
5.4	4.4	4.0	3.8
8.5	5.6	3.1	2.7
24.0	5.8	4.1	1.3

It may be seen that these spectra have more pronounced peaks and have higher frequency content than occurs in typical earthquake records. The peak accelerations in the three pulses are 3.8 G's, 2.3 G's and 0.93 G's.

The variation of the free field motion with depth is shown on the spectra at a range of 200 feet and depths of 5 feet, 20 feet and 62.5 feet. The 5 feet deep spectra is given in Fig. B.5 while the 20 feet and 62.5 feet spectra is shown on Figs. B.7 and B.8. The motion may be seen to be rather uniform over the top 20 feet but there are significant attenuations of the motion of the lower frequency content by a depth of 62.5 feet. The high frequency end

of the spectra may be seen to be larger at the deeper depths, however. The peak accelerations in all of the pulses are associated with firing of the back array. These peaks at the 200 feet range are 2.3 G's at the 5 feet and 20 feet depths while the peak increases to 5.0 G's at the 62.5 feet depth. It would appear that the high frequency end of the free field spectra are associated with energy generated when the back array is fired and that this energy travels through the deeper stiffer soil.

Spectra of the vertical, 200 feet range free field motion are shown on Figs. B.9 and B.10 for depths of 5 feet and 20 feet. These spectra contain spectral peaks 6.0 and 7.0 cps in addition to the peaks which occur for the horizontal spectra. The ratios of vertical to horizontal spectral peak accelerations appear to increase as the frequency increases.

2.3 Other Studies of SIMQUAKE II

Higgins (Ref. 5) described the SIMQUAKE series of tests and analyzed the data. Comparisons were made between the measured free field and in-structure motions to determine the form of the soil/structure interaction process. Large rocking motion of the test structures was noted. This rocking motion was associated with a nonlinear interaction model. The nonlinearities in the model were associated with separation of the structure base from the soil (liftoff), and separation of the sidewalls from the backfill.

Nonlinear finite element analyses of S01 and S02 were made by Vaughan and Isenberg (Ref. 6). A soil island ranging from 150 feet to 300 feet from the front array was modeled. The measured motions were used as input to the boundaries of this model. Crack elements were included at the soil/structure interface so that liftoff effects could be included. The soil is generally modeled with a plasticity cap model (Coulomb-Mohr model with a cap on the compression zone). Good correlation is found between measured and computed response values.

3.0 COMPARISONS OF CALCULATED AND MEASURED DATA

Comparisons are made between the measured and calculated response of structures S01, S02, S05 and S06. Response spectra (2% damping) are used to make the comparisons. Spectra of the measured horizontal motions at the top and bottom of the structure and the measured vertical motion of the structures' base are compared with spectra of the calculated responses. The geometry of the structures and their ranges from the front array are given in Table 2.1.

SIM Code (Ref. 3) is used to perform the calculations. This code is described in some detail in Section 4.1 of Appendix A. It is a lumped parameter code which carries out the solution of the equations of motion in the time domain. Springs and dampers are used to represent the soil/structure interaction process. Since the frequencies of the test structures are all greater than 40 cps rigid models of the structures are used for the calculations. The form of the interaction parameters are described in Section 3.1.

The test data indicate that liftoff occurred for all of the test structures. All of the lumped parameter soil/structure interaction computer codes use linear models to represent the interaction process. Therefore they cannot be expected to give a good representation of interaction effects when liftoff occurs. A primary objective of these comparisons is to evaluate the extent to which liftoff effects may be modeled with a linear interaction law. The amount of liftoff which occurred in the SIMQUAKE experiments is discussed in Section 3.2.

The detailed comparisons of the measured and calculated in-structure response spectra are made in Section 3.3. Parameters of the interaction model are varied to obtain a "best fit" of the measured spectra. These variations allow conclusions to be drawn regarding the sensitivity of the results to the actual parameters used to model the interaction forces.

3.1 Soil/Structure Interaction Parameters

Two models are used to represent the interaction process for the SIMQUAKE structures. One models interaction forces at the basemat and the second models forces transmitted through the sidewalls (the structures are embedded 25% into the free field).

The basemat interaction model is based on the analytic solutions for a rigid circular foundation vibrating on a homogeneous elastic half space. The equations used to calculate the interaction springs and dampers are:

$$K_H = \frac{28.8 G R (1-\mu)}{7-8\mu}$$

$$C_H = \frac{18.24 \rho_c R^2 (1-\mu)}{7-8\mu}$$

$$K_V = \frac{4 G R}{1-\mu}$$

$$C_V = \frac{3.4 R^2 \rho_c}{1-\mu}$$

$$K_\theta = \frac{2.13 G R^3}{1-\mu}$$

$$C_\theta = \frac{0.4 \rho_c R^4}{(1-\mu)}$$

where K_H , K_V , K_θ = horizontal, vertical and rocking springs

C_H , C_V , C_θ = horizontal, vertical and rocking dampers

G = soil shear modulus

R = foundation radius

μ = soil Poisson's ratio

$\rho_c = \sqrt{\gamma G/g}$

γ = soil density

g = gravitational constant

The sidewall interaction model represents the pressures exerted on the wall of the structure as proportional to the relative displacement and velocity normal to the wall surface. This model is based (Ref. 7) on the form of analytic solutions and parameters of the model are based on experimental data. The specific form of the model is

$$\sigma_r = k \Delta u + c \dot{\Delta u}$$

where σ_r = radial pressure acting on radial

Δu = relative radial displacement

$\dot{\Delta u}$ = relative radial velocity

A summary of the interaction parameters for the SIMQUAKE test structures is given in Table 3.1. These parameters are based on the following soil properties:

Shear Modulus 3170 ksf

Poisson's Ratio 0.3

Density 113 pcf

The dimensions of the structures are given in Table 2.1.

Table 3.1

Interaction Parameters (All Units-Kip-Feet-Seconds)

Parameter	Structure #		
	S01	S02=S06	S05
Base Model:			
Rotational Spring	4070000.	1210000.	1510000.
Trans. Spring	104000.	69500.	34700.
Vertical Spring	135800.	90550.	45280.
Rotational Damper	6030.	1191.	74.5
Trans. Damper	521.	231.	57.9
Vertical Damper	911.	405.	101.3
Sidewall Model:			
Rotational Spring	1034000.	325000.	38300.
Trans. Spring	98030.	66600.	32680.
Rotational Damper	4361.	914.	53.8
Trans. Damper	414.	188.	46.0
Horizontal Freq (cps)	25.5	27.7	75.3
Rotational Freq (cps)	10.6	16.0	31.7
Vertical Freq (cps)	20.9	30.0	61.7
Horizontal Damp (% crit)	37.5	36.5	36.5
Rotational Damp (% crit)	6.8	6.9	6.7
Vertical Damp (% crit)	44.1	43.2	26.4

It may be seen that the interaction frequencies are rather high and that the sidewall model parameters are relatively small as compared with the base model parameters. The free field motion has significant content and frequencies up through at least 30 cps (see Figs. 2.4 through 2.10). One would expect that soil/structure interaction effects are important for the experiment therefore.

3.2 Uplift Effects

The vertical axes of all of the structures were permanently rotated during the SIMQUAKE II experiment. This is reported in Refs. 1, 5, and 6. It was also reported that a gap existed after the experiment between the sidewall and the backfill. The input free field motion was sufficiently large to cause separation of the foundation from the soil (i.e., uplift). This uplift may be observed in the interface pressure measurement shown on Fig. B.11. This pressure gage was mounted under the downstream side of the basemat. The upstream gage shows a similar record with the cycles out of time phase indicating a rocking motion. The negative pressures indicate tensile pressure. The 0.8 MPA pressure is equivalent to 11.6 psi. The bearing pressure due to the weight of S01 is 10.0 psi. The difference between the 11.6 psi pressure and the 10.0 psi is most likely due to the additional restraint against overturning provided by sidewall interaction effects. Therefore, one may conclude that liftoff occurred when the tensile pressure reached the bearing pressure.

Uplift is a nonlinear phenomena, and one would expect difficulty in matching nonlinear results with the use of a linear interaction model. All of the currently used lumped parameter interaction models are linear. The objectives of the comparisons are to determine the magnitude and character of errors which occur when the linear interaction models are applied. A study is also conducted to determine whether a simple variation of the linear interaction model could be made which account for the nonlinear effects. These investigations are reported in Section 3.3.

It is of interest to investigate the magnitude of the seismic disturbance which would be expected to result in uplift. Consider the simple model shown in Fig. B.12 and constrained so that the base moves with the free field. A base motion is input of magnitude (x) and duration (t). The duration is sufficiently small so that it may be considered as an impulse. This motion would represent a single spike in an overall seismic time history. The recorded peak acceleration spikes in the SIMQUAKE II data has durations of about 0.03 seconds. This imposed base motion is equivalent to an initial

rotational velocity of

$$\dot{\theta}_0 = \frac{M(\ddot{x}\Delta t)}{J} \ell$$

The equation of motion for the system shown in Fig. B.12 is

$$J\ddot{\theta} + K\theta = 0$$

For zero initial rotation and the initial rotational velocity developed above, this system has the solution

$$\theta = \frac{\dot{\theta}_0}{\omega} \sin \omega t$$

$$\text{where } \omega^2 = K/J$$

The maximum rotational response is

$$\theta_{\max} = \dot{\theta}_0 / \omega$$

This corresponds to a base moment (m) and peak interaction stress (σ) of

$$m = K\dot{\theta}_0 / \omega$$

$$\sigma = \frac{m}{S} = \frac{4K\dot{\theta}_0}{\omega\pi R^3}$$

Liftoff will occur when the peak stress exceeds the interaction stress due to the weight of the structure. Therefore the required magnitude of the peak accelerations to produce liftoff may be determined as

$$\frac{4K\dot{\theta}_0}{\omega\pi R^3} = \frac{gM}{\pi R^2}$$

$$(\ddot{x}_m \Delta t) = \frac{gR}{\Delta \ell} \sqrt{\frac{J}{K}}$$

The values of this peak acceleration for structures S01 and S06 are

$m = 0.11$ G's for S01

$m = 0.07$ G's for S06

While the model is based upon rather gross approximations to the real situation, it does indicate that liftoff is expected in the SIMQUAKE II tests. Since the actual accelerations are much larger than the predicted liftoff accelerations, one would also expect the effects associated with liftoff to be significant.

3.3 Comparisons of Measured with Calculated In-Structure Spectra

Predictions are made for the response of structures S01 and S06. These structures are used because the S01 is closest to the explosive arrays and S06 is furthest from the arrays of all of the test structures. The test structure properties are given in Table 2.3 and the interaction parameters are given in Table 3.1. The input free field motion used for both cases is the measured pulse directly below the structure. Comparisons are made between the measured and calculated response spectra. Horizontal spectra are compared at the top and bottom of the structure and vertical spectra at the base of the structure are compared. In all cases 2% damped spectra are used.

The horizontal spectra are shown on Fig. B.13 for S01 using the standard interaction parameters. The solid curves represent the calculated values while the dashed curves shown the measured data. As may be seen the correlation is reasonable at the base of the structure but it is poor at the top of the structure. The calculated spectra indicate a much higher frequency content than does the spectra of the measured data. This undoubtedly is caused by liftoff. One would expect lower frequencies when the structure lifted off and tipped from front toe of the foundation to the back toe of the foundation. The interaction parameters were then varied in an attempt to obtain a better correlation between the measured and calculated

data. Figure B.14 shows the spectral comparisons when sidewall interaction is neglected. The correlation is better, but still quite poor at the top of the structure. Comparisons are shown on Figs. B.15 and B.16 for spectra calculated using interaction parameters based on 50% and 25% of the measured soil modulus. Once again it is seen that the general shape of the calculated spectra is quite different from that of the measured spectra. A comparison of the calculated and measured vertical spectra is shown on Fig. B.17. The calculated spectra is significantly lower than the measured spectra. This once again may be attributed to liftoff effects. When liftoff does not occur there is no coupling between the horizontal and vertical response. However when the structure lifts off due to the horizontal force, a net upward vertical resultant force occurs on the base causing a vertical response. This coupling is additive to the normal vertical response of the structure. Therefore one would expect that liftoff will cause larger vertical responses than would be anticipated with a linear model.

Similar comparisons are made for structure S06. The comparison of the horizontal spectra using the standard interaction parameters given in Table 3.1 is shown on Fig. B.18. The comparisons neglecting sidewall interaction is shown on Fig. 3.19, and the comparisons using 50% and 20% of the soil modulus to calculate interaction parameters are shown on Figs. B.20 and B.21. The comparison of the vertical spectra is shown on Fig. B.22. The same correlations are found for the S06 structure as is discussed above for the S01.

4.0 CONCLUSIONS

Several "scale" model reactor containment structures were subjected to a blast induced loading during the SIMQUAKE II experiment. The loading was designed (to the extent possible) to simulate large magnitude seismic motions. Extensive instrumentation was placed in the free field and on the structures.

The measured free field pulse is used as input to rigid body models of the structure. Lumped parameter SSI analysis is then performed to calculate spectra of the induced structural motions. These spectra of the induced structural motions. These spectra are then compared with spectra of the measured in-structure motions. The following conclusions are drawn based on the results of these analyses:

1. The measured free field motion is fairly uniform throughout the site with no indication that feedback from the structure had an effect on the free field motion.
2. Significant liftoff occurred for all of the test structures. This is confirmed from: pressure measurements taken at the foundation/soil interface; the permanent notational displacement of the structure, and the disturbance of the soil backfill.
3. Comparisons of the measured and calculated horizontal spectra indicate rather good agreement at the base, but poor agreement at the top of the structure. The calculated spectra indicates much higher frequency content of the motion than was measured and also contains more energy than the measured spectra. Both of these effects are attributable to liftoff effects.

4. The good correlation of the horizontal base spectra indicate that liftoff does not effect the translation interaction, so it only effects the rocking interaction model.
5. The spectra of the measured vertical pulse has much higher peaks than the spectra of the calculated vertical motion. This effect may also be attributed to rocking motions effected by liftoff. When liftoff occurs, the rocking motion results in a net upward force acting on the structure. This couples the vertical response to the horizontal input. This coupling effect is not present when a linear interaction law (which neglects liftoff) is used.
6. Soil parameters were varied in an attempt to obtain a "fit" of the measured spectra with spectra generated from a lumped parameter solution. The soil shear modulus was varied from 20% to 100% of the measured data. The comparison of the measured and computed spectra was still poor indicating that it is not possible to model the nonlinear liftoff phenomena with an equivalent linear model.

B-19

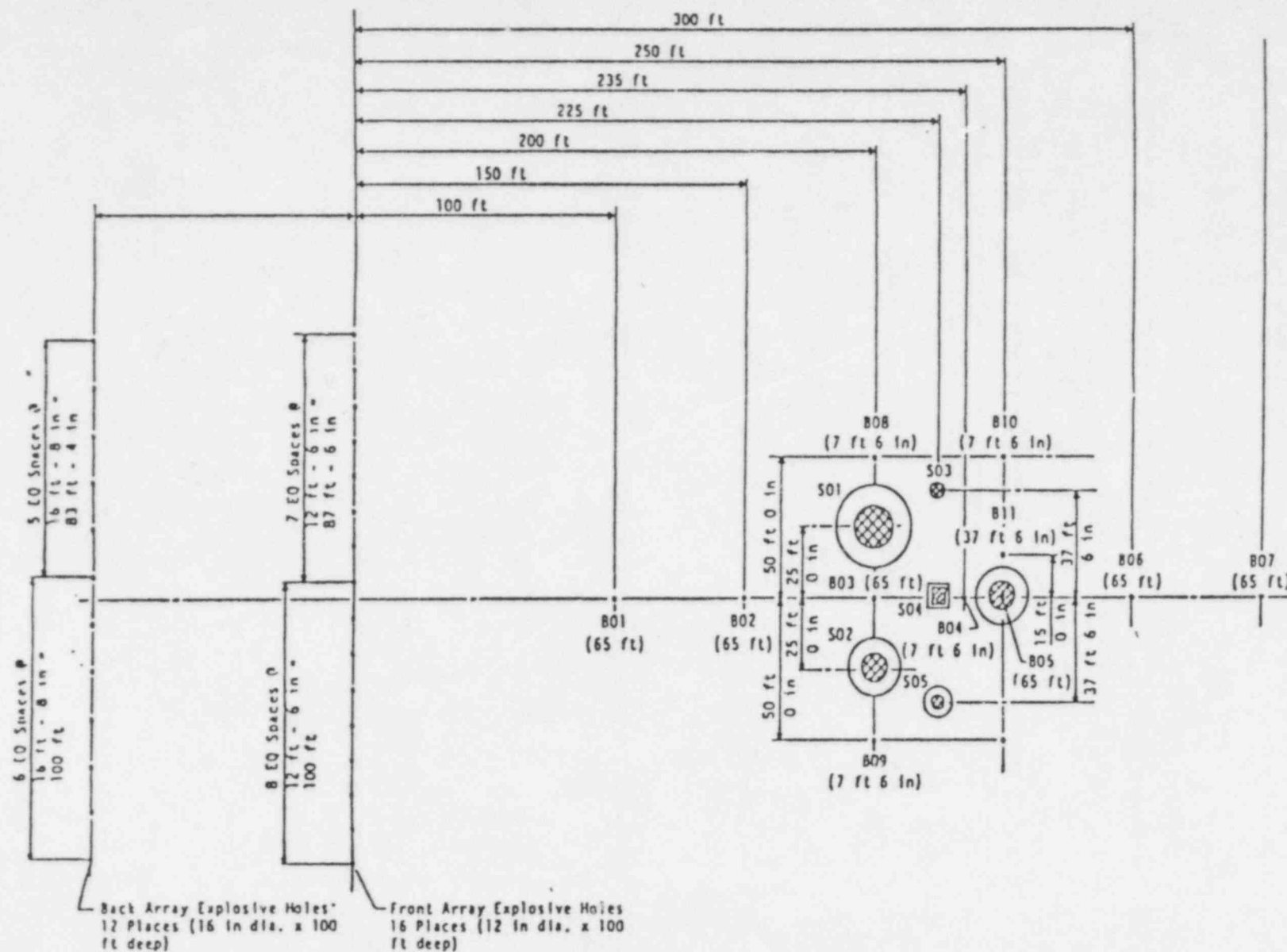


Fig. B.1 SIMQUAKE II Testbed Plan. (Ref. SQ-3)

SIMQUAKE II Front Array

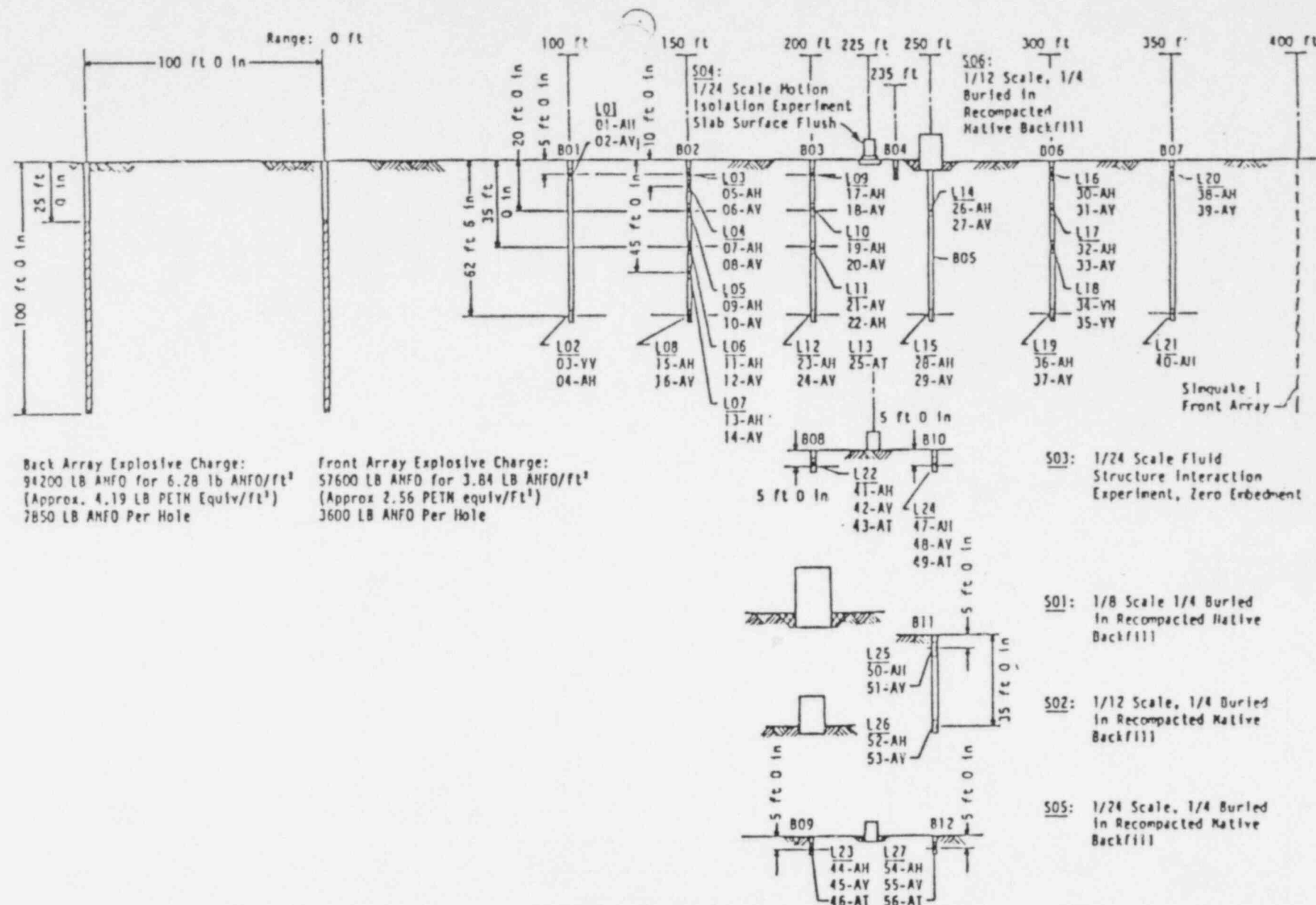


Fig. B.2 SIMQUAKE II Testbed Elevation. (Ref. SQ-3)

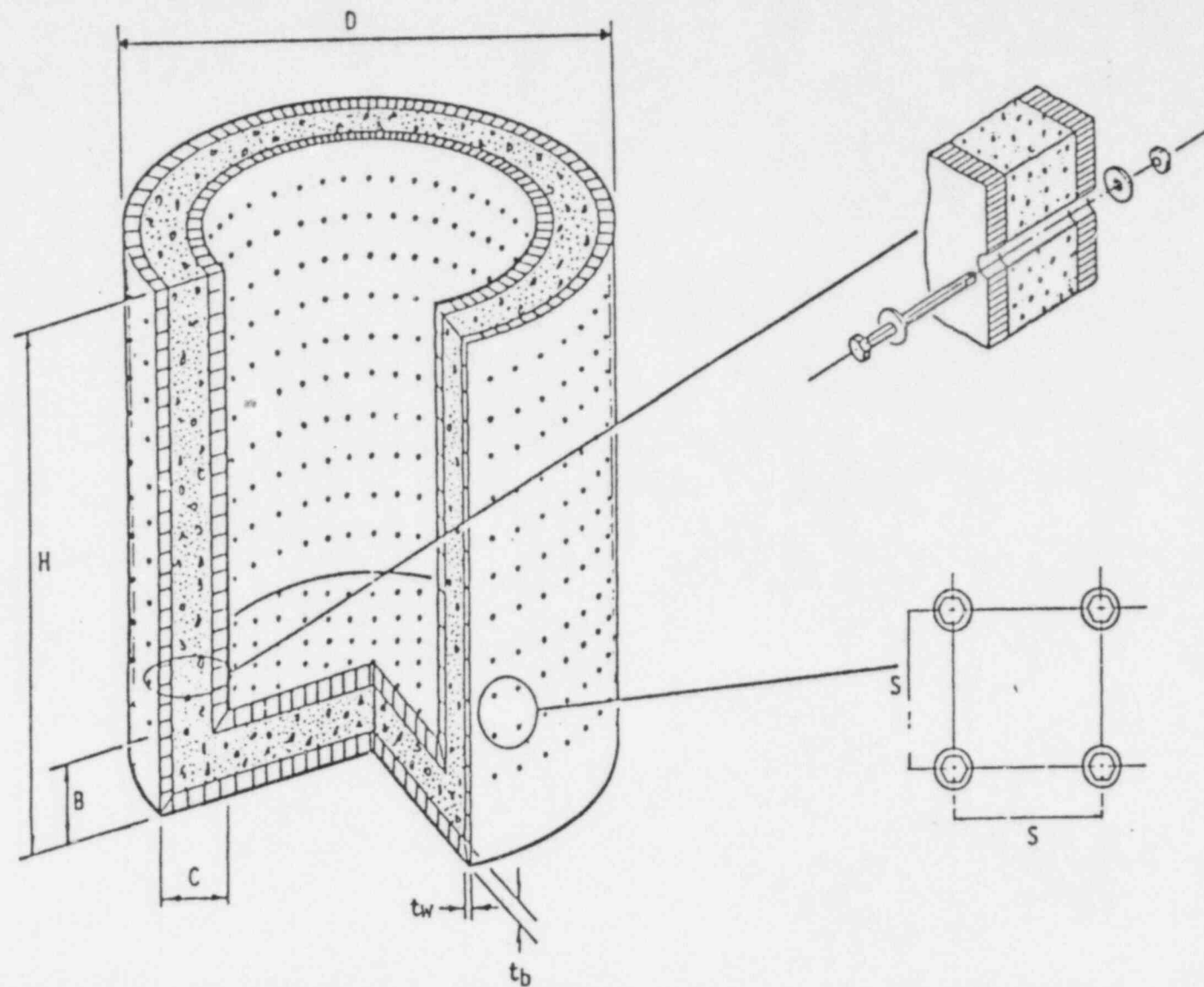


Fig. B.3 Typical SIMQUAKE Model Structure. (Ref. SQ-2)

Fig. B.4 Free Field HOR X=45.72 Y=0 Z=1.52

2.0 PERCENT DAMPING NODE-5

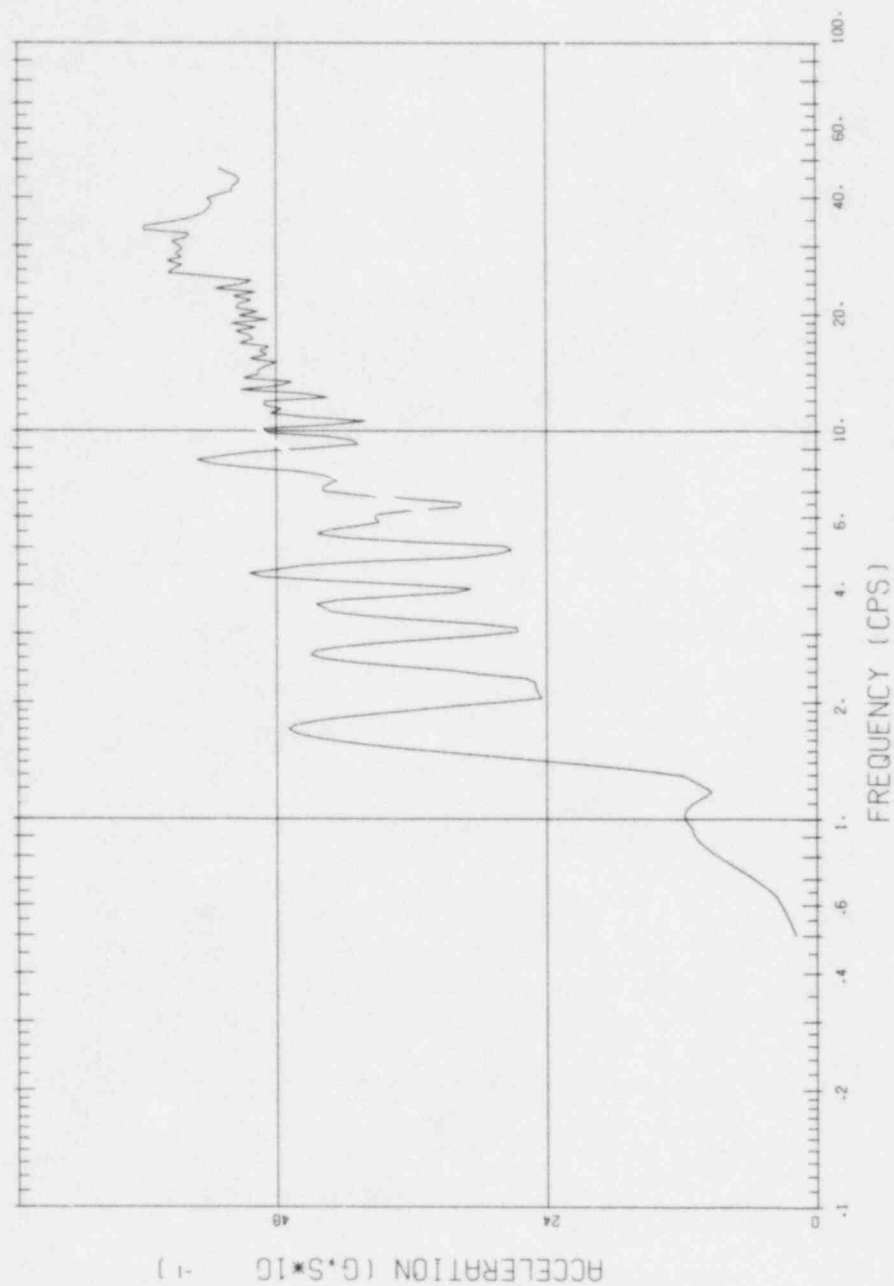


Fig. B.5 Free Field HOR X=60.96 Y=0 Z=1.52

2.0 PERCENT DAMPING

NODE=17

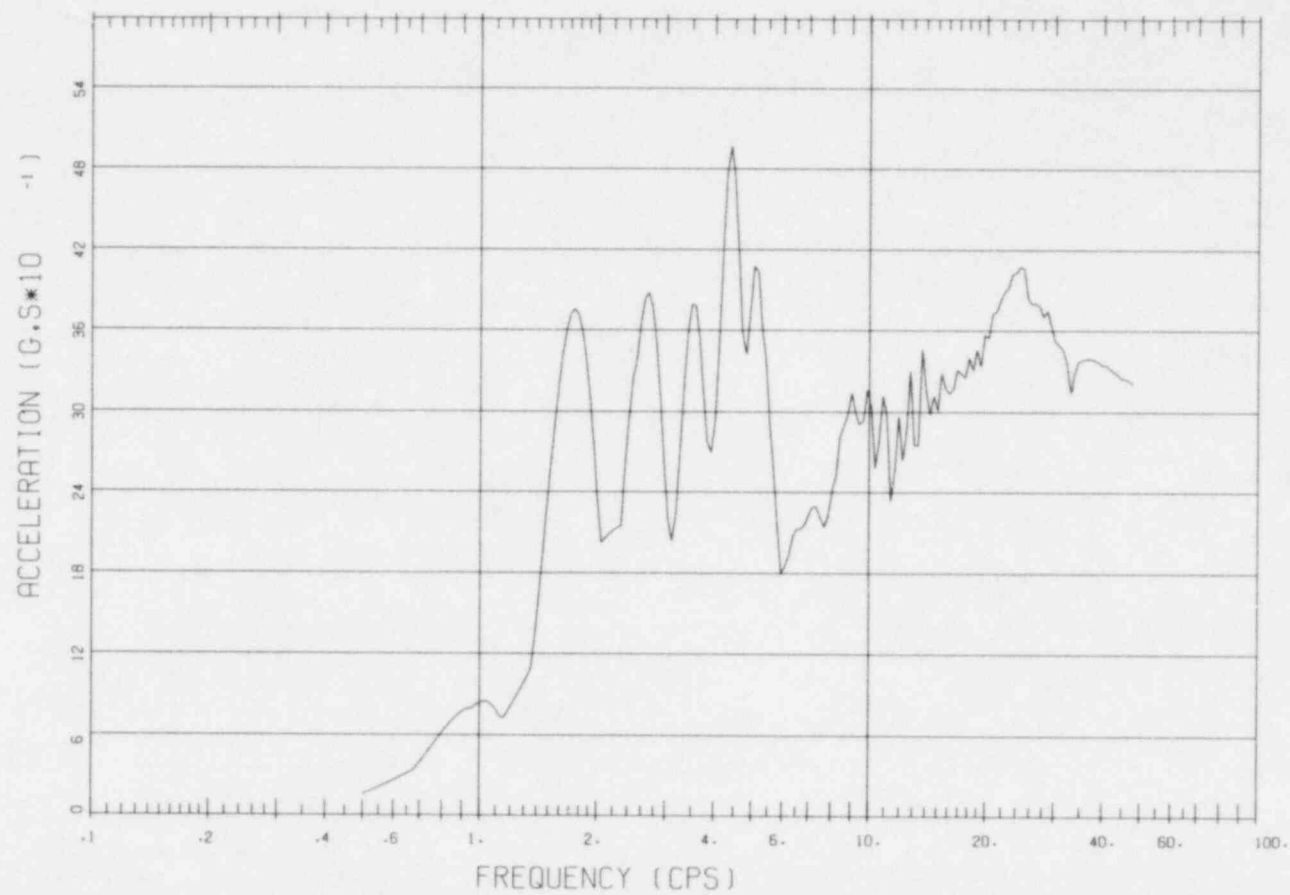


Fig. B.6 Free Field HOR X=91.44 Y=0 Z=1.52

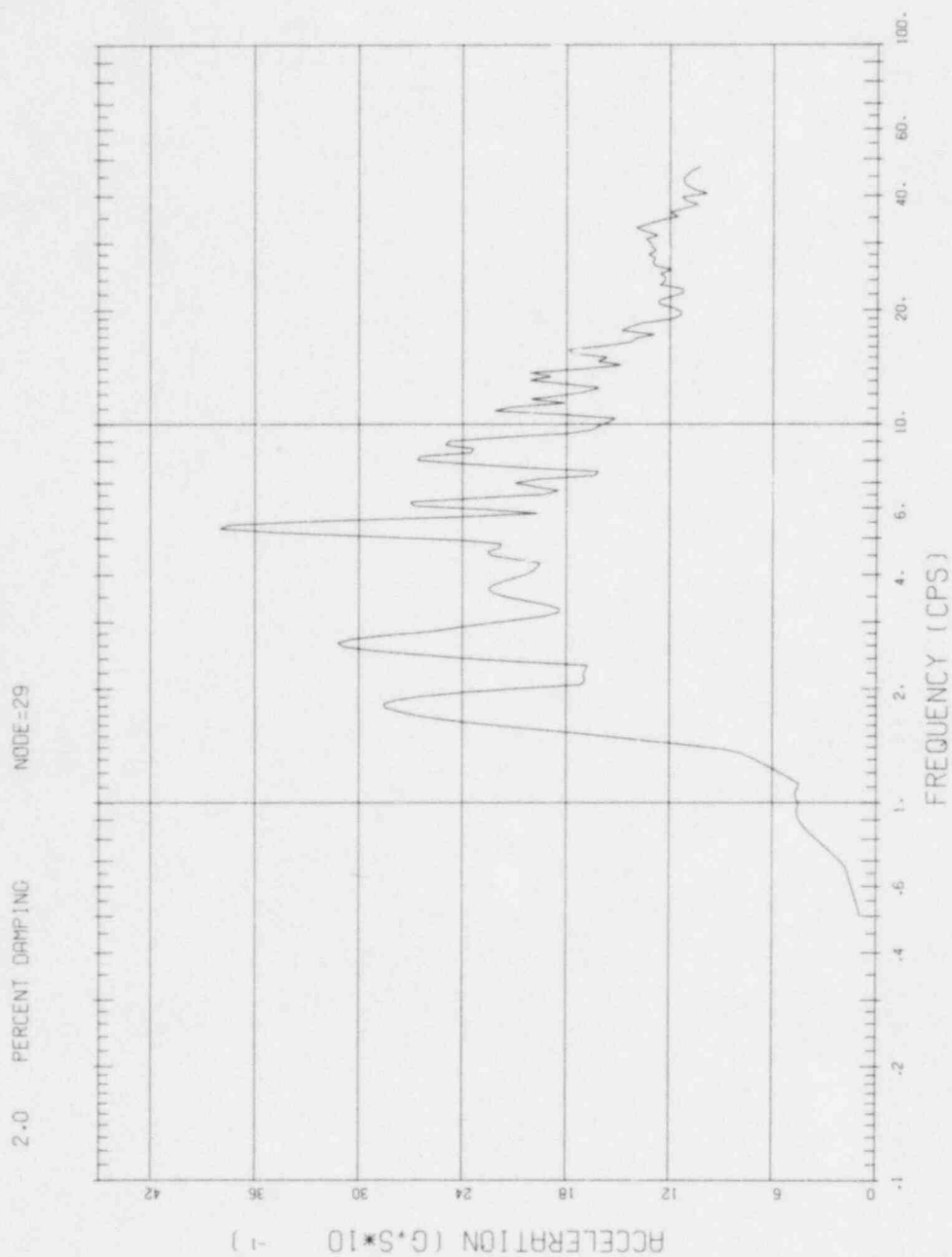


Fig. B.7 Free Field HOR X=60.98 Y=0 Z=6.1

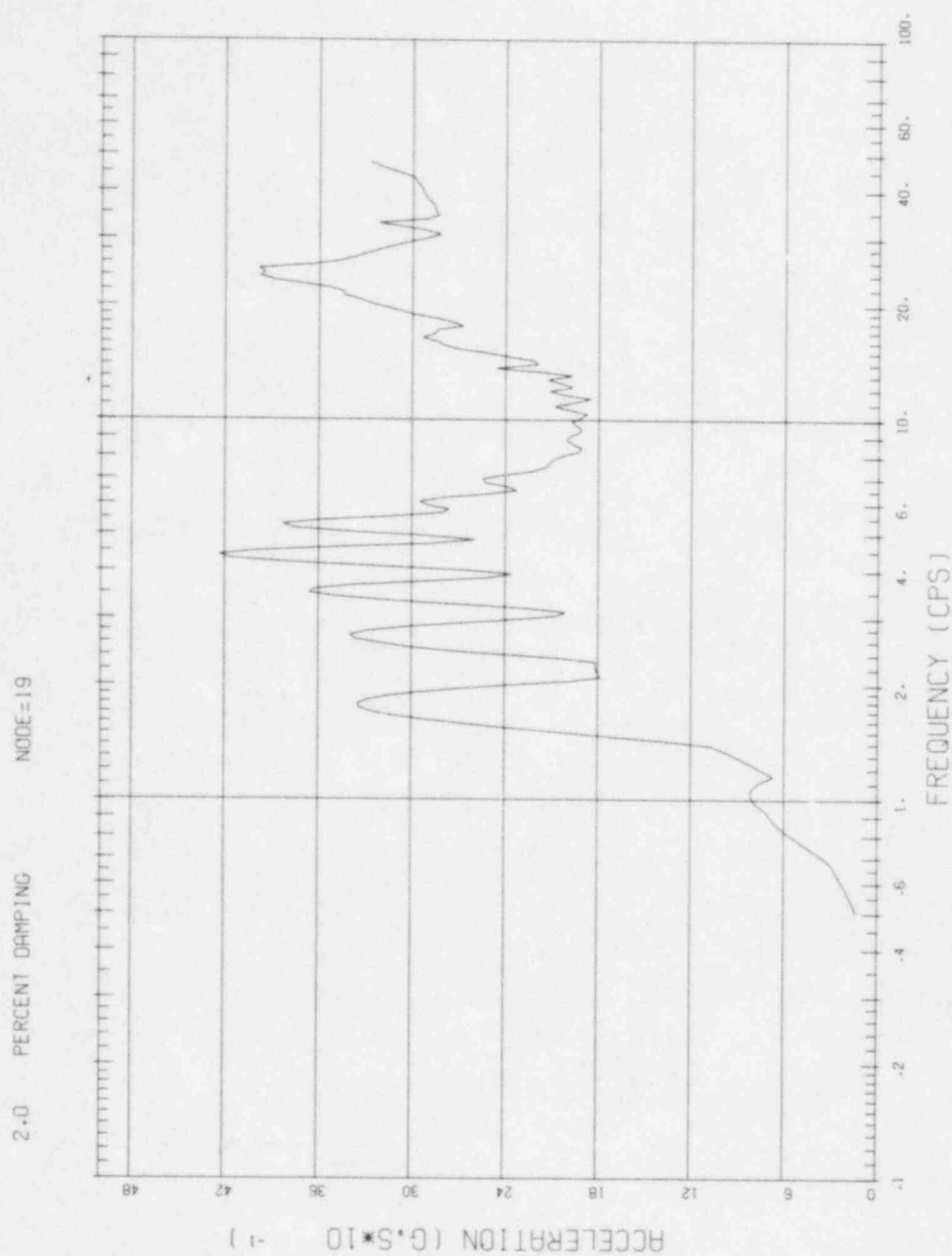


Fig. B.8 Free Field HOR X=60.96 Y=0 Z=19.05

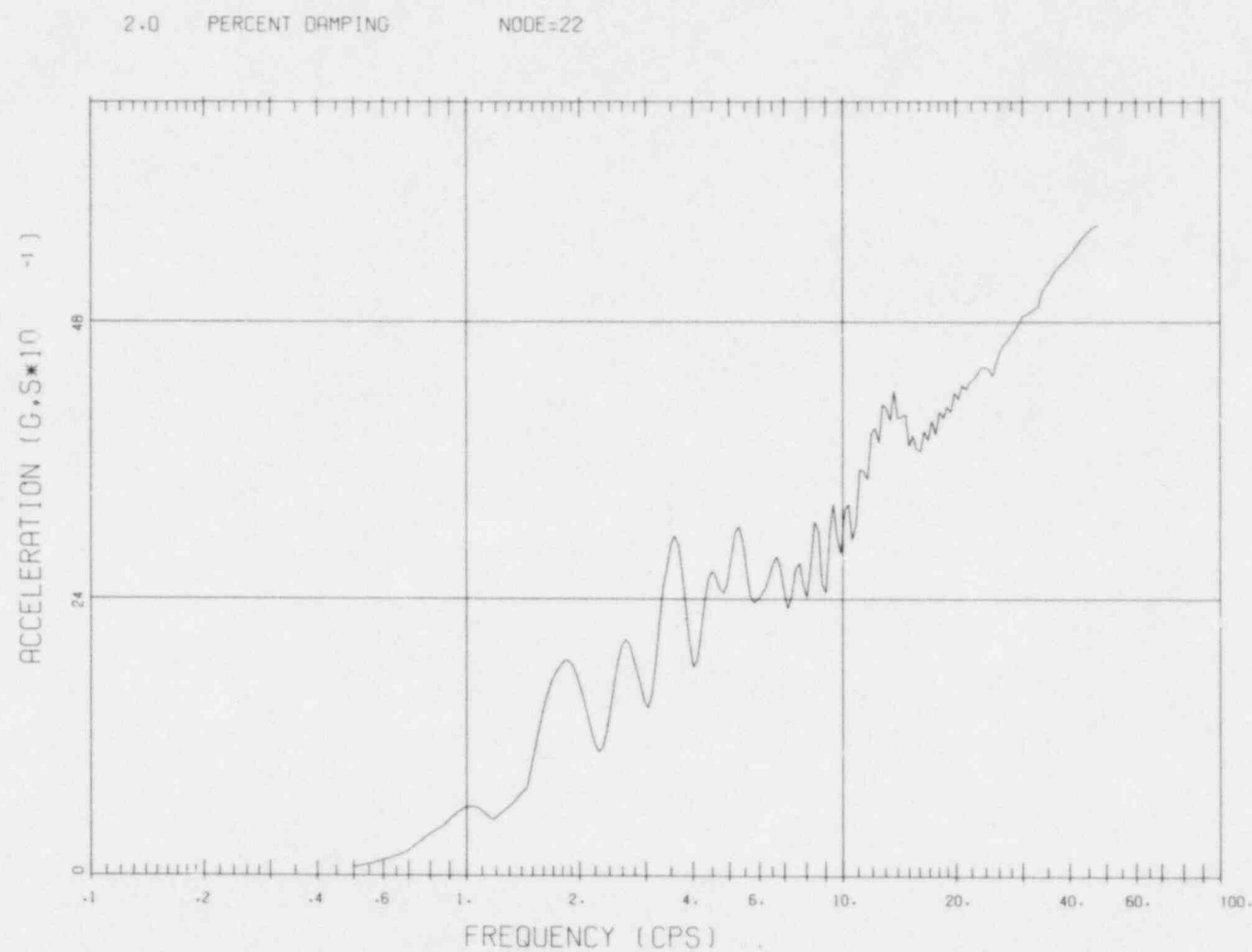


Fig. B.9 Free Field VERT X=60.96 Y=0 Z=1.52

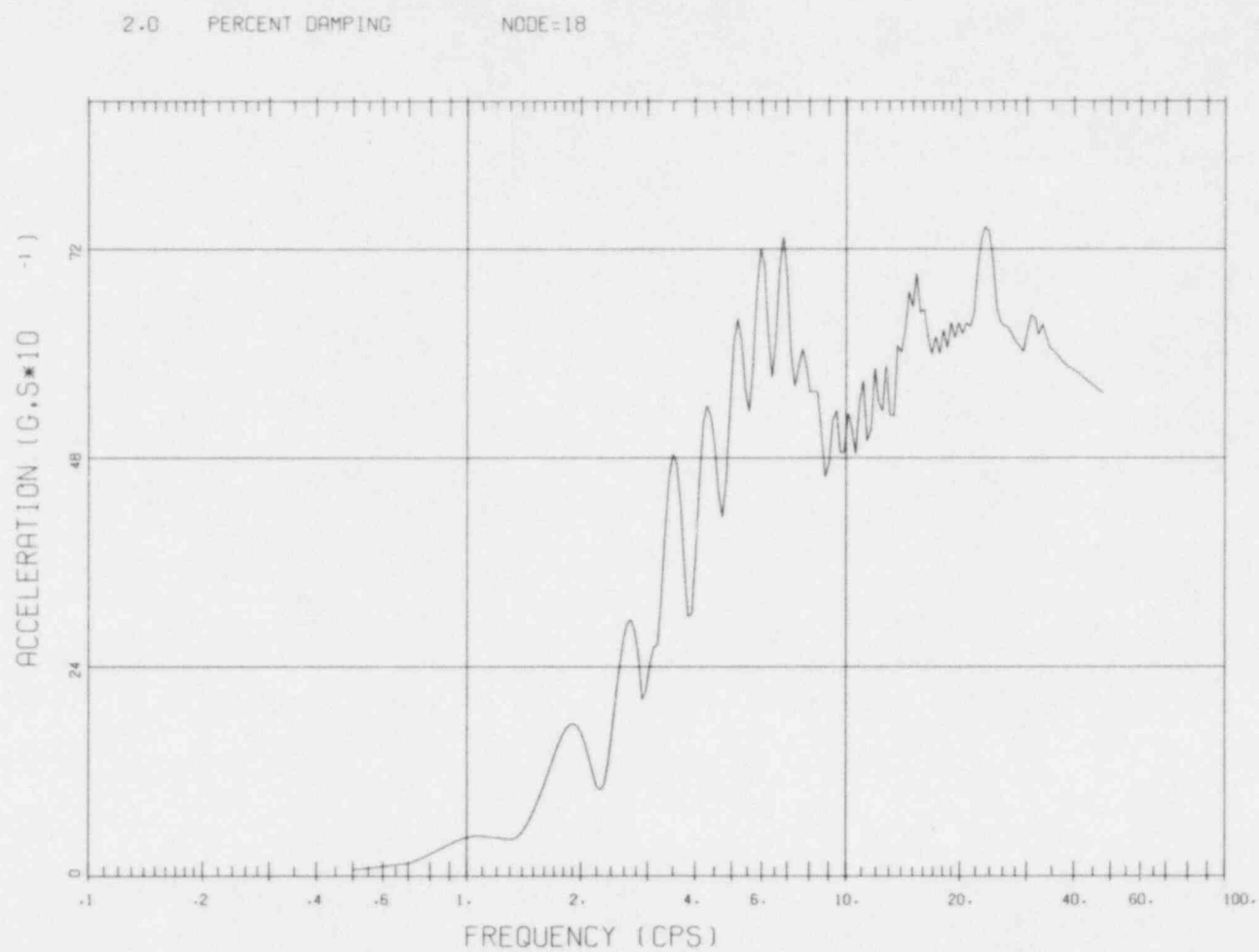
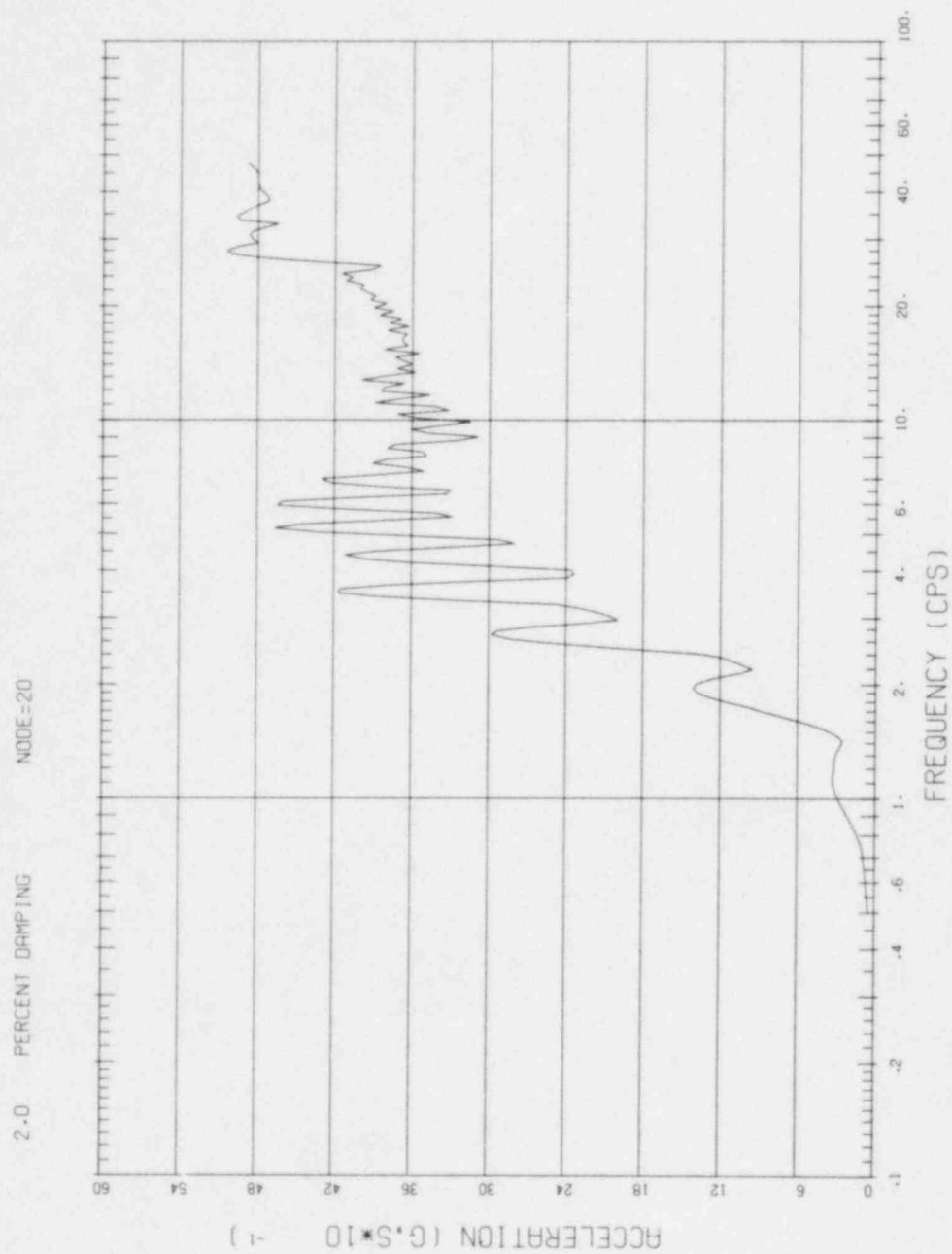


Fig. B.10 Free Field VERT X=60.96 Y=0 Z=6.1



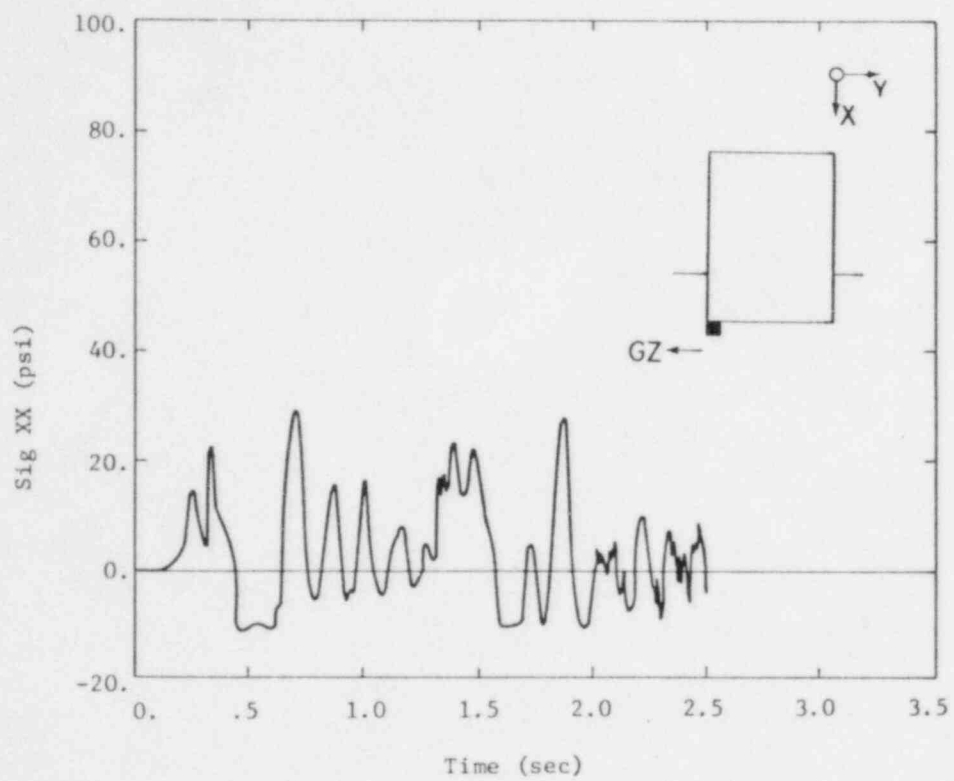


Fig. B.11 Interface Pressure - S01

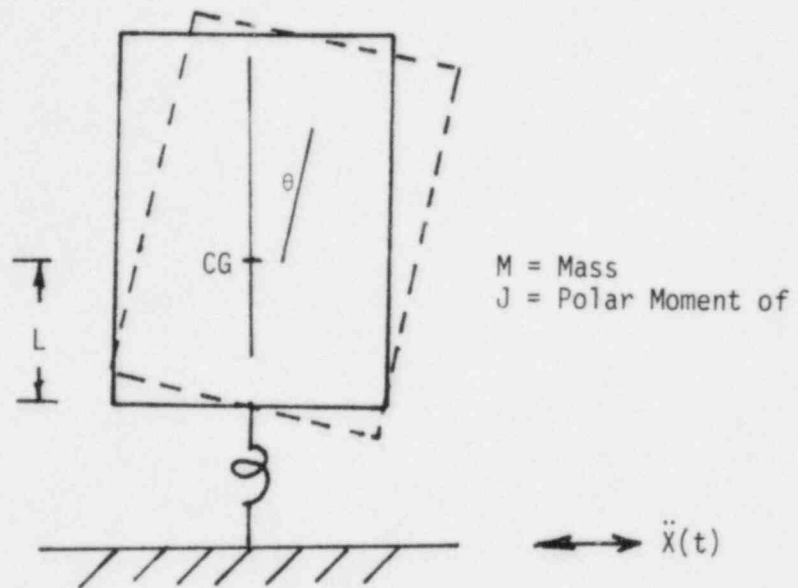


Fig. B.12 Uplift Model

B-31

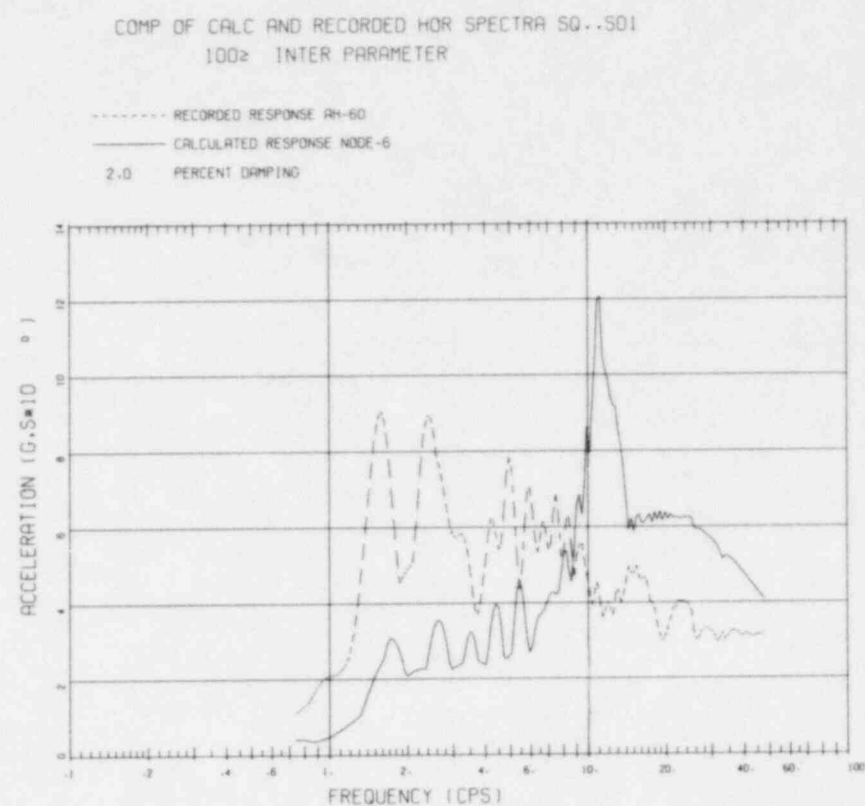
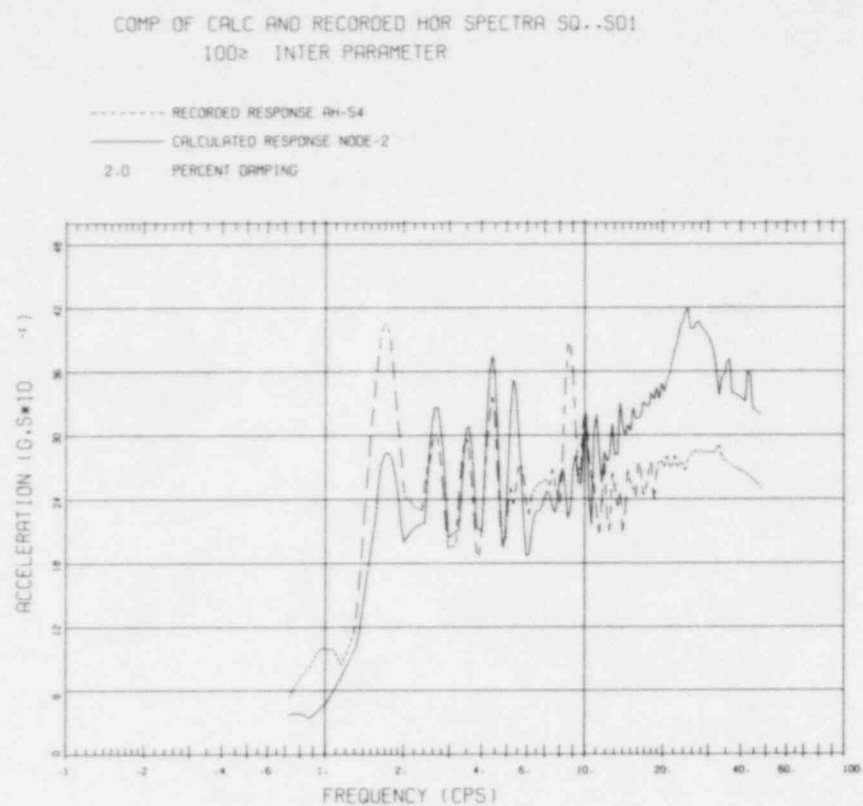


Fig. B.13 Comparison of Calculated and Recorded HOR Spectra SQ..S01
100% Interaction Parameter

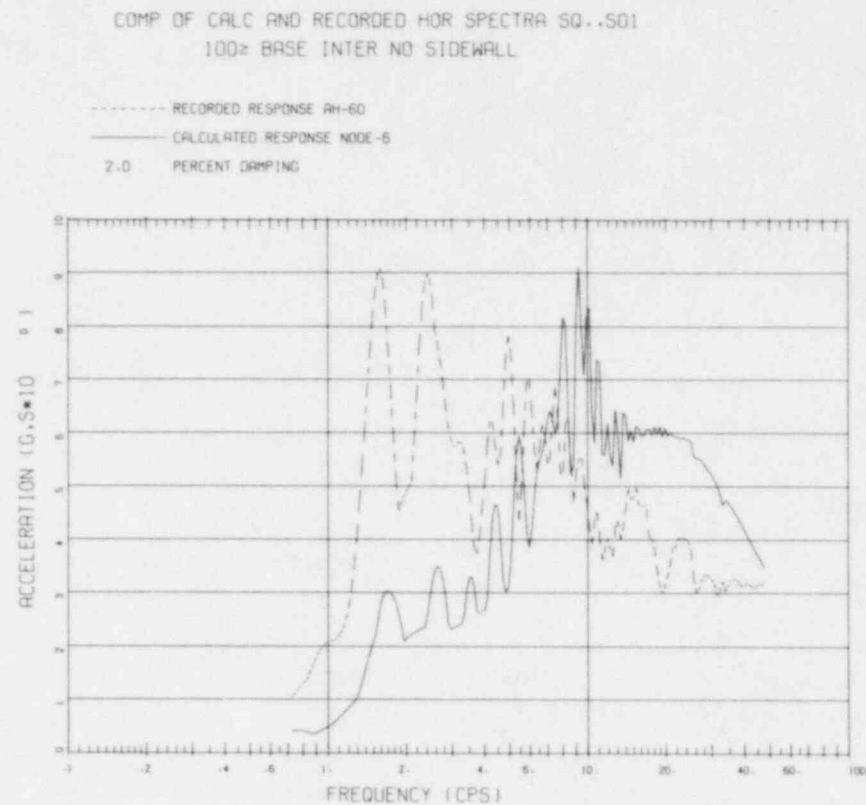
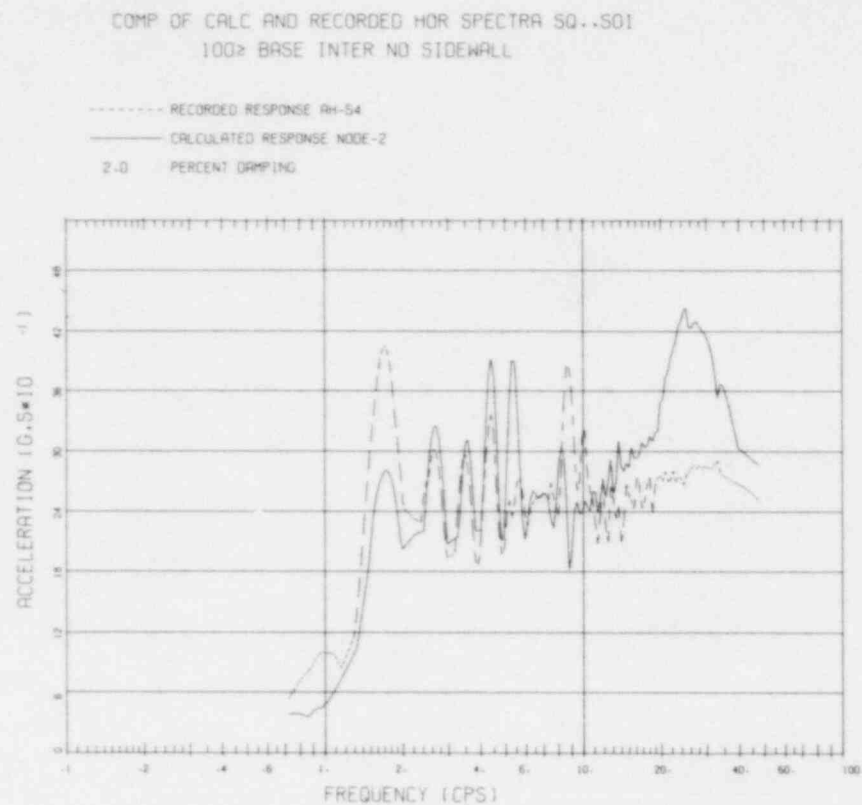
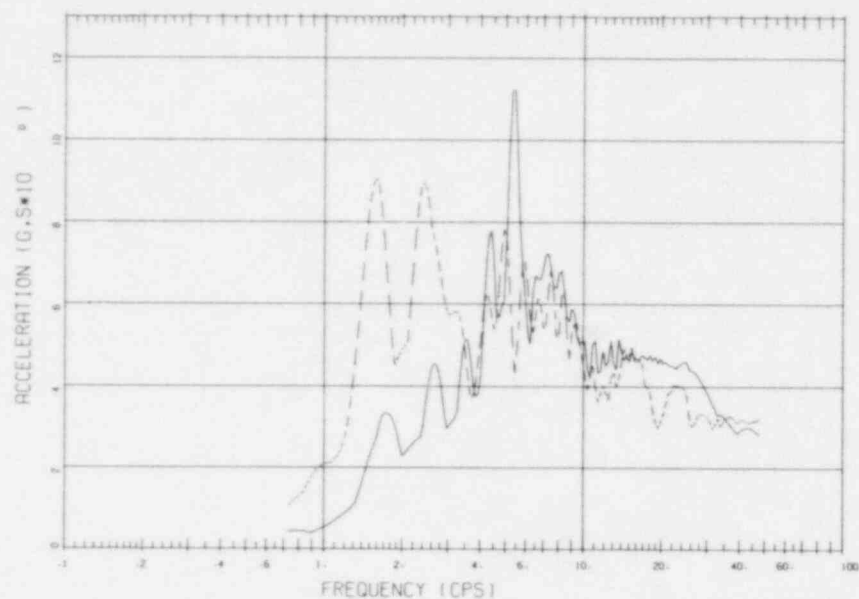


Fig. B.14 Comparison of Calculated and Recorded HOR Spectra SQ..S01
100% Base Interaction No Sidewall

B-33

COMP OF CALC AND RECORDED HOR SPECTRA SQ..S01
NO SIDEWALL...50% BASE MODULUS

----- RECORDED RESPONSE AH-60
----- CALCULATED RESPONSE NODE-6
2.0 PERCENT DAMPING



COMP OF CALC AND RECORDED HOR SPECTRA SQ..S01
NO SIDEWALL...50% BASE MODULUS

----- RECORDED RESPONSE AH-54
----- CALCULATED RESPONSE NODE-2
2.0 PERCENT DAMPING

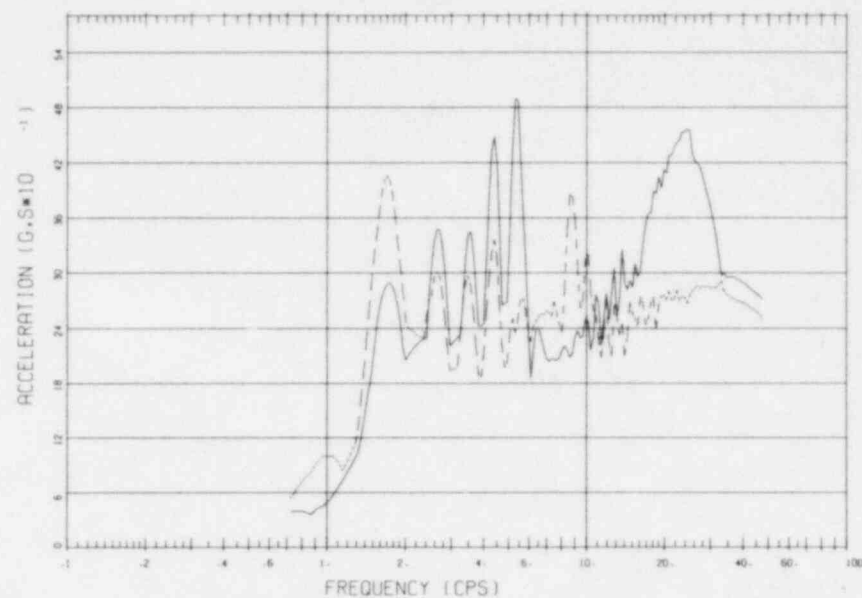
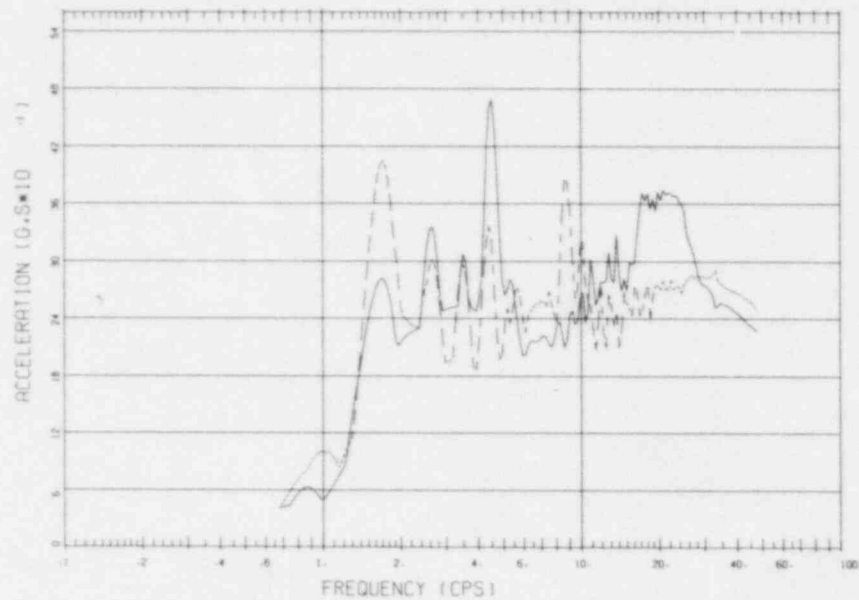


Fig. B.15 Comparison of Calculated and Recorded HOR Spectra AQ..S01
No Sidewall...50% Base Modulus

COMP OF CALC AND RECORDED HOR SPECTRA SQ..S01
NO SIDEWALL...25% BASE MODULUS

----- RECORDED RESPONSE RH-54
——— CALCULATED RESPONSE NODE-2
2.0 PERCENT DAMPING



COMP OF CALC AND RECORDED HOR SPECTRA SQ..S01
NO SIDEWALL...25% BASE MODULUS

----- RECORDED RESPONSE RH-60
——— CALCULATED RESPONSE NODE-6
2.0 PERCENT DAMPING

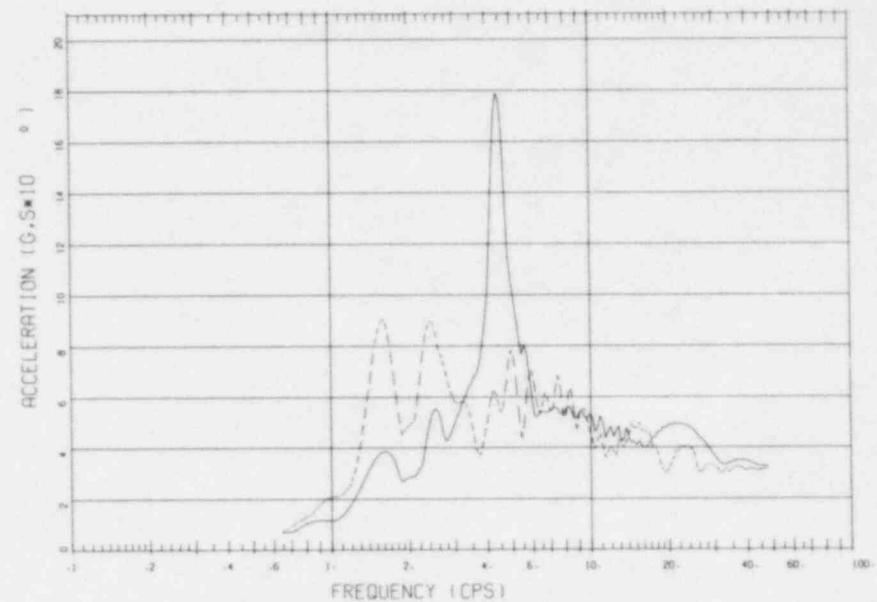


Fig. B.16 Comparison of Calculated and Recorded HOR Spectra SQ...S01
No Sidewall...25% Base Modulus

COMP OF CALC AND RECORDED VER SPECTRA SQ..SQ1
F INPUT 100% INTER PARAMETERS

----- RECORDED RESPONSE RH-56
——— CALCULATED RESPONSE NODE-2
2.0 PERCENT DAMPING

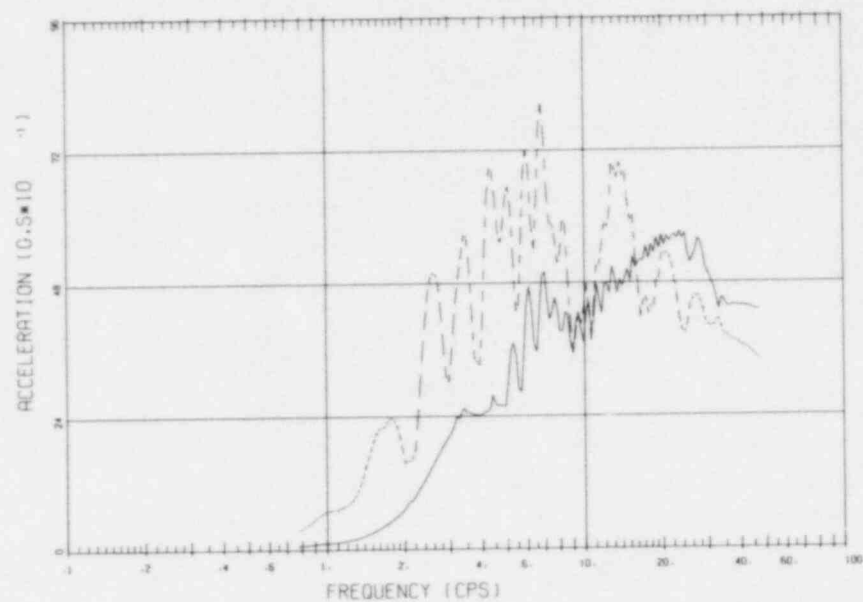
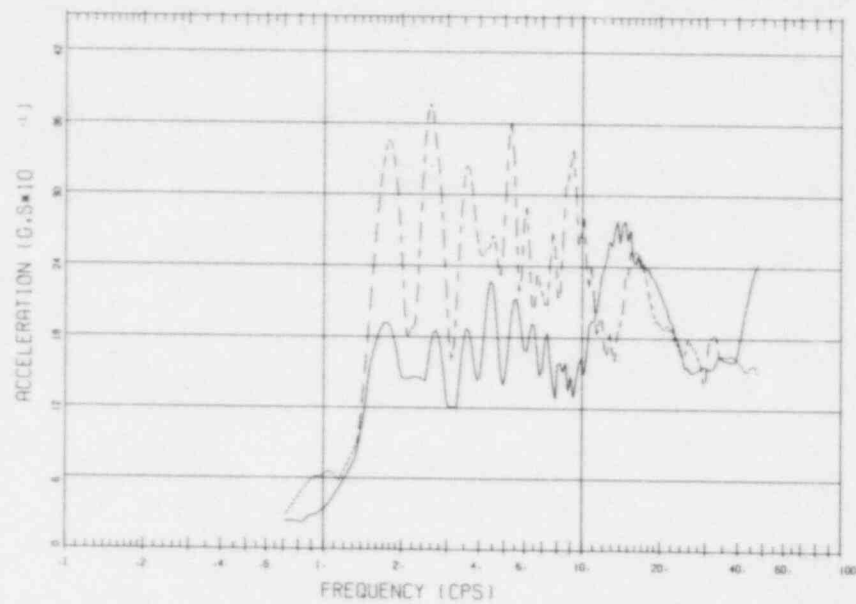


Fig. B.17 Comparison of Measured and Calculated Vertical Spectra for SIMQUAKE II Structure Using Standard Interaction Parameters

COMP OF CALC AND RECORDED HOR SPECTRA SQ...S06
SIDEWALL...100% BASE MODULUS

----- RECORDED RESPONSE AH-57
——— CALCULATED RESPONSE NODE-2
2.0 PERCENT DAMPING



COMP OF CALC AND RECORDED HOR SPECTRA SQ...S06
SIDEWALL...100% BASE MODULUS

----- RECORDED RESPONSE AH-64
——— CALCULATED RESPONSE NODE-6
2.0 PERCENT DAMPING

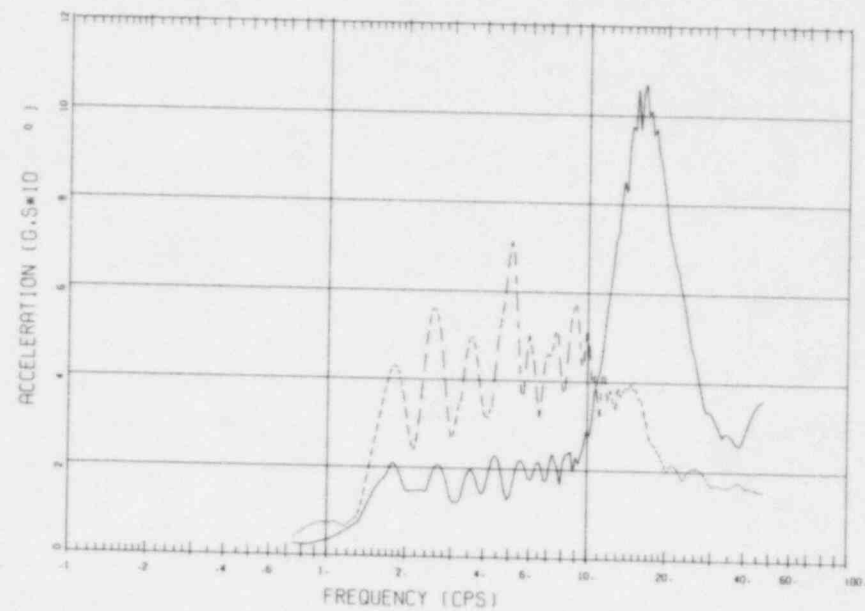
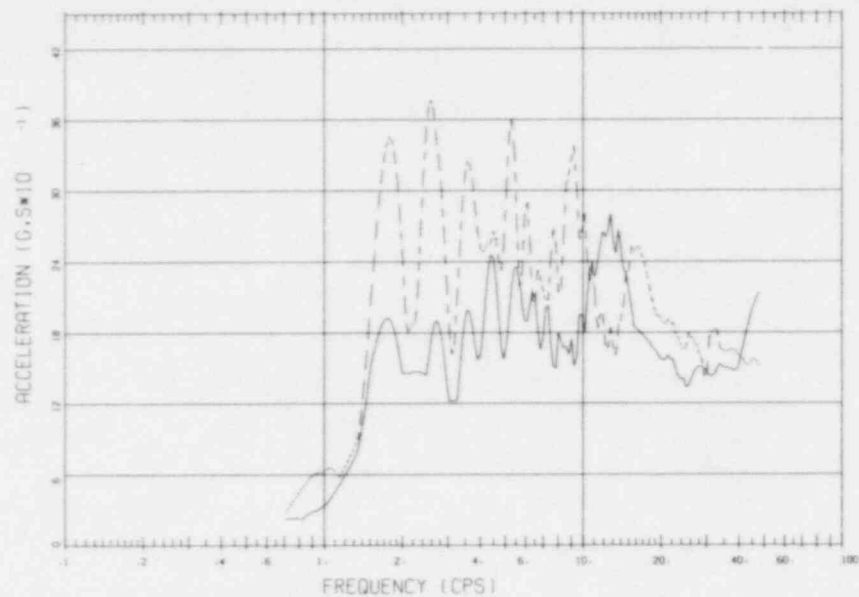


Fig. B.18 Comparison of Calculated and Recorded HOR Spectra SQ...S06
Sidewall...100% Base Modulus

COMP OF CALC AND RECORDED HOR SPECTRA SQ..S06
NO SIDEWALL..100% BASE MODULUS

----- RECORDED RESPONSE RH-57
——— CALCULATED RESPONSE NODE-2
2.0 PERCENT DAMPING



COMP OF CALC AND RECORDED HOR SPECTRA SQ..S06
NO SIDEWALL..100% BASE MODULUS

----- RECORDED RESPONSE RH-64
——— CALCULATED RESPONSE NODE-6
2.0 PERCENT DAMPING

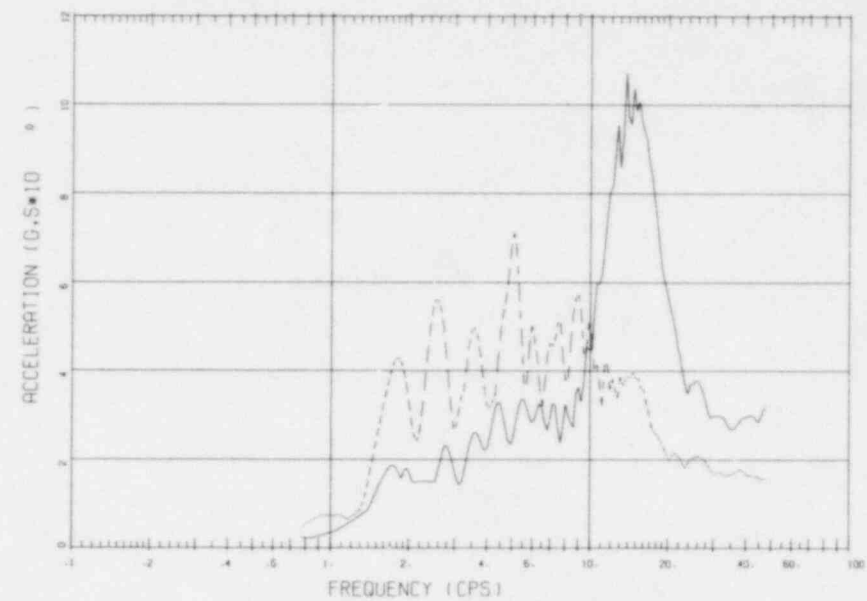
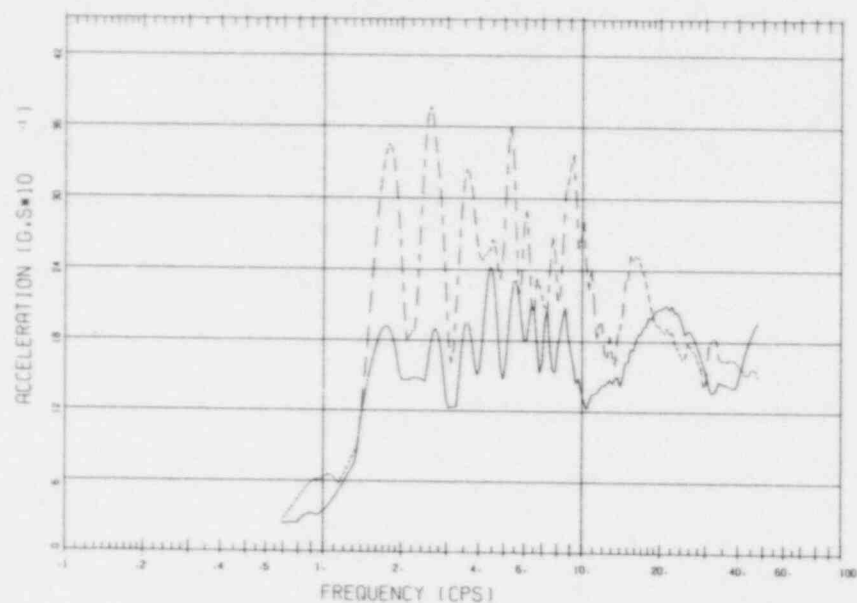


Fig. B.19 Comparison of Calculated and Recorded HOR Spectra SQ..S06
No Sidewall..100% Base Modulus

COMP OF CALC AND RECORDED HOR SPECTRA SQ..S06
NO SIDEWALL...50% BASE MODULUS

----- RECORDED RESPONSE RH-57
——— CALCULATED RESPONSE NODE-2
2.0 PERCENT DAMPING



COMP OF CALC AND RECORDED HOR SPECTRA SQ..S06
NO SIDEWALL...50% BASE MODULUS

----- RECORDED RESPONSE RH-64
——— CALCULATED RESPONSE NODE-6
2.0 PERCENT DAMPING

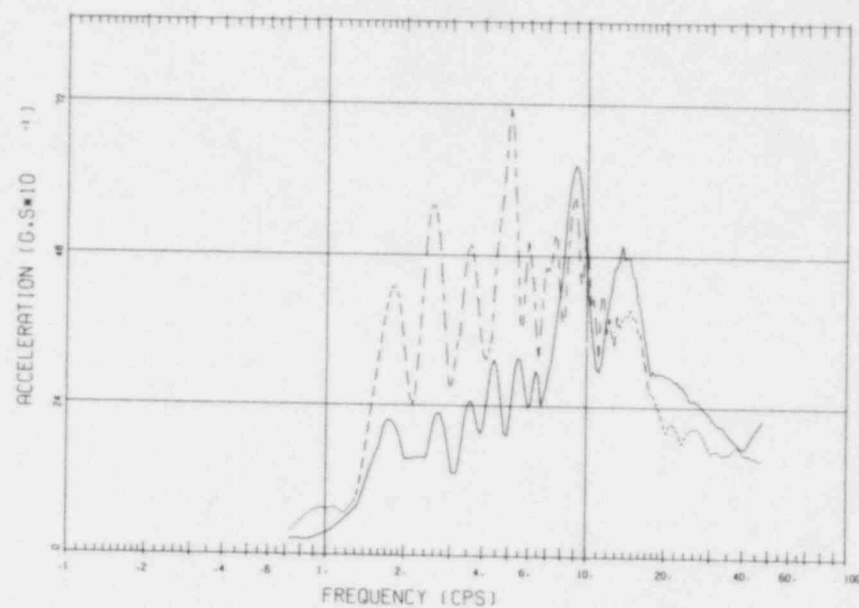
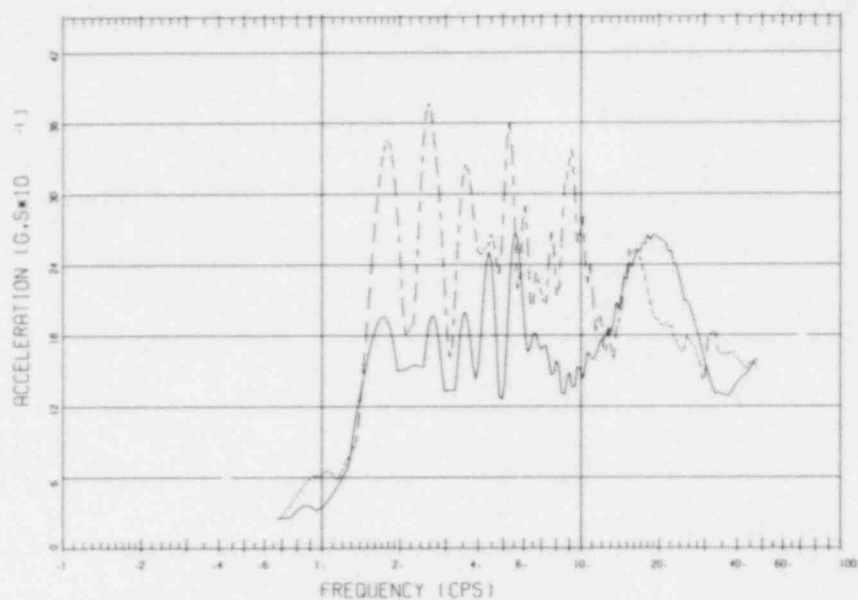


Fig. B.20 Comparison of Calculated and Recorded HOR Spectra SQ..S06
No Sidewall...50% Base Modulus

COMP OF CALC AND RECORDED HOR SPECTRA SQ..S06
NO SIDEWALL...20% BASE MODULUS

----- RECORDED RESPONSE RH-57
——— CALCULATED RESPONSE NODE-2
2.0 PERCENT DAMPING



COMP OF CALC AND RECORDED HOR SPECTRA SQ..S06
NO SIDEWALL...20% BASE MODULUS

----- RECORDED RESPONSE RH-64
——— CALCULATED RESPONSE NODE-6
2.0 PERCENT DAMPING

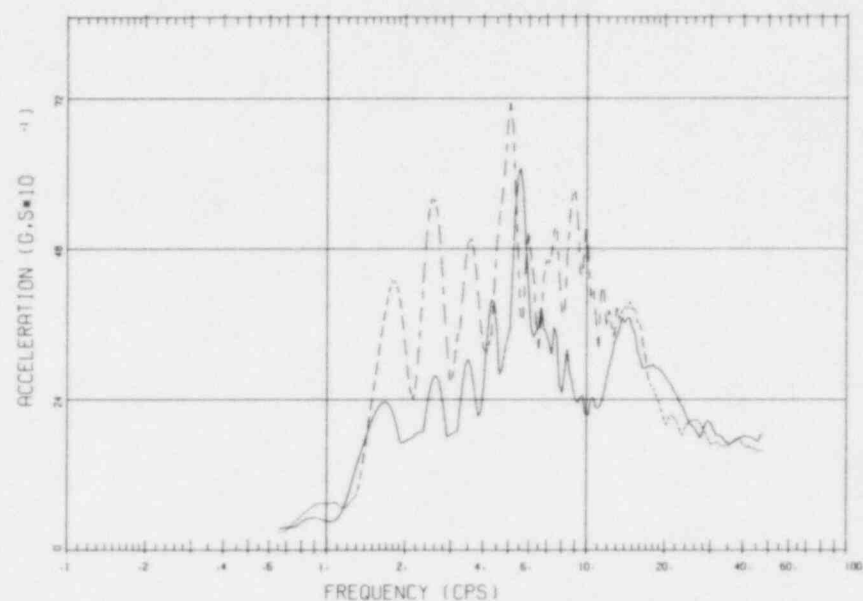


Fig. B.21 Comparison of Calculated and Recorded HOR Spectra SQ..S06
No Sidewall...20% Base Modulus

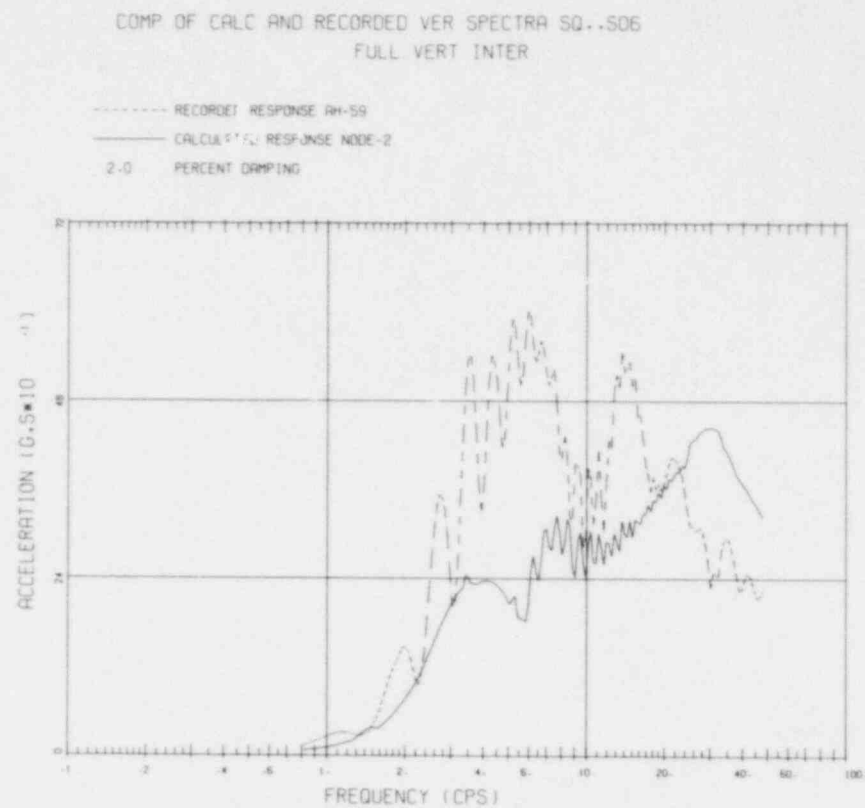


Fig. B.22 Comparison of Calculated and Recorded VER Spectra
SQ..S06 Full VERT Interaction

REFERENCES

1. C.J. Higgins, et al. (University of New Mexico), R.E. Crawford, et al., (Civil Nuclear Sytem), C.F. Howard and P.J. Banez (ANCO Engineers, Inc.), "SIMQUAKEI - An explosive Test Series Designed to Simulate the Effects of Earthquake-Like Ground Motions on Nuclear Power Plant Models", University of New Mexico and ANCO Engineers, Summary Report to EPRI, NO-1728, 1981.
2. C.J. Higgins, K.B. Simmons and S.F. Pickett, "SIMQUAKEII - A Multiple Detonation Explosive Test to Simulate the Effects of Earthquake-Like Ground Motions on Nuclear Power Plant Models", University of New Mexico Summary Report to EPRI, Contract RP810-1, 1979.
3. C.A. Miller and C.J. Costantino' "Soil-Structure Interaction Methods - SIM Code", NUREG/CR-1717, Vol. III, Sept. 1979.
4. "SIMQUAKE II - "An Explosive Test to Simulate Earthquake Ground Motion Effects on Model Nuclear Power Plant Structures", University of New Mexico for EPRI, Vols. I to VIII, February 1979.
5. C.J. Higgins, "Rocking Response of Embedded Model Structures", Proc. ASCE Convention, Las Vegas, Nevada, April 1982.
6. J. Isenberg, D.K. Vaughan, I. Sandler, "Nonlinear Soil-Structure Interaction", EPRI-NP-945, December 1978.
7. C.J. Costantino, E. Vey, Response of Burned Cylinder Encased in Foam", Journal of Soil Mechanics, ASCE, September 1969.

Correlation of Fukushima Data With
Finite Element Codes
Appendix C

CORRELATION OF FUKUSHIMA DATA WITH FINITE ELEMENT CODES

1.0 INTRODUCTION

This report presents the results obtained from the SSI study making use of the finite element method of analysis. A variation of parameter study was conducted using the FLUSH computer program, with the results compared with the measured output from the Fukushima Nuclear Power Plant, subjected to the 1978 earthquake of magnitude 7.4. The objective of the study has been to ascertain and perhaps quantify the discrepancies that develop in a standard method of analysis used in SSI calculations. Although the FLUSH Code was used, the discrepancies that are noted can be ascribed to most finite element codes used in the industry, and not just FLUSH. This is particularly true for this exercise, since only simple linear soil models were used for the Fukushima site properties. Iteration did not have to be used to account for nonlinear soil properties.

A relatively detailed description of the FLUSH program is presented in Section 3.0 below and in Ref. 1. The basic assumption used in its development, however, is based on the concept of upward propagating shear waves generated from horizontal seismic disturbances applied at some deep bedrock/soil interface. To make the problem tractable, simplified linear material properties are used in conjunction with an approximate transmitting boundary formulation to restrict the size of the finite element mesh. The remainder of the finite element formulation is similar to that used in many other computer codes. The applicability of the approach to the SSI problem then rests on the adequacy of the primary assumptions, namely, upward propagating shear waves through linear soils.

2.0 DESCRIPTION OF FUKUSHIMA DATA

A detailed description of the Fukushima site has previously been presented in Appendix A. For completeness of this appendix, a brief outline of the site is presented. An E-W elevation through the Reactor Building is shown in Fig. C.1. The building, about 40 meters square, is embedded in the

foundation to a depth of 14 meters. Eight accelerometers were located as shown, four on the structure and four in the free-field. The motions measured were N-S horizontal motions, or those normal to the plane of Fig. 1.

The free-field at the site is a mudstone extending from the operating floor level to a depth of about 160 meters, below which is a stiffer sandstone basement rock. The wave speeds through the rock are as listed in Fig. C.1, while the hysteretic damping ratio recommended is 10%. These data were obtained from Ref. 2, although no specific information was presented concerning the tests performed to obtain this data, nor variation of this data with depth. As may be noted from the wave speed data, the mudstone is a relatively soft rock. It is composed of very fine-grained clay minerals and, similar to shales, is often laminated and splintery.

3.0 DESCRIPTION OF FLUSH CODE

The FLUSH finite computer code is a two-dimensional finite element program designed (Ref. 1) to address the SSI problem from a particular point of view. The program is capable of treating a plane section through one or more buildings located at or near the ground surface. This structural model consists of a network of beam/spring elements interconnecting a series of node points which may have both mass and rotary inertia. The soil/rock free-field is represented by a mesh of solid plane strain finite elements which is terminated at a bottom horizontal boundary. The seismic input motion history is applied to nodes along this bottom boundary as shown in Fig. C.2.

The vertical sides of the finite element mesh can be made transmitting boundaries in an attempt to simulate the infinite lateral extent of the actual soil/rock free-field. This transmitting formulation is based upon solutions obtained for free harmonic Rayleigh wave motion. For the case where the bottom boundary of the mesh is placed at a depth corresponding to a physical boundary (say at a soil/rock interface) where the impedance between the two layers is significantly different, this representation of the free-field is reasonable. However, for the case where the bottom boundary is arbitrarily located at a depth where there is no impedance mismatch, this bottom boundary can be considered as fixed and will transmit energy back into the mesh,

essentially trapping the energy artificially within the finite element mesh. Such a representation can lead to computational inaccuracies.

While the model used in FLUSH is two-dimensional, some three-dimensional effects are simulated by including horizontal and vertical dampers along the planar faces of the soil/rock mesh. The damping forces are proportional to the differences between nodal velocities and free-field velocities. The intent of this formulation is to allow some energy dissipation in the third dimension. Its effectiveness when compared to exact solutions is unclear, however. The constitutive model used for the soil/rock material is based upon the linear-hysteretic formulation, in which energy dissipation due to nonlinear stress-strain behavior is represented by the frequency independent hysteretic damping ratio (see Appendix A).

The equations of motion for both the soil/rock mesh and the structure, placed in matrix form, are solved using standard Fourier techniques (e.g., FFT method). Amplitudes of motion are obtained at each frequency within the frequency range of interest, which, by using inverse Fourier operations, leads to the time-dependent displacement output. This superposition method of analysis obviously leads to the requirement for linear materials. Nonlinear strain-dependent properties of the soil are treated by the approximate equivalent linear iterative approach, using estimates of peak shear strains obtained from a previous trial.

Ground shaking is applied to the finite element mesh at the bottom boundary. The program is designed to accept either the horizontal or vertical control input motion for one run. If the response to both horizontal and vertical inputs are desired, two separate runs must be made, which must be superimposed to obtain the desired response. However, this requirement leads to a difficulty when dealing with the equivalent iterative technique. Iteration on peak element shear strain can be applied on only one of the two ground motion components, typically the horizontal run. The final soil properties from this run are then used for the vertical run, with no iteration applied. It is assumed of course that this second run does not change the value of the peak shear strains.

4.0 CHARACTERISTICS OF INPUT MOTION

As mentioned above, the FLUSH type analysis consists of inputting a motion-time history at the base of a combined finite element/structural model. For this particular study, the input motion considered was the known horizontal accelerogram measured under the Reactor Building at an elevation of -40 meters. The recorded motion is shown in Fig. C.3 and consists of a 60 second duration pulse with a peak acceleration of 0.062 g's. As may be noted, the strong motion is restricted to the first 30 seconds of shaking.

The Fourier components of this pulse are shown in Fig. C.4, while the corresponding response spectrum is shown in Fig. C.5. The majority of the energy content of the motion is restricted to frequencies less than 10 cps, with significant content at frequencies of about 0.6, 1.6, 3.0 and 4.8 hz.

5.0 STRUCTURAL MODEL

The model used to represent the Reactor Building is shown in Fig. C.6, which was obtained by reducing the structural stick model used in the lumped parameter phase of this program. This stick model is shown in Fig. C.6a and represents an E-W cross-section of the structure. To simplify the finite element study, this structural system was condensed into the single of Fig. C.6b up to the operating floor level, with a foundation structure added to account for the effects of embedment into the free-field mudstone. To ensure proper moment continuity between the stick and the foundation structure, a fictitious structural element of large stiffness and small mass was extended from the operating floor level into the foundation mat. The density of the foundation mat material was taken to yield the proper total mass of the foundation structure.

6.0 FINITE ELEMENT MODELS

In an attempt to study various aspects of the finite element approach to SSI calculations, a series of finite element meshes were drawn and digitized which showed differences in mesh width, element size, material damping and

interaction formulation. These meshes are shown in Figs. C.7 through C.12. The first mesh used in Mesh 51 shown in Fig. C.7. This mesh was generated (purposely) by an inexperienced analyst with little guidance in an attempt to see if this factor had any impact on computed responses. As may be noted, the mesh has a restricted zone of finer elements immediately around the foundation, with coarser elements used to extend the mesh to the side and bottom boundaries. The obvious purpose of this approach, often used in structural analysis, is to minimize the size of the computational problem while at the same time yielding extensive meshes. As is well known in dynamic problems, however, it is the frequency transmission capability of the coarse elements between the structure and the input that control the adequacy of the computation. For this mesh, the vertical frequency capability of the coarse elements of the mesh is about 9 cps. Considering that the frequency content of the input inadequate to determine structural response.

Meshes 61, 71 and 81 are all fine meshes with various distances to the lateral transmitting boundary. The vertical transmission capability of this mesh is 35 cps, a capability which would be expected to yield adequate response to a frequency of about 17 cps. Only Mesh 81 was run for this study since the bigger meshes would not fit in the BNL version of FLUSH without extensive program modifications. Since other data generated on this study indicates that the lateral extent of the mesh for this problem is not too significant (together with other indications in the literature), only the results of Mesh 81 were used for the finer meshes.

Mesh 91 of Fig. C.11 is the same as Mesh 81, with the exception that coarser vertical elements were used through the free-field. The vertical frequency transmission is about 17 cps. Mesh A1 of Fig. C.12 also has a transmission capability of about 17 cps, but the lateral extent of the mesh is much larger.

7.0 NUMERICAL RESULTS

The first series of problems run made use of the coarse Mesh 51, which has the low frequency transmission capability of only 9 cps. Four separate

problems were run, varying two aspects of the problem. The first three problems assumed free-field (or rock) material damping of 10%, 20% and 30%. Full interaction between the free-field and the structure is maintained since the same set of nodes connect the foundation structure directly to the free-field. For this problem, with an embedded foundation mat, this direct connection may lead to erroneous rocking behavior of the structure, since the tendency of the mat to lift off is artificially restrained by the stiffness of the elements to the side of the foundation structure. To estimate the effect of this problem for the Fukushima configuration, a modified problem was investigated in which the shear stiffness of the elements immediately to the side of the mat is reduced to zero while maintaining the compression stiffness of these elements.

Some of the results of this problem series are shown in Fig. C.13, in which the peak computed accelerations at various levels through the structure are shown and compared to measured peak values. As may be noted, the effects of sidewall shear for this configuration are small. The results of this set of data also indicate that to match the peak accelerations to the measured values requires that the effective material damping for the mudstone be set at between 20% and 30%, what is normally considered relatively high values for rock foundations.

A similar set of problems was run using the finer, but narrower Mesh 81 with the results shown in Fig. C.14. For this problem set, the effect of sidewall shear appears more pronounced. However, since only a single element is placed between the foundation and the transmitting boundary, and this is the element that has an artificially reduced shear modulus, these comparisons must be considered suspect. Again the results for the three damping cases seems to indicate that material damping for the mudstone should be set at about 20%. The specific values of peak accelerations at the various floor levels are tabulated in Tables 1 and 2.

TABLE 1
PEAK STRUCTURAL ACCELERATIONS (G'S) USING MESH 51

Soil Damping			Full Sidewall Interaction			No Shear
			10%	20%	30%	10%
Measured						
ROOF			0.921	0.591	0.418	0.878
(AH4)	0.553					
7th Floor			0.699	0.438	0.305	0.666
5th Floor (AH3)	0.193		0.436	0.259	0.182	0.411
3rd Floor (AH2)	0.140		0.293	0.193	0.139	0.277
Basemat (AH1)	0.085		0.082	0.064	0.056	0.081

TABLE 2
PEAK STRUCTURAL ACCELERATIONS (G'S) USING MESH 81

Soil Damping			Full Sidewall Interaction			No Shear
			10%	20%	30%	10%
Measured						
ROOF			0.636	0.460	0.348	0.615
(AH4)	0.553					
7th Floor			0.491	0.345	0.255	0.373
5th Floor (AH3)	0.193		0.320	0.225	0.169	0.179
3rd Floor (AH2)	0.140		0.189	0.140	0.110	0.127
Basemat (AH1)	0.085		0.084	0.066	0.057	0.124

Before considering characteristics of computed response spectra, a summary of peak accelerations computed at the various floor levels is presented in Table 3 for the various meshes mentioned, all for a rock material damping value of 10%. If we first compare the results of Meshes 91 and A1, we can deduce that the transmitting boundary formulation is adequate for this problem, since the only difference between the two meshes is the location of the lateral boundary. The results from Meshes 81, 91 and 51, the primary difference being the frequency transmission capability of the elements, indicate that the rocking calculation is directly related to element stiffness, while the horizontal behavior does not appear to be as dependent. It is well known that the coarser the element, the stiffer the element and the greater the resistance to both shear and compression. However, it may be noted from Appendix A that the rocking frequency for this site is about 3.5 cps, while the translational frequency is about 11 cps. The smaller dependence of peak horizontal acceleration on element size is more probably related to the fact that most of the energy in the input pulse is at the lower frequency range.

A comparison of spectra generated with Mesh 51 is presented in Figs. C.15 through C.17 for the problems with and without sidewall shear. Again, the effect of this parameter for this configuration appears to be unimportant. As may be noted, the spectra generated at the roof truss and 5th floor elevation indicate a second peak at 4.8 cps, which is not as pronounced at the third floor elevation. It should be noted that this frequency corresponds to the peak frequency of the input basement motion at -40 meters, as seen in Fig. C.5. Apparently this peak is transmitted through the coarse mesh, inducing a rocking motion at the nearby frequency.

Figures C.18 and C.19 present a comparison of the results obtained between Meshes 91 and A1, the only differences being the location of the lateral transmitting boundary of the meshes. The results at both the 5th floor and roof indicate similar spectra, supporting the conclusion stated above that the transmitting formulation is adequate for this problem. Again, a second peak seems to be transmitted through the structural model is not

TABLE 3

PEAK COMPUTED STRUCTURAL ACCELERATIONS (G'S)
FROM ALL MESHES USING 10% SOIL DAMPING

	Roof	7th Flr	5th Flr	3rd Flr	Basemat
Fine Mesh 81 Near Boundary 35 Cps Transmission Freq.	0.636	0.491	0.320	0.189	0.082
Medium Mesh 91 Near Boundary 17 Cps Transmission Freq.	0.430	0.290	0.182	0.132	0.088
Medium Mesh A1 Inter. Boundary 17 Cps Transmission Freq.	0.431	0.289	0.176	0.131	0.085
Coarse Mesh 51 Far Boundary 9 Cps Transmission Freq.	0.921	0.699	0.436	0.293	0.082

noted in the actual recordings, this at a frequency of about 7 cps. At the lower frequency of about 3 cps, however, the recorded spectra is higher than the computed, indicating that the effective system damping may in fact be frequency dependent.

Figs. C.20 and C.21 present some comparisons from the results of Meshes 81 and 91. As mentioned above, the effect of element size (and therefore frequency transmission) is significant. It can be noted that the results indicate a significant shift in frequencies of the system, with the stiffer mesh yielding the higher frequencies of peak response.

Figs. C.22 through C.25 present results for the effect of assumed rock damping modulus on computed response, with the output being from Mesh 51 and Mesh 81. The results again indicate that the simplified frequency independent material damping is in fact not applicable to this rock material. The higher frequencies input to the meshes appear to be transmitted unimpeded, whereas the recorded results seem to indicate that these higher frequencies are in fact damped out and do not reach the structure.

8.0 CONCLUSIONS

The results of this series of runs using the finite element approach to the SSI problem has lead to the following conclusions:

1. Comparisons of the computed response spectra indicate that, for this soft rock site, the transmitting boundary concept can be reasonably applied to the calculation.
2. The computed responses are significantly affected by the frequency transmission capacity of the elements in the free-field between the input motion and the structure. The usual concept of including larger elements away from the structure does not lead to acceptable response calculations.

3. For this soft rock site, the concept of frequency independent material damping appears to be inadequate. It seems that an increase in damping with frequency, similar to simple viscous damping, is required to simulate recorded response. This would be more in agreement with intuitive understanding of dampign in rock. Required material damping at low frequency, similar to that of most cyclic tests (say 1 cps), is low as the test would indicate. At higher frequencies of about 10 cps, material damping rates would be higher.

Diagram illustrating the geological cross-section and seismic data for the reactor building area.

Reactor Building Dimensions and Elevations:

- Overall width: 40.56
- Internal width: 30.42
- Ground Surface: +10.0
- Reactor Building Elevation: +54.9
- Reactor Building Elevation: +38.9
- Reactor Building Elevation: +25.9
- Reactor Building Elevation: +10.0
- Reactor Building Elevation: -4.0
- Reactor Building Elevation: -14.0
- Reactor Building Elevation: -40.0

Seismic Data:

- MUDSTONE: $V_p \approx 1700$ m/s, $V_s \approx 530$ m/s
- SANDSTONE: $V_p \approx 1900$ m/s, $V_s \approx 680$ m/s

Key Points and Distances:

- Point AH9: 28.0
- Point AH1: 27.0
- Point AH10: -40.0
- Point AH11: -14.0
- Point AH12: -4.0
- Point AH1: -4.0
- Point AH2: +25.9
- Point AH3: +38.9
- Point AH4: +54.9

C-13

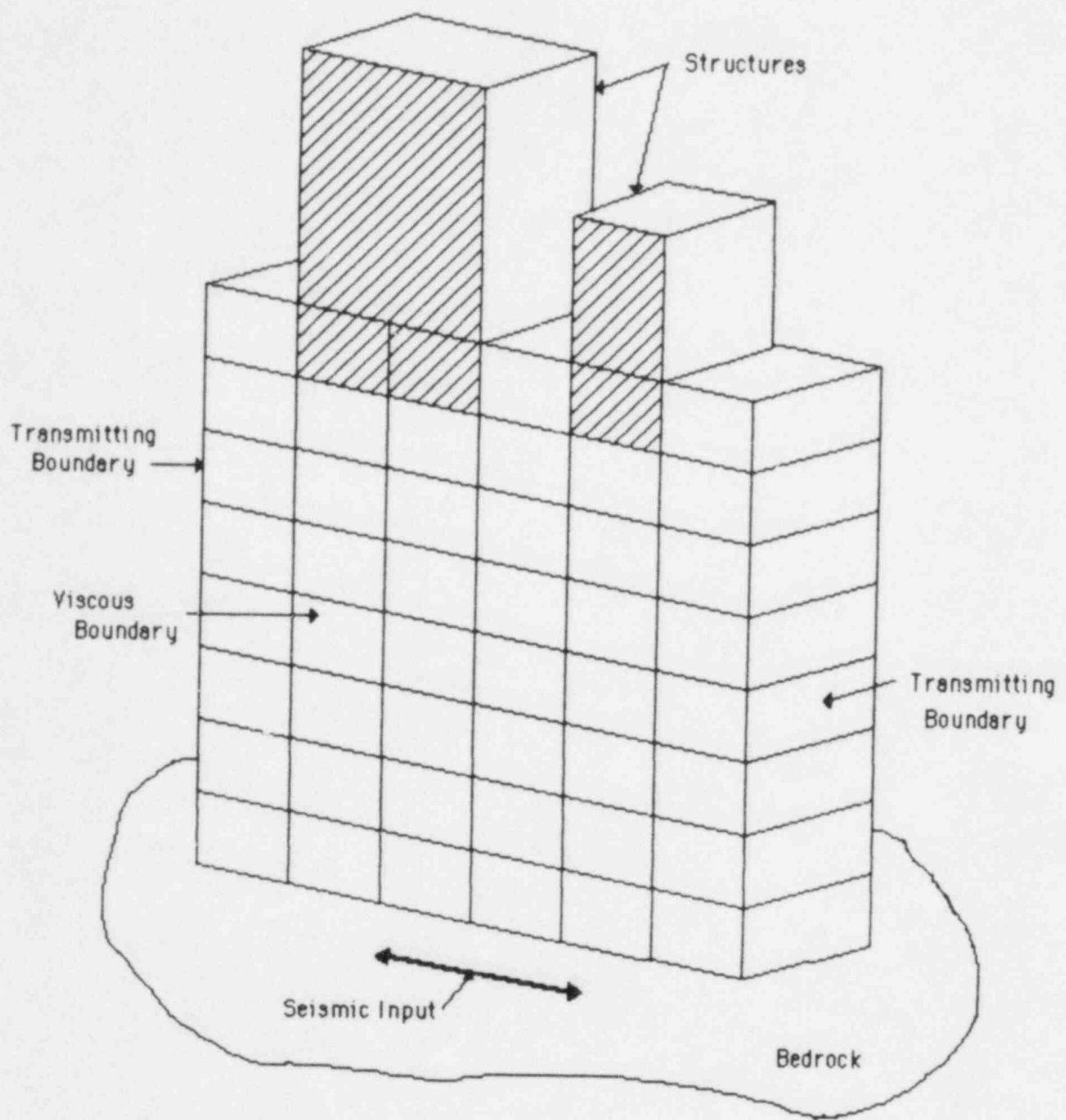


Fig. C.2 SCHEMATIC OF FINITE ELEMENT MODEL
USED IN FLUSH CODE

Fig. C.3 Recorded Pulse at -40M Under Reactor Building

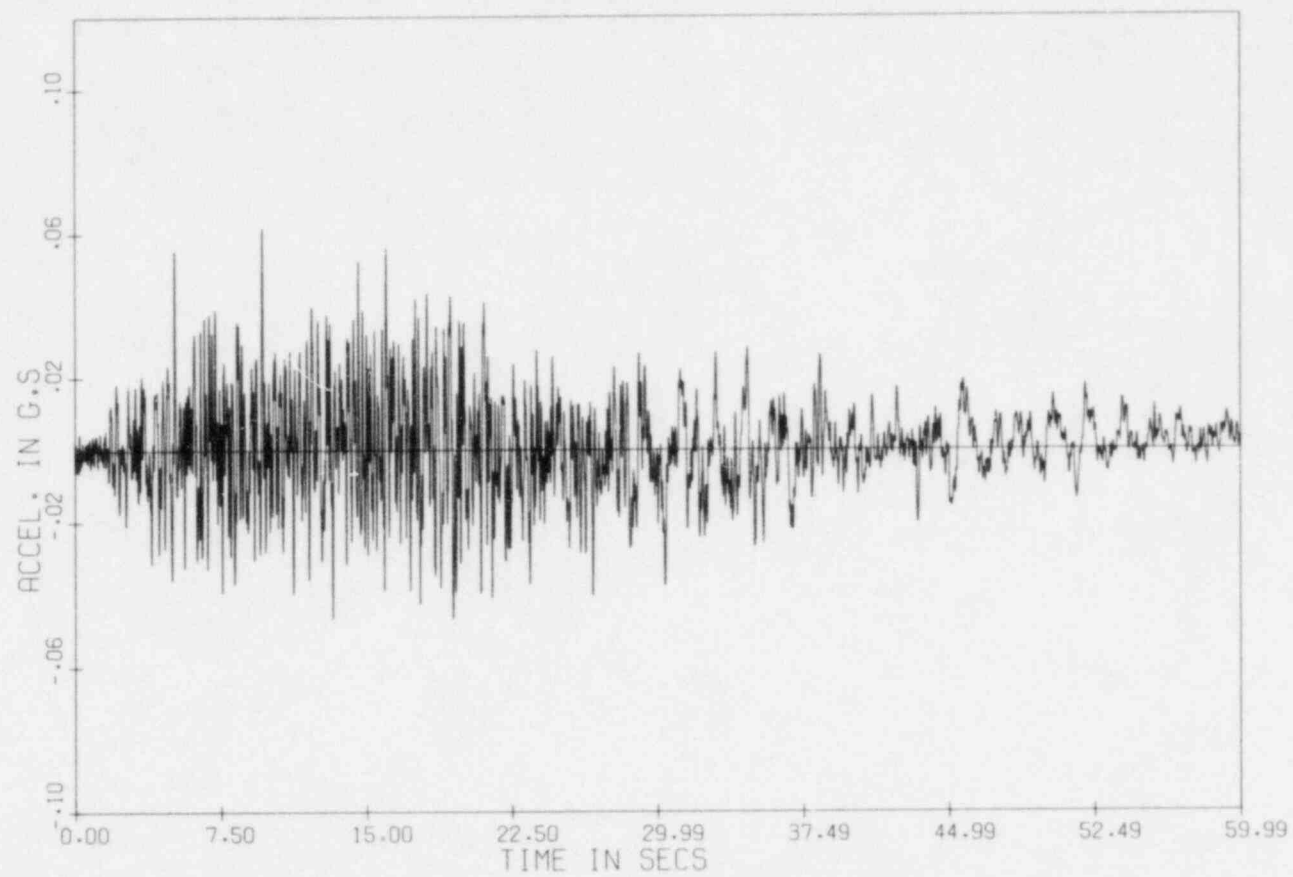


Fig. C.4 Frequency Content of Recorded Pulse at -40M

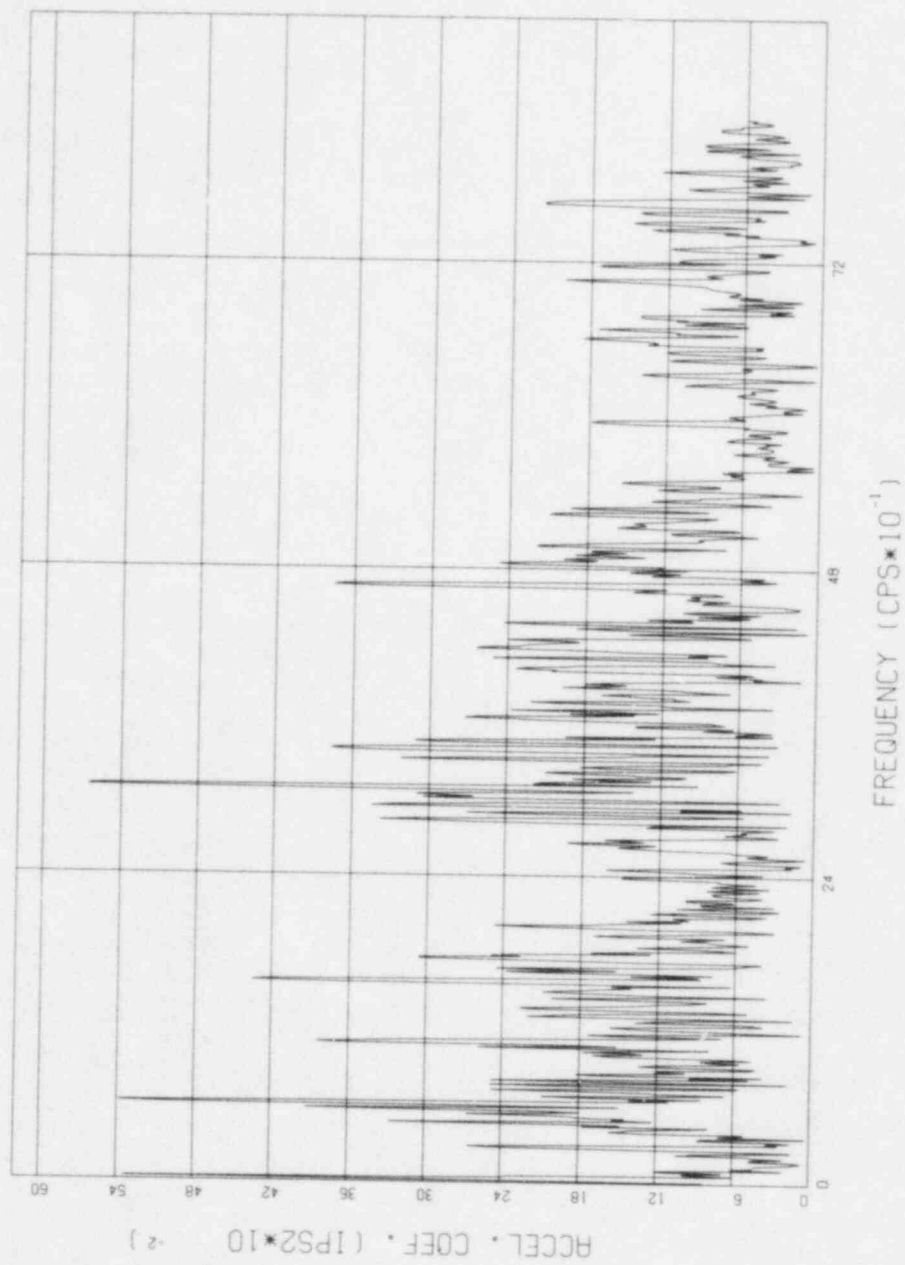
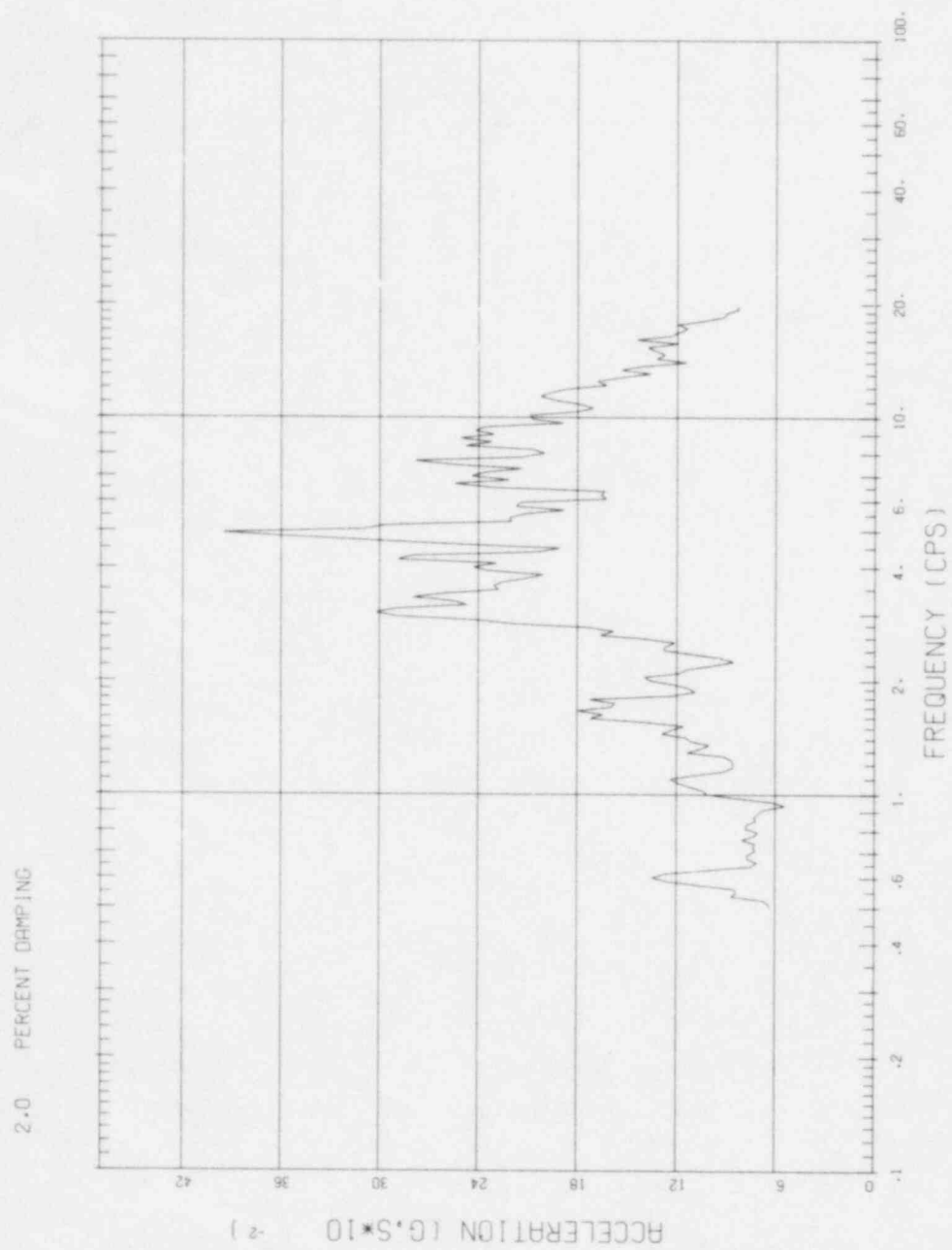


Fig. C.5 Spectrum of -40M Recorded Pulse Under Reactor Building



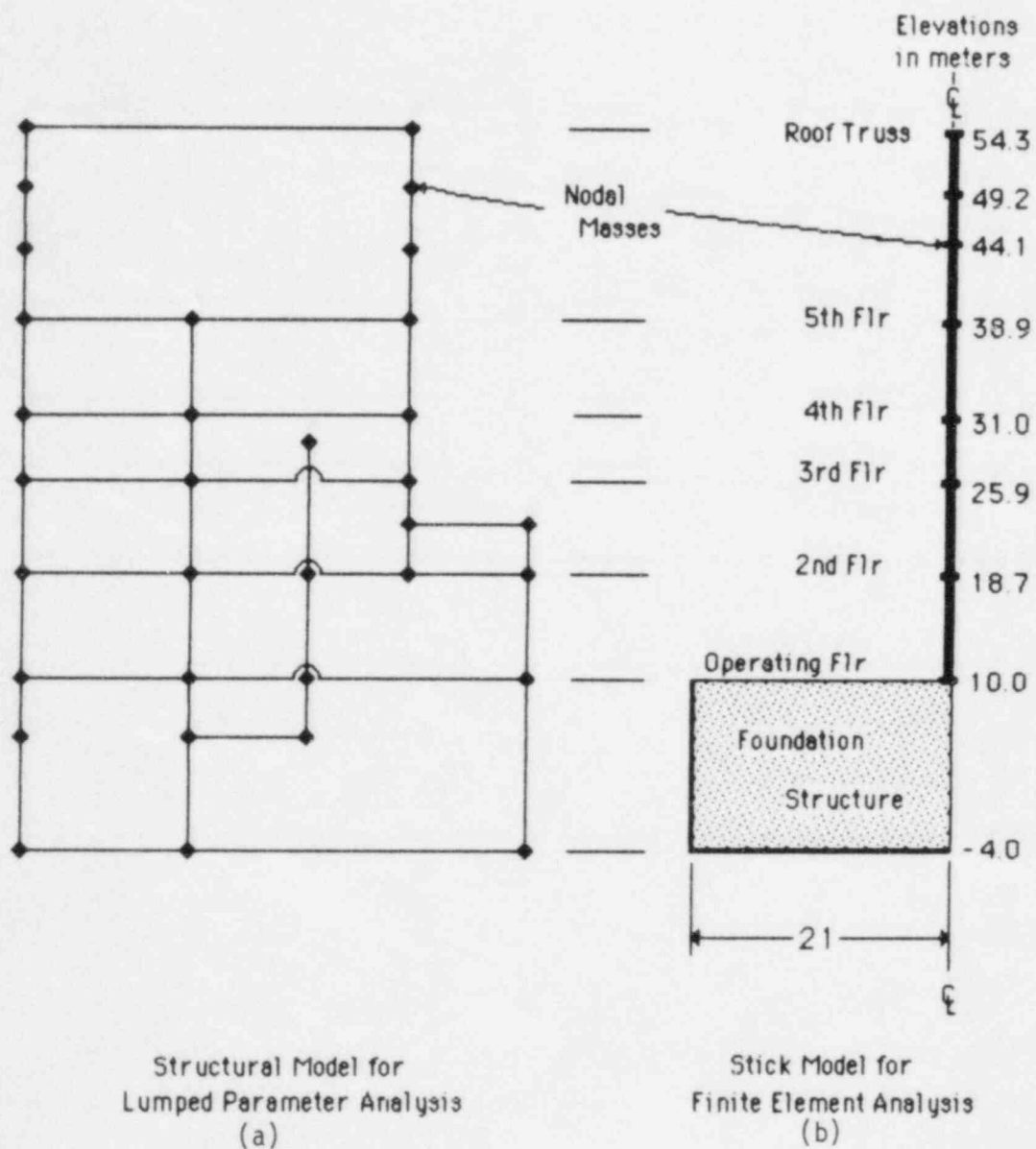


Fig. C.6 STRUCTURAL MODELS

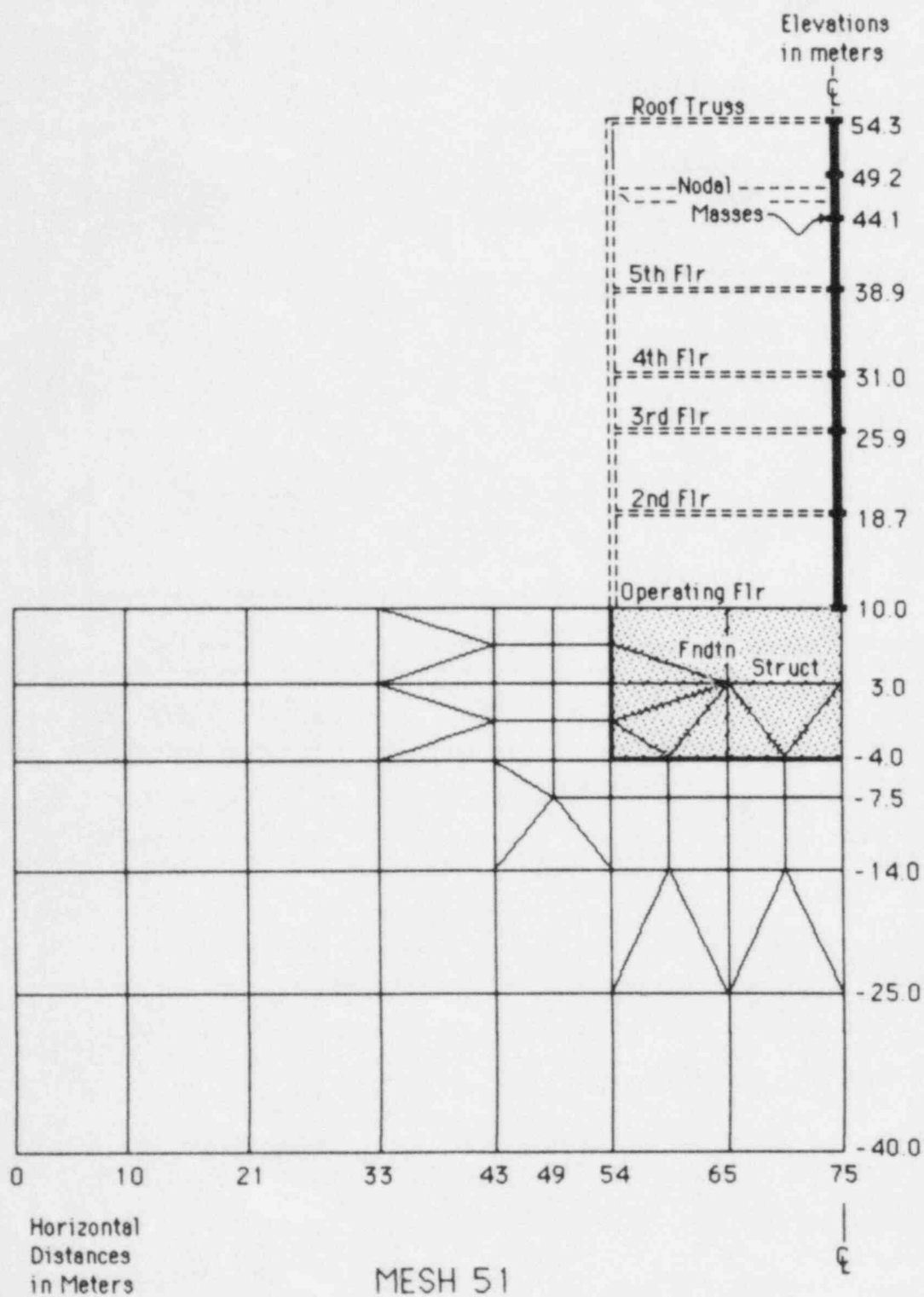


Fig. C.7 Low Frequency Transmission Mesh

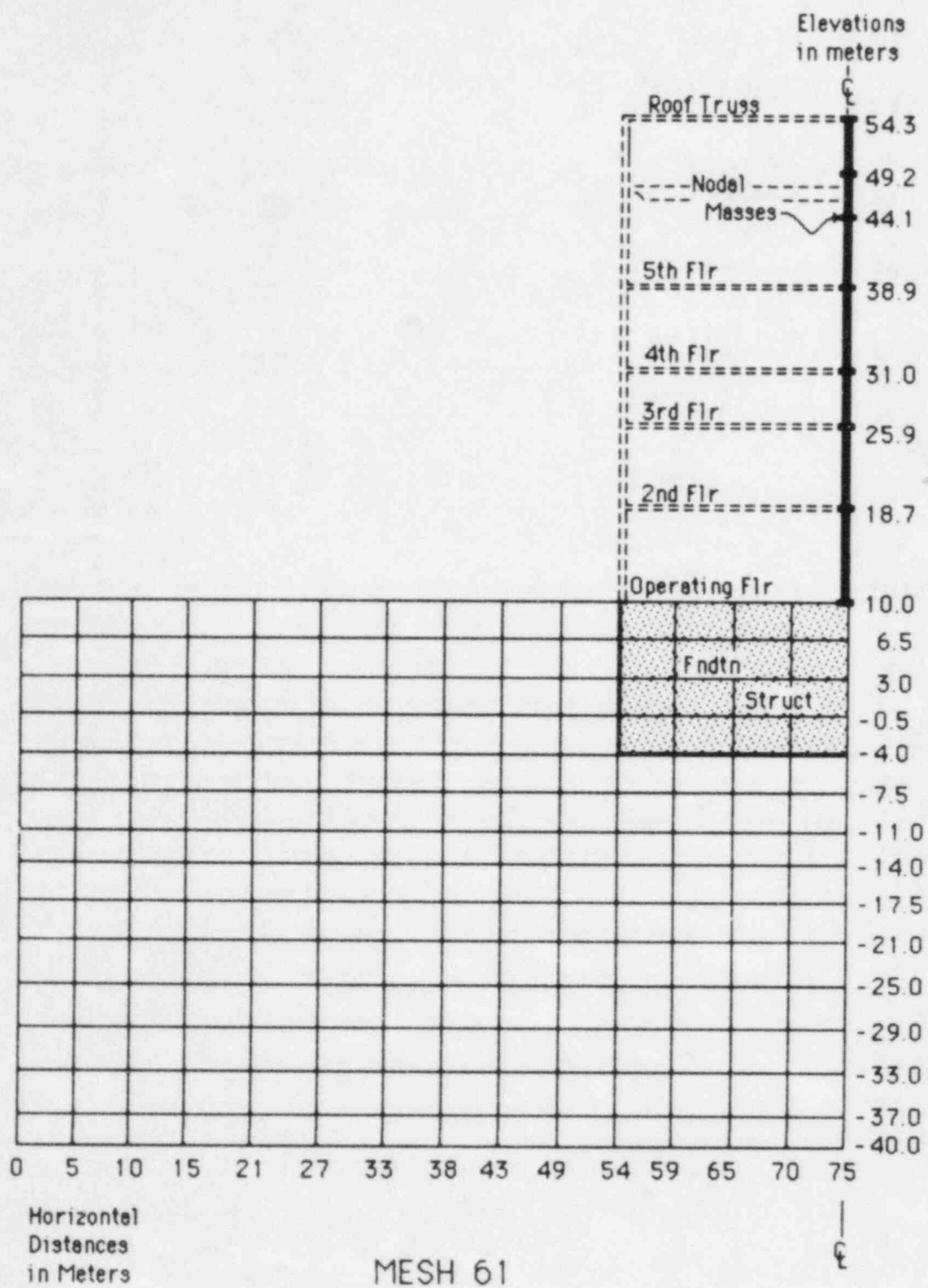


Fig. C.8 High Frequency Transmission Mesh

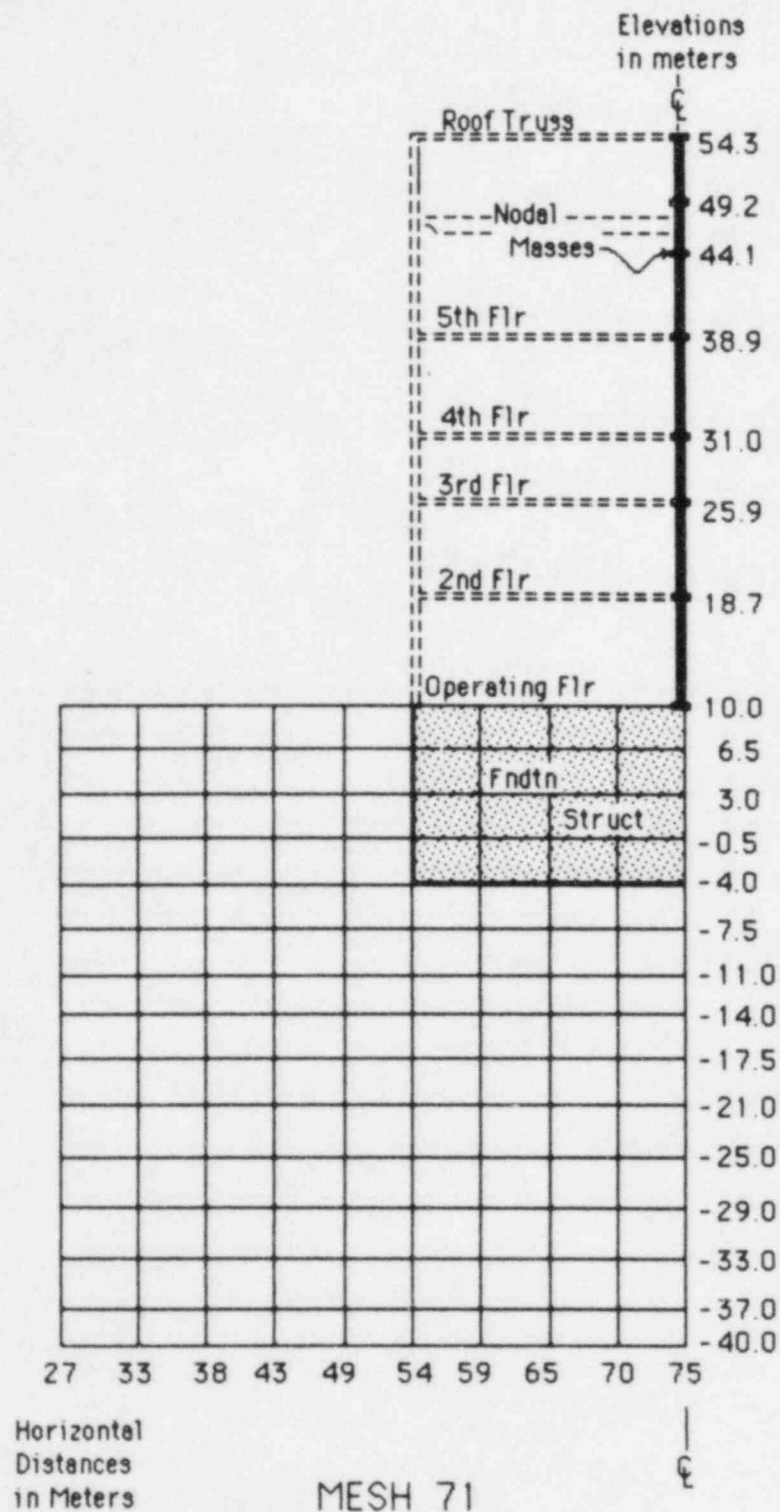


Fig. C.9 Intermediate Mesh

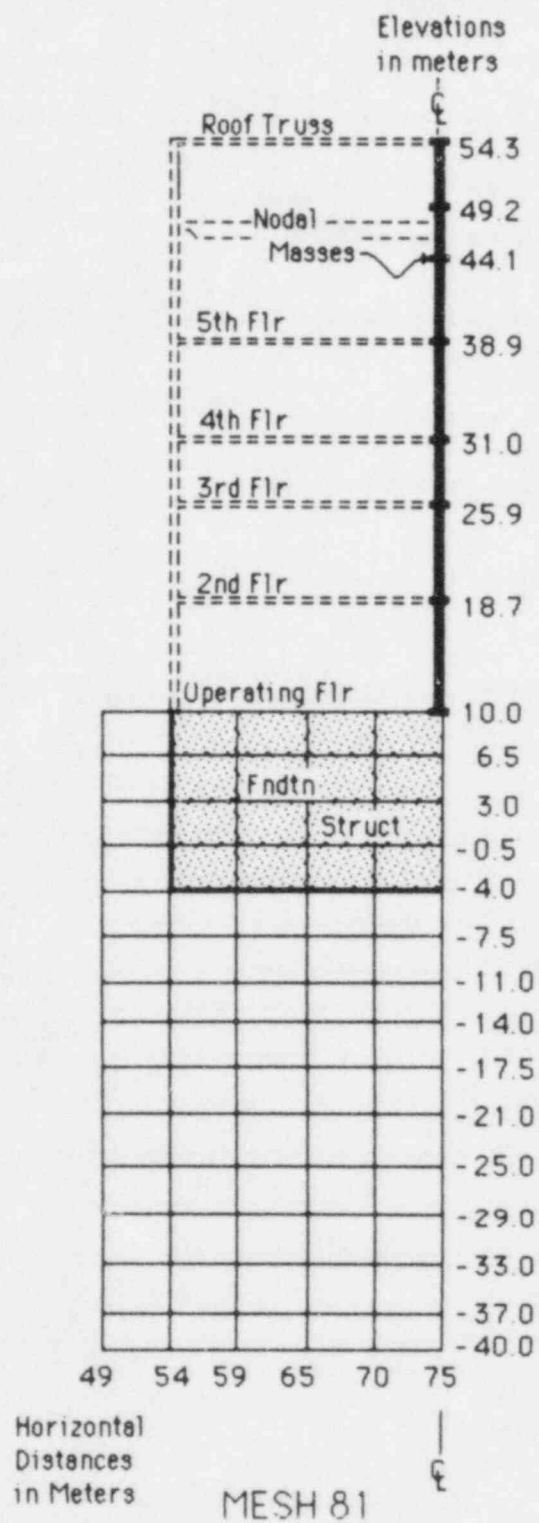


Fig. C.10 Close Vertical Boundary

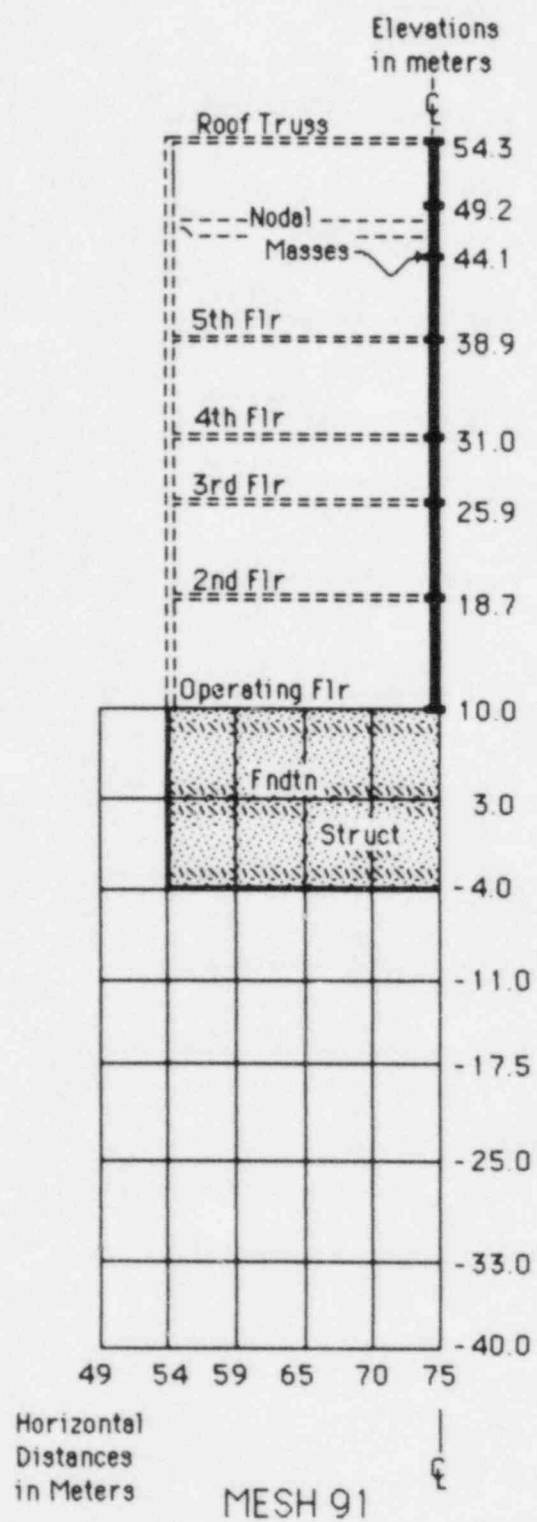


Fig. C.11 Intermediate Frequency Mesh

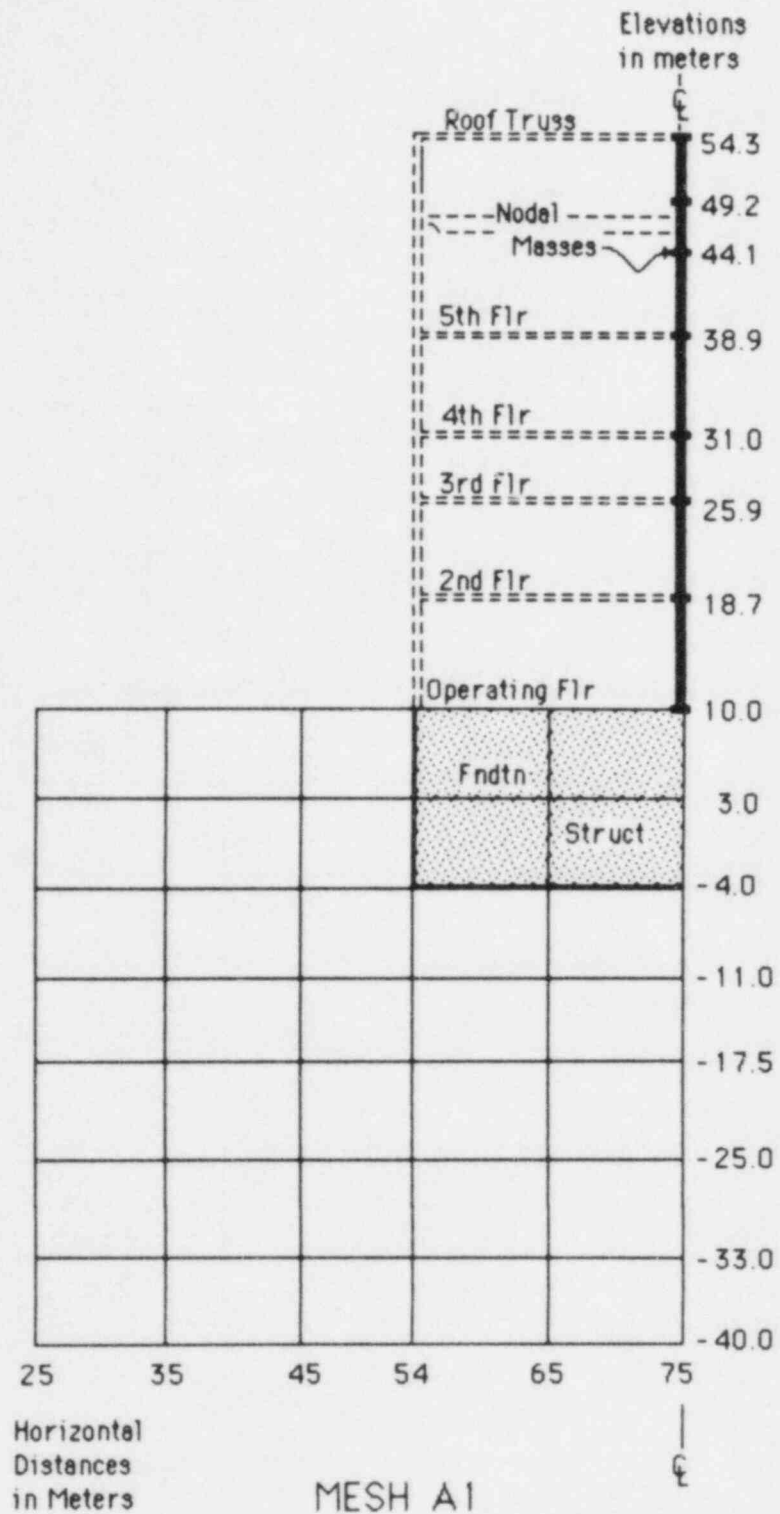


Fig. C.12 Intermediate Frequency/Intermediate Boundary Mesh

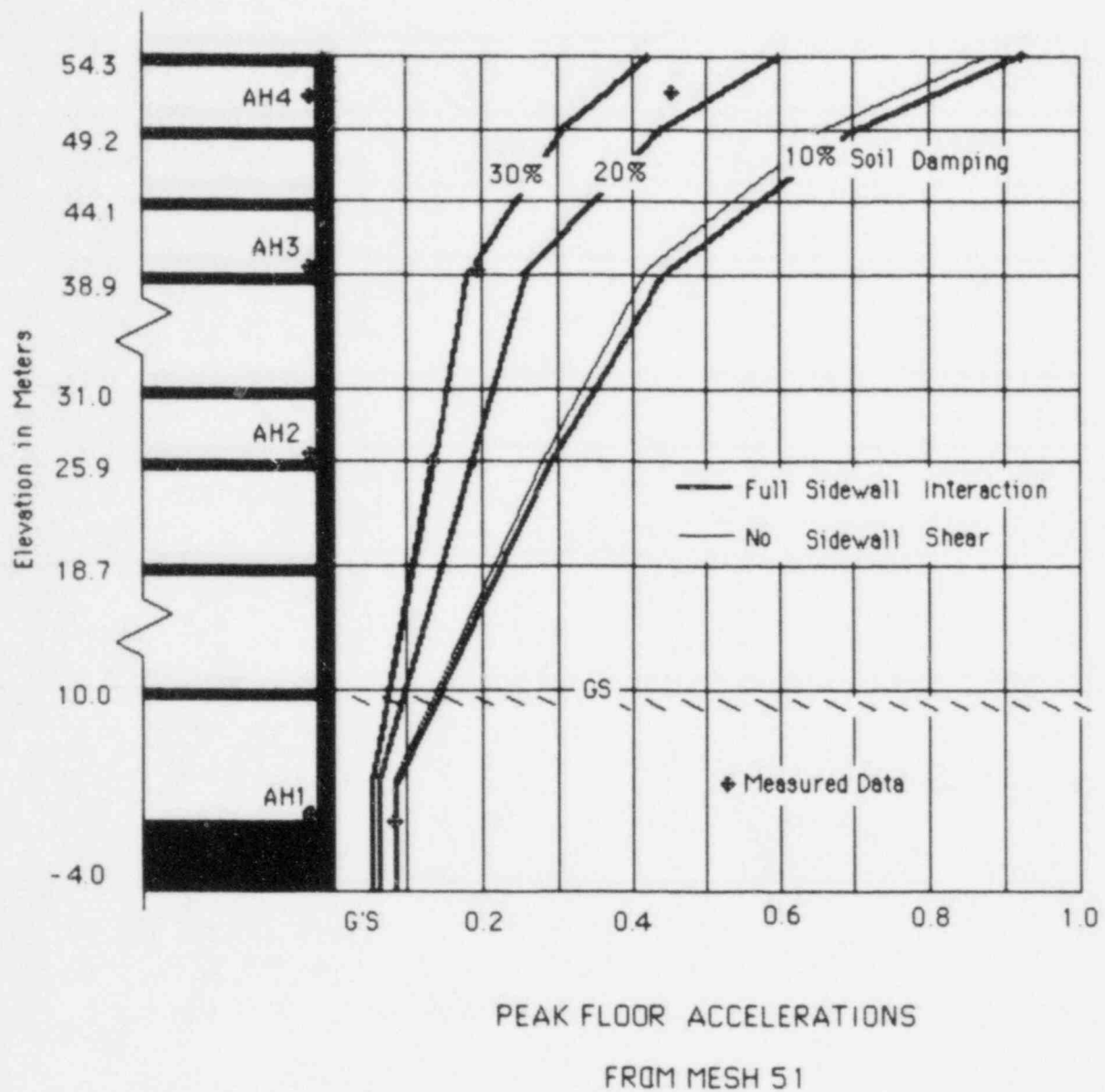


Fig. C.13 Comparison of Peak Floor Accelerations for Low Frequency Mesh

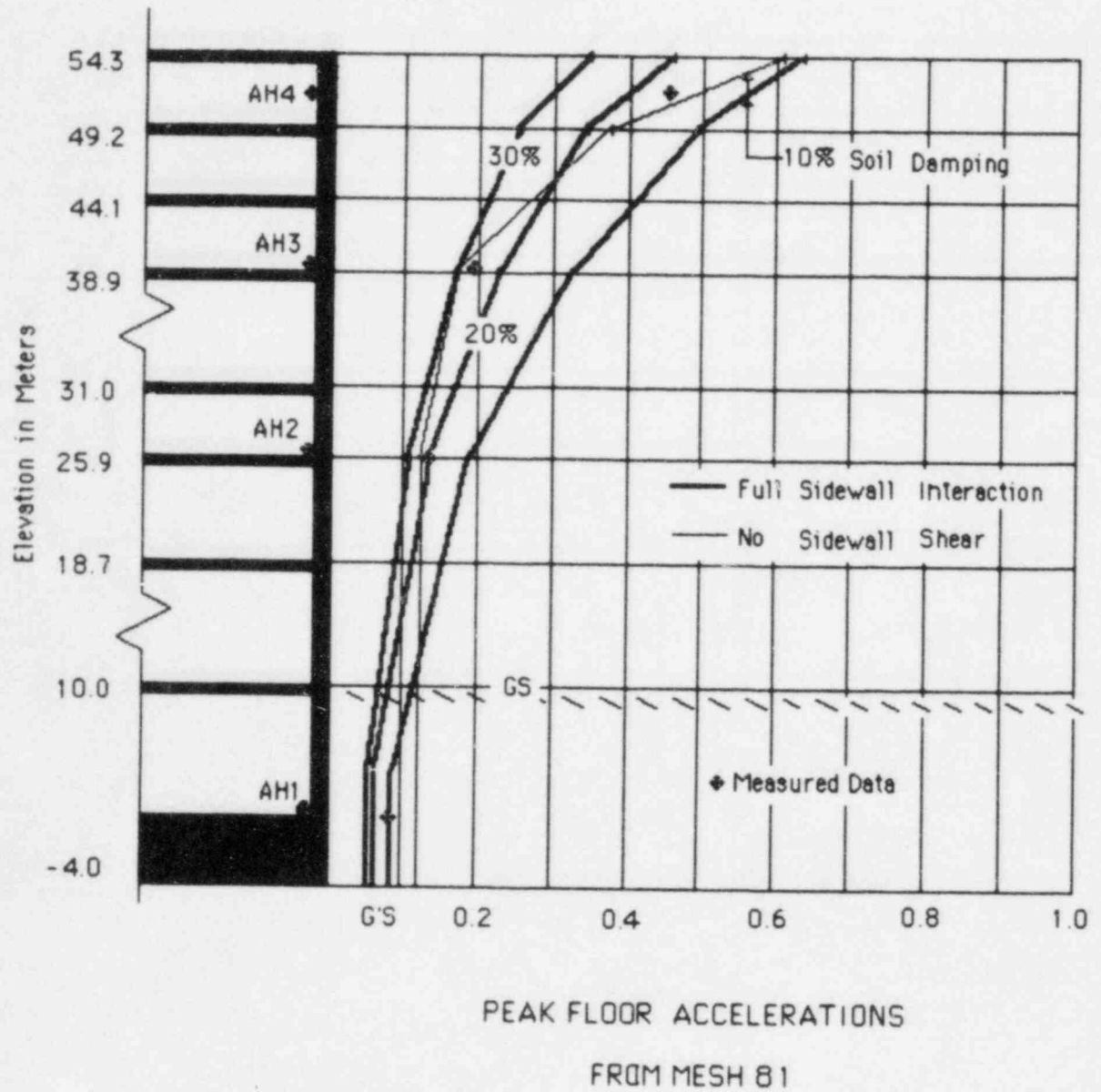
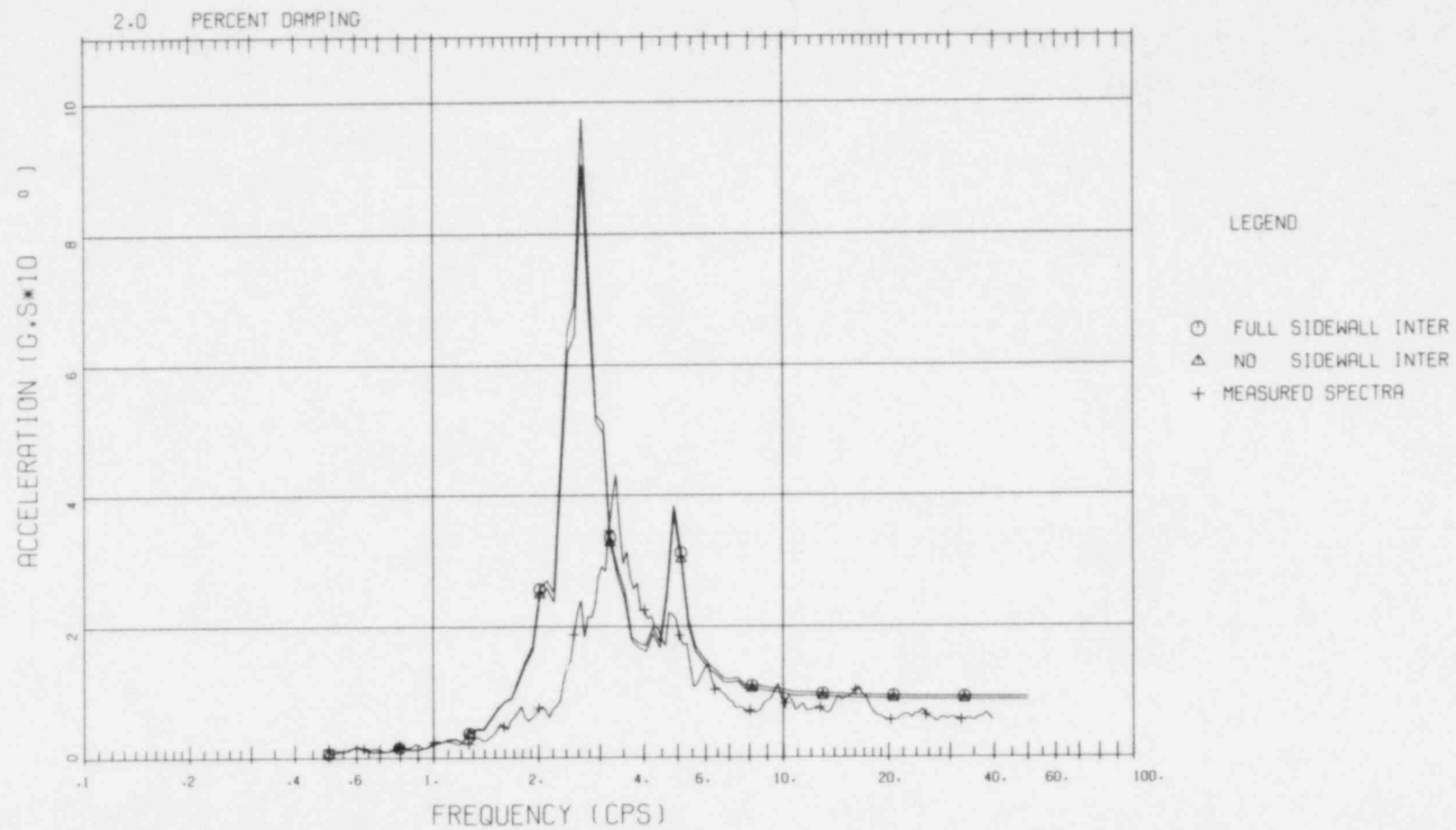
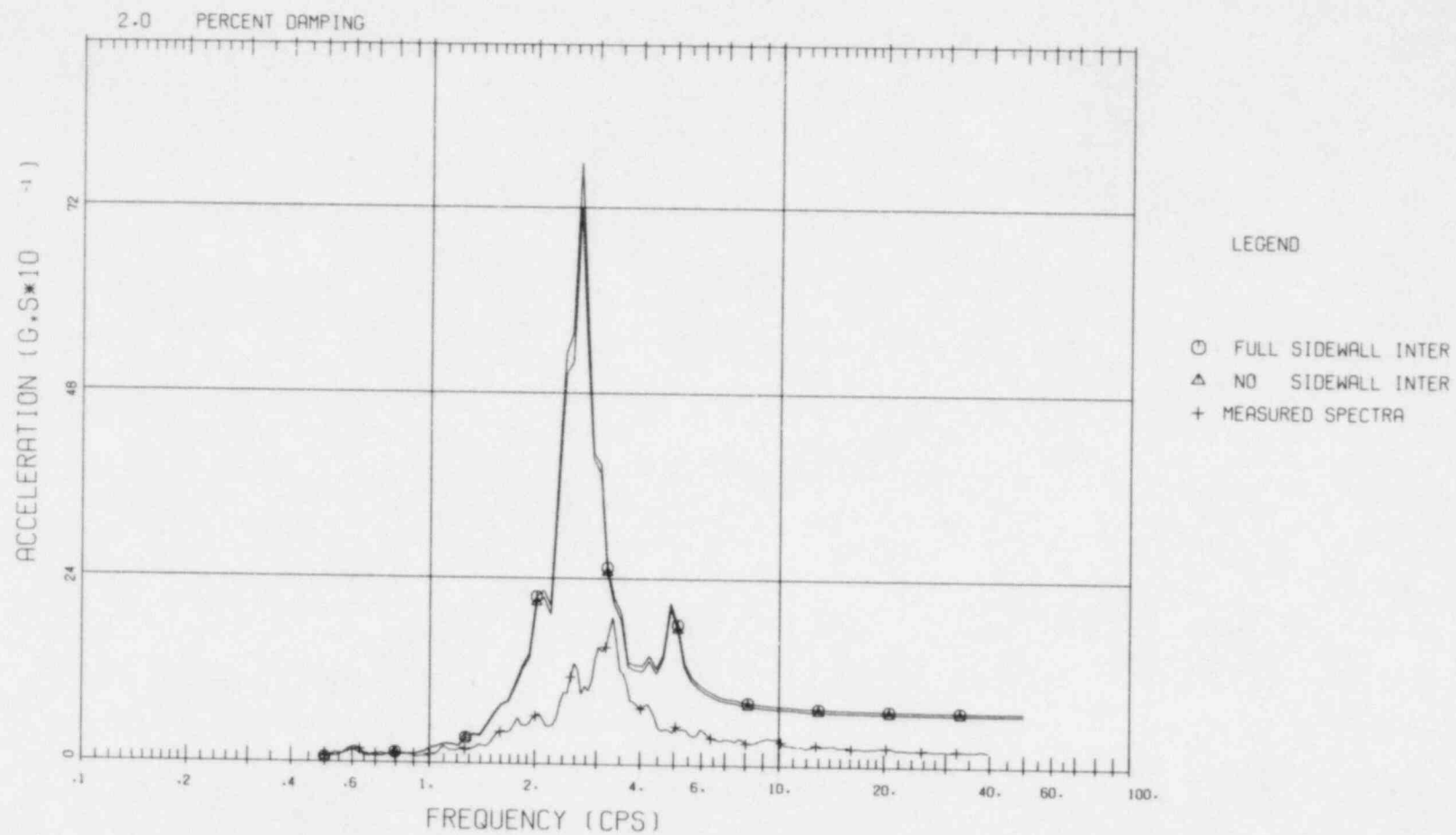


Fig. C.14 Comparison of Floor Accelerations for High Frequency Mesh

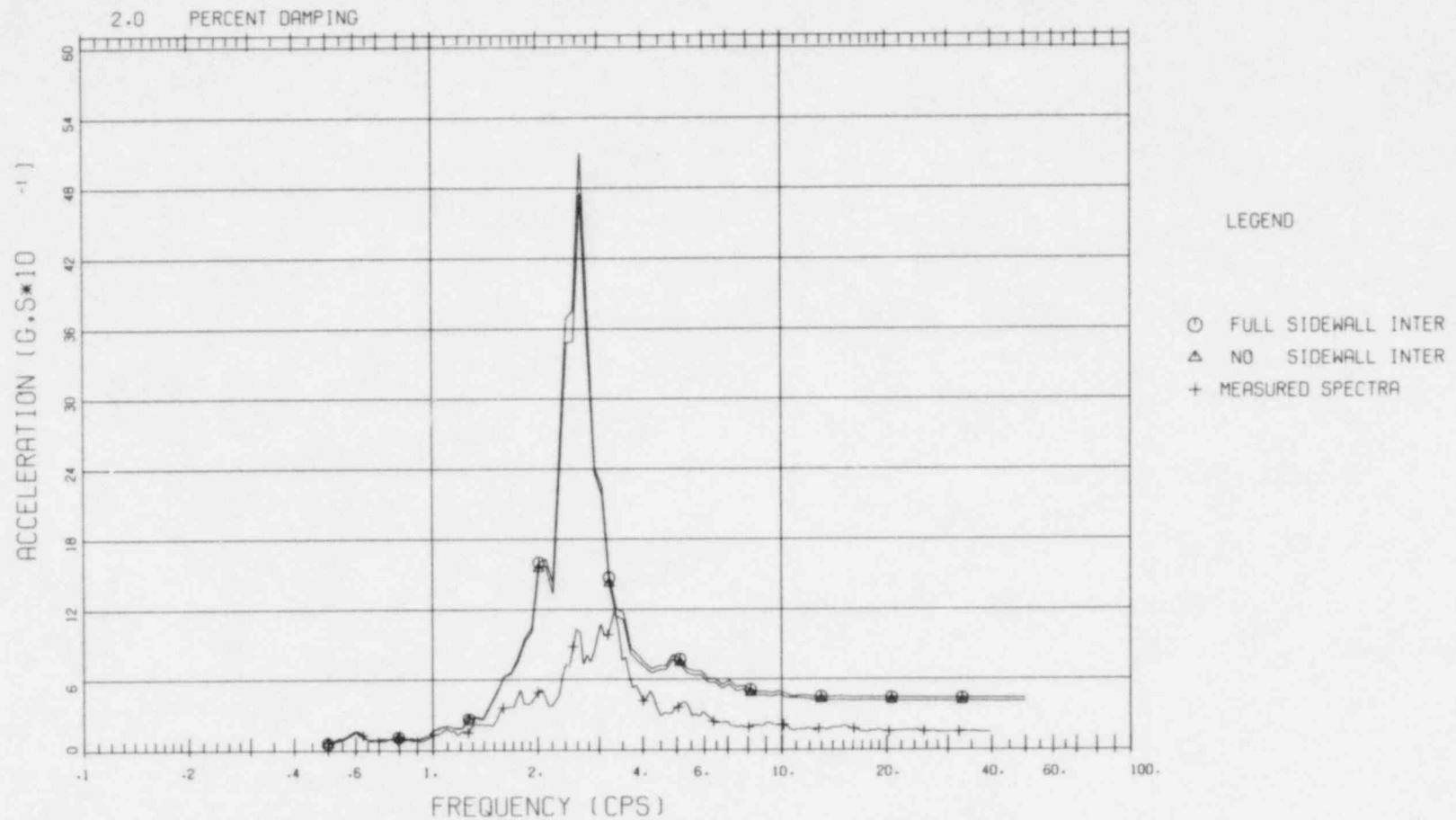
I
Fig. C.15 SIDEWALL FRICTION EFFECTS 10PCT SOIL DAMPING, ROOF TRUSS



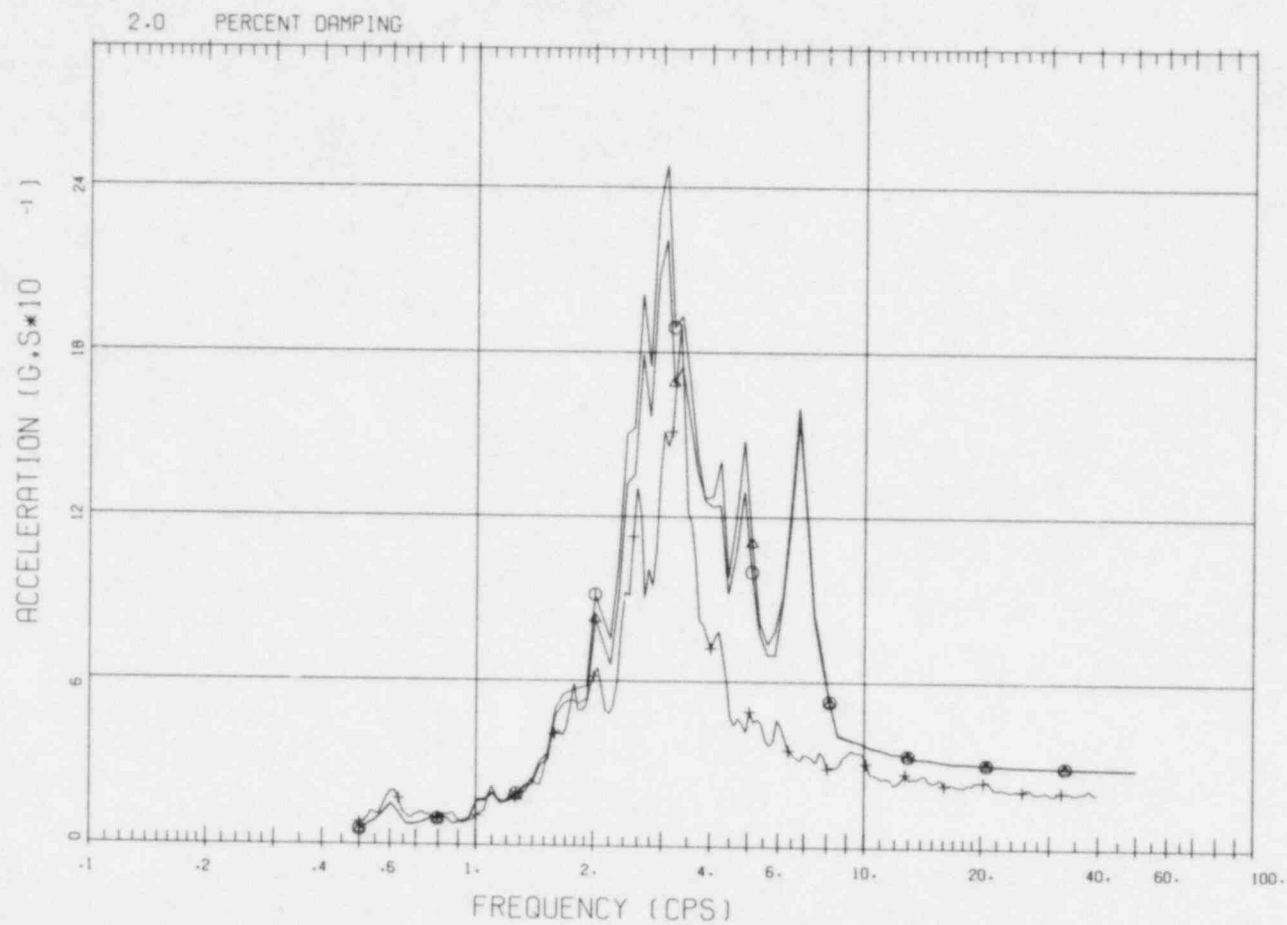
I
Fig. C.16 SIDEWALL FRICTION EFFECTS 10PCT SOIL DAMPING, 5TH FLR



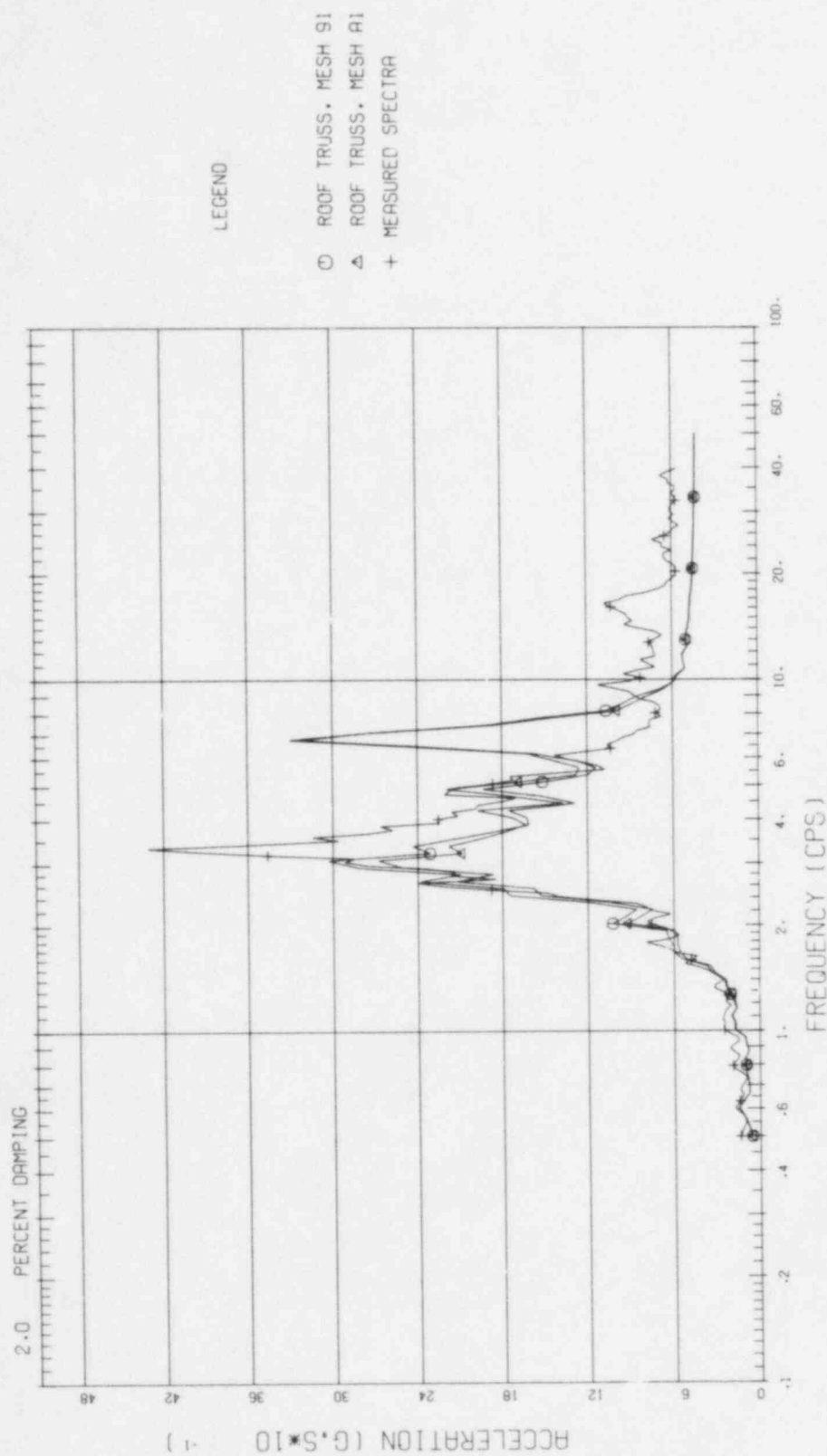
I
Fig. C.17 SIDEWALL FRICTION EFFECTS 10PCT SOIL DAMPING, 3RD FLR



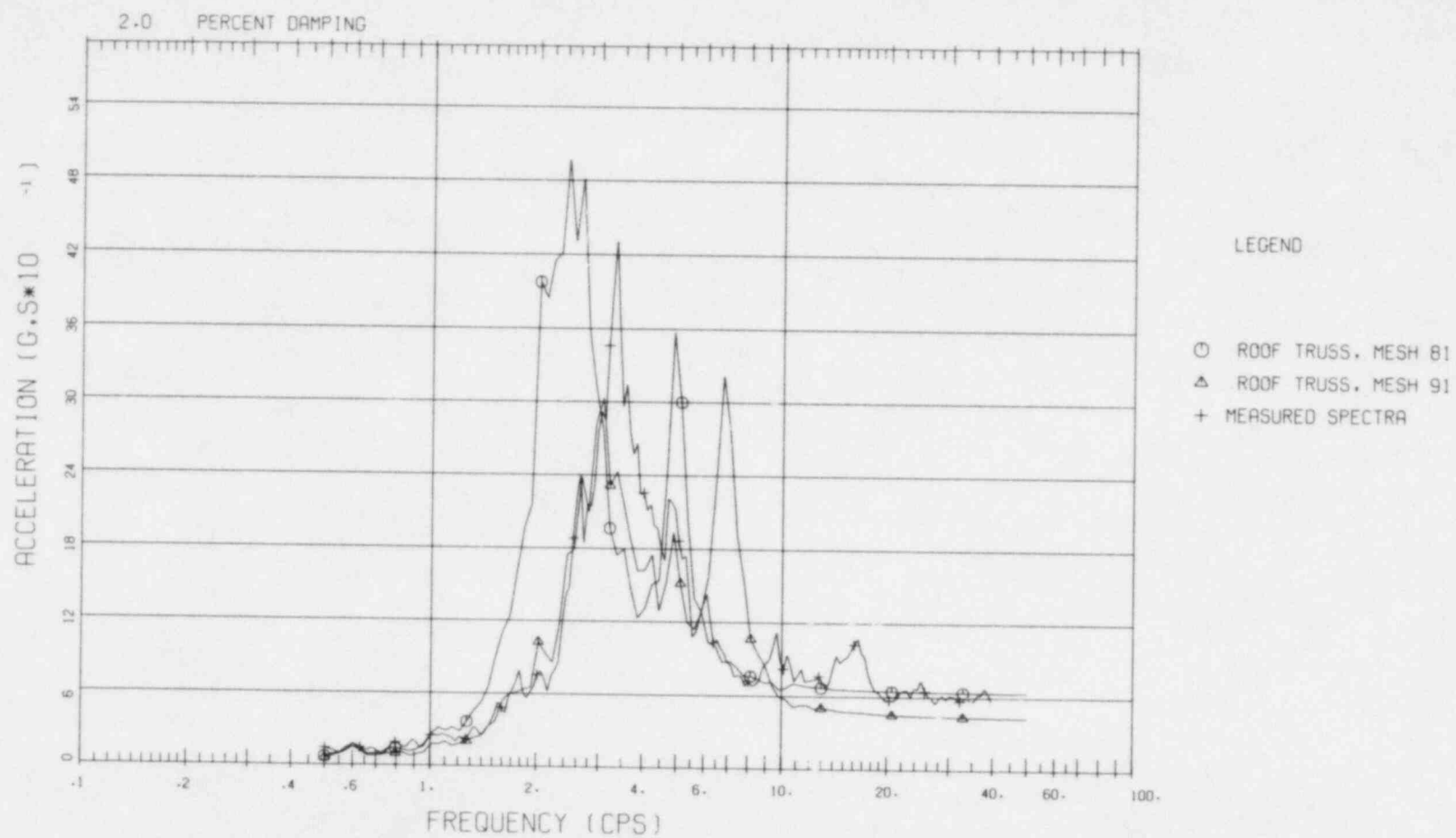
I
Fig. C.18 MESH WIDTH EFFECT. 10PCT SOIL DAMPING



I
Fig. C.19 MESH WIDTH EFFECT, 10PCT SOIL DAMPING



I
Fig. C.20 ELEMENT SIZE EFFECT ON SPECTRA, 10PCT SOIL DAMPING



I
Fig. C.21 ELEMENT SIZE EFFECT ON SPECTRA, 10PCT SOIL DAMPING

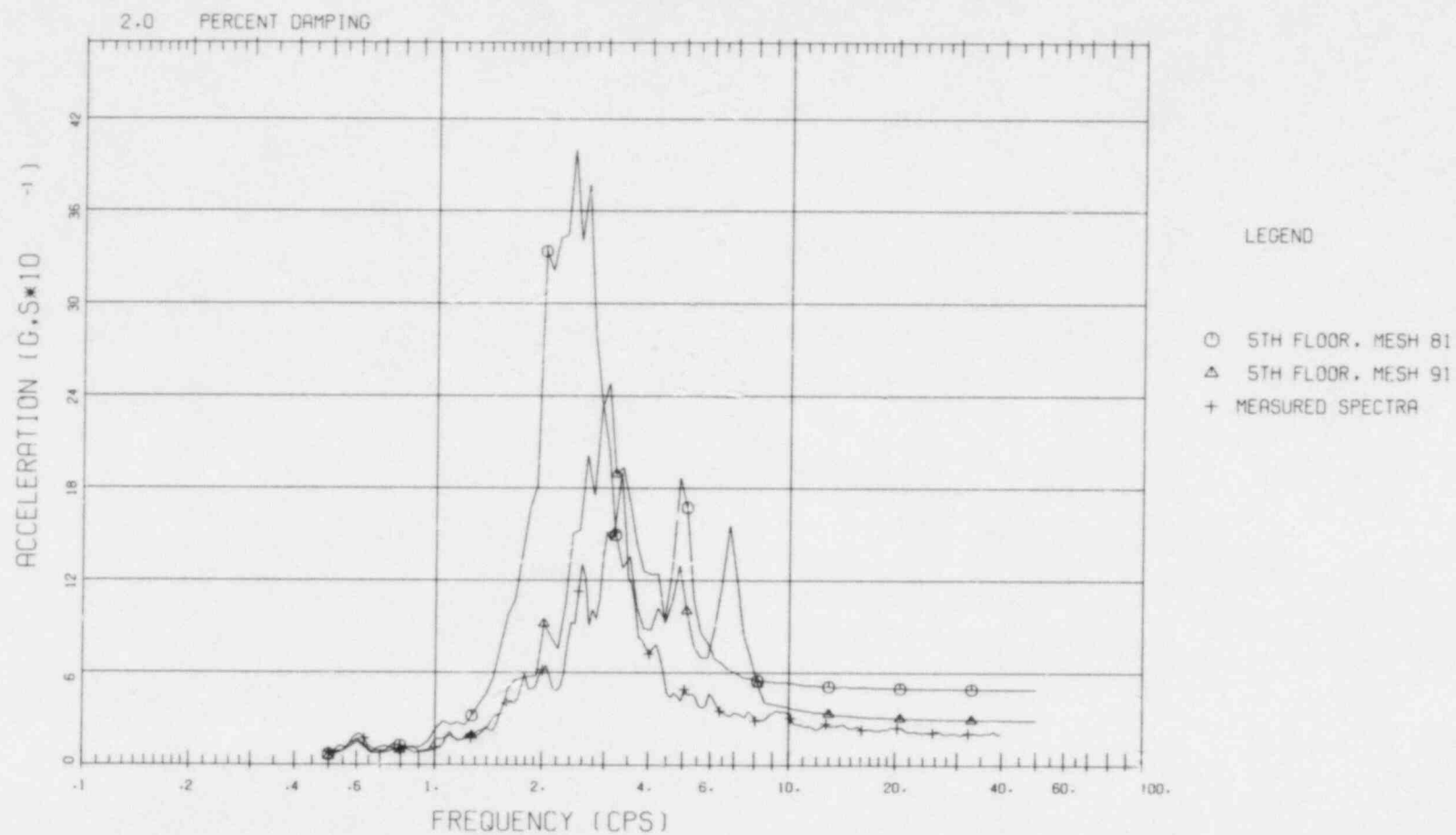


Fig. C.22 SOIL DAMPING EFFECT AT ROOF TRUSS. MESH 51

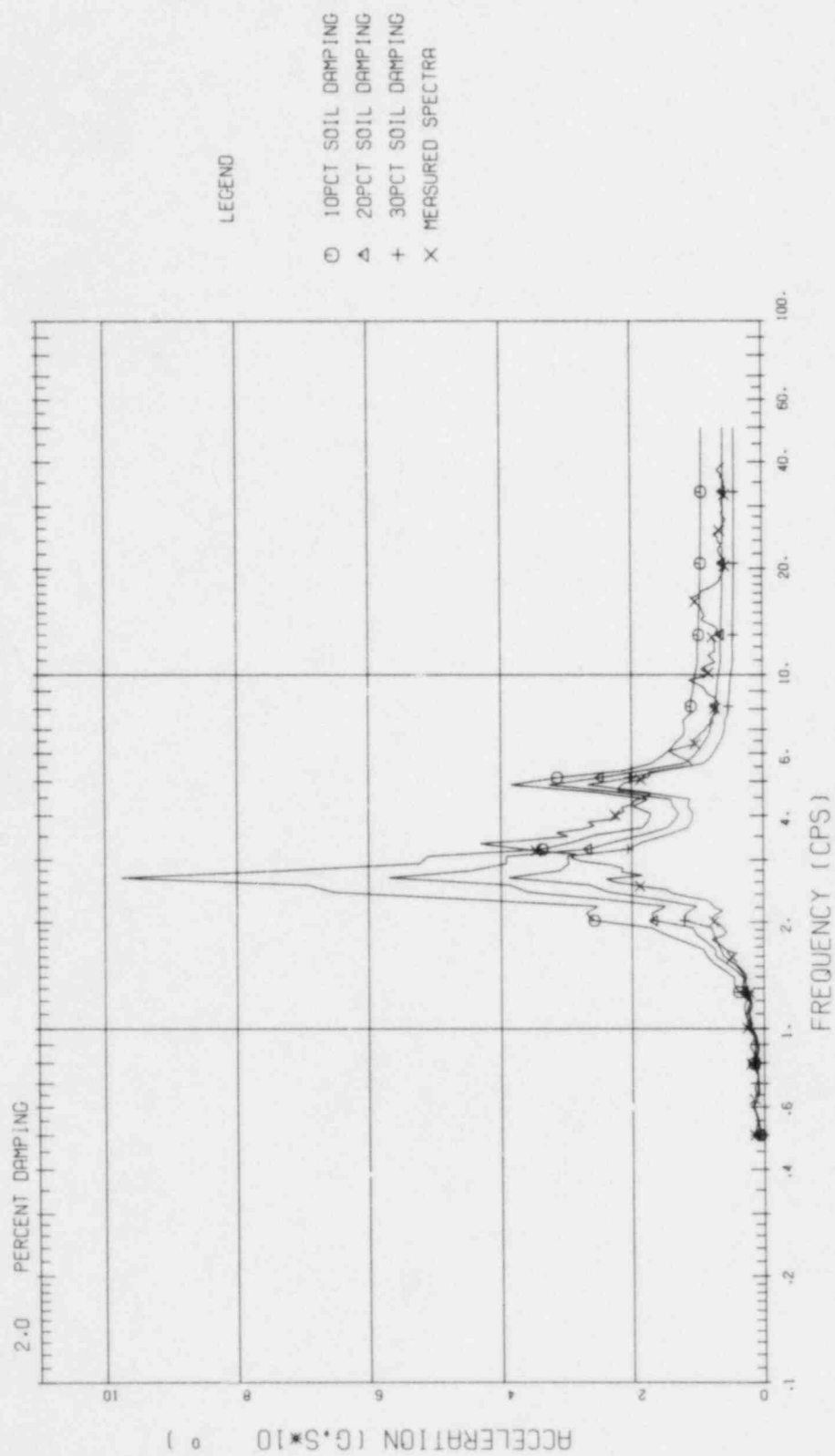


Fig. C.23 SOIL DAMPING EFFECT AT 5TH FLR. MESH 51

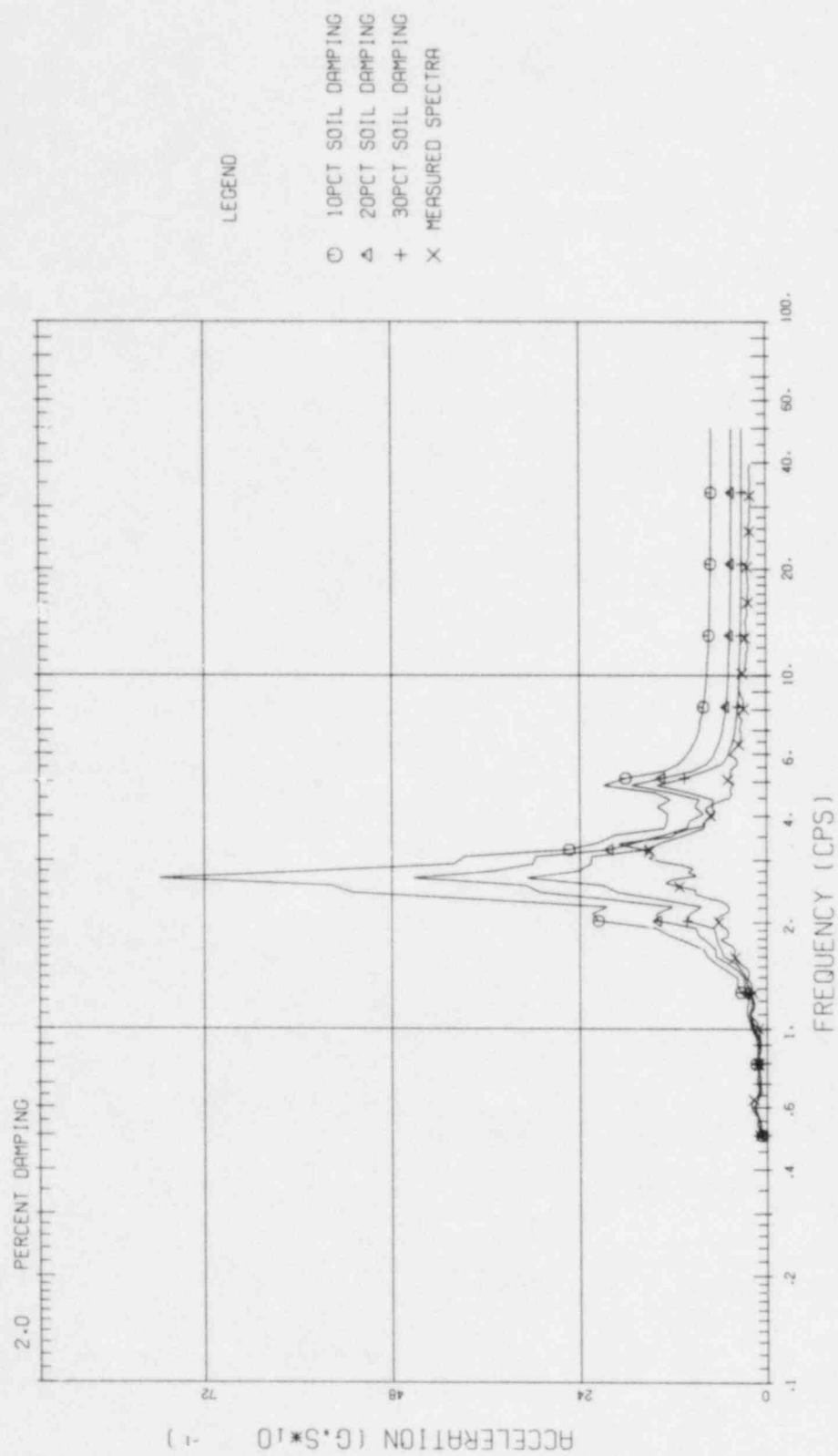


Fig. C.24 SOIL DAMPING EFFECT AT ROOF TRUSS. MESH 81

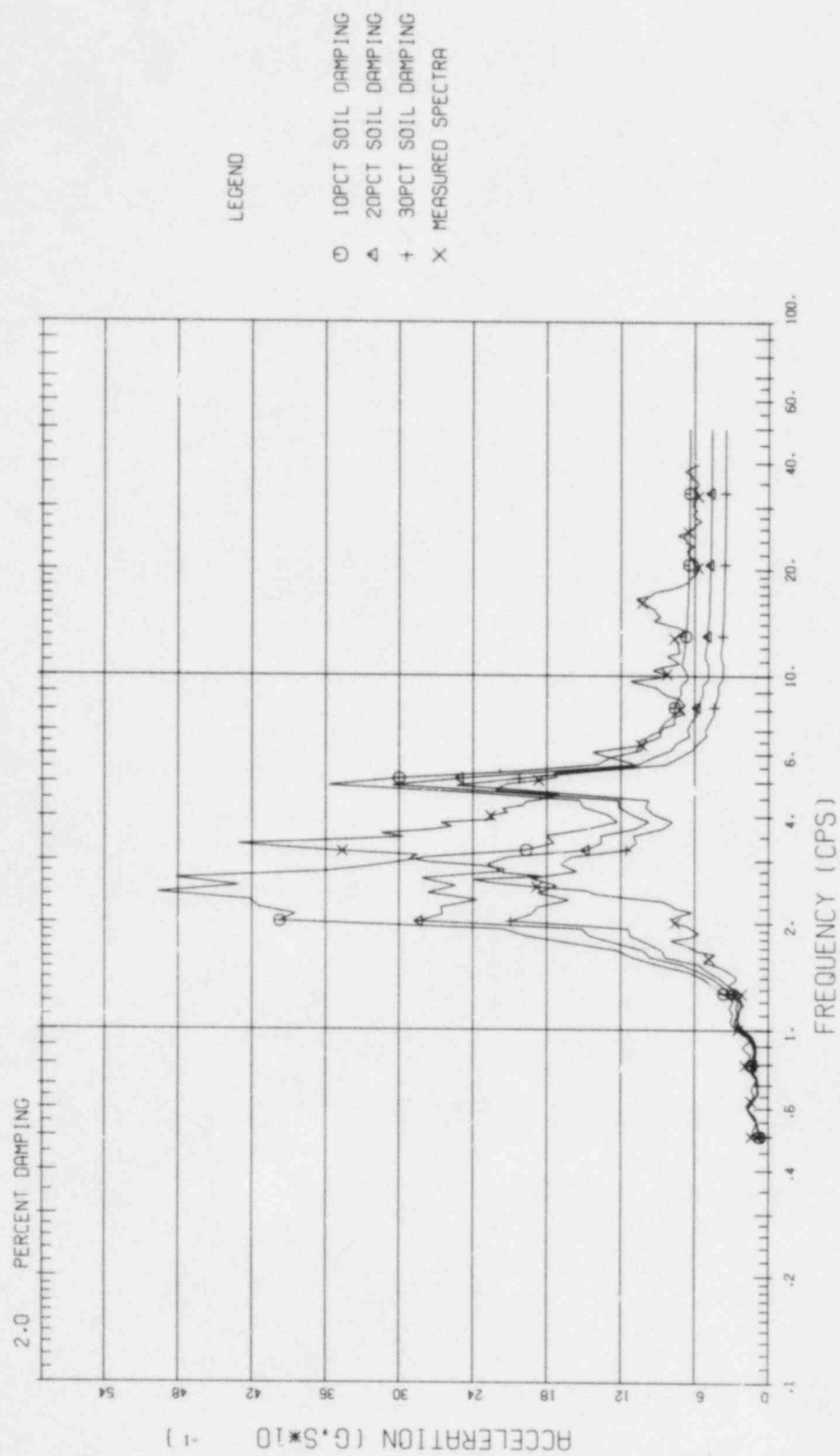
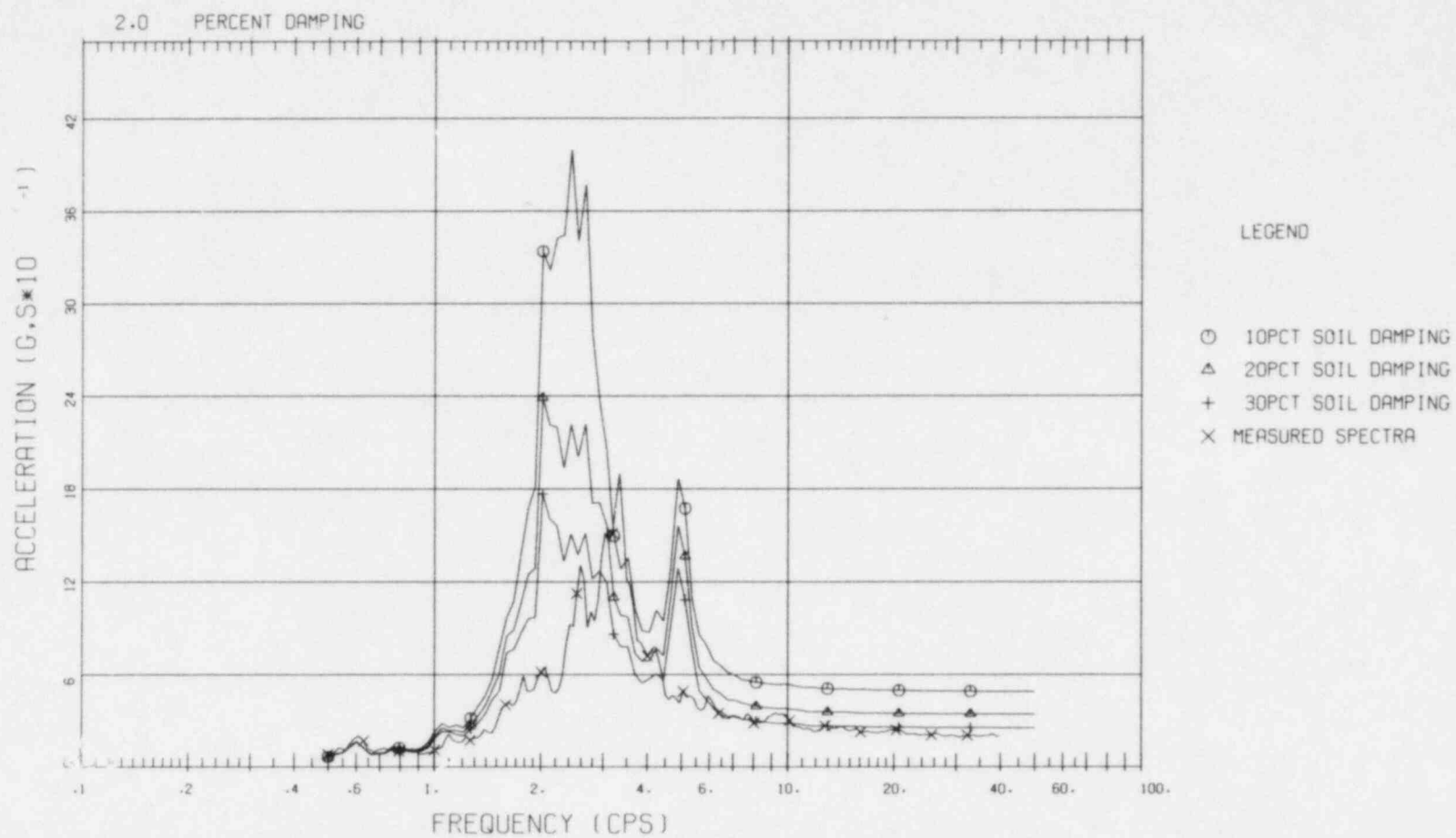


Fig. C.25 SOIL DAMPING EFFECT AT 5TH FLR. MESH 81



REFERENCES

1. "FLUSH: A Computer Program for Approximate 3-D Analysis of Soil-Structure Interaction Problems", by J. Lysmer, et al., Report No. EERC 75-30, Univ. of California, Nov. 1975.
2. "Investigation of Soil-Building Interaction Behavior of a BWR Nuclear Power Plant During Miyagiken-Oki Earthquake of 1978", by H. Tanaka and M. Nakahara.

☆U.S. GOVERNMENT PRINTING OFFICE:1985 515 034 10023

BIBLIOGRAPHIC DATA SHEET

SEE INSTRUCTIONS ON THE REVERSE

1. REPORT NUMBER (Assigned by TIDC, add Vol. No., if any)

BNL-NUREG-51893

NUREG/CR-4182

2. TITLE AND SUBTITLE

Verification of Soil Structure Interaction Methods

3. LEAVE BLANK

4. DATE REPORT COMPLETED

MONTH

YEAR

February

1985

6. DATE REPORT ISSUED

MONTH

YEAR

May

1985

5. AUTHOR(S)

C.A. Miller, C.J. Costantino, A.J. Philippacopoulos
and M. Reich

7. PERFORMING ORGANIZATION NAME AND MAILING ADDRESS (Include Zip Code)

Structural Analysis Division
Department of Nuclear Energy
Brookhaven National Laboratory
Upton, NY 11973

8. PROJECT/TASK/WORK UNIT NUMBER

9. FIN OR GRANT NUMBER

A-3242

10. SPONSORING ORGANIZATION NAME AND MAILING ADDRESS (Include Zip Code)

Office of Nuclear Regulatory Research
U.S. Nuclear Regulatory Commission
Washington, DC 20555

11a. TYPE OF REPORT

Technical Report

b. PERIOD COVERED (Inclusive dates)

12. SUPPLEMENTARY NOTES

NA

13. ABSTRACT (200 words or less)

Soil-structure interaction (SSI) methods currently used by industry to evaluate the seismic response of nuclear power plant facilities are reviewed with the aim of evaluating those areas of uncertainty which still exist in the analytic approaches. The primary methodologies used by various agencies generally can be grouped into three areas, namely, lumped parameter methods, finite element methods of combined soil/structure systems, and substructuring methods of analysis. Each of these are discussed in the report.

In general, it was found that lumped parameter approaches yield reasonable results provided that the site is relatively uniform and the seismic inputs are low enough such that nonlinear effects are unimportant. The finite element results are reasonable provided that extreme care is taken in determining mesh geometry, boundary conditions, 3D effects, etc. Similar conclusions can be applied to the structuring approaches.

14. DOCUMENT ANALYSIS - a. KEYWORDS/DESCRIPTORS

soil-structure interaction, lumped parameter methods, finite element
methods, substructure methods, Fukushima data, SIMQUAKE data

b. IDENTIFIERS/OPEN ENDED TERMS

15. AVAILABILITY
STATEMENT

16. SECURITY CLASSIFICATION

(This page)

Unclassified

(This report)

Unclassified

17. NUMBER OF PAGES

18. PRICE

120555078877 1 1AN1RD
US NRC
ADM-DIV OF TIDC
POLICY & PUB MGT BR-PDR NUREG
W-501
WASHINGTON DC 20555